

TECHNISCHE UNIVERSITÄT DRESDEN

INSTITUT FÜR BAHNFAHRZEUGE UND BAHNTECHNIK
PROFESSUR FÜR FAHRZEUGMODELLIERUNG UND -SIMULATION

Model Order Reduction in Structural Mechanics Coupling the Rigid and Elastic Multi Body Dynamics

Vollständiger Abdruck der von der Fakultät Verkehrswissenschaften
“Friedrich List” der Technischen Universität Dresden
zur Erlangung des akademischen Grades

Doktor der Ingenieurwissenschaften (Dr.-Ing.)

genehmigten Dissertation

von

MSc.-Math. Panagiotis Koutsovasilis

geboren am 15. August 1979 in Athen, Griechenland

Tag der Einreichung: 9. April 2009
Tag der Verteidigung: 21. September 2009

Vorsitzender der
Prüfungskommission: Prof. Dr.-Ing. J. Trinckauf

Prüfer der Dissertation: Prof. Dr.-Ing. M. Beitelshmidt
Prof. Dr. rer. nat. M. Arnold

Vorwort

Die vorliegende Arbeit entstand in der Zeit von August 2005 bis Juli 2009 im Rahmen meiner Tätigkeit als wissenschaftlicher Mitarbeiter von Prof. Dr.-Ing. M. Beitelschmidt an der Professur für Fahrzeugmodellierung und -simulation der Technischen Universität Dresden. Ich möchte all jenen danken, die mich bei der Erstellung dieser Arbeit unterstützt haben.

Mein besonderer Dank geht an Herrn Prof. Dr.-Ing. M. Beitelschmidt für die Anregung und Förderung dieser Arbeit. Mit seiner steten Diskussions- und Hilfsbereitschaft hat er einen entscheidenden Beitrag zum Gelingen der Arbeit geleistet.

Ein weiterer besonderer Dank ergeht an Herrn Dr.-Ing. V. Quarz für die enge und fruchtbare Zusammenarbeit während der gesamten Zeit meiner wissenschaftlichen Arbeit. Durch seine Ratschläge und Hinweise trug er erheblich zur Steigerung der Qualität der vorliegenden Dissertation bei. Herrn Prof. Dr. rer. nat. M. Arnold der Martin-Luther-Universität Halle-Wittenberg danke ich für die freundliche Übernahme des Korreferats und die entstandenen Ideen und Anregungen im Rahmen der Korrekturphase meiner Dissertation. Weiterhin bedanke ich mich bei Herrn Prof. Dr.-Ing. habil. V. Ulbricht für seine gesamte Unterstützung für die notwendigen Prüfungen infolge der Promotionsordnung. Dem Vorsitzenden der Promotionsordnung Herrn Prof. Dr.-Ing. J. Trinckau als auch Herrn Prof. Dr.-Ing. G. Löffler möchte ich ebenfalls danken.

Den jetzigen und den ehemaligen Kollegen sowohl an der Professur für Fahrzeugmodellierung und -simulation als auch an der Professur für Technik spurgeführter Fahrzeuge der Technischen Universität Dresden danke ich für die stets angenehme Arbeitsatmosphäre und die heiteren Doktorandentreffen. Insbesondere danke ich Herrn Dipl.-Ing. M. Harter für seine stetige Hilfe und unsere zahlreichen fruchtbaren Diskussionen.

Ein weiterer Dank ergeht an Herrn E. Börner, der im Rahmen seiner Studienarbeit unter meiner Anleitung Beiträge zu meiner Dissertation geleistet hat.

Nicht zuletzt möchte ich mich bei meiner Freundin Medea bedanken, die mir immer ein großer Rückhalt war. Weiterhin danke ich allen meinen Freunden, die dafür gesorgt haben, dass mein Aufenthalt in Dresden zu der schönsten Zeit meines Lebens zählt. Ein ganz besonderer Dank gilt meinen Eltern. Sie haben mir mein gesamtes Studium ermöglicht und mich immer nach besten Kräften ununterbrochen und entscheidend unterstützt. Ihnen wie auch meinem früh verstorbenen liebsten Onkel und Kollegen Georgios Kopanias ist diese Arbeit gewidmet.

Contents

Nomenclature	IX
1 Introduction	1
1.1 Mechanical multi body systems	1
1.2 Coupling the rigid and elastic multi body dynamics	2
1.3 Model Order Reduction in structural mechanics	3
1.4 Software availability and restrictions	6
1.5 Structure of the thesis	8
2 Model Order Reduction	11
2.1 Equations of motion for Finite Element structures	11
2.1.1 Kinematics of Finite Element structures	11
2.1.2 Kinetics of Finite Element structures	13
2.1.3 Dimension of Finite Element discretized structures	16
2.2 Master and slave degrees of freedom	17
2.3 Categorization of model order reduction methods	21
2.4 Physical space reduction-expansion methods	22
2.4.1 Static condensation and variants	22
2.4.2 Dynamic condensation and variants	25
2.4.3 Improved Reduction System method and variants	27
2.4.4 System Equivalent Reduction Expansion Process	30
2.5 Semi physical subspace reduction-expansion methods	33
2.5.1 Component Mode Synthesis and variants	33
2.5.2 Krylov spanned Component Mode Synthesis	36
2.5.3 Improved Component Mode Synthesis	37
2.6 Non physical subspace reduction-expansion methods	39
2.6.1 First order Krylov Subspace method	40
2.6.2 Second order Krylov Subspace method	44
2.6.3 First order Balanced Truncation	50
2.6.4 Second order Balanced Truncation	54
2.6.5 Second Order Modal Truncation	57
2.7 Two-step reduction-expansion methods	58
3 Validation of reduced order models	61
3.1 Eigenvalue analysis in structural mechanics	61
3.1.1 Undamped free vibrated systems	61
3.1.2 Orthogonality properties	63
3.1.3 Proportionally damped free vibrated systems	64
3.1.4 Practical implementation for mechanical structures	65
3.2 Model Correlation Criteria	66

3.2.1	Eigenfrequency related criteria	66
3.2.2	Eigenvector related criteria	68
3.2.3	Switching process updating methodology	74
3.3	Application examples	78
3.3.1	3D solid bar structure - Case 1	78
3.3.2	3D solid bar structure - Case 2	91
3.3.3	UIC60 elastic rail - Case 1	93
3.3.4	UIC60 elastic rail - Case 2	97
3.3.5	Elastic rod	101
3.3.6	Elastic crankshaft	106
4	Numerical issues in model order reduction	113
4.1	Diagonal perturbation methodology	115
4.2	Diagonal perturbation - application examples	116
4.2.1	Iterative model order reduction	116
4.2.2	Direct model order reduction	122
4.3	Stabilization of the matrix polynomial in structural mechanics	124
5	Flexible body dynamics in multi body systems	129
5.1	Floating frame of reference formulation	130
5.1.1	Kinematics of flexible multi body systems	130
5.1.2	Ritz approximation for deformations	131
5.1.3	Kinetics of flexible multi body systems	132
5.2	Evaluation of the elastic body information	135
5.3	Back-projection approach	137
5.4	Standard Input Data file	140
6	Model Order Reduction Package	143
6.1	Functionality of the MORPACK toolbox	144
6.1.1	Inner interfaces	144
6.1.2	Application levels	145
6.2	Algorithmic procedures for free and fixed structures	146
6.3	Application examples	147
6.3.1	3D solid bar structure	147
6.3.2	UIC60 rail	148
6.4	Non successful SID generation	154
7	Summary	155
7.1	Summary in English	155
7.2	Summary in German	157
Literature		159
List of Figures		167
List of Tables		171

A MORPACK User's Guide	173
A.1 MORPACK version 1.0	173
A.2 ANSYS FE data	173
A.3 Procedures I & II	174
A.4 MORPACK GUI	175
A.5 Compatibility with commercial FEM software packages	178

Nomenclature

BEM	Boundary Element Method
BT	Balanced Truncation
CAD	Computer Aided Design
CG	Conjugate Gradient (method)
CMP	Correlated Modal Pair
CMS	Component Mode Synthesis
COMAC	Coordinate Modal Assurance Criterion
DAE	Differential and Algebraic Equation
DoF	Degrees of Freedom
DP	Diagonal Perturbation
FBI	Flexible Body Input Data
FE	Finite Element
FEM	Finite Element Method
FEMBS	Finite Element - Multi Body Systems interface
FV	Free Velocity (Gramians)
GMRES	Generalized Minimal Residual (method)
HSV	Hankel Singular Value
ICMS	Improved Component Mode Synthesis
IKCMS	Improved Krylov spanned Component Mode Synthesis
IRS	Improved Reduction System (method)
ISS	International Space Station
KCMS	Krylov spanned Component Mode Synthesis
KSM	Krylov Subspace Method
KV	Krylov Vector
LTI	Linear Time Invariant
MAC	Modal Assurance Criterion
MBS	Multi Body Systems
MCC	Model Correlation Criteria
MCCM	Modal Comparison Criteria Matrix
MEMS	Micro Electro Mechanical Systems

MIMO	Multi Input Multi Output
MNVD	Mass Normalized Vector Difference
modMAC	Modified Modal Assurance Criterion
MOR	Model Order Reduction
MORPACK	Model Order Reduction PACKage
MSF	Modal Scale Factor
NFD	Natural Frequency Difference
NMD	Normalized Modal Difference
NRFD	Normalized Relative Frequency Difference
ODE	Ordinary Differential Equation
PCG	Preconditioned Conjugate Gradient (method)
PDE	Partial Differential Equation
ROM	Reduced Order Model
SEREP	System Equivalent Reduction Expansion Process
SID	Standard Input Data
SISO	Single Input Single Output
SNVD	Stiffness Normalized Vector Difference
SOBT	Second Order Balanced Truncation
SOKSM	Second Order Krylov Subspace Method
SOMT	Second Order Modal Truncation
SOSSB	Second-Order State-Space Balancing algorithm
SSB	State-Space Balancing algorithm
UIC	Union Internationale des Chemins de fer
w.r.t	with respect to
ZV	Zero Velocity (Gramians)

1 Introduction

1.1 Mechanical multi body systems

The modelling procedure of mechanical Multi Body Systems (MBS) constitutes an essential tool being used in various research disciplines, e.g. engine dynamics, vehicle simulation, robotics, mechanisms, microelectromechanical systems (MEMS), etc. The mechanical and structural systems consist of numerous subsystems or components (bodies), which are interconnected by different types of joints, thus enforcing kinematic constraints. Based on each subsystem's dynamic properties the MBS theory is divided into two major categories, namely, the rigid and the elastic multi body dynamics [110, 112].

In rigid body dynamics the body is assumed to undergo no deformation or more accurately the body's deformation is small enough, in comparison to its overall motion, to be neglected. Therefore, the distance between two material points of the body is constant. Based on this modelling approach the equations of motion can be derived and are given either by a set of second-order, index-3 Differential and Algebraic Equations (DAEs) [21], if kinematic constraints are present and the generalized coordinates have been used to model the MBS, or by a set of second-order Ordinary Differential Equations (ODEs) in case of absence of kinematic constraints or utilization of the so called minimal coordinates. In both cases advantages concerning the accuracy of solution as well as the computational time are present: the system's discretization leads to a fairly low number of bodies, joints, force elements, and components of control resulting in a total number of Degrees of Freedom (DoF) generally smaller than one thousand (6 DoF per rigid body). Thus, the low number of ODEs or DAEs in combination with efficient existing $O(n)$ formalisms [40, 6, 7, 108] contribute to a fairly low computation time. The major disadvantage of rigid body dynamics lies in the nature of its definition: the neglect of the deformation effect can lead to the derivation of mathematical models, which describe poorly the actual system. Cases of such systems might be mechanical structures, which operate at high speeds or with sufficient force loads.

In elastic multi body dynamics, on the other hand, the deformation effect is taken into consideration. In this case, though, the dynamic behavior of the elastic MBS is given by a set of Partial Differential Equations (PDEs) the solution of which, e.g. the computation of the body's deformation or stress state, is in seldom cases analytically possible. This is due to systems with complex geometry, or with boundary conditions analytically not describable, or with non linear material properties. Therefore, various numerical methods have been developed over the last decades [48, 95, 128], e.g. the Ritz-Galerkin method, the Ritz method, the Finite Element Method (FEM), the Boundary Element Method (BEM), or their combination depending on the nature of the problem in order to approximate the solution of the PDE. The choice of the so called shape

functions over the domain of interest is what makes each method different from the others.

The most commonly used numeric approach in elastic multi body dynamics is the FEM [128]. Due to the structure's complexity, it is not easy to find an appropriate shape function over the whole domain, which satisfies the essential geometric and kinetic boundary conditions of the system. Thus, the domain is partitioned into geometrical elements known as Finite Elements (FE), i.e. lines, areas and volumes for the one-, two- and three-dimensional case respectively, and for these elements local shape functions (Ritz shape functions) are defined, which should assure the fulfillment of kinetic, material and boundary condition properties. Under certain assumptions the whole set of FE can capture the system's deformation field. This discretization procedure leads to the definition of second-order ODEs. Also, in this case advantages are present: the FEM is easy to apply, independent of the geometry's complexity, and the system matrices of the derived ODE possess a specific sparse pattern. The accuracy of solution is high with respect to the linear or non linear theory applied. Still, in FEM the term accuracy is accompanied by several disadvantages. In many applications, a large number of elastic coordinates have to be considered in order to sufficiently describe the deformation of the MBS. This leads to a large number of FE and nodes (6 DoF per node), increasing the dimension of the ODE's system matrices to a number usually larger than half a million, when complex MBS are considered. For static problems this causes no major difficulties, since efficient direct and iterative sparse algorithms are invoked, which exploit the specific pattern of the system matrices. In the case of dynamic procedures, though, and under normal hardware configuration any computation is practically pointless.

1.2 Coupling the rigid and elastic multi body dynamics

In an effort to accurately model and efficiently simulate mechanical MBS, the coupling of rigid and elastic multi body dynamics takes place. Herewith, the dynamic analysis of complex MBS is based on both the above mentioned modelling formalisms, since the MBS consist of various interconnected sets of rigid and deformable bodies. Certain compatibility adjustments, though, are necessary in order to feasibly enable the coupling procedure. These adjustments constitute the basic approximation steps or levels during the modelling work flow in continuum mechanics (Table 1.1).

Firstly, the geometry of the mechanical MBS is constructed. This is accomplished by the use of Computer Aided Design (CAD) technology and the appropriate software therefor. The design's accuracy is important, still specific details that might have minor influence on the model's dynamics are disregarded, e.g. very small areas and angled curves. This approximation depends, of course, both on the user and on the model's definition and has vast influence on the second step, namely, the consideration of the elastic nature for the deformable bodies of the MBS. The FEM is applied with the help of the analogous FE software and the accuracy of the resulting ODE depends on the discretization level and the element types used. As already mentioned, the discretization

level is usually very high generating ODEs with a large number of DoF. Thus, it is essential to apply the third approximation procedure known as DoF condensation or Model Order Reduction (MOR). Herewith, a reduced dimension ODE is generated, i.e. the initial large number of DoF is reduced, and the aim is to keep the dynamics of the original model as intact as possible. This is done within the FE software and the approximation error depends on the condensation method used as well as the dimension of the Reduced Order Model (ROM). At last, the fourth approximation step ensures the utilization of both the rigid and elastic body information in a generalized set of ODEs or DAEs according to the MBS formalism. It is based on the Ritz approximation and realized via interfaces between FE and MBS software packages.

Table 1.1: Modelling work flow in continuum mechanics

Approximation levels	Modelling tools	Information loss due to
Geometry	CAD software	Small areas, angled curves
PDE → ODE	FE software	Discretization, element type
FE DoF	FE software	DoF condensation
Elastic DoF	FEM/MBS software	Ritz approximation

The four major approximation levels of the rigid-elastic coupling contribute to an information loss concerning the dynamics of the actual mechanical MBS. The user's intervention is restricted up to a certain point to the first level, while constructing the CAD geometry. For the rest of the levels the algorithms are semi or fully black-boxed in the source codes of the software tools or interfaces, i.e. the user should only define certain parameter sets for the algorithmic initialization. The MOR approximation procedure constitutes the necessary link for the rigid-elastic coupling, since the ROMs can be effectively used in MBS codes avoiding memory capacity problems and vast computation times. Thus, the correct application or appropriate selection of the MOR method is important.

1.3 Model Order Reduction in structural mechanics

The restrictions concerning both the numerical algorithms and the hardware configuration in combination with the constant increase of the systems' complexity in mechanics constitute the solution of engineering problems a rather difficult task. The possibility of results' inaccuracy under such circumstances is high. Furthermore, in fields such as control engineering, the effort of designing a controller for very large models poseses several difficulties. Various examples from different research disciplines, e.g. the International Space Station (ISS) [54] in structural mechanics, the CD player [30] in electrical engineering or the Butterfly gyro [1] in Micro Electro Mechanic Systems (MEMS), fully depict the problems of dealing with high ordered systems. Thus, it is necessary to find a way of reducing the system's dimension and simultaneously keeping the important dynamic properties intact. This is accomplished by MOR, which

succeeds in simplifying the simulation and controller design tasks by finding a low order approximation of the original high order model.

In structural mechanics, as MOR is considered to be the approach of reducing the dimension of the second-order ODE by neglecting certain unimportant or unwanted DoF of the spatially discretized mechanical structure. The ROM's quality depends on how well it captures the dynamics of the original model. Based on the way the MOR proceeds, several methods have been developed during the last decades.

The first condensation technique, directly applied to models originating from structural mechanics, was proposed by GUYAN [55] and IRONS [60]. According to this method, the inertia terms contributing to the model's dynamics are ignored. Herewith, the method is exact only for static problems and it is therefore addressed as static condensation. In the latter years several variations of the static condensation followed, which contributed to taking into account the dynamic effects of the model and thus, generating qualitatively better ROMs. In this area belong the dynamic condensation method by LEUNG [79], the Improved Reduction System (IRS) method and the System Equivalent Reduction Expansion Process (SEREP) introduced by O' CALLAHAN, AVITABILE and RIEMER [25, 26], a method similar to SEREP by KAMMER [63], and the iterated IRS approach proposed by FRISWELL [46, 47]. A breakthrough in the field of dynamic MOR is considered to be the Component Mode Synthesis (CMS) by CRAIG and BAMPTON [32, 33, 34]. The CMS method belongs to the category of sub-structuring techniques: the model is split up into sub-structures and for each sub-structure the CMS algorithm is applied. It is based on computing the static part, according to the static condensation, and a dynamic part according to the definition of a certain set referred to as the Craig-Bampton (CB) set. Several variations of the CMS method are also introduced, e.g. the Rubin's CMS MOR by KRAKER and VAN CAMPEN [73] and the CMS_x MOR proposed by LIAO, BAI and GAO [83]. Finally, the Improved Component Mode Synthesis method (ICMS) introduced by KOUTSOVASILIS and BEITELSCHMIDT [69] constitutes a promising MOR scheme, which utilizes the advantages of both the IRS and CMS methods. ICMS adopts the algorithmic principle of the CMS method, but the static part is in this case defined based on the IRS properties.

The algorithmic basis of the above mentioned MOR methods is the theory of master (or external) and slave (or internal) DoF. As master DoF set is defined the subset of the structure's total DoF, which remains in the DoF set of the ODE after the reduction and therefore constitutes the DoF of the ROM. The slave DoF set consists of the unwanted DoF and therefore, it is the set to be removed from the ODE of the original model. The selection of the master and slave DoF sets proceeds with the help of specific criteria. It is not a trivial task, since it is model dependent and requires advanced engineering experience. Based on the aforesaid, several studies and applications have been conducted either in an effort to capture the advantages and disadvantages of these MOR methods or simply to generate ROMs, since some of the methods are considered to be state of the art in structural mechanics [13, 22, 38, 50, 64, 65, 70, 67, 72, 88, 92, 96, 97].

The mathematical area of systems and control theory offers a great variety of MOR schemes conceived for first-order Linear Time Invariant (LTI) systems. According to these approaches, the definition of the ROM is generally based on matching certain

parameters of the reduced and the original model or deleting specific states from the system, which are of less importance. Thus, the MOR methods belonging to this area are divided into two categories, namely, the Padé and Padé-type approximations, and the balancing-related truncation techniques.

The category of Padé and Padé-type approximations corresponds to techniques developed for obtaining a ROM, based on the theory of moment matching or partial realization. This separation depends on whether or not the coefficients of the transfer function of the LTI system tend to zero or to infinity, respectively. The first case would represent the system's dynamics at low frequencies and the second at high frequencies. The ROMs are computed with the help of Krylov subspaces [74] and the utilization of efficient algorithms, provided by ARNOLDI [8], LANCZOS [75] or variations of these two [35]. This type of MOR referred to as Krylov Subspace Method (KSM) has been extensively used over the last years for reducing numerous first-order LTI systems from different research areas [4, 5, 9, 12, 15, 18, 14, 20, 49, 52, 53, 84, 117, 45, 44, 17, 113].

The balancing-related truncation concept was firstly proposed by MULLIS and ROBERTS [90] and later on applied by MOORE [89] and LAUB, HEATH, PAIGE, and WARD [76], introducing the Balanced Truncation (BT) method. MOR methods belonging to this category succeed in generating ROMs by eliminating those states of the LTI, which require a large amount of energy to be reached and/or yield small amounts of energy to be observed. The basic tools for representing the input and output amount of energy are the controllability and observability gramians, respectively. These concepts, though, are basis dependent and thus, a basis should be found with which they become equivalent. This balanced basis is provided by the, so called, Hankel Singular Values (HSVs) [17, 4]. The importance of Balanced Truncation (BT) is the fact that it preserves stability and moreover, a global error bound exists. This second aspect constitutes in general a disadvantage of all the previously mentioned MOR methods, since there exists no such reliable criterion for determining a priori the dimension of the ROM. The techniques of this category have also been extensively studied and tested on various applications, which result in first-order LTI systems [17, 4, 18, 16, 80, 113].

In structural mechanics the system of equations derived by the FEM is a set of second-order ODEs or DAEs. In this case, the direct utilization of Padé and Padé-type approximations or the balancing-related truncation techniques is not advised. The reason is that the ROM does not preserve the second-order structure of the original model, e.g. the definiteness properties of the system matrices are damaged. Therefore, reduction schemes for systems in second-order form have been developed.

For the category of Padé and Padé-type approximations a first approach was given by SU and CRAIG [120], which actually preserves the second-order structure, but lacks in matching sufficient moments in comparison to the standard KSM MOR for first-order LTI systems. SALIMBAHRAMI proposed [107] the Second Order Krylov Subspace Method (SOKSM) for Single Input Single Output (SISO) systems. SOKSM and its variants have been successfully tested on several applications including structural mechanics [11, 41, 13, 64, 65, 70, 67, 72, 100, 77, 81, 82, 106, 105, 103, 104, 17].

Analogously, for the category of balancing-related truncation techniques a first approach in

handling second-order systems was introduced by MEYER and SRINIVASAN [87]. Therein, the so called free-velocity and zero-velocity gramians are given, which succeed in defining a balanced realization for second-order systems. This method was later extended by CHAHLAOUI, LEMONNIER, VANDENDORPE and VAN DOOREN, by proposing the Second Order Balanced Truncation (SOBT) [28, 29]. STYKEL and REIS investigate several variants [119, 98, 99] of reducing second-order systems with BT and propose various projection approaches therefor. The mentioned balancing-related MOR methods for second-order systems are a matter of current research and various comparisons are being conducted referring to the handling of large sparse systems and the quality of the ROMs [17, 4, 57, 118, 116].

A last MOR category consists of various combinations of certain of the above mentioned MOR methods. Thus, this category concerns hybrid or two-step MOR approaches. CARNEY, ABDALLAH, and HUCKLEBRIDGE introduced an alternation of the CMS method by using the same MOR scheme, but instead of defining the CB set a subspace spanned by Krylov vectors is utilized [27]. Based on this approach, the Improved Krylov spanned Component Mode Synthesis method (IKCMS) is introduced by KOUTSOVAMILIS and BEITELSCHMIDT [69], the algorithmic scheme of which proceeds analogously to the ICMS MOR approach. LEHNER and EBERHARD proposed the two-step approach [78] based on a combination of the BT and KSM for second-order systems. A similar methodology is found in KOUTSOVAMILIS, QUARZ, and BEITELSCHMIDT [71], where various combinations of MOR schemes, e.g. SEREP-KSM, KSM-BT, etc., for second-order systems are tested.

1.4 Software availability and restrictions

The decision of applying a certain MOR method depends not only on the model's specifics and the engineer's experience, but also on the software availability. Taking into account the modelling work flow, as given in Table 1.1, numerous software tools exist, which support the coupling of rigid and elastic multi body dynamics (Table 1.2).

Table 1.2: Rigid & elastic MBS: software sample

CAD Software	FEM Software	MBS Software
CATIA	ABAQUS	ADAMS
I-DEAS	ADINA	SIMPACK
Pro/ENGINEER	ANSYS	
SolidWorks	MSC Nastran	

The MOR algorithms are implemented as toolboxes integrated into the FE software. Thus, the dimension of the FE structure can be reduced within the FE software environment and output files are generated for the transfer of the elastic data into a MBS code. Usually, at this point an interface is activated in order to interpret the

elastic information and write it in a suitable format for further usage in MBS software packages.

For the purpose of this Thesis, the author restricts himself to the utilization of two specific software packages for the rigid-elastic MBS coupling, namely, ANSYS [3] and SIMPACK [115].

The software coupling between ANSYS and SIMPACK (Fig. 1.1) during a rigid-elastic body formulation is conducted with the help of an interface implemented as a toolbox within SIMPACK, namely, the FEMBS interface [114]. The FEMBS program generates the input data for the flexible body representation in SIMPACK. This is accomplished based on certain assumptions [114], e.g. linear material properties, the choice of shape functions (Ritz approximation), and the linearized equations of motion in terms of the deformation coordinates, all to be found in the works of WALLRAPP, SCHWERTASSEK, DOMBROWSKI, and SHABANA [111, 109, 110, 125, 122, 124, 112]. Thereafter, the ROM's elastic information is written in the so called Standard Input Data (SID) file format, introduced by WALLRAPP [123]. The SID file is saved in an ASCII format according to the structure-based object oriented techniques proposed by OTTER, HOCKE, DABERKOW, and LEISTER [94], and it constitutes the SIMPACK input file for further computations.

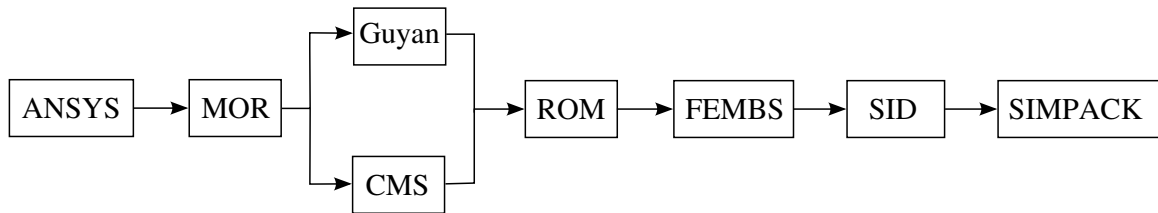


Fig. 1.1: FEM-MBS coupling using ANSYS and SIMPACK

The above mentioned ANSYS-SIMPACK work flow is, of course, accompanied by a restriction, which is regarded as a disadvantage and its nature is threefold.

Firstly, and most important, is the fact that ANSYS, as almost all the other frequently used FEM program packages, supports only two MOR methods, namely, the static and the CMS method (Fig. 1.1). With CMS being the standardized MOR method in structural mechanics, the application of other MOR schemes, which could offer qualitatively better ROMs at a reduced cost, i.e. smaller system matrices, is not feasible.

The second disadvantage is an immediate consequence of the first problematic aspect and refers to the fact that the FEMBS interface copes with ROMs generated only by the previously mentioned methods. In case that the FE information is extracted from ANSYS and an alternative MOR method is applied, it is essential for the ROM's information to be written in the SID file format. Otherwise, the ROM's data is not importable into SIMPACK.

Finally, the third disadvantage concerns the quality of the ROM generated within the ANSYS code. The measure of validating the dynamic properties of a ROM in ANSYS is based, solely, on a comparison of the eigenfrequency spectrum for both the original

and ROM. Several studies, e.g. by EWINS [43], IMANOVIC [58], GLOTH [50], and KOUTSOVASILIS, QUARZ, and BEITELSCHMIDT [13, 64, 65, 70, 67, 72], have shown that simply an eigenfrequency correlation gives no precise information regarding the ROM's dynamic behavior. In fact, the whole eigenvalue (eigenfrequency and eigenvector) information is required, which combined with the system matrices of both the original and ROM, delivers a plethora of criteria, known as Model Correlation Criteria (MCC). A well established MCC is, for example, the Modal Assurance Criterion (MAC) firstly introduced by ALLEMANG [2].

On the basis of the aforesaid, the kernel of this Thesis is built. The goal is to adjust the properties of alternative MOR methods, presented in the previous Section, to the requirements of structural mechanics and exploit several MOR variations based on each model's configuration. Thus, the dynamic properties of the alternative ROMs have to be validated assuring that the important structure properties are not damaged. It should be accomplished utilizing only the FE discretization in ANSYS. Thereafter, the appropriate toolbox has to be built, which should obtain the FE information and then initialize a MOR interface according to the user's demands. A further interface has to be implemented, which should enable the SID file format generation enabling thus, the data import into SIMPACK. In between, the MCC should be available providing sufficient information for the ROMs prior to their import into SIMPACK. Numerous comparisons among the MOR methods are necessary, under various model considerations (free and fixed structures) in order to derive constructive results for the applied/compared MOR method. These comparisons should take place not only within the independent toolbox, but also within SIMPACK in order to validate the ROM's behavior in a commercial software package. All the above, shortly outlined, in combination with several novel theoretical aspects, necessary to enable the FEM-MBS coupling by the use of alternative MOR methods, constitute the structure of the Thesis, which is given, in details, in the following Section.

1.5 Structure of the thesis

Apart from the Introduction, the present Thesis is comprised of six Chapters, the contents of which are outlined in this Section.

Chapter 2 covers the area of MOR in structural mechanics. After a short introduction on the application of the FEM and the use of the shape functions in continuum mechanics, the second-order ODEs are derived, which describe the equations of motion for mechanical systems. Based on the theory of master and slave DoF for such ODE systems, various MOR schemes are analyzed and divided into three general categories, namely, the physical-, the semi physical-, and the non physical space MOR methods. The issue of the preservation of the second-order structure for the ROMs is thoroughly discussed.

The utilization and application of the MCC for validating the ROMs is the topic of Chapter 3. The ROMs are validated according to various eigenfrequency and eigenvector criteria. Based on certain orthogonality conditions mainly derived from the modal

analysis theory, the importance of each criterion is outlined. Several MOR schemes are applied to four models originating from the field of structural mechanics, namely, the 3D solid bar structure, the elastic piston rod, the elastic crankshaft, and the UIC60 elastic rail. Thus, the efficiency of the applied MOR method is tested based on the MCC, and depending on the model's configuration several conclusions are derived, e.g. the master and slave DoF dependence for free and fixed structures.

The numerical algorithmic approach during the application of a MOR method is outlined in Chapter 4. The high complexity of models in continuum mechanics results in FE structures with a large number of DoF. Although efficient direct methods exist, which handle large sparse systems, the utilization of iterative algorithms is unavoidable, since under normal hardware configuration memory capacity problems occur. A common fact when dealing with large models in structural mechanics are ill-conditioned system matrices (especially the stiffness matrix), which contribute to vast computation times during an iterative solution. For this reason the diagonal perturbation method is proposed. Herewith, a set of model dependent perturbation parameters is given, with which the iterative solution is accelerated and the model's structural properties are kept intact. Furthermore, the diagonal perturbation algorithm finds an interesting use when the BT method is applied to second-order systems. A necessary condition therefor is the stability of the system's matrix polynomial. Under certain model configurations, e.g. non-fixed mechanical structures, this property is damaged and thus, the balancing related schemes are not applicable. Based on the properties of the diagonal perturbation method this problem is overcome.

Chapter 5 consists of two parts. In the first part, the necessary theory for coupling rigid and elastic multi body dynamics is presented. According to the floating frame of reference formulation and the Ritz approximation for deformation, the kinetics of a representative body are outlined. The symmetric system matrices are partitioned into the sub-parts, based on the rigid and elastic contribution for both the translational and rotational coordinates. The system's integrals are given, namely, the generalized mass and forces. Their evaluation is derived under consideration of several approximating assumptions and the final equations of motions for the coupled FEM-MBS formulation are presented in the, so called, descriptor form. The evaluation of the system's integrals is completed by simple vector-matrix multiplications.

The second part of Chapter 5 copes with the transferring procedure of the elastic body data into SIMPACK. It is accomplished by generating the necessary SID file format. Therefore, the structure of the SID file is shortly described and various specifications are outlined, e.g. the FE units, the data scaling based on the elastic model's units, and the categorization of the system matrices. Furthermore, the back-projection approach is proposed. When a non physical space MOR method is used, the DoF set of the reduced vector lies on a non physical space. Thus, the direct generation of the kinematic and kinetic information in MBS codes is not possible, since SIMPACK requires all the system's information to be defined in the Euclidean space. An extra sub-space is required in order to project the ROM back onto the physical configuration space. Thereafter, the SID file for the back-projected ROM should be generated, but a prior verification of the ROM's structure preservation is essential. This method is tested on a

3D solid bar structure and the UIC60 elastic rail.

The Model Order Reduction PACKage (MORPACK) is the topic of Chapter 6. Herein, all the above mentioned theoretical aspects are combined and implemented into the MORPACK toolbox. It concerns a Matlab-based interface adapted both to the modelling requirements and compatibilities of coupling FE models originating from ANSYS into SIMPACK. It consists of two inner interfaces, namely, the MOR and the SID interface. Four application levels operate either as data transfer and conversion tools or as functions, which validate the ROM's dynamics or transform their state-space definition in order to import and export compatible models for the above mentioned inner interfaces. The functionality of the MORPACK toolbox is divided into two categories according to the user's requirements. Two application examples of SIMPACK flexible models generated with MORPACK are given, namely, the 3D solid bar structure and the UIC60 elastic rail, and their validation within SIMPACK is outlined comparing different MOR schemes. Finally, the case of non successful SID generation is discussed and realized by certain model configurations.

Chapter 7 concludes the Thesis, in English and in German, by summarizing the results of Chapters 2 to 6 and suggesting several aspects for future work.

2 Model Order Reduction

2.1 Equations of motion for Finite Element structures

The derivation of the motion equations for flexible structures with the help of the FEM is the topic of this Section. As mentioned in the Introduction, the dynamic state of an elastic body is described by a set of PDEs, the solution of which is approximated according to the Ritz method [128]. Herewith, the discretization of space leads to the formulation of second-order linear time invariant ODEs. It is accomplished by considering both the kinematic and kinetic information for the elastic structure, which is shortly analyzed in the following Subsections 2.1.1 and 2.1.2.

2.1.1 Kinematics of Finite Element structures

In all preceding formulations the motion of an element e within a three dimensional continuum K is considered. Therefore, the notation $\alpha = \{1, 2, 3\}$ will correspond to the three directions of the referred coordinate system.

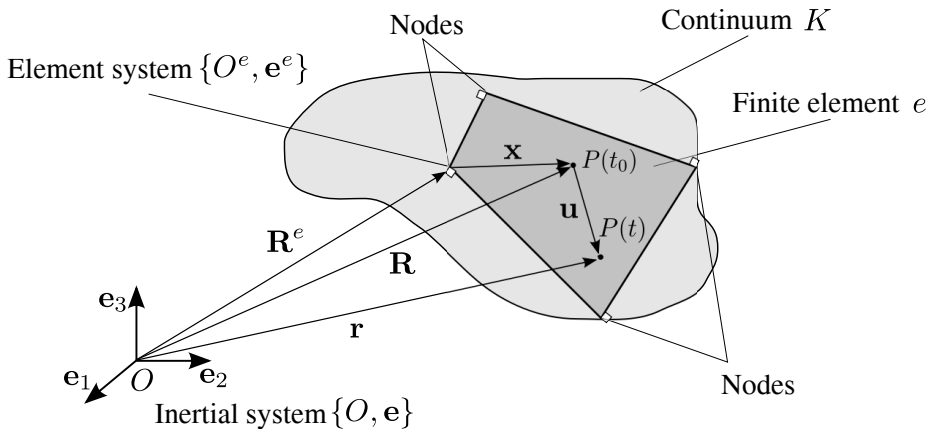


Fig. 2.1: Motion of an element e of a FE structure

On the basis of Fig. 2.1, which is introduced in SCHWERTASSEK and WALLRAPP [110], the definition of several parameters will be given, with which the full kinematic description of a Finite Element (FE) structure is derived.

Thus, according to Fig. 2.1, let $\mathbf{x} = [x_\alpha]$ be the vector of coordinates for a material point P , within a FE e with respect to (w.r.t) the element coordinate system $\{O^e, e^e\}$. Due to deformation, the displacement of the material point P w.r.t $\{O^e, e^e\}$ will be

given by the displacement vector

$${}^e\mathbf{u}(\mathbf{x}, t) = [{}^e u_\alpha(\mathbf{x}, t)], \quad (2.1)$$

and the description of the element coordinate system $\{O^e, \mathbf{e}^e\}$ w.r.t the inertial system $\{O, \mathbf{e}\}$ will be defined based on the vectors of both the position \mathbf{R}^e and rotation \mathbf{e}^e , respectively, i.e.

$$\mathbf{R}^e = [R_\alpha^e] \text{ and } \mathbf{e}^e = \boldsymbol{\Gamma}^e \mathbf{e}. \quad (2.2)$$

The notation $\boldsymbol{\Gamma}^e = [\Gamma_{\alpha\beta}^e]$ corresponds to the rotation matrix with the index β being defined analogously to the index α . Eq. (2.2) gives the necessary information for the description of the displacement vector (Eq. (2.1)) in terms of the inertial coordinate system $\{O, \mathbf{e}\}$, i.e.

$$\mathbf{u}(\mathbf{R}, t) = \boldsymbol{\Gamma}^{eT} {}^e\mathbf{u}(\mathbf{x}, t), \text{ where } \mathbf{x} = \boldsymbol{\Gamma}^e(\mathbf{R} - \mathbf{R}^e) \text{ for } \mathbf{R} \text{ in } e, \quad (2.3)$$

and therefore the motion of the point P (Fig. 2.1) within the element e w.r.t $\{O, \mathbf{e}\}$ is ascertained:

$$\mathbf{r}(\mathbf{R}, t) = \mathbf{R} + \mathbf{u}(\mathbf{R}, t) = \mathbf{R}^e + \boldsymbol{\Gamma}^{eT}(\mathbf{x} + {}^e\mathbf{u}(\mathbf{x}, t)). \quad (2.4)$$

The Ritz method approximates the displacement field (Eq. (2.1)) by introducing certain space-dependent shape functions and time-dependent coordinates. In case of flexible structures being discretized with FE, it is a common procedure to define the set of the time-dependent Ritz coordinates w.r.t the boundary points, also called nodes, for each element e of the FE structure. On that basis, the mathematical formulation for the Ritz approximation of the displacement field w.r.t $\{O^e, \mathbf{e}^e\}$ is derived:

$${}^e\mathbf{u}(\mathbf{x}, t) = \sum_{i=1}^{n_z^e} \mathbf{N}_i^e(\mathbf{x}) z_i^e(t) = \mathbf{N}^e(\mathbf{x}) \mathbf{z}^e(t), \quad i = 1, 2, \dots n_z^e. \quad (2.5)$$

Here, n_z^e denotes the total number of the element's nodal coordinates $z_i^e(t)$, and $\mathbf{N}^e(\mathbf{x}) = [\mathbf{N}_i^e(\mathbf{x})] = [N_{\alpha i}^e(\mathbf{x})]$ constitutes the, so called, interpolation matrix, which provides the displacement shape functions and depends only on the vector's definition for the local coordinates $\mathbf{x} = [x_\alpha]$. The matrix $\mathbf{z}^e(t) = [z_i^e(t)]$ represents the matrix of the element's nodal coordinates.

Eq. (2.5) is practically useless, if FE structures are considered, which consist of n_E elements and n_N nodes. Therefore, the definition of a matrix of FE coordinates w.r.t a global coordinate system is essential. Considering Fig. 2.1, let the global coordinate system be identical to the inertial system $\{O, \mathbf{e}\}$ and thus, the matrix of FE coordinates w.r.t $\{O, \mathbf{e}\}$ will be defined, i.e.

$$\mathbf{z}_F = \left[\dots \begin{bmatrix} \mathbf{u}^{kT} & \boldsymbol{\theta}^{kT} \end{bmatrix} \dots \right]^T, \quad k = 1, 2, \dots n_N. \quad (2.6)$$

The terms $\mathbf{u}^k = [u_\alpha^k]$ and $\boldsymbol{\theta}^k = [\theta_\alpha^k]$ represent the vectors of translational and rotational coordinates, respectively. The relationship between the matrix of the element's nodal coordinates $\mathbf{z}^e(t)$ and the system coordinates $\mathbf{z}_F(t)$ is ascertained by use of an orthogonal

transformation matrix of dimension $n_z^e \times n_F$, i.e.

$$\mathbf{T}^e = [T_{ij}^e], \quad i = 1, 2, \dots, n_z^e, \quad j = 1, 2, \dots, n_F \quad (2.7)$$

and thus, the following equation holds:

$$\mathbf{z}^e(t) = \mathbf{T}^e \mathbf{z}_F(t), \quad e = 1, 2, \dots, n_E. \quad (2.8)$$

The combination of Eq. (2.5) and (2.8) results in a formulation, which depends on the definition of $\mathbf{z}_F(t)$, but still describes the displacement field of the points of the element e w.r.t. $\{O^e, \mathbf{e}^e\}$, i.e.

$${}^e\mathbf{u}(\mathbf{x}, t) = \mathbf{N}^e(\mathbf{x}) \mathbf{z}^e(t) = \mathbf{N}^e(\mathbf{x}) \mathbf{T}^e \mathbf{z}_F(t). \quad (2.9)$$

In order to be able to express the displacement field (Eq. (2.9)) w.r.t $\{O, \mathbf{e}\}$, an extra transformation is required. This information is provided by the Eq. (2.3) and thus, the displacement vector $\mathbf{u}(\mathbf{R}, t)$ for the points of the representative element e w.r.t $\{O, \mathbf{e}\}$ is obtained:

$$\mathbf{u}(\mathbf{R}, t) = \boldsymbol{\Gamma}^{eT} {}^e\mathbf{u}(\mathbf{x}, t) = \boldsymbol{\Gamma}^{eT} \mathbf{N}^e(\mathbf{x}) \mathbf{T}^e \mathbf{z}_F(t). \quad (2.10)$$

Eq. (2.10) is valid only for the representative element e and therefore, a generalization is compulsory such that the description holds for every element of a FE discretized structure. This is feasible, if the following conditions are fulfilled [110]:

$$\mathbf{N}^e(\mathbf{x}) \equiv \mathbf{0} \quad \forall \mathbf{x} = \boldsymbol{\Gamma}^e(\mathbf{R} - \mathbf{R}^e) \text{ and } \mathbf{R} \text{ not in the element } e. \quad (2.11)$$

Herewith, the global Ritz-approximation for the displacement field of a FE structure is defined, i.e.

$$\mathbf{u}(\mathbf{R}, t) = \boldsymbol{\Phi}(\mathbf{R}) \mathbf{z}_F(t) = \left(\sum_{e=1}^{n_E} \boldsymbol{\Gamma}^{eT} \mathbf{N}^e(\mathbf{x}) \mathbf{T}^e \right) \mathbf{z}_F(t), \quad \text{with } \mathbf{x} = \boldsymbol{\Gamma}^e(\mathbf{R} - \mathbf{R}^e). \quad (2.12)$$

Eq. (2.12) in combination with the Eq. (2.4) completes the kinematic description of a, geometrically non-constrained, FE structure.

2.1.2 Kinetics of Finite Element structures

The derivation of the kinetic formulation for FE structures is based both on the above outlined global Ritz-approximation for the structure's displacement field and the principle of D' ALEMBERT in the Lagrangian formulation [23, 110].

Let the inertial system be identical to the coordinate system $\{O, \mathbf{e}\}$ (as depicted in Fig. 2.1). Thus, for the virtual displacement and velocity of the point P in the continuum K holds:

$$\delta \mathbf{r} = \delta \mathbf{u} \text{ and } \delta \dot{\mathbf{r}} = \delta \dot{\mathbf{u}}. \quad (2.13)$$

According to the principle of D' ALEMBERT, the sum of the virtual work of all forces acting on a body must be zero. Hence, the sum of the virtual work of the inertial forces, the internal forces and the applied external body force over an infinitesimal

volume V_0 , and the applied surface force over an infinitesimal area A_0 of V_0 equals zero, i.e.

$$-\int_{V_0} \delta \mathbf{u}^T \rho_0 \ddot{\mathbf{u}} dV_0 - \int_{V_0} \delta \boldsymbol{\epsilon}^T \mathbf{H} \boldsymbol{\epsilon} dV_0 + \int_{V_0} \delta \mathbf{u}^T \mathbf{b}_0 dV_0 + \int_{A_0} \delta \mathbf{u}^T \mathbf{p}_0 dA_0 = \mathbf{0}. \quad (2.14)$$

In Eq. (2.14) let ρ_0 represent the material density, \mathbf{b}_0 the vector of the applied external body force over V_0 , \mathbf{p}_0 the vector of the applied external surface force over A_0 and $\boldsymbol{\epsilon}$ the strain tensor. The term \mathbf{H} is the, so called, material matrix defined for homogeneous, elastic and isotropic materials, with which the material law is described. Thus, for each element and without pre-load stresses or thermal strains [110], it holds:

$$\boldsymbol{\sigma}^e(\mathbf{x}, \mathbf{z}_F) = \mathbf{H}^e \boldsymbol{\epsilon}^e(\mathbf{x}, \mathbf{z}_F). \quad (2.15)$$

A simplification of Eq. (2.14) is obtained by utilizing the Ritz-approximated displacement field, given in Eq. (2.12). Additionally, the conditions in Eq. (2.11) as well as the orthogonality properties of the rotation matrix, defined in Eq. (2.2), are taken into consideration, i.e.

$$\boldsymbol{\Gamma}^e \boldsymbol{\Gamma}^{eT} = \mathbf{I}, \quad (2.16)$$

with \mathbf{I} being the unit matrix. Also, the time dependence of \mathbf{z}_F will be omitted, i.e. $\mathbf{z}_F := \mathbf{z}_F(t)$. On that basis, each summand of Eq. (2.14) will be analyzed separately.

The substitution of Eq. (2.12) into the first summand of Eq. (2.14) leads to the following series of equations:

$$\int_{V_0} \delta \mathbf{u}^T \rho_0 \ddot{\mathbf{u}} dV_0 = \delta \mathbf{z}_F^T \sum_{e=1}^{n_E} \left(\mathbf{T}^{eT} \int_{V_0^e} \mathbf{N}^{eT}(\mathbf{x}) \rho_0^e(\mathbf{x}) \mathbf{N}^e(\mathbf{x}) dV \mathbf{T}^e \right) \ddot{\mathbf{z}}_F \quad (2.17)$$

$$= \delta \mathbf{z}_F^T \sum_{e=1}^{n_E} \mathbf{T}^{eT} \mathbf{M}^e \mathbf{T}^e \ddot{\mathbf{z}}_F \quad (2.18)$$

$$= \delta \mathbf{z}_F^T \mathbf{M}_F \ddot{\mathbf{z}}_F. \quad (2.19)$$

Here, the term $\mathbf{M}^e = \int_{V_0^e} \mathbf{N}^{eT}(\mathbf{x}) \rho^e(\mathbf{x}) \mathbf{N}^e(\mathbf{x}) dV$ is defined as the mass matrix for each element e of the FE structure. Hence, $\mathbf{M}_F = \sum_{e=1}^{n_E} \mathbf{T}^{eT} \mathbf{M}^e \mathbf{T}^e$ constitutes the mass matrix of the whole FE structure.

The second summand of Eq. (2.14) possesses no direct connection to the element's displacement vector and therefore, Eq. (2.12) cannot be directly applied. A relationship between the strain tensor $\boldsymbol{\epsilon}$ and $\mathbf{u}(\mathbf{R}, t)$ is required. This information is provided by the strain-displacement relationship [110, 128, 112, 95], which is introduced below for each element e , i.e.

$$\boldsymbol{\epsilon}^e(\mathbf{x}, \mathbf{z}_F) = \mathbf{L}(\mathbf{u}) {}^e \mathbf{u}(\mathbf{x}, t) \stackrel{(2.5)}{=} \mathbf{L}(\mathbf{u}) \mathbf{N}^e(\mathbf{x}) \mathbf{z}^e(t) \stackrel{(2.8)}{=} \mathbf{L}(\mathbf{u}) \mathbf{N}^e(\mathbf{x}) \mathbf{T}^e \mathbf{z}_F = \mathbf{B}^e(\mathbf{x}) \mathbf{T}^e \mathbf{z}_F. \quad (2.20)$$

Without loss of generality, let Eq. (2.20) describe the linear version of the strain-displacement relationship. Under this assumption, the notation $\mathbf{L}(\mathbf{u})$ corresponds to the linear operator matrix, which is defined according to SCHWERTASSEK and WALLRAPP

[110], as follows:

$$\mathbf{L} = \begin{pmatrix} \vartheta_1 & 0 & 0 \\ 0 & \vartheta_2 & 0 \\ 0 & 0 & \vartheta_3 \\ \vartheta_2 & \vartheta_1 & 0 \\ 0 & \vartheta_3 & \vartheta_2 \\ \vartheta_3 & 0 & \vartheta_1 \end{pmatrix}, \text{ where } \vartheta_\alpha = \frac{\vartheta}{\vartheta R_\alpha}. \quad (2.21)$$

The substitution of Eq. (2.12) and Eq. (2.20) in the second summand of Eq. (2.14) leads to the following:

$$\int_{V_0} \delta \boldsymbol{\epsilon}^T \mathbf{H} \boldsymbol{\epsilon} dV_0 = \delta \mathbf{z}_F^T \sum_{e=1}^{n_E} \left(\mathbf{T}^{eT} \int_{V_0^e} \mathbf{B}^{eT}(\mathbf{x}) \mathbf{H}^e \mathbf{B}^e(\mathbf{x}) dV \mathbf{T}^e \right) \mathbf{z}_F \quad (2.22)$$

$$= \delta \mathbf{z}_F^T \sum_{e=1}^{n_E} \mathbf{T}^{eT} \mathbf{K}^e \mathbf{T}^e \mathbf{z}_F \quad (2.23)$$

$$= \delta \mathbf{z}_F^T \mathbf{K}_F \mathbf{z}_F. \quad (2.24)$$

Analogously to the previous definitions, the term $\mathbf{K}^e = \int_{V_0^e} \mathbf{B}^{eT}(\mathbf{x}) \mathbf{H}^e \mathbf{B}^e(\mathbf{x}) dV$ represents the linear stiffness matrix for each element e of the FE structure and $\mathbf{K}_F = \sum_{e=1}^{n_E} \mathbf{T}^{eT} \mathbf{K}^e \mathbf{T}^e$ the linear stiffness matrix of the whole FE structure.

In case of introducing pre-load stresses or non-linearities in Eq. (2.14), the relationships defined in Eq. (2.15) and (2.20) would include a pre-load stress term and a non-linear operator, respectively. This would result in the definition of certain additional summands in Eq. (2.22) for the derivation of the FE structure's stiffness properties [110].

For the third summand of Eq. (2.14), the definition of the body force for each element of the FE structure is used, i.e. $\mathbf{b}_0^e = \rho_0^e \mathbf{g}$, with ρ_0^e being the element's material density and \mathbf{g} the acceleration of gravity w.r.t $\{O, \mathbf{e}\}$. Herewith, the following relationship is obtained:

$$\int_{A_0} \delta \mathbf{u}^T \mathbf{b}_0 dA_0 = \delta \mathbf{z}_F^T \sum_{e=1}^{n_E} \left(\mathbf{T}^{eT} \int_{V_0^e} \mathbf{N}^{eT}(\mathbf{x}) \rho_0^e(\mathbf{x}) dV \mathbf{\Gamma}^e \right) \mathbf{g} \quad (2.25)$$

$$= \delta \mathbf{z}_F^T \sum_{e=1}^{n_E} \mathbf{T}^{eT} \mathbf{f}_g^e = \delta \mathbf{z}_F^T \mathbf{F}_g, \quad (2.26)$$

where $\mathbf{f}_g^e = \int_{V_0^e} \mathbf{N}^{eT}(\mathbf{x}) \rho_0^e(\mathbf{x}) dV \mathbf{\Gamma}^e \mathbf{g}$ is the element's vector of body force and $\mathbf{F}_g = \sum_{e=1}^{n_E} \mathbf{T}^{eT} \mathbf{f}_g^e$ the vector of body force for the FE structure.

Finally, for the last summand of Eq. (2.14) the utilization of Eq. (2.12) gives

$$\int_{V_0} \delta \mathbf{u}^T \mathbf{p}_0 dV_0 = \delta \mathbf{z}_F^T \sum_{e=1}^{n_E} \mathbf{T}^{eT} \int_{A_0^e} \mathbf{N}^{eT}(\mathbf{x}) {}^e \mathbf{p}_0^e(\mathbf{x}) dA \mathbf{\Gamma}^e \quad (2.27)$$

$$= \delta \mathbf{z}_F^T \sum_{e=1}^{n_E} \mathbf{T}^{eT} \mathbf{f}_p^e = \delta \mathbf{z}_F^T \mathbf{F}_p. \quad (2.28)$$

Herein, $\mathbf{f}_p^e = \int_{A_0^e} \mathbf{N}^{eT}(\mathbf{x}) {}^e\mathbf{p}_0^e(\mathbf{x}) dA \Gamma^e$ represents the external applied surface force for each element e and $\mathbf{F}_p = \sum_{e=1}^{n_E} \mathbf{T}^{eT} \mathbf{f}_p^e$ the external surface force applied on the FE structure.

Gathering Eq. (2.19), (2.24), (2.26), and (2.28) and substituting them in Eq. (2.14) leads to

$$\delta \mathbf{z}_F^T (\mathbf{M}_F \ddot{\mathbf{z}}_F + \mathbf{K}_F \mathbf{z}_F - \mathbf{F}_g - \mathbf{F}_p) = 0 \quad (2.29)$$

and thus, the general second-order LTI equation of motion for undamped FE structures is derived. It is written in compact matrix form, as shown below:

$$\mathbf{M}_F \ddot{\mathbf{z}}_F + \mathbf{K}_F \mathbf{z}_F = \mathbf{F}_g + \mathbf{F}_p = \mathbf{F}. \quad (2.30)$$

If damping effects are to be considered, the definition of the associated parameter is essential. The simplest, and most commonly used, damping model assumes the damping to be linearly proportional to the structure's velocity. This leads to the following equation for linearly damped FE structures

$$\mathbf{M}_F \ddot{\mathbf{z}}_F + \mathbf{D}_F \dot{\mathbf{z}}_F + \mathbf{K}_F \mathbf{z}_F = \mathbf{F}, \quad (2.31)$$

with \mathbf{D}_F being the structural damping matrix. It can be obtained based on the structural damping \mathbf{D}^e for each element of the FE structure via the relationship $\mathbf{D}_F = \sum_{e=1}^{n_E} \mathbf{T}^{eT} \mathbf{D}^e \mathbf{T}^e$.

2.1.3 Dimension of Finite Element discretized structures

The dimension of the system matrices and vectors in Eq. (2.31) is calculated based on the number of both the elements n_E and the nodes n_N utilized to discretize the FE structure (Eq. (2.14)). For models discretized with n_E different elements, i.e. $n_E = \{E_1, E_2, \dots, E_n\}$ with $E_i \neq E_j$ for every $i \neq j$ and $i = 1, 2, \dots, n$, the dimension number is defined as follows

$$n_{dim} = \sum_{i=1}^{n_E} n_N^{E_i} = \sum_{i=1}^{n_E} \left(\alpha^{E_i} n_{F_u}^{E_i} + \beta^{E_i} n_{F_\theta}^{E_i} \right) \quad (2.32)$$

and it consists of two summands, namely, the dimension number provided by the translational $n_{F_u}^{E_i}$ and rotational $n_{F_\theta}^{E_i}$ coordinates (Eq. (2.6)) for each element E_i , respectively. Both dimension numbers of coordinates are accompanied by two sets α^{E_i} and β^{E_i} , which are also defined in an element manner and give the DoF range of each node, respectively, i.e. $\alpha^{E_i} = \{1, 2, 3\}$ representing the translational DoF $\{\mathbf{u}_1, \mathbf{u}_2, \mathbf{u}_3\}$ and $\beta^{E_i} = \{1, 2, 3\}$ representing the rotational DoF $\{\boldsymbol{\theta}_1, \boldsymbol{\theta}_2, \boldsymbol{\theta}_3\}$ in the three dimensional space. The value of these sets varies according to the type of E_i and the dimension of the configuration space (1D, 2D, 3D).

On the basis of the aforesaid, the dimension of the system matrices and vectors of Eq. (2.31) is written in a compact form:

$$[] \in \mathbb{R}^{n_{dim} \times n_{dim}}, [] := \{\mathbf{M}_F, \mathbf{D}_F, \mathbf{K}_F\} \quad (2.33)$$

$$[] \in \mathbb{R}^{n_{dim} \times 1}, [] := \{\mathbf{z}_F, \mathbf{F}\}. \quad (2.34)$$

Eq. (2.33)-(2.34) give the dimension of non-constrained FE structures. In case of having parts of the system's DoF grounded, the resulting dimension of the fixed system matrices and vectors is given below:

$$[]_{\text{fixed}} \in \mathbb{R}^{(n_{\text{dim}} - n_{\text{dim}}^{\text{fix}}) \times (n_{\text{dim}} - n_{\text{dim}}^{\text{fix}})}, [] := \{\mathbf{M}_F, \mathbf{D}_F, \mathbf{K}_F\} \quad (2.35)$$

$$[]_{\text{fixed}} \in \mathbb{R}^{(n_{\text{dim}} - n_{\text{dim}}^{\text{fix}}) \times 1}, [] := \{\mathbf{z}_F, \mathbf{F}\}, \quad (2.36)$$

where in this case the number of the fixed DoF, given by $n_{\text{dim}}^{\text{fix}}$ and defined analogously to n_{dim} (Eq. (2.32)), is removed from the total set of the non-fixed structure's DoF.

In continuum mechanics the dimension of either the fixed or non-fixed system matrices and vectors is large. The more complex the parts of the mechanical MBS system are, the larger the dimension is. This fact, in combination with the required accuracy levels, which are usually high, results in dimension numbers of the order $n_{\text{dim}} \geq 5 \cdot 10^5$. Thus, several simulation and control procedures, as already outlined in the Introduction, are either impossible to conduct or suffer from storage capacity and vast computational time problems.

MOR overcomes the mentioned problems by reducing the order of the system matrices. Especially in the field of structural mechanics, several traditional MOR schemes are based on the theory of master and slave DoF. This topic is handled in the next Section.

In the following, the subscript notation F used for denoting the system matrices and vectors of a FE structure will be omitted, e.g. the LTI second-order ODE from Eq. (2.31) will be written as given below:

$$\mathbf{M}\ddot{\mathbf{z}} + \mathbf{D}\dot{\mathbf{z}} + \mathbf{K}\mathbf{z} = \mathbf{F}. \quad (2.37)$$

Furthermore, the dimension number n_{dim} (Eq. (2.32)), which defines the dimension of the system matrices and vectors in Eq. (2.37), will be denoted as n .

2.2 Master and slave degrees of freedom

The general concept of MOR in structural mechanics is to find a low dimension subspace $\mathbf{T} \in \mathbb{R}^{n \times m}$, $m \ll n$ in order to approximate the state vector \mathbf{z} of Eq. (2.37), i.e.

$$\mathbf{z} \approx \mathbf{T}\mathbf{z}_R. \quad (2.38)$$

By substituting Eq. (2.38) in Eq. (2.37) and then projecting Eq. (2.37) on the subspace \mathbf{T} , a lower dimension LTI second-order ODE is obtained

$$\mathbf{M}_R\ddot{\mathbf{z}}_R + \mathbf{D}_R\dot{\mathbf{z}}_R + \mathbf{K}_R\mathbf{z}_R = \mathbf{F}_R, \quad (2.39)$$

with $\mathbf{M}_R = \mathbf{T}^T \mathbf{M} \mathbf{T}$, $\mathbf{D}_R = \mathbf{T}^T \mathbf{D} \mathbf{T}$, $\mathbf{K}_R = \mathbf{T}^T \mathbf{K} \mathbf{T}$ being the reduced system matrices and $\mathbf{F}_R = \mathbf{T}^T \mathbf{F}$ the reduced load vector of dimensions $\mathbb{R}^{m \times m}$ and $\mathbb{R}^{m \times 1}$, respectively.

Alternatively, the ROM's mass and stiffness matrices can be derived in an energetic

manner, namely, by computing the kinetic E_k and potential (elastic) E_p energy of the original model, i.e.

$$E_k = \frac{1}{2} \dot{\mathbf{z}}^T \mathbf{M} \dot{\mathbf{z}} \stackrel{(2.38)}{\approx} \frac{1}{2} (\mathbf{T} \dot{\mathbf{z}}_R)^T \mathbf{M} (\mathbf{T} \dot{\mathbf{z}}_R) = \frac{1}{2} \dot{\mathbf{z}}_R^T (\mathbf{T}^T \mathbf{M} \mathbf{T}) \dot{\mathbf{z}}_R = \frac{1}{2} \dot{\mathbf{z}}_R^T \mathbf{M}_R \dot{\mathbf{z}}_R = E_{k,R} \quad (2.40)$$

$$E_p = \frac{1}{2} \mathbf{z}^T \mathbf{K} \mathbf{z} \stackrel{(2.38)}{\approx} \frac{1}{2} (\mathbf{T} \mathbf{z}_R)^T \mathbf{K} (\mathbf{T} \mathbf{z}_R) = \frac{1}{2} \mathbf{z}_R^T (\mathbf{T}^T \mathbf{K} \mathbf{T}) \mathbf{z}_R = \frac{1}{2} \mathbf{z}_R^T \mathbf{K}_R \mathbf{z}_R = E_{p,R}. \quad (2.41)$$

The reduced damping matrix can only be calculated by direct projection. It is accomplished based on the model's type used for its definition, e.g. Rayleigh damping. This matter is handled in Section 3.1.3.

In any case, the allocation of the original structure's DoF, which should constitute the DoF set of the ROM (Eq. (2.39)), is of great importance. Therefore, the theory of master (m) or external and slave (s) or internal DoF is applied, which defines as master those DoF that form the DoF set of the ROM (hence the utilization of the same notation m for both the dimension of the ROM and the master set) and consequently, as slave the DoF set, which is eliminated from the Eq. (2.37) after the MOR procedure.

According to this theory, the system matrices and vectors of Eq. (2.37) have to be partitioned into sub-blocks forming thus, a transformed (with different DoF-sorting) second-order system of equations, i.e.

$$\tilde{\mathbf{M}} \ddot{\mathbf{z}} + \tilde{\mathbf{D}} \dot{\tilde{\mathbf{z}}} + \tilde{\mathbf{K}} \tilde{\mathbf{z}} = \tilde{\mathbf{F}}. \quad (2.42)$$

This partitioning procedure takes place prior to the application of the MOR method and the sorted system matrices, and vectors of Eq. (2.42) are defined, as given below:

$$\widetilde{[]} := \begin{pmatrix} []_{mm} & []_{ms} \\ []_{sm} & []_{ss} \end{pmatrix}, \quad [] = \{ \mathbf{M}, \mathbf{D}, \mathbf{K} \}, \quad \widetilde{\mathbf{z}} := \begin{pmatrix} \mathbf{z}_m \\ \mathbf{z}_s \end{pmatrix}, \quad \widetilde{\mathbf{F}} := \begin{pmatrix} \mathbf{F}_m \\ \mathbf{F}_s \end{pmatrix}. \quad (2.43)$$

The structure of the original and sorted system matrices, as defined in Eq. (2.43), is visualized in Fig. 2.2, Fig. 2.3 and Fig. 2.4. Herein, the mass matrices of three different models are depicted, namely, the 3D solid bar (Fig. 2.2), the elastic UIC60 rail (Fig. 2.3), and the elastic rod (Fig. 2.4).

It is observed that for small dimension models the sub-blocks (mm , ms , sm , ss) are distinguishable, e.g. the mm sub-block in Fig. 2.2 with $m/n = 60\%$. The larger the dimension of the model is, the more difficult it is to clearly distinguish the aforementioned sub-blocks, since $m \ll n$ ($m/n \approx 1\%$ in Fig. 2.3 and $m/n \approx 0.04\%$ in Fig. 2.4). The observation of the rest of the system matrices would have exactly the same structure result. The sole difference would be the notably larger number of non zero entries.

The sorted equation system (Eq. (2.42)) is valid, if and only if the following conditions are fulfilled

$$m \cup s = n \quad \text{and} \quad m \cap s = \emptyset, \quad \text{where } n : \text{total DoF}. \quad (2.44)$$

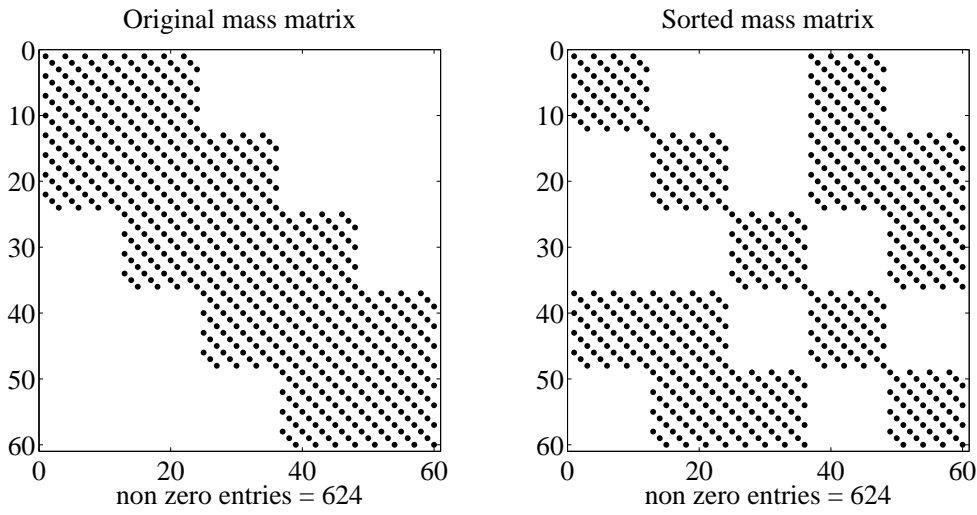


Fig. 2.2: Mass matrix of a 3D solid bar before and after the m & s sorting

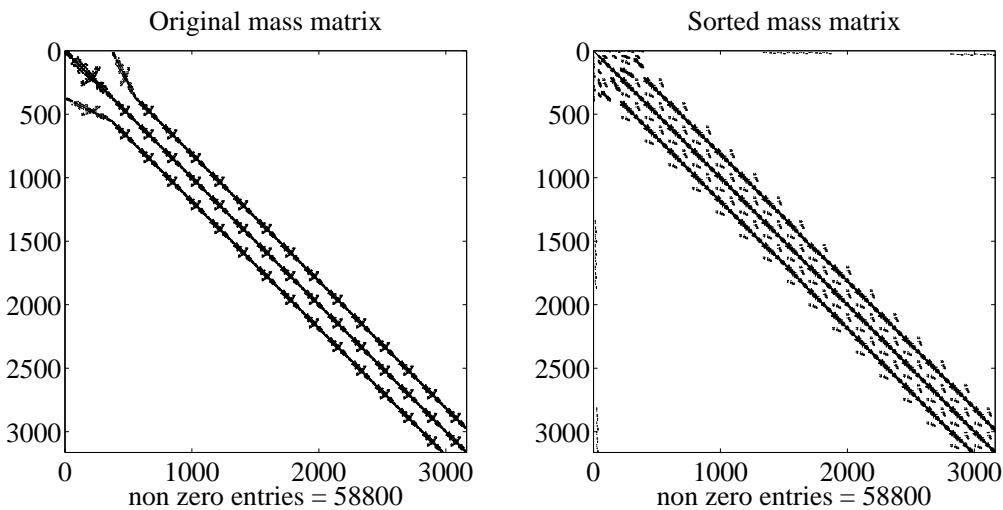


Fig. 2.3: Mass matrix of an elastic UIC60 rail before and after the m & s sorting

Eq. (2.44) states, firstly that the sum of both the master and slave DoF should equal the total DoF of the FE structure, and secondly that it is not allowed for a DoF to coexist in the master and slave set. These conditions can be easily verified by confirming the consistency of the dimension and the non zero entries (Fig. 2.2 - 2.4) for both the original and the sorted versions of the system matrices.

The decision of which DoF should be appointed to the m or s set, under the assumption the necessary conditions (Eq. (2.44)) to be fulfilled, is not a trivial task. It is model dependent and requires advanced engineering experience. As it will be shown in the forthcoming Chapter 3, the definition of the m set is crucial for the quality of the ROM by certain MOR methods. Therefore, specific criteria exist [127], which indicate how

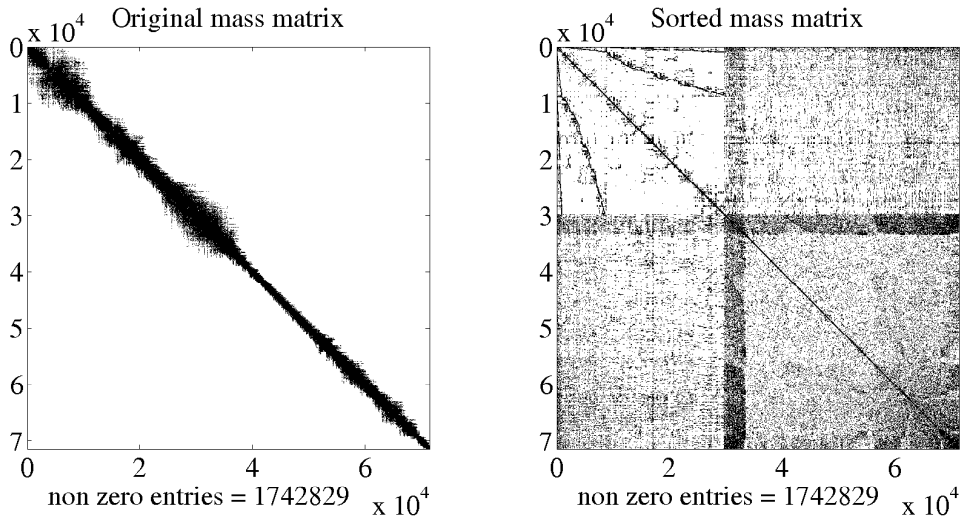


Fig. 2.4: Mass matrix of an elastic rod before and after the m & s sorting

the m set should be acquired. Thus, it is advised to select master DoF at positions:

- where large deformation is expected,
- such that all possible deformations can be visualized,
- which are equally distributed in the structure,
- which possess the characteristic of having large concentrated mass and at the same time small local stiffness.

The last criterion is the standard criterion integrated in commercial FE software packages, e.g. ANSYS, whenever the automatic selection of the m set is activated. Its pseudo-algorithmic formulation is given below:

$$\text{while } i \leq n \text{ formulate } b_i = \frac{\mathbf{K}(i,i)}{\mathbf{M}(i,i)} \text{ and sequentially choose } \min(b_j)_{1 \leq j \leq m}. \quad (2.45)$$

Nonetheless, in case of the FEM-MBS coupling process, e.g. coupling mechanical models from ANSYS into SIMPACK, certain of the model's DoF must be *de facto* appointed to the m set in order for the coupling procedure to be feasible. Thus, in addition to the previously mentioned criteria, master DoF must be chosen at positions:

- such as the origin of coordinates [114],
- where forces and boundary constraints are to be defined in the MBS codes,
- where displacements are to be calculated or joint types (for connecting the elastic body with other rigid bodies) are to be defined in the MBS codes, respectively.

The definition of the master and slave DoF sets initiates the application of the chosen MOR procedure, the analysis of which is covered in the next Section.

2.3 Categorization of model order reduction methods

The general MOR scheme proceeds in finding an appropriate subspace $\mathbf{T} \in \mathbb{R}^{n \times m}$, $m << n$ (Eq. (2.38)), also referred to as coordinate transformation matrix, with which the ROM is obtained. Based on the theory applied to obtain this subspace, the MOR methods are divided into three categories widely used by several authors [17, 4, 10, 107]:

1. Modal truncation, sub-structuring, and static condensation,
2. Padé and Padé-type approximations, and
3. balancing-related truncation techniques.

In this Thesis a different categorization is developed, which stems from the requirement of importing alternative MOR methods into MBS codes. Thus, according to the definition of the coordinate transformation matrix and therefore the definition of the reduced state vector \mathbf{z}_R (Eq. (2.39)), the MOR techniques are divided into the following three categories:

1. *Physical subspace reduction-expansion methods.* This is the case where the whole DoF set of the reduced model, e.g. by the static condensation, lies on the physical configuration space, i.e.

$$\mathbf{z}_R \in \mathbb{R}^n, \quad 1 \leq n \leq 3. \quad (2.46)$$

MOR methods belonging to this category are the:

- (a) static (Guyan) condensation and variants [55, 60],
- (b) dynamic condensation and variants [79, 50, 96],
- (c) Improved Reduction System method (IRS) and variants [25, 46],
- (d) System Equivalent Reduction Expansion Process (SEREP) [26],
- (e) SEREP-IRS and SEREP-Guyan two-step MOR [71].

2. *Semi physical subspace reduction-expansion methods.* In this category one part of the reduced state vector lies on the physical configuration space and the other part is defined on a non-physical space, i.e.

$$\mathbf{z}_R = [\mathbf{z}_1 \quad \mathbf{z}_2]^T \in \{\mathbb{R}^n \cup \mathbb{X}^n : \mathbb{R}^n \cap \mathbb{X}^n = 0, \quad 1 \leq n \leq 3\}. \quad (2.47)$$

MOR methods belonging to this category are the:

- (a) Component Mode Synthesis (CMS) [32, 33, 34],
- (b) CMS spanned by Krylov vectors (KCMS) [27],
- (c) Improved CMS (ICMS) [69],
- (d) Improved KCMS (IKCMS) [69],
- (e) SEREP-CMS, SEREP-KCMS, SEREP-ICMS and SEREP-IKCMS two-step MOR [71].

Here, one part of the reduced vector consists of the model's physical space DoF and the rest are either the modal coordinates obtained by the CB set or the Krylov

coordinates defined by the eigenvectors, which span a certain Krylov subspace.

3. *Non physical subspace reduction-expansion methods.* Here, the DoF set of the ROM resides on a subspace \aleph^n , which is spanned by non-physical eigenvectors, e.g. let \mathbb{K}^n be a subspace spanned by Krylov vectors, then

$$\mathbf{z}_R \in \aleph^n = \mathbb{K}^n := \{\mathbf{z}_R \in \mathbb{K}^n : \mathbb{R}^n \cap \mathbb{K}^n = 0, 1 \leq n \leq 3\}. \quad (2.48)$$

MOR methods belonging to this category are the:

- (a) second order Krylov Subspace Method (KSM) [107, 17, 4],
- (b) second order balancing-related techniques, e.g. Balanced Truncation (BT) [118, 98, 28],
- (c) Second Order Modal Truncation (SOMT),
- (d) KSM-BT, SEREP-KSM, SEREP-BT, SOMT-KSM, and SOMT-BT two-step MOR [78, 71].

For the above outlined categories, the annotation $\{\mathbb{R}^n, 1 \leq n \leq 3\}$ refers to the three physical space dimensions (1D, 2D and 3D). The maximum number of the state vector's DoF per node (n_N^{DoF}) varies according to the definition of the configuration space $\{\mathbb{R}^n, 1 \leq n \leq 3\}$, on which it resides, i.e.

$$n_N^{\text{DoF}} = \begin{cases} 1, & \mathbb{R} : 1\text{D Space} \\ 3, & \mathbb{R}^2 : 2\text{D Space} \\ 6, & \mathbb{R}^3 : 3\text{D Space} \end{cases} \quad (2.49)$$

The methodology of the MOR schemes originating from the first two categories is affiliated to the theory presented in the previous Section 2.2, namely, the master and slave DoF partitioning. Furthermore, the derivation of the coordinate transformation matrix (Eq. (2.38)) is ascertained for the undamped version of Eq. (2.42), i.e.

$$\tilde{\mathbf{M}}\ddot{\mathbf{z}} + \tilde{\mathbf{K}}\tilde{\mathbf{z}} = \tilde{\mathbf{F}}. \quad (2.50)$$

Finally, the two-step MOR approaches, which appear in all of the three above outlined MOR categories, will be treated separately in Section 2.7, since their algorithmic scheme is identical and independent of the category they belong to.

2.4 Physical space reduction-expansion methods

2.4.1 Static condensation and variants

The static condensation constitutes a standard MOR method integrated into several FEM software packages. Its algorithmic approach is based on two major approximations. They are applied to the undamped second-order ODE (Eq. (2.50)), the analytical expression

of which is given below:

$$\begin{pmatrix} \mathbf{M}_{mm} & \mathbf{M}_{ms} \\ \mathbf{M}_{sm} & \mathbf{M}_{ss} \end{pmatrix} \begin{pmatrix} \ddot{\mathbf{z}}_m \\ \ddot{\mathbf{z}}_s \end{pmatrix} + \begin{pmatrix} \mathbf{K}_{mm} & \mathbf{K}_{ms} \\ \mathbf{K}_{sm} & \mathbf{K}_{ss} \end{pmatrix} \begin{pmatrix} \mathbf{z}_m \\ \mathbf{z}_s \end{pmatrix} = \begin{pmatrix} \mathbf{F}_m \\ \mathbf{F}_s \end{pmatrix}. \quad (2.51)$$

Firstly, it is assumed that there is no force applied to the internal DoF, i.e. $\mathbf{F}_s = \mathbf{0}$, and secondly, the structure's equivalent inertia terms are omitted (hence the static nature). According to Eq. (2.51), the second approximation is mathematically expressed as follows:

$$\mathbf{M}_{mm}\ddot{\mathbf{z}}_m + \mathbf{M}_{ms}\ddot{\mathbf{z}}_s = \mathbf{0} \quad \text{and} \quad \mathbf{M}_{sm}\ddot{\mathbf{z}}_m + \mathbf{M}_{ss}\ddot{\mathbf{z}}_s = \mathbf{0}. \quad (2.52)$$

By expanding the second part of Eq. (2.51) and utilizing the information provided by Eq. (2.52), an expression is derived, which relates the slave DoF state vector \mathbf{z}_s to the master DoF state vector \mathbf{z}_m :

$$(2.51) \Rightarrow \mathbf{z}_s = -\mathbf{K}_{ss}^{-1}(\mathbf{M}_{sm}\ddot{\mathbf{z}}_m + \mathbf{M}_{ss}\ddot{\mathbf{z}}_s + \mathbf{K}_{sm}\mathbf{z}_m) \quad (2.53)$$

$$\stackrel{(2.52)}{=} (-\mathbf{K}_{ss}^{-1}\mathbf{K}_{sm})\mathbf{z}_m. \quad (2.54)$$

As stated in Eq. (2.38), the purpose is to express the state vector of the full model (Eq. (2.50)) in terms of the state vector of the potential ROM. In this case, it is accomplished based on the information provided in Eq. (2.54), i.e.

$$\mathbf{z} = \begin{pmatrix} \mathbf{z}_m \\ \mathbf{z}_s \end{pmatrix} \stackrel{(2.54)}{=} \begin{pmatrix} \mathbf{z}_m \\ (-\mathbf{K}_{ss}^{-1}\mathbf{K}_{sm})\mathbf{z}_m \end{pmatrix} = \begin{pmatrix} \mathbf{I}_m \\ -\mathbf{K}_{ss}^{-1}\mathbf{K}_{sm} \end{pmatrix} \cdot \mathbf{z}_m = \mathbf{T}_{\text{static}} \cdot \mathbf{z}_m \quad (2.55)$$

where $\mathbf{I}_m \in \mathbb{R}^{m \times m}$ is the unit matrix. The structure of the $\mathbf{T}_{\text{static}}$ matrix, with its $m \times m$ sub-block being given by the unit matrix, can be elegantly observed when small dimension models are examined (Fig. 2.5). The system matrices and the vector of

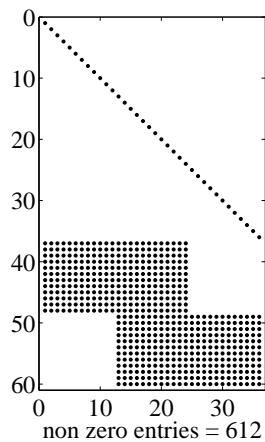


Fig. 2.5: $\mathbf{T}_{\text{static}}$ by MOR of a 3D solid bar - $m = 36$

applied forces for the static-ROM are obtained according to Eq. (2.39), i.e.

$$[\cdot]_{\text{static}} = \mathbf{T}_{\text{static}}^T \cdot [\tilde{\cdot}] \cdot \mathbf{T}_{\text{static}}, \quad [\cdot] := \{\mathbf{M}, \mathbf{D}, \mathbf{K}\} \quad \text{and} \quad \mathbf{F}_{\text{static}} = \mathbf{T}_{\text{static}}^T \tilde{\mathbf{F}}. \quad (2.56)$$

The static reduction is a good approximation (exact for static analyses) for the low eigenvalue (eigenfrequency and eigenvector) spectrum of a FE structure. In general, when high frequency motion is considered, the influence of the inertia terms is significant. Thus, the second basic assumption of the static MOR is contradicted under such circumstances and the method becomes inaccurate.

CHEN and PAN have developed a methodology [31], which introduces the valid eigenfrequency range $[0, \omega_c]$ for the static MOR. In this annotation ω_c represents the lowest eigenfrequency of either the model's slave structure, the dynamic state of which is given by the equation

$$\mathbf{M}_{ss} \ddot{\mathbf{z}}_s + \mathbf{K}_{ss} \mathbf{z}_s = \mathbf{0}, \quad (2.57)$$

or the full model's structure, but with all its master DoF being fixed (both expressions are equivalent). The more master DoF are present, the higher the lowest eigenfrequency of the fixed structure will be, and thus, the larger the valid eigenfrequency range is. Hence, the suggestion of selecting as many master DoF as possible during the static MOR.

On this basis, the error produced by the static MOR depends upon the ratio of the cut eigenfrequency ω_c to the wished eigenfrequency ω , i.e. the higher the ratio ω_c/ω is, the more accurate the static-ROM is. Of course, the increase in size for the m set should be accompanied by an adequate choice for their position in the structure (selection of master DoF in Section 2.2), since awkwardly selected master DoF result in slave structures with low lower-eigenfrequencies. This matter will be examined in Chapter 3.

The necessity to improve the dynamics of the Guyan ROM has led to several variations of the classical static condensation, one of which is the, so called, generalized static condensation [96]. This method will be annotated in the following as g-Guyan in order to distinguish it from the classical Guyan condensation.

The algorithmic scheme of the g-Guyan method assumes the same master and slave DoF partitioning as for the classical Guyan approach. The difference resides on the formulation of the block-partitioned system of equations (Eq. (2.51)), since the g-Guyan approach requires the following re-formulation of Eq. (2.51):

$$(\hat{\mathbf{M}}_m \quad \hat{\mathbf{M}}_s) \begin{pmatrix} \ddot{\mathbf{z}}_m \\ \ddot{\mathbf{z}}_s \end{pmatrix} + (\hat{\mathbf{K}}_m \quad \hat{\mathbf{K}}_s) \begin{pmatrix} \mathbf{z}_m \\ \mathbf{z}_s \end{pmatrix} = \begin{pmatrix} \mathbf{F}_m \\ \mathbf{F}_s \end{pmatrix} = \tilde{\mathbf{F}}, \quad (2.58)$$

$$[\hat{\cdot}]_m = \begin{pmatrix} [\cdot]_{mm} \\ [\cdot]_{sm} \end{pmatrix} \in \mathbb{R}^{n \times m}, \quad [\hat{\cdot}]_s = \begin{pmatrix} [\cdot]_{ms} \\ [\cdot]_{ss} \end{pmatrix} \in \mathbb{R}^{n \times s}, \quad [\cdot] := \{\mathbf{M}, \mathbf{K}\}. \quad (2.59)$$

On this account, the approximation procedures of the classical Guyan MOR are invoked

with a slight modification regarding the assumption for the vector of the external forces, namely, it is assumed no force to be applied to neither the slave nor the master DoF set of the structure, i.e. $\tilde{\mathbf{F}} = \mathbf{0}$. Thence, the two approximations are mathematically formulated as follows

$$\hat{\mathbf{M}}_m \ddot{\mathbf{z}}_m + \hat{\mathbf{M}}_s \ddot{\mathbf{z}}_s = \mathbf{0} \text{ and } \tilde{\mathbf{F}} = \mathbf{0}. \quad (2.60)$$

The combination of Eq. (2.58)-(2.60) leads to the definition of the coordinate transformation matrix $\mathbf{T}_{\text{g-Guyan}}$ for the g-Guyan MOR method, i.e.

$$\mathbf{z} = \begin{pmatrix} \mathbf{z}_m \\ \mathbf{z}_s \end{pmatrix} \stackrel{(2.60)}{=} \begin{pmatrix} \mathbf{z}_m \\ (-\hat{\mathbf{K}}_s^+ \hat{\mathbf{K}}_m) \mathbf{z}_m \end{pmatrix} = \begin{pmatrix} \mathbf{I}_m \\ -\hat{\mathbf{K}}_s^+ \hat{\mathbf{K}}_m \end{pmatrix} \cdot \mathbf{z}_m = \mathbf{T}_{\text{g-Guyan}} \cdot \mathbf{z}_m, \quad (2.61)$$

where $\mathbf{I}_m \in \mathbb{R}^{m \times m}$ is, as previously, the unit matrix, and the term $\hat{\mathbf{K}}_s^+ \in \mathbb{R}^{s \times n}$ denotes the pseudo-inverse [51] of the non-square stiffness matrix $\hat{\mathbf{K}}_s$, i.e.

$$\hat{\mathbf{K}}_s^+ = (\hat{\mathbf{K}}_s^T \hat{\mathbf{K}}_s)^{-1} \hat{\mathbf{K}}_s^T. \quad (2.62)$$

The g-Guyan ROM data, i.e. the reduced system matrices and the reduced force vector, are generated according to the directives given in Eq. (2.56).

The g-Guyan condensation is considered to be more accurate than the classical Guyan MOR, at least for ROMs at a low frequency range. Unfortunately, this advantage is in case of large models accompanied by severe computational problems due to the calculation of the pseudo-inverse $\hat{\mathbf{K}}_s^+$.

Nonetheless, the neglect of the structure's inertia in the Guyan scheme is a major source of information loss. Therefore, other MOR approaches were developed in the effort to include the model's dynamic effects into their reduction algorithm, one of which is the, so called, dynamic condensation and is discussed in the next Subsection.

2.4.2 Dynamic condensation and variants

The dynamic condensation, also referred to as classical dynamic condensation, belongs to the category of MOR methods, the algorithm of which utilizes the inertia information of the FE structure.

It was originally conceived for reducing systems, as given in Eq. (2.50), which undergo a harmonic or periodical excitation. Therefore, a variation of Eq. (2.50) is introduced, which includes the time dependency for the force vector:

$$\tilde{\mathbf{M}} \ddot{\mathbf{z}} + \tilde{\mathbf{K}} \tilde{\mathbf{z}} = \tilde{\mathbf{F}}(t). \quad (2.63)$$

Eq. (2.63) provides the dynamic state of a FE structure in time domain. The application of the Laplace transformation allows the analogous description of Eq. (2.63) in the frequency domain, as shown below:

$$(\tilde{\mathbf{M}} s^2 + \tilde{\mathbf{K}}) \tilde{\mathbf{Z}}(\mathbf{s}) = \tilde{\mathbf{F}}_L(\mathbf{s}). \quad (2.64)$$

Herein, the terms $\tilde{\mathbf{Z}}(\mathbf{s})$ and $\tilde{\mathbf{F}}_L(\mathbf{s})$ annotate the Laplace functions of the time-dependent vectors of displacement $\tilde{\mathbf{z}}(t)$ and $\tilde{\mathbf{F}}(t)$, respectively, i.e.

$$\tilde{\mathbf{Z}}(\mathbf{s}) := \mathcal{L}\{\tilde{\mathbf{z}}\}(\mathbf{s}) = \int_0^\infty e^{-st} \tilde{\mathbf{z}}(t) dt \quad \text{and} \quad \tilde{\mathbf{F}}_L(\mathbf{s}) := \mathcal{L}\{\tilde{\mathbf{F}}\}(\mathbf{s}) = \int_0^\infty e^{-st} \tilde{\mathbf{F}}(t) dt. \quad (2.65)$$

The term $\mathbf{s} \in \mathbb{C}^{n \times 1}$ generally lies in the complex plane if damping is introduced (Chapter 3). Considering the undamped system of Eq. (2.64), the term $\mathbf{s} := \mathbf{s}_{\text{imag}} = j\omega \in \mathbb{I}^{n \times 1}$ represents the eigen angular frequency ω , which relates to the structure's natural eigenfrequency f via the relationship $f = \omega/2\pi$.

The expansion of (2.64) according to the master and slave DoF partitioning leads to the following equation, written in compact form, as shown below:

$$\underbrace{(-\tilde{\mathbf{M}}\omega^2 + \tilde{\mathbf{K}})}_{\tilde{\mathbf{B}}(\omega)} \tilde{\mathbf{Z}}(\omega) = \tilde{\mathbf{F}}_L(\omega) \Leftrightarrow \quad (2.66)$$

$$\underbrace{\begin{pmatrix} \mathbf{B}(\omega)_{mm} & \mathbf{B}(\omega)_{ms} \\ \mathbf{B}(\omega)_{sm} & \mathbf{B}(\omega)_{ss} \end{pmatrix}}_{\tilde{\mathbf{B}}(\omega)} \begin{pmatrix} \mathbf{Z}(\omega)_m \\ \mathbf{Z}(\omega)_s \end{pmatrix} = \begin{pmatrix} \mathbf{F}_L(\omega)_m \\ \mathbf{F}_L(\omega)_s \end{pmatrix}. \quad (2.67)$$

At this point, the first approximation of the static condensation is invoked, namely, the assumption that no forces are applied on the slave DoF, i.e. $\mathbf{F}_L(\omega)_s = \mathbf{0}$. Thus, following exactly the algorithmic scheme as outlined in Subsection 2.4.1, the coordinate transformation matrix \mathbf{T}_{dyn} for the dynamic MOR method is obtained, i.e.

$$\mathbf{T}_{\text{dyn}} = \begin{pmatrix} \mathbf{I}_m \\ -\mathbf{B}(\omega)^{-1}_{ss} \mathbf{B}(\omega)_{sm} \end{pmatrix}, \quad \text{with } \mathbf{B}(\omega)_{ij} := -\mathbf{M}_{ij}\omega^2 + \mathbf{K}_{ij}, \quad \{i, j\} = \{s, m\}. \quad (2.68)$$

Eq. (2.68) explicitly states the dependence of the subspace \mathbf{T}_{dyn} on the parameter ω . The choice of ω should not be conducted randomly, but it should constitute a value out of the model's frequency spectrum ω_F . If not, the free-vibration version of Eq. (2.64), i.e. with $\tilde{\mathbf{F}}_L(\mathbf{s}) = \mathbf{0}$, is not satisfied:

$$\text{if } \omega^2 \neq \omega_F^2 \stackrel{(2.64)}{\Rightarrow} \tilde{\mathbf{B}}(\omega)\tilde{\mathbf{Z}} \neq \mathbf{0}. \quad (2.69)$$

Having fulfilled the condition of Eq. (2.69), the system matrices and the vector of applied forces for the dynamic-ROM are obtained according to Eq. (2.39), i.e.

$$[\]_{\text{dyn}} = \mathbf{T}_{\text{dyn}}^T \cdot [\] \cdot \mathbf{T}_{\text{dyn}}, \quad [\] := \{\mathbf{M}, \mathbf{D}, \mathbf{K}\} \quad \text{and} \quad \mathbf{F}_{\text{dyn}} = \mathbf{T}_{\text{dyn}}^T \tilde{\mathbf{F}}. \quad (2.70)$$

The accuracy of the dynamic-ROM is limited to the spectrum defined around the parameter $\omega := \omega_0$ chosen for the MOR initialization. Hence, the reference at the Subsection's beginning of this MOR scheme being developed for systems under harmonic or periodical excitation, which for the latter case the accuracy is high.

The classical dynamic reduction constitutes a special case of the, so called, exact or generalized dynamic reduction introduced by LEUNG [79]. According to this method, there is no specific assignment for the frequency value, e.g. $s := \omega = \omega_0$, but the MOR scheme proceeds in keeping the frequency term s defined as a variable. Thus, the coordinate transformation matrix as well as the ROM's data are s -dependent.

Finally, according to Eq. (2.68), it is noticed that the dynamic MOR maps itself into the static MOR method when $\omega = \mathbf{0}$. Therefore, the static condensation is considered to be a special case of the dynamic MOR.

2.4.3 Improved Reduction System method and variants

The IRS MOR method constitutes an alternative approach in the effort to include the inertia terms of the original model in the definition of the coordinate transformation matrix (Eq. (2.38)). The kernel of the IRS algorithm is the classical Guyan condensation and on that basis the static information is perturbed by taking into account the inertia terms as pseudo-static forces [25].

Let the dynamic equations of a free vibrated Guyan ROM be given as follows:

$$\mathbf{M}_R \ddot{\mathbf{z}}_m + \mathbf{K}_R \mathbf{z}_m = \mathbf{0} \Rightarrow \ddot{\mathbf{z}}_m = -\mathbf{M}_R^{-1} \mathbf{K}_R \mathbf{z}_m. \quad (2.71)$$

The double differentiation of Eq. (2.54) gives

$$(2.54) \Rightarrow \ddot{\mathbf{z}}_s = (-\mathbf{K}_{ss}^{-1} \mathbf{K}_{sm}) \ddot{\mathbf{z}}_m \quad (2.72)$$

and the substitution of Eq. (2.71) in Eq. (2.72) leads to the description of the slave DoF acceleration \mathbf{z}_s in terms of the ROM's system data, i.e. the reduced system matrices and the unknown reduced state vector \mathbf{z}_m , and the sub-blocks of the original model's stiffness matrix utilized for defining the Guyan-subspace (Eq. (2.55)):

$$(2.71), (2.72) \Rightarrow \ddot{\mathbf{z}}_s = \mathbf{K}_{ss}^{-1} \mathbf{K}_{sm} \mathbf{M}_R^{-1} \mathbf{K}_R \mathbf{z}_m. \quad (2.73)$$

Eq. (2.73) is substituted in Eq. (2.53) and the relationship between the slave DoF \mathbf{z}_s and the master DoF \mathbf{z}_m is ascertained (Eq. (2.74)). Herein, the dependence on the ROM's system matrices and the inertia terms of the original model is described in Eq. (2.74) - (2.75), i.e.

$$\mathbf{z}_s = (-\mathbf{K}_{ss}^{-1} \mathbf{K}_{sm} + \mathbf{K}_{ss}^{-1} \mathbf{S} \mathbf{M}_R^{-1} \mathbf{K}_R) \mathbf{z}_m \quad (2.74)$$

$$\mathbf{S} = \mathbf{M}_{sm} - \mathbf{M}_{ss} \mathbf{K}_{ss}^{-1} \mathbf{K}_{sm}. \quad (2.75)$$

Thus, the block-partitioned state vector \mathbf{z} is expressed in terms of the vector \mathbf{z}_m according to the following formulation:

$$\mathbf{z} = \begin{pmatrix} \mathbf{z}_m \\ \mathbf{z}_s \end{pmatrix} \stackrel{(2.74)}{=} \begin{pmatrix} \mathbf{I}_m \\ -\mathbf{K}_{ss}^{-1} \mathbf{K}_{sm} + \mathbf{K}_{ss}^{-1} \mathbf{S} \mathbf{M}_R^{-1} \mathbf{K}_R \end{pmatrix} \cdot \mathbf{z}_m = \mathbf{T}_{IRS} \cdot \mathbf{z}_m, \quad (2.76)$$

$$\mathbf{T}_{\text{IRS}} \stackrel{(2.75)}{=} \underbrace{\begin{pmatrix} \mathbf{I}_m \\ -\mathbf{K}_{ss}^{-1}\mathbf{K}_{sm} \end{pmatrix}}_{\mathbf{T}_{\text{static}}} + \underbrace{\begin{pmatrix} \mathbf{0} & \mathbf{0} \\ \mathbf{0} & \mathbf{K}_{ss}^{-1} \end{pmatrix}}_{\mathbf{P}} \underbrace{\begin{pmatrix} \mathbf{M}_{mm} & \mathbf{M}_{ms} \\ \mathbf{M}_{sm} & \mathbf{M}_{ss} \end{pmatrix}}_{\tilde{\mathbf{M}}} \underbrace{\begin{pmatrix} \mathbf{I}_m \\ -\mathbf{K}_{ss}^{-1}\mathbf{K}_{sm} \end{pmatrix}}_{\mathbf{T}_{\text{static}}} \mathbf{M}_R^{-1} \mathbf{K}_R \quad (2.77)$$

The utilization of Eq. (2.75) allows the expansion of the \mathbf{T}_{IRS} subspace and thus, the $\mathbf{T}_{\text{static}}$ subspace dependence is directly stated. Eq. (2.77) can be written in compact matrix form, as shown below:

$$\mathbf{T}_{\text{IRS}} = \mathbf{T}_{\text{static}} + \mathbf{P} \tilde{\mathbf{M}} \mathbf{T}_{\text{static}} \mathbf{M}_R^{-1} \mathbf{K}_R. \quad (2.78)$$

The system matrices and the vector of applied forces for the IRS-ROM are obtained according to Eq. (2.39), i.e.

$$[]_{\text{IRS}} = \mathbf{T}_{\text{IRS}}^T \cdot [\tilde{ }] \cdot \mathbf{T}_{\text{IRS}}, \quad [] := \{\mathbf{M}, \mathbf{D}, \mathbf{K}\} \quad \text{and} \quad \mathbf{F}_{\text{IRS}} = \mathbf{T}_{\text{IRS}}^T \tilde{\mathbf{F}}. \quad (2.79)$$

The IRS MOR method generates ROMs, which capture the dynamics of the original model better than the classical or generalized Guyan condensation. It is expected so, since Eq. (2.78) includes an extra summand, apart from the static information, i.e. $\mathbf{T}_{\text{static}}$, which contains the inertia information of the original model. Nevertheless, the basis of the reduction scheme is the classical Guyan MOR and the greatest amount of the produced error is due to the static nature of the algorithm.

A variant of the standard IRS reduction is considered to be the dynamic IRS MOR introduced by FRISWELL [47]. The methodology of this approach resides, simply, on combining the classical dynamic MOR with the algorithmic scheme of the standard IRS method. Herewith, it is attempted to minimize the error of the standard, also called static, IRS MOR by introducing the inertia effect into the definition for the static part of the \mathbf{T}_{IRS} subspace (Eq. (2.78)).

In this case, Eq. (2.71) would hold, but the free vibrated dynamic ROM and the double differentiation of the second part of the Eq. (2.68) would give

$$(2.68) \Rightarrow \ddot{\mathbf{z}}_s = (-\mathbf{B}(\omega)_{ss}^{-1}\mathbf{B}(\omega)_{sm}) \ddot{\mathbf{z}}_m \quad (2.80)$$

and thus, a relationship between the vectors of the slave and master DoF is obtained, analogously to Eq. (2.73), i.e.

$$(2.71), (2.80) \Rightarrow \ddot{\mathbf{z}}_s = \mathbf{B}(\omega)_{ss}^{-1}\mathbf{B}(\omega)_{sm}\mathbf{M}_R^{-1}\mathbf{K}_R\mathbf{z}_m. \quad (2.81)$$

Based on analogous matrix manipulation the combination of Eq. (2.74) and Eq. (2.81) leads to the definition of the \mathbf{T}_{DIRS} subspace for the dynamic IRS MOR:

$$\mathbf{T}_{\text{DIRS}} = \mathbf{T}_{\text{dyn}} + \mathbf{P}_{\text{dyn}} \tilde{\mathbf{M}} \mathbf{T}_{\text{dyn}} \mathbf{M}_R^{-1} \mathbf{K}_R. \quad (2.82)$$

$$\mathbf{P}_{\text{dyn}} := \begin{pmatrix} \mathbf{0} & \mathbf{0} \\ \mathbf{0} & \mathbf{B}(\omega)_{ss}^{-1} \end{pmatrix} = \begin{pmatrix} \mathbf{0} & \mathbf{0} \\ \mathbf{0} & (\mathbf{K}_{ss} - \omega^2 \mathbf{M}_{ss})^{-1} \end{pmatrix}, \quad (2.83)$$

where $\omega := \omega_0$ and the definition of the \mathbf{T}_{dyn} coordinate transformation matrix is given in Eq. (2.68). On the basis of the \mathbf{T}_{DIRS} definition the static IRS constitutes a special case of the dynamic IRS, i.e. when $\omega := \omega_0 = 0$.

The DIRS MOR method is, as expected, appropriate for structures, which undergo a harmonic or periodical excitation and the generated DIRS ROMs capture the dynamics of the original model better than the classical dynamic condensation.

Both the aforementioned IRS variants, i.e. the static and dynamic IRS, rely on the ROM data obtained from the classical Guyan or dynamic condensation, respectively. An improvement of the estimates for the IRS variants was proposed by FRISWELL [47] in the so called, iterated IRS scheme.

In the following, only the iterated static IRS is considered, since the subspace derivation for the iterated dynamic IRS MOR is conducted in an analogous way.

There exist two versions of the static iterated IRS MOR, namely, the first being an immediate result of the \mathbf{T}_{IRS} defined in Eq. (2.78), i.e.

$$\mathbf{T}_{\text{IRS}, i+1} = \mathbf{T}_{\text{static}} + \mathbf{P}\tilde{\mathbf{M}}\mathbf{T}_{\text{IRS}, i} \mathbf{M}_{\text{IRS}, i}^{-1} \mathbf{K}_{\text{IRS}, i}. \quad (2.84)$$

and the second being introduced by BLAIR, CAMINO and DICKENS [19], which adopts the scheme of Eq. (2.84) with its second term being retained to the standard $\mathbf{T}_{\text{static}}$ subspace, i.e.

$$\mathbf{T}_{\text{IRS}, i+1} = \mathbf{T}_{\text{static}} + \mathbf{P}\tilde{\mathbf{M}}\mathbf{T}_{\text{static}} \mathbf{M}_{\text{IRS}, i}^{-1} \mathbf{K}_{\text{IRS}, i}. \quad (2.85)$$

In Eq. (2.84)-(2.85) the new coordinate transformation matrix $\mathbf{T}_{\text{IRS}, i+1}$ is derived, which then becomes the current IRS transformation for the next iteration step. The algorithm of Eq. (2.85) results in the generation of ROM data, which do not accurately reproduce the eigenvalue spectrum of the original model. Thus, it will not be further considered in this Thesis.

The utilization of the iterative scheme in Eq. (2.84) leads to generation of ROMs, which become stepwise more accurate. Actually, it has been shown [46] that the iterated static IRS MOR converges monotonically to the SEREP method. The convergence rate, though, is absolutely dependent on the choice of the master DoF set.

In case of Eq. (2.84) being convergent, the ROM is in the position to reproduce the lower eigenvalue spectrum (eigenfrequency and eigenvector) of the original model. Therefor, a reformulation of the Eq. (2.84) is required:

$$(2.84) \Rightarrow \mathbf{T}_{\text{IRS}, i+1} = \begin{pmatrix} \mathbf{I}_m \\ \mathbf{t}_{\text{IRS}, i+1} \end{pmatrix}, \quad (2.86)$$

$$\mathbf{t}_{\text{IRS}, i+1} = -\mathbf{K}_{ss}^{-1} \mathbf{K}_{sm} + \mathbf{K}_{ss}^{-1} (\mathbf{M}_{sm} + \mathbf{M}_{ss} \mathbf{t}_{\text{IRS}, i}) \mathbf{M}_{\text{IRS}, i}^{-1} \mathbf{K}_{\text{IRS}, i}. \quad (2.87)$$

The relationship between the slave and master DoF via the $\mathbf{T}_{\text{IRS}, i+1}$ subspace holds not only for the physical configuration space $\{\mathbb{R}^n, n = 1, 2, 3\}$, but also for the space

spanned by the eigenvectors, i.e.

$$\Phi = \begin{pmatrix} \Phi_m \\ \Phi_s \end{pmatrix} = T_{IRS, i+1} \Phi_m, \quad (2.88)$$

where the term Φ denotes the $n \times q$ modal matrix consisting of q eigenvectors and Φ_m and Φ_s the $m \times q$ and $s \times q$ sub-blocks of the modal matrix Φ , respectively. For the ROM the dynamic equation in the frequency domain holds:

$$M_{IRS} \omega^2 \Phi_m = K_{IRS} \Phi_m \Leftrightarrow M_{IRS}^{-1} K_{IRS} \Phi_m = \omega^2 \Phi_m, \quad (2.89)$$

with ω representing the eigen angular frequency of the ROM. The substitution of Eq. (2.89) in the second part of Eq. (2.88) leads to the derivation of the following relationship:

$$(2.88), (2.89) \xrightarrow{(2.87)} K_{ss} \Phi_s = -K_{sm} \Phi_m + \omega^2 K_{sm} \Phi_m + \omega^2 M_{ss} \Phi_s \quad (2.90)$$

$$\Leftrightarrow \omega^2 [M_{sm} \ M_{ss}] \Phi = [K_{sm} \ K_{ss}] \Phi. \quad (2.91)$$

Eq. (2.89) can be expressed in terms of the original model's information by taking into consideration the definition of the ROM data given in Eq. (2.79), i.e.

$$(2.79), (2.89) \Rightarrow \omega^2 T_{IRS}^T \tilde{M} \underbrace{T_{IRS} \Phi_m}_{\Phi} = T_{IRS}^T \tilde{K} \underbrace{T_{IRS} \Phi_m}_{\Phi} \quad (2.92)$$

$$\xleftarrow{(2.86)} \omega^2 [I_m \ t_{IRS}^T] \tilde{M} \Phi = [I_m \ t_{IRS}^T] \tilde{K} \Phi \quad (2.93)$$

$$\Leftrightarrow \omega^2 [M_{mm} \ M_{ms}] \Phi = [K_{mm} \ K_{ms}] \Phi. \quad (2.94)$$

The combination of Eq. (2.91) and Eq. (2.94) gives the dynamic equation of the original model in the frequency domain, i.e. $\omega^2 \tilde{M} \Phi = \tilde{K} \Phi$ for the chosen frequency ω and the associated eigenvector Φ . Herewith, it is proved that the ROM reproduces the lower observable eigenvalues of the original model.

The versions of the IRS algorithms presented in this Section, especially the iterated cases, succeed in generating ROMs, which capture the dynamics of the original model very well. Still, as observed throughout this Section, the IRS scheme depends on the definition of the T_{static} subspace. Thus, for several cases where the inertia terms become significant, e.g. in gun dynamics or high acceleration events, the standard IRS and its variants deliver only fair results. This problematic situation is overcome by the application of the last MOR belonging to the category of *Physical space reduction-expansion algorithms*, namely, the SEREP MOR method.

2.4.4 System Equivalent Reduction Expansion Process

SEREP is a powerful MOR approach, which has been extensively used in various disciplines of structural mechanics. It was introduced by O' CALLAHAN, AVITABILE,

and RIEMER [26]. A similar methodology was proposed by KAMMER [63].

The algorithmic basis of SEREP is the modal matrix of the FE discretized structure, which contains the structure's eigenvectors arranged in a column-wise format. Thus, let Φ be the $n \times q$ modal matrix, where the terms n and q denote the dimension of the model and the number of the computed eigenvectors, respectively. Considering the undamped dynamic system described in the time domain (Eq. (2.50)), the associated dynamic system described in the frequency domain can be derived (Eq. (2.64)). On that basis, the following equation holds

$$\tilde{\mathbf{z}} = \Phi \mathbf{q}, \quad (2.95)$$

which relates the state space vector $\tilde{\mathbf{z}}$ to the vector of modal coordinates \mathbf{q} of dimension $q \times 1$. The analytical expression of the master and slave DoF sets for the state space vector $\tilde{\mathbf{z}}$ leads to an analogous derivation for the modal matrix, i.e.

$$\begin{pmatrix} \mathbf{z}_m \\ \mathbf{z}_s \end{pmatrix} = \begin{pmatrix} \Phi_{m \times q} \\ \Phi_{s \times q} \end{pmatrix} \mathbf{q}. \quad (2.96)$$

The index annotation for the sub-blocks of the modal matrix in the previous as well as the following equations gives the dimension of the current state of the matrix, i.e. the index in $\mathbf{A}_{x \times y}^T$ represents the $x \times y$ dimension of the transposed matrix \mathbf{A}^T .

According to the first part of Eq. (2.96) the modal coordinates can be expressed in terms of the master DoF coordinates, if the pseudo-inverse definition for a non-square vector is used (Eq. (2.62)):

$$\mathbf{q} = \Phi_{q \times m}^+ \mathbf{z}_m = (\Phi_{q \times m}^T \Phi_{m \times q})^{-1} \Phi_{q \times m}^T \mathbf{z}_m. \quad (2.97)$$

By substituting the relationship of Eq. (2.97) in Eq. (2.96) the expression of the full model's state space vector w.r.t to the master DoF vector is derived and thus, the $\mathbf{T}_{\text{SEREP}}$ coordinate transformation matrix is defined, i.e.

$$(2.97), (2.96) \Rightarrow \tilde{\mathbf{z}} = \begin{pmatrix} \mathbf{z}_m \\ \mathbf{z}_s \end{pmatrix} = \begin{pmatrix} \Phi_{m \times q} \Phi_{q \times m}^+ \\ \Phi_{s \times q} \Phi_{q \times m}^+ \end{pmatrix} \mathbf{z}_m = \mathbf{T}_{\text{SEREP}} \cdot \mathbf{z}_m. \quad (2.98)$$

As in the previous Subsections, the system matrices and the vector of applied forces for the SEREP-ROM are obtained according to Eq. (2.39), i.e.

$$[\]_{\text{SEREP}} = \mathbf{T}_{\text{SEREP}}^T \cdot [\tilde{\mathbf{z}}] \cdot \mathbf{T}_{\text{SEREP}}, \quad [\] := \{\mathbf{M}, \mathbf{D}, \mathbf{K}\} \quad \text{and} \quad \mathbf{F}_{\text{SEREP}} = \mathbf{T}_{\text{SEREP}}^T \tilde{\mathbf{F}}. \quad (2.99)$$

In this case, though, the specific nature of the $\mathbf{T}_{\text{SEREP}}$ subspace allows the analytical expression of the reduced mass and stiffness matrices, which result in the following formulation:

$$\mathbf{M}_{\text{SEREP}} = \Phi_{q \times m}^T \Phi_{q \times m} \quad \text{and} \quad \mathbf{K}_{\text{SEREP}} = \Phi_{q \times m}^T \Lambda_{q \times q} \Phi_{q \times m}. \quad (2.100)$$

In Eq. (2.100) $\Lambda_{q \times q}$ denotes the eigenvalue matrix, for which in accordance to the

annotation introduced in the previous Subsections, it holds:

$$\boldsymbol{\Lambda}_{q \times q} := \boldsymbol{\Omega}_{q \times q}^2 = \text{diag} [\omega_i^2], \quad i = 1, \dots, q. \quad (2.101)$$

Thence, according to Eq. (2.100) it is not necessary to apply the matrix multiplications of Eq. (2.99) for the generation of the ROM, since the reduced system matrices can be directly computed based only on the eigenvalue data.

An analogous expression for the damping matrix depends on the modelling scheme used for its definition. The Rayleigh damping modelling (Chapter 3) permits the plausible description of the reduced damping matrix, as shown below:

$$\mathbf{D}_{\text{SEREP}} = \boldsymbol{\Phi}_{q \times m}^T (\alpha \mathbf{I}_{q \times q} + \beta \boldsymbol{\Lambda}_{q \times q}) \boldsymbol{\Phi}_{q \times m}, \quad \alpha, \beta = \text{const.} \quad (2.102)$$

The SEREP-ROM preserves exactly all the modes selected from the original model and therefore, SEREP is considered to be a powerful MOR technique. As given in Eq. (2.98), the reduction's quality depends only on the selection of the full eigenvectors and not on the definition of the master DoF within the structure (master DoF free method). Still, the precise allocation of the m set is important and should be taken into consideration during the FEM-MBS coupling procedure (Section 2.2). Despite the positive aspects, this reduction scheme is accompanied by several drawbacks, the nature of which is twofold and thus, divided into the following two categories.

The application of SEREP is only feasible, if the modal matrix, i.e. the selected set of eigenvectors, of the original model is available. This aspect can be computationally expensive in case of large models. The utilization, though, of specific sparse algebra techniques [51] for either the direct [36] or the iterative [102] solution of large eigenvalue problems in combination with the, so called, lumped mass approximation [3] could overcome this problem. Furthermore, in several disciplines the selection of the important eigenvectors of the original model is not a trivial task. Fortunately, in the area of structural mechanics the vectors of interest are the smallest magnitude eigenvalues, i.e. the larger the magnitude property of an eigenvalues becomes, the less it corresponds to the low-frequency dynamics of the model.

The second drawback of the SEREP method refers to the nature of the ROM's system matrices (Eq. (2.100)). The non-proper definition of the parameters m and p could lead to the generation of rank-deficient matrices. For example, this is the case when $m < q$ in Eq. (2.98) [26, 96]. It is generally advised for m to be larger or equal than q , i.e. $m \geq q$, although here it should also be proceeded with caution as suggested by QU [96]. Thence, it is vital to check the consistency of the ROM. A rank-deficient mass matrix is not positive definite and thus, the structure of the mechanical model is not preserved. As it will be seen in the next Chapter (Subsection 3.1.4), the modal analysis of a FE structure should always be conducted based on the Cholesky decomposition of the mass matrix. Herewith, it is verified if the essential structure properties of the FE discretized model are preserved or not.

2.5 Semi physical subspace reduction-expansion methods

The Component Mode Synthesis method (CMS) [34] is the main topic of this category. It is regarded as the state of the art MOR algorithm integrated into commercial FE software packages. A modification of the CMS, namely, the Krylov spanned CMS MOR is also included. It will be seen that both MOR approaches highly depend on the static modes defined by the Guyan reduction scheme. An improvement of this algorithmic scheme considers the replacement of the Guyan-static modes by the IRS-static modes and thus, two interesting MOR approaches are created: the Improved CMS (ICMS) and the Improved KCMS (IKCMS) MOR accompanied by their iterated versions.

2.5.1 Component Mode Synthesis and variants

As already mentioned, the CMS method is the preferable MOR algorithm widely used in various disciplines of structural mechanics. It succeeds in generating ROMs, which capture very well the dynamics of the original model while keeping intact the important structural properties, i.e. the definiteness properties of the system matrices.

The general algorithmic scheme of CMS is divided into three categories resulting thus, in three CMS variants [32, 33, 34]: the fixed-interface (FIX), the free-interface (FREE), and the residual-flexible free interface (RFFB) method (Fig. 2.6). The decision of which

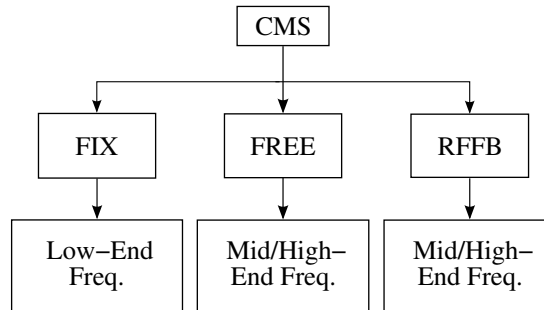


Fig. 2.6: Categorization of the CMS variants

method to apply is model dependent. For the majority of the analysis procedures in structural mechanics the fixed-interface CMS method is advised, since the accuracy on the lower eigenvalues of the FE structure is required. In several cases, though, it is compulsory for the computed eigenvalues to be more accurate at the mid- to high-end of the model's eigenvalue spectrum. Thence, the application of either the FREE or the RFFB CMS method is recommended.

In this Thesis, the FEM-MBS coupling is investigated, i.e. we cope with elastic MBS and their data transfer into MBS codes. For such dynamical systems the spectrum

of interest lies in the domain of the structure's lower eigenvalues. Thus, only the fixed-interface CMS method will be considered and will be simply referred to as the CMS MOR.

The CMS algorithm is based, as all the previously stated MOR methods, on the theory of the master and slave DoF (Eq. (2.51)). The kernel of this method resides on the observation that the slave DoF vector \mathbf{z}_s can be expressed as a superposition of the slave DoF vector \mathbf{z}_s (Guyan) generated according to the Guyan reduction scheme, and the slave DoF vector \mathbf{z}_s (CB) defined according to the Craig-Bampton (CB) modes, i.e.

$$\mathbf{z}_s = \mathbf{z}_s(\text{Guyan}) + \mathbf{z}_s(\text{CB}). \quad (2.103)$$

A detailed insight into the CB definition clarifies the validity of Eq. (2.103). The CB set consists of some lower eigenvectors of the internal (slave) structure, which are calculated imposing the blocking condition on the master DoF of Eq. (2.51) (hence, the fixed-interface characterization):

$$\mathbf{z}_m = \ddot{\mathbf{z}}_m = 0 \stackrel{(2.51)}{\Rightarrow} \mathbf{M}_{ss}\ddot{\mathbf{z}}_s + \mathbf{K}_{ss}\mathbf{z}_s = \mathbf{F}_s. \quad (2.104)$$

The free-vibrated version of Eq. (2.104), i.e. $\mathbf{F}_s = \mathbf{0}$ given in the frequency domain, allows the computation of the slave structure's modal matrix Φ_{ss} :

$$(\mathbf{K}_{ss} - \mathbf{M}_{ss}\omega_{ss}^2)\Phi_{ss} = \mathbf{0}. \quad (2.105)$$

Eq. (2.105) describes the general eigenvalue problem of the block-structure defined by the slave DoF. For the definition of the CB set the calculation of l eigenvectors of the smallest frequency magnitude suffices, i.e.

$$\mathbf{z}_s(\text{CB}) = \Phi_{CB}, \quad \text{with} \quad \Phi_{ss} = \begin{bmatrix} \Phi_{CB}^{s \times l} & \Phi_2^{s \times (s-l)} \end{bmatrix} \quad \text{and} \quad l \ll s = n - m. \quad (2.106)$$

The substitution of Eq. (2.54) and Eq. (2.106) in Eq. (2.103) gives the full description of the structure's slave DoF in terms of master DoF vector \mathbf{z}_m and the vector of modal coordinates \mathbf{y} , i.e.

$$\mathbf{z}_s = \underbrace{-\mathbf{K}_{ss}^{-1}\mathbf{K}_{sm}\mathbf{z}_m}_{\mathbf{T}_s} + \underbrace{\sum_{k=1}^l \boldsymbol{\phi}_k y_k}_{\Phi_{CB}} = \mathbf{T}_s \mathbf{z}_m + \Phi_{CB} \mathbf{y}. \quad (2.107)$$

Thus, the \mathbf{T}_{CMS} coordinate transformation matrix of the CMS MOR method is ascertained:

$$\mathbf{z} = \begin{pmatrix} \mathbf{z}_m \\ \mathbf{z}_s \end{pmatrix} \stackrel{(2.107)}{=} \begin{pmatrix} \mathbf{z}_m \\ \mathbf{T}_s \mathbf{z}_m + \Phi_{CB} \mathbf{y} \end{pmatrix} = \underbrace{\begin{pmatrix} \mathbf{I}_m^{m \times m} & \mathbf{0}^{m \times l} \\ \mathbf{T}_s^{s \times m} & \Phi_{CB}^{s \times l} \end{pmatrix}}_{\mathbf{T}_{\text{CMS}}} \cdot \begin{pmatrix} \mathbf{z}_m \\ \mathbf{y} \end{pmatrix} = \mathbf{z}_{\text{CMS}}. \quad (2.108)$$

The definition of the reduced system vector \mathbf{z}_{CMS} in Eq. (2.108) exemplifies the reason

for CMS residing in the *Semi physical subspace reduction-expansion methods* category. The system matrices and the vector of applied forces for the CMS-ROM are computed via the basic scheme of Eq. (2.39), i.e.

$$[\cdot]_{\text{CMS}} = \mathbf{T}_{\text{CMS}}^T \cdot [\tilde{\cdot}] \cdot \mathbf{T}_{\text{CMS}}, \quad [\cdot] := \{\mathbf{M}, \mathbf{D}, \mathbf{K}\} \quad \text{and} \quad \mathbf{F}_{\text{CMS}} = \mathbf{T}_{\text{CMS}}^T \tilde{\mathbf{F}}. \quad (2.109)$$

Two aspects should be taken into consideration regarding the reduced data in Eq. (2.109). Firstly, the dimension of the CMS ROM's system matrices and vectors are determined based on the number of both the master DoF m and the modal coordinates l , i.e.

$$[\cdot]_{\text{CMS}}^{(m+l) \times (m+l)}, \quad [\cdot] := \{\mathbf{M}, \mathbf{D}, \mathbf{K}\}, \quad \mathbf{z}_{\text{CMS}}^{(m+l) \times 1} \quad \text{and} \quad \mathbf{F}_{\text{CMS}}^{(m+l) \times 1}. \quad (2.110)$$

Secondly, under the assumption of a unit norm for the eigenvectors w.r.t the mass (Chapter 3), the reduced mass and stiffness matrices have a characteristic structure (Fig. 2.7), which is obtained by expanding the terms in Eq. (2.109):

$$\mathbf{M}_{\text{CMS}} = \begin{pmatrix} \mathbf{M}^{m \times m} & \mathbf{M}^{m \times l} \\ \mathbf{M}^{l \times m} & \mathbf{I}_{CB}^{l \times l} \end{pmatrix} \quad \text{and} \quad \mathbf{K}_{\text{CMS}} = \begin{pmatrix} \mathbf{K}^{m \times m} & \mathbf{K}^{m \times l} \\ \mathbf{K}^{l \times m} & \mathbf{\Lambda}_{CB}^{l \times l} \end{pmatrix}. \quad (2.111)$$

The block matrices \mathbf{I}_{CB} and $\mathbf{\Lambda}_{CB}$ denote the unit and the eigenvalue matrix, respectively, the latter being defined as given in Eq. (2.101). If the Rayleigh modelling scheme

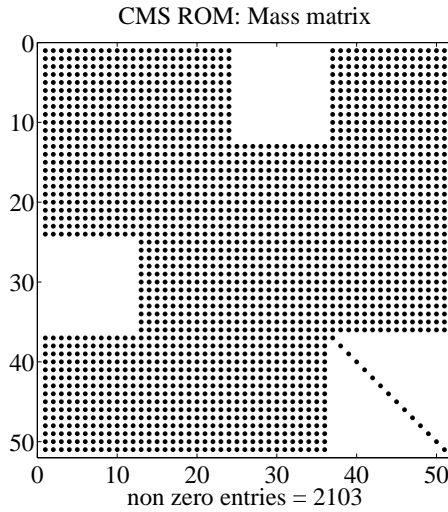


Fig. 2.7: \mathbf{M}_{CMS} of 3D solid bar with $m = 36$ and $\text{CB} = 15$

is chosen for the definition of the model's damping, then the structure of the reduced damping matrix is analogously defined, i.e.

$$\mathbf{D}_{\text{CMS}} = \begin{pmatrix} \mathbf{D}^{m \times m} & \mathbf{D}^{m \times l} \\ \mathbf{D}^{l \times m} & (\alpha \mathbf{I} + \beta \mathbf{\Lambda})_{CB}^{l \times l} \end{pmatrix}, \quad \alpha, \beta = \text{const.} \quad (2.112)$$

As stated at the beginning of the Subsection, the CMS method generates ROMs, which capture very well the dynamics of the original model. The utilization of fast sparse algorithms during the lower eigenvector calculation of the slave structure contributes to reducing the computation time and thus, indicating this approach as an important MOR tool. Furthermore, the fact that this method is implemented as the standard and most reliable MOR algorithm in several FE software packages can only be regarded as a positive aspect.

Nevertheless, as the rest of the so far introduced MOR methods, the CMS algorithmic procedure is accompanied by certain disadvantages. The dependence of the ROM's quality on the number and the position of the master DoF is high. In contrast to SEREP and other approaches belonging to the category of *Non physical subspace reduction-expansion methods*, the allocation of the m set directly affects both the static \mathbf{z}_s (Guyan) and the dynamic \mathbf{z}_s (CB) part of the slave DoF vector in Eq. (2.103). When two different m sets of the same dimension in the same structure are selected, the CB modes are different, since the slave structure is not the same. This dependence becomes more significant, if fixed structures are considered. Here, the error produced during the generation of the static part (Subsection 2.4.1) should be accompanied by an increase in the number of the CB modes in order for a good quality ROM to be ascertained.

2.5.2 Krylov spanned Component Mode Synthesis

The Krylov spanned CMS method can be regarded as a modification of the classical CMS, since the same superposition principle is adopted for the description of the slave DoF state vector \mathbf{z}_s (Eq. (2.103)). The only difference to the classical approach is situated in the definition of the dynamic contribution for the slave structure.

The classical CMS proceeds in introducing the CB modes set (Eq. (2.106)), whereas the algorithmic scheme of the KCMS method is based on the definition of the, so called, Krylov Vectors (KV) [74] for the slave structure. Thus, the modified version of Eq. (2.103) is ascertained:

$$\mathbf{z}_s = \mathbf{z}_s(\text{Guyan}) + \mathbf{z}_s(\text{KV}), \quad (2.113)$$

where the term $\mathbf{z}_s(\text{KV})$ represents the slave DoF displacement vector due to the eigenvectors, which span the associated Krylov subspace.

For a given constant matrix $\tilde{\mathbf{A}} \in \mathbb{R}^{n \times n}$, a starting vector $\tilde{\mathbf{b}} \in \mathbb{R}^{n \times 1}$, and $q \in \mathbb{N}^*$ the Krylov subspace is defined as the subspace spanned by the q column vectors $\tilde{\mathbf{b}}, \tilde{\mathbf{A}}\tilde{\mathbf{b}}, \dots, \tilde{\mathbf{A}}^{q-1}\tilde{\mathbf{b}}$, i.e.

$$K_q(\tilde{\mathbf{A}}, \tilde{\mathbf{b}}) := \text{span} \left\{ \tilde{\mathbf{b}}, \tilde{\mathbf{A}}\tilde{\mathbf{b}}, \dots, \tilde{\mathbf{A}}^{q-1}\tilde{\mathbf{b}} \right\}. \quad (2.114)$$

Considering the undamped version of Eq. (2.37), it is proved (a detailed proof therefor is given in Subsection 2.6.2) the terms $\tilde{\mathbf{A}}$ and $\tilde{\mathbf{b}}$ in Eq. (2.114) to be defined as follows:

$$(2.114) \stackrel{(2.37)}{\Rightarrow} \tilde{\mathbf{A}} := \mathbf{K}^{-1}\mathbf{M} \quad \text{and} \quad \tilde{\mathbf{b}} := \mathbf{K}^{-1}\mathbf{F} \quad (2.115)$$

Thence, according to Eq. (2.114) and Eq. (2.115) the full description of the Krylov

subspace regarding the structure defined by the internal DoF is derived:

$$K_q^{\text{slave}} := K_q(\mathbf{K}_{ss}^{-1}\mathbf{M}_{ss}, \mathbf{K}_{ss}^{-1}\mathbf{F}_s) \quad (2.116)$$

$$= \text{span} \left\{ \underbrace{\mathbf{K}_{ss}^{-1}\mathbf{F}_s}_{\Phi_1^{\text{Krylov}}}, \underbrace{(\mathbf{K}_{ss}^{-1}\mathbf{M}_{ss})\mathbf{K}_{ss}^{-1}\mathbf{F}_s}_{\Phi_2^{\text{Krylov}}}, \dots, \underbrace{(\mathbf{K}_{ss}^{-1}\mathbf{M}_{ss})^{q-1}\mathbf{K}_{ss}^{-1}\mathbf{F}_s}_{\Phi_q^{\text{Krylov}}} \right\} \quad (2.117)$$

and the slave DoF vector \mathbf{z}_s can be expressed in terms of the master DoF vector \mathbf{z}_m and the vector of Krylov coordinates $\mathbf{y}^{\text{Krylov}}$:

$$\mathbf{z}_s = \underbrace{-\mathbf{K}_{ss}^{-1}\mathbf{K}_{sm}\mathbf{z}_m}_{\mathbf{T}_s} + \sum_{k=1}^q \Phi_k^{\text{Krylov}} y_k^{\text{Krylov}} = \mathbf{T}_s \mathbf{z}_m + K_q^{\text{slave}} \mathbf{y}^{\text{Krylov}}. \quad (2.118)$$

Analogously to the classical CMS case, the coordinate transformation matrix \mathbf{T}_{KCMS} for the KCMS MOR method is ascertained, i.e.

$$\mathbf{z} = \begin{pmatrix} \mathbf{z}_m \\ \mathbf{z}_s \end{pmatrix} \stackrel{(2.118)}{=} \begin{pmatrix} \mathbf{z}_m \\ \mathbf{T}_s \mathbf{z}_m + K_q^{\text{slave}} \mathbf{y}^{\text{Krylov}} \end{pmatrix} = \underbrace{\begin{pmatrix} \mathbf{I}_m & \mathbf{0} \\ \mathbf{T}_s & K_q^{\text{slave}} \end{pmatrix}}_{\mathbf{T}_{\text{KCMS}}} \cdot \underbrace{\begin{pmatrix} \mathbf{z}_m \\ \mathbf{y}^{\text{Krylov}} \end{pmatrix}}_{\mathbf{z}_{\text{KCMS}}} \quad (2.119)$$

and the associated ROM data is computed based on the relationships given in Eq. (2.109) - (2.112).

The ROMs generated by the KCMS MOR method possess almost the same dynamical properties as the CMS-ROMs, at least for the low frequency range of interest. Since the coordinate transformation matrices of both methods (Eq. (2.108) and Eq. (2.119)) contain the term \mathbf{T}_s , it is expected the same static error to be produced. The major advantage of KCMS in comparison to the classical CMS is the partial dependence of the transformation matrix on the allocation of the master DoF set. As already mentioned in the previous Subsection, the quality of the CB set depends both on the number and the position of the structure's master DoF. On the contrary, the definition of the K_q^{slave} subspace depends only on the initialization parameter q , which denotes the dimension of the associated Krylov subspace. Thus, for structures where a non-usual DoF allocation is necessary the KCMS reduction scheme results in ROMs, which capture the dynamics better than the classical CMS MOR.

2.5.3 Improved Component Mode Synthesis

In the effort to reduce the error produced by the classical CMS reduction, the Improved CMS method (ICMS) is proposed by KOUTSOVASILIS and BEITELSCHMIDT [69].

The dynamics of a $(m+l) \times (m+l)$ CMS-ROM model, under the assumption of the m set being predefined, can always be improved by increasing the number of the CB modes l and thus, generating a larger dimension ROM. In view of coupling the ROM

into a MBS code, though, this dimension increase would aggravate any further MBS simulation. Therefore, the ICMS MOR is introduced, which succeeds in improving the algorithmic scheme of the classical CMS method, while keeping unaltered the dimension of CB modes set.

The major source of information loss in the CMS algorithm is the contribution of the static part \mathbf{z}_s (Guyan) in the superposition definition of the slave DoF vector (Eq. (2.103)). The reason is obviously the neglect of the inertia terms, which is partially compensated by the utilization of the CB set. A methodology for reducing the static error within the superposition of \mathbf{z}_s is offered by the IRS MOR method (Subsection 2.4.3), since according to the IRS algorithm the inertia terms of the original model are included into the definition of the IRS subspace. Thus, the term \mathbf{z}_s (Guyan) in Eq. (2.103) can be substituted by the static term \mathbf{z}_s (IRS) and a different superposition principle is derived, i.e.

$$\mathbf{z}_s = \mathbf{z}_s(\text{IRS}) + \mathbf{z}_s(\text{CB}). \quad (2.120)$$

The reformulation of Eq. (2.76) indicates the coordinate transformation matrix, which should be used for the \mathbf{z}_s (IRS) definition in Eq. (2.120), i.e.

$$\mathbf{z}_s(\text{IRS}) = \begin{pmatrix} \mathbf{z}_m \\ \mathbf{z}_s \end{pmatrix} \stackrel{(2.74)}{=} \begin{pmatrix} \mathbf{I}_m \\ -\mathbf{K}_{ss}^{-1}\mathbf{K}_{sm} + \mathbf{K}_{ss}^{-1}\mathbf{S}\mathbf{M}_R^{-1}\mathbf{K}_R \end{pmatrix} \cdot \mathbf{z}_m = \begin{pmatrix} \mathbf{I}_m^{m \times m} \\ \mathbf{t}_{\text{IRS}}^{s \times m} \end{pmatrix} \cdot \mathbf{z}_m \quad (2.121)$$

with \mathbf{S} being ascertained as given in Eq. (2.75). Taking into account the CB definition in Eq. (2.106), the coordinate transformation matrix \mathbf{T}_{ICMS} of the ICMS MOR method is obtained:

$$\mathbf{z} = \begin{pmatrix} \mathbf{z}_m \\ \mathbf{z}_s \end{pmatrix} \stackrel{(2.121)}{=} \begin{pmatrix} \mathbf{z}_m \\ \mathbf{t}_{\text{IRS}}\mathbf{z}_m + \Phi_{CB}\mathbf{y} \end{pmatrix} = \underbrace{\begin{pmatrix} \mathbf{I}_m^{m \times m} & \mathbf{0}^{m \times l} \\ \mathbf{t}_{\text{IRS}}^{s \times m} & \Phi_{CB}^{s \times l} \end{pmatrix}}_{\mathbf{T}_{\text{ICMS}}} \cdot \underbrace{\begin{pmatrix} \mathbf{z}_m \\ \mathbf{y} \end{pmatrix}}_{\mathbf{z}_{\text{ICMS}}}. \quad (2.122)$$

The calculation of the ICMS ROM data is accomplished based on the previously stated relationships given throughout the Eq. (2.109) - (2.112).

A further improvement of the \mathbf{T}_{ICMS} subspace is feasible by the utilization of the iterative scheme presented in Eq. (2.84). It leads, as in the static IRS case, to the generation of ROMs, which become stepwise more accurate, i.e.

$$\mathbf{T}_{\text{ICMS}, i+1} = \begin{pmatrix} \mathbf{I}_m & \mathbf{0} \\ \mathbf{t}_{\text{IRS}, i+1} & \Phi_{CB} \end{pmatrix}, \quad (2.123)$$

with the iterated IRS term $\mathbf{t}_{\text{IRS}, i+1}$ being defined in Eq. (2.87).

As observed in Eq. (2.123), the iteration scheme concerns only the lower left sub-block of the \mathbf{T}_{ICMS} coordinate transformation matrix, namely, the \mathbf{t}_{IRS} subspace. On this account, the iterative ICMS MOR retains the convergence properties of the iterative static IRS method.

The ICMS algorithm generates ROMs, which succeed in capturing the dynamics of the original model better than the classical CMS and IRS reduction methods. The consideration of the inertia terms in the definition of both the static and the dynamic part of the aforesaid superposition principle (Eq. (2.120)) leads to the definition of ROMs with improved accuracy also in the higher eigenvalue spectrum. The disadvantages of the classical CMS case when dealing with fixed FE structures are overcome by the utilization of the iterated ICMS scheme, which actually competes even with the powerful Krylov Subspace Method (KSM), to be presented in the next Section.

The same error-correction idea can be used in order to improve the algorithm of the KCMS MOR. Thence, the Improved KCMS method (IKCMS) is created, which differs from the ICMS case in the definition of the slave structure's Krylov subspace. The IKCMS coordinate transformation matrix and ROM data can be derived according to the Eq. (2.120) - (2.123), where the term K_q^{slave} (Eq. (2.116)) should be used instead of the CB modes. The IKCMS MOR scheme utilizes the advantages of the classical KCMS reduction, the magnitude of which is increased when its iterative version is applied.

The IKCMS reduction concludes the cycle of MOR approaches belonging to the category of *Semi physical subspace reduction-expansion methods*. The following Section copes with the last MOR family, namely, the *Non physical subspace reduction-expansion methods*.

2.6 Non physical subspace reduction-expansion methods

The kernel of this last category consists of two important MOR procedures, namely, the Krylov Subspace Method (KSM) [4, 5, 9, 12, 15, 18, 14, 20, 49, 52, 53, 84, 117, 45, 44, 17, 113] and the techniques of the general Balanced Truncation (BT) approach [90, 89, 76, 17, 4, 18, 16, 80, 113]. Both methods originate from the mathematical field of control theory and were initially developed for LTI first-order ODEs, e.g. systems that describe the dynamic state of electrical networks. A direct application of either the KSM or the BT method for reducing the order of mechanical MBS is not advised, since there is no guarantee for the preservation of the ROM's structure. Thence, several modifications to the basic KSM [107, 4, 17, 42] and BT [87, 28, 119] algorithms are necessary for the methods to be applicable in structural mechanics.

The theory of adapting the KSM and BT methods for reducing second-order systems is highly connected to the associated first-order theory. Thus, in this Section the first-order algorithms of both MOR methods will be presented and on that basis the equivalent second-order schemes will be derived.

Additionally to the above mentioned MOR reductions, the *Non physical subspace reduction-expansion methods* category includes the Second Order Modal Truncation method (SOMT). It is simply a truncated representation of the original model in the subspace spanned by its eigenvectors and thus, directly applicable to second-order models.

2.6.1 First order Krylov Subspace method

The first-order KSM was initially developed for reducing the dimension of Multi Input Multi Output (MIMO) dynamical systems of the form:

$$\mathbf{E}\dot{\mathbf{z}}(t) = \mathbf{A}\mathbf{z}(t) + \mathbf{B}\mathbf{u}(t) \quad (2.124)$$

$$\mathbf{y}(t) = \mathbf{C}\mathbf{z}(t), \quad (2.125)$$

where $\{\mathbf{E}, \mathbf{A}\} \in \mathbb{R}^{N \times N}$, $\mathbf{B} \in \mathbb{R}^{N \times k}$ and $\mathbf{C} \in \mathbb{R}^{p \times N}$ are the, so called, system input and output matrices, respectively. The terms $\mathbf{u} \in \mathbb{R}^{k \times 1}$, $\mathbf{y} \in \mathbb{R}^{p \times 1}$ and $\mathbf{z} \in \mathbb{R}^{N \times 1}$ represent the associated input, output and state vectors of the system.

The KSM reduction scheme is based on the definition of two important quantities, namely, the *moments* and the *Markov parameters*, which are derived after the Laplace transformation of Eq. (2.124) - (2.125) and the introduction of the transfer matrix $\mathbf{H}(s)$, i.e.

$$\mathbf{H}(s) = \mathbf{C}(s\mathbf{E} - \mathbf{A})^{-1}\mathbf{B}. \quad (2.126)$$

Under the assumption of \mathbf{A} being non singular, the transfer matrix $\mathbf{H}(s)$ can be expanded about zero with the help of the Taylor method, i.e.

$$\mathbf{H}(s) = -\underbrace{\mathbf{C}\mathbf{A}^{-1}\mathbf{B}}_{\bar{m}_0} - \underbrace{\mathbf{C}(\mathbf{A}^{-1}\mathbf{E})\mathbf{A}^{-1}\mathbf{B}s}_{\bar{m}_1} - \dots - \underbrace{\mathbf{C}(\mathbf{A}^{-1}\mathbf{E})^i\mathbf{A}^{-1}\mathbf{B}s^i}_{\bar{m}_i} - \dots \quad (2.127)$$

and herein, the resulting non-negative coefficients of the series are referred to as the system's moments:

$$\mathbb{R}^{p \times k} \ni \bar{m}_i := \mathbf{C}(\mathbf{A}^{-1}\mathbf{E})^i\mathbf{A}^{-1}\mathbf{B}, \quad i = 1, 2, \dots. \quad (2.128)$$

If in the definition of the transfer matrix (Eq. (2.126)) the eigenvalue term s is replaced by $1/\lambda$, i.e. $s = 1/\lambda$, the Taylor expansion of $\mathbf{H}(s = 1/\lambda)$ about $\lambda = 0$ delivers a different version of series:

$$\mathbf{H}(s) = -\underbrace{\mathbf{C}\mathbf{E}^{-1}\mathbf{B}s^{-1}}_{\bar{M}_0} - \underbrace{\mathbf{C}(\mathbf{E}^{-1}\mathbf{A})\mathbf{E}^{-1}\mathbf{B}s^{-2}}_{\bar{M}_1} - \dots - \underbrace{\mathbf{C}(\mathbf{E}^{-1}\mathbf{A})^i\mathbf{E}^{-1}\mathbf{B}s^{-i}}_{\bar{M}_i} - \dots \quad (2.129)$$

and in this case the non-negative coefficients are the, so called, Markov parameters, which are defined under the assumption of \mathbf{E} being non singular:

$$\mathbb{R}^{p \times k} \ni \bar{M}_i := \mathbf{C}(\mathbf{E}^{-1}\mathbf{A})^i\mathbf{E}^{-1}\mathbf{B}, \quad i = 1, 2, \dots. \quad (2.130)$$

The general concept of MOR for first-order dynamical systems (Eq. (2.124) - (2.125)) is similar to the approach presented in Eq. (2.38) - (2.39). Therefore, the aim is to find a certain subspace $\mathbf{T}_r \in \mathbb{R}^{N \times q}$ with $q \ll N$ in order to approximate the state space vector \mathbf{z} of the original system as well as possible, i.e.

$$\mathbf{z} \approx \mathbf{T}_r \mathbf{z}_R, \quad (2.131)$$

and thereafter to project the dynamical system onto the subspace spanned by another coordinate transformation matrix $\mathbf{T}_l \in \mathbb{R}^{N \times q}$:

$$\mathbf{T}_l^T \mathbf{E} \mathbf{T}_r \dot{\mathbf{z}}_R = \mathbf{T}_l^T \mathbf{A} \mathbf{T}_r \mathbf{z}_R + \mathbf{T}_l^T \mathbf{B} \mathbf{u} \quad (2.132)$$

$$\mathbf{y}(t) = \mathbf{C} \mathbf{T}_r \mathbf{z}_R. \quad (2.133)$$

For symmetric systems it is typical to choose the projection matrices \mathbf{T}_l and \mathbf{T}_r to be identical, i.e. $\mathbf{T}_l \equiv \mathbf{T}_r$ and thus, the MOR is referred to as a one-sided MOR. Nevertheless, for the preceding relationships the general case of the two-sided MOR will be considered, whereas a simplified version of the MIMO case will be regarded, namely, the SISO systems, i.e. $\mathbf{B} \equiv \mathbf{b}$, $\mathbf{C} \equiv \mathbf{c}^T$, $\mathbf{u} \equiv u$ and $\mathbf{y} \equiv y$. On this account, the system information of the ROM is obtained:

$$[]_R = \mathbf{T}_l^T \cdot [] \cdot \mathbf{T}_r, \quad []_R := \{\mathbf{E}, \mathbf{A}\} \quad \text{and} \quad \mathbf{b}_R = \mathbf{T}_l^T \mathbf{b}, \quad \mathbf{c}_R^T = \mathbf{c}^T \mathbf{T}_r. \quad (2.134)$$

Analogously to the relationships in Eq. (2.126) - (2.130), the transfer function, the moments and the Markov parameters of the associated ROM can be defined. The KSM algorithm provides certain Krylov subspaces (Eq. (2.114)) for the assignment of the \mathbf{T}_l and \mathbf{T}_r projection matrices, such that the moments and Markov parameters of the original and the ROM match. A close observation on the definition of these two quantities leads to the conclusion for the first to be reflecting the dynamic behavior of a system at a low frequency range, whereas the latter the dynamic behavior at high frequencies. In this Thesis, the main interest resides on the low frequency range and thus, for the following proofs only the moment matching case will be considered.

On the basis of the aforesaid, the following **Theorem 2.1** is stated as given in SALIMBAHRAWI [107], which shows that the basis vectors of suitable Krylov subspaces can be utilized in the MOR projection scheme of Eq. (2.132) - (2.133):

Theorem 2.1 *If the columns of the matrices \mathbf{T}_l and \mathbf{T}_r constitute the basis vectors of the Krylov subspaces $K_q(\mathbf{A}^{-1}\mathbf{E}, \mathbf{A}^{-1}\mathbf{b})$ and $K_q(\mathbf{A}^{-T}\mathbf{E}^T, \mathbf{A}^{-T}\mathbf{c})$, respectively, then the first $2q$ moments of the original and the ROM match, i.e. $\bar{m}_{R,i} = \bar{m}_i$, $\forall i \in [0, 2q-1]$. Herein, it is assumed that \mathbf{A} and \mathbf{A}_R are non singular matrices.*

The proof of the above mentioned theorem is straightforward based on the induction procedure and will be divided into three parts. Firstly, it will be proved that the first q moments of both the original and the ROM match in case of the input Krylov subspace $K_q^{\text{input}} = K_q(\mathbf{A}^{-1}\mathbf{E}, \mathbf{A}^{-1}\mathbf{b})$ and a random matrix \mathbf{T}_l , which fulfills the non singularity conditions of \mathbf{A} and \mathbf{A}_R . Secondly, the analogous proof will be regarded for the associated output Krylov subspace $K_q^{\text{output}} = K_q(\mathbf{A}^{-T}\mathbf{E}^T, \mathbf{A}^{-T}\mathbf{c})$ and an equivalent projection matrix \mathbf{T}_r under the same \mathbf{A} and \mathbf{A}_R inversion assumptions. Finally, both outcomes will be used for the total moment matching properties.

Regarding the first part, the validity of the following relationship should be proved:

$$\mathbf{c}^T \mathbf{T}_r (\mathbf{A}_R^{-1} \mathbf{E}_R)^i \mathbf{A}_R^{-1} \mathbf{b}_R = \mathbf{c}^T (\mathbf{A}^{-1} \mathbf{E})^i \mathbf{A}^{-1} \mathbf{b}, \quad \forall i \in [0, q-1] \quad \text{and} \quad \mathbf{T}_r \in K_q^{\text{input}}. \quad (2.135)$$

For $i = 0$, the first part of Eq. (2.135) is reformulated taking into account that the

vector $\mathbf{A}^{-1}\mathbf{b} \in K_0^{\text{input}}$, i.e.

$$\exists \mathbf{r}_0 \in \mathbb{R}^{q \times 1} : \mathbf{A}^{-1}\mathbf{b} = \mathbf{T}_r \mathbf{r}_0 \quad (2.136)$$

$$\mathbf{c}^T \mathbf{T}_r \mathbf{A}_R^{-1} \mathbf{b}_R \stackrel{(2.134)}{=} \mathbf{c}^T \mathbf{T}_r (\mathbf{T}_l^T \mathbf{A} \mathbf{T}_r)^{-1} \mathbf{T}_l^T \mathbf{b} = \mathbf{c}^T \mathbf{T}_r (\mathbf{T}_l^T \mathbf{A} \mathbf{T}_r)^{-1} \mathbf{T}_l^T (\mathbf{A} \mathbf{A}^{-1}) \mathbf{b} \quad (2.137)$$

$$\stackrel{(2.136)}{=} \mathbf{c}^T \mathbf{T}_r (\mathbf{T}_l^T \mathbf{A} \mathbf{T}_r)^{-1} \mathbf{T}_l^T \mathbf{A} \mathbf{T}_r \mathbf{r}_0 = \mathbf{c}^T \mathbf{T}_r \mathbf{r}_0 = \mathbf{c}^T \mathbf{A}^{-1} \mathbf{b} \quad (2.138)$$

According to the induction algorithm, if the relationship in Eq. (2.135) holds for $i = 0, 1, \dots, k$, then it should be proved that it holds for $i = k + 1$:

$$\bar{m}_{R,i} = \mathbf{c}^T \mathbf{T}_r (\mathbf{A}_R^{-1} \mathbf{E}_R)^{k+1} \mathbf{A}_R^{-1} \mathbf{b}_R \quad (2.139)$$

$$= \mathbf{c}^T \mathbf{T}_r \mathbf{A}_R^{-1} \mathbf{E}_R (\mathbf{A}_R^{-1} \mathbf{E}_R)^k \mathbf{A}_R^{-1} \mathbf{b}_R \quad (2.140)$$

$$\stackrel{(2.134)}{=} \mathbf{c}^T \mathbf{T}_r (\mathbf{T}_l^T \mathbf{A} \mathbf{T}_r)^{-1} \mathbf{T}_l^T \mathbf{E} \mathbf{T}_r (\mathbf{A}_R^{-1} \mathbf{E}_R)^k \mathbf{A}_R^{-1} \mathbf{b}_R \quad (2.141)$$

$$\stackrel{k\text{-induction}}{=} \mathbf{c}^T \mathbf{T}_r (\mathbf{T}_l^T \mathbf{A} \mathbf{T}_r)^{-1} \mathbf{T}_l^T \mathbf{E} (\mathbf{A}^{-1} \mathbf{E})^k \mathbf{A}^{-1} \mathbf{b} \quad (2.142)$$

$$= \mathbf{c}^T \mathbf{T}_r (\mathbf{T}_l^T \mathbf{A} \mathbf{T}_r)^{-1} \underbrace{\mathbf{T}_l^T \mathbf{A} (\mathbf{A}^{-1} \mathbf{E})^{k+1} \mathbf{A}^{-1} \mathbf{b}}_{\in K_{k+1}^{\text{input}}} \quad (2.143)$$

$$= \mathbf{c}^T \mathbf{T}_r (\mathbf{T}_l^T \mathbf{A} \mathbf{T}_r)^{-1} \mathbf{T}_l^T \mathbf{A} \mathbf{T}_r \mathbf{r}_{k+1} \quad (2.144)$$

$$= \mathbf{c}^T (\mathbf{A}^{-1} \mathbf{E})^{k+1} \mathbf{A}^{-1} \mathbf{b} = \bar{m}_i, \quad (2.145)$$

where in Eq. (2.143) the under braced vector belongs to the K_{k+1}^{input} subspace and thus, it can be written as a linear combination of the columns of \mathbf{T}_r , i.e.

$$\exists \mathbf{r}_{k+1} \in \mathbb{R}^{q \times 1} : (\mathbf{A}^{-1} \mathbf{E})^{k+1} \mathbf{A}^{-1} \mathbf{b} = \mathbf{T}_r \mathbf{r}_{k+1}. \quad (2.146)$$

The proof of the second part is conducted in an analogous way and an equivalent relationship for $\mathbf{T}_l \in K_q^{\text{input}}$ and a random matrix \mathbf{T}_r is derived:

$$\mathbf{c}_R^T (\mathbf{A}_R^{-1} \mathbf{E}_R)^i \mathbf{A}_R^{-1} \mathbf{T}_l^T \mathbf{b} = \mathbf{c}^T (\mathbf{A}^{-1} \mathbf{E})^i \mathbf{A}^{-1} \mathbf{b}, \quad \forall i \in [0, q-1] \quad \text{and} \quad \mathbf{T}_l \in K_q^{\text{output}} \quad (2.147)$$

The final part, which completes the statement of **Theorem 2.1** is accomplished by utilizing the relationships obtained in Eq. (2.145) and Eq. (2.147). Herewith, it will be shown that $\forall i \in [0, 2q-1]$ the first $2q$ moments of the original and the ROM match:

$$\bar{m}_{R,i} = \mathbf{c}_R^T (\mathbf{A}_R^{-1} \mathbf{E}_R)^i \mathbf{A}_R^{-1} \mathbf{b}_R \quad (2.148)$$

$$= \mathbf{c}_R^T (\mathbf{A}_R^{-1} \mathbf{E}_R)^{i-q} (\mathbf{A}_R^{-1} \mathbf{E}_R) (\mathbf{A}_R^{-1} \mathbf{E}_R)^{q-1} \mathbf{A}_R^{-1} \mathbf{b}_R \quad (2.149)$$

$$\stackrel{(2.134)}{=} \underbrace{\mathbf{c}_R^T (\mathbf{A}_R^{-1} \mathbf{E})^{i-q} \mathbf{A}_R^{-1} \mathbf{T}_l^T}_{(2.147)} \underbrace{\mathbf{E} \mathbf{T}_r (\mathbf{A}_R^{-1} \mathbf{E}_R)^{q-1} \mathbf{A}_R^{-1} \mathbf{b}_R}_{(2.145)} \quad (2.150)$$

$$= \mathbf{c}^T (\mathbf{A}^{-1} \mathbf{E})^{i-q} \mathbf{A}^{-1} \mathbf{E} (\mathbf{A}^{-1} \mathbf{E})^{q-1} \mathbf{A}^{-1} \mathbf{b} = \mathbf{c}^T (\mathbf{A}^{-1} \mathbf{E})^i \mathbf{b} = \bar{m}_i. \quad (2.151)$$

Eq. (2.135)-(2.151) give the full proof of **Theorem 2.1** concerning the general two-sided KSM MOR and thus, the projection matrices in Eq. (2.132) - (2.133) are defined based on the aforementioned input and output Krylov subspaces. At this point, the KSM reduction scheme requires a numerically stable algorithm, which allows the accurate computation of the basis vectors of K_q^{input} and K_q^{output} . It is accomplished by utilizing either the ARNOLDI [8] or the LANCZOS [75] algorithms, with the first being more suitable for one-sided MOR approaches, whereas the latter for the two-sided version.

The MOR concept presented in Eq. (2.38) - (2.39) requires the application of an equivalent one-sided MOR approach. On this account, only the ARNOLDI method will be considered, the algorithm of which is given below. Here, the basis vector computation $\mathbf{V}_q = [\mathbf{v}_1 \ \mathbf{v}_2 \ \dots \ \mathbf{v}_q] \in K_q(\tilde{\mathbf{A}}, \tilde{\mathbf{b}})$ (Eq. (2.114)) is demonstrated:

1. $i = 1$: Normalize the starting vector $\tilde{\mathbf{b}}$, i.e.

$$\mathbf{v}_1 = \frac{\tilde{\mathbf{b}}}{\sqrt{\tilde{\mathbf{b}}^T \tilde{\mathbf{b}}}} = \frac{\tilde{\mathbf{b}}}{\|\tilde{\mathbf{b}}\|_2} \quad (2.152)$$

2. *FOR* $i = 2, 3, \dots, q$ *DO*

- (a) Calculate the next basis vector, i.e.

$$\hat{\mathbf{v}}_i = \mathbf{A}\mathbf{v}_{i-1} \quad (2.153)$$

- (b) Gram-Schmidt orthogonalization: *FOR* $j = 1$ to $i-1$

$$\mathbf{h}_{j,i-1} = \hat{\mathbf{v}}_i^T \mathbf{v}_j \quad (2.154)$$

$$\hat{\mathbf{v}}_i = \hat{\mathbf{v}}_i - \mathbf{h}_{j,i-1} \mathbf{v}_j \quad (2.155)$$

- (c) Normalization: *BREAK* the loop *IF* $\hat{\mathbf{v}}_i = \mathbf{0}$ *ELSE*

$$\mathbf{v}_i = \frac{\hat{\mathbf{v}}_i}{\sqrt{\hat{\mathbf{v}}_i^T \hat{\mathbf{v}}_i}} \quad (2.156)$$

- (d) *END IF* $i = q$ *ELSE* go to step (a) and increase i .

The Gram-Schmidt orthogonalization (Eq. (2.154) - (2.155)) and the normalization step in Eq. (2.156) assure that the column vectors of \mathbf{V}_q are normalized and orthogonal to each other, i.e.

$$\mathbf{V}_q^T \mathbf{V}_q = \mathbf{I}^{q \times q}. \quad (2.157)$$

In case of the term q , which indicates the dimension of the ROM, being large enough, the ARNOLDI algorithm might generate vectors, which are not linearly independent. Therefore, several deflation techniques [24] exist, based on which the linear dependent vectors are stepwise deleted during the iteration scheme.

The shortly outlined first-order moment-matching KSM MOR theory constitutes the basis, according to which the second-order KSM MOR is developed.

2.6.2 Second order Krylov Subspace method

In this Subsection an equivalent formulation of the classical second-order ODEs in Eq. (2.37) is considered, i.e.

$$\mathbf{M}\ddot{\mathbf{z}} + \mathbf{D}\dot{\mathbf{z}} + \mathbf{K}\mathbf{z} = \mathbf{Qu} \quad (2.158)$$

$$\mathbf{y} = \mathbf{L}\mathbf{z}, \quad (2.159)$$

where the terms \mathbf{y} and \mathbf{L} are defined analogously to the terms in Eq. (2.125). The right hand side of Eq. (2.158) can be regarded as the applied force vector $\mathbf{F} = \mathbf{Qu} \in \mathbb{R}^{n \times 1}$. It consists of the scatter matrix $\mathbf{Q} \in \mathbb{R}^{n \times p}$, which allocates the designated input u in the domain of the FE structure, and the input vector $\mathbf{u} \in \mathbb{R}^{p \times 1}$.

Several realizations of Eq. (2.158) - (2.159) exist, which allow the description of the second-order system as a set of first-order ODEs [107]. For the purpose of the preceding proofs, the following realization will be used (Eq. (2.160) - (2.161)) and according to its structure the matrix notations of Eq. (2.124) - (2.125) are adopted, i.e.

$$\underbrace{\begin{pmatrix} -\mathbf{K} & \mathbf{0} \\ \mathbf{0} & \mathbf{M} \end{pmatrix}}_{\mathbf{E}} \underbrace{\begin{pmatrix} \dot{\mathbf{z}} \\ \ddot{\mathbf{z}} \end{pmatrix}}_{\dot{\mathbf{x}}} = \underbrace{\begin{pmatrix} \mathbf{0} & -\mathbf{K} \\ -\mathbf{K} & -\mathbf{D} \end{pmatrix}}_{\mathbf{A}} \underbrace{\begin{pmatrix} \mathbf{z} \\ \dot{\mathbf{z}} \end{pmatrix}}_{\mathbf{x}} + \underbrace{\begin{pmatrix} \mathbf{0} \\ \mathbf{Q} \end{pmatrix}}_{\mathbf{B}} \mathbf{u} \quad (2.160)$$

$$\mathbf{y} = \underbrace{[\mathbf{L} \ \mathbf{0}]}_{\mathbf{C}} \begin{pmatrix} \mathbf{z} \\ \dot{\mathbf{z}} \end{pmatrix} \quad (2.161)$$

Here (Eq. (2.160) - (2.161)), the dimension of the system matrices is twice as large as the dimension of the associated system matrices in the second-order form (Eq. (2.158) - (2.159)):

$$\{\mathbf{E}, \mathbf{A}\} \in \mathbb{R}^{N \times N} \quad \text{and} \quad \mathbf{B} \in \mathbb{R}^{N \times k}, \quad \mathbf{C} \in \mathbb{R}^{p \times N} \quad \text{with} \quad N = 2n. \quad (2.162)$$

As already mentioned in the introductory part of this Section, the direct application of the first-order KSM techniques for reducing second-order systems, i.e. the associated first-order realizations, is not advised. In order to assure the preservation of the ROM's structure properties the structure of the associated moments should be exploited. According to the definition in Eq. (2.128), the moments of the system described in Eq. (2.160) - (2.161) are ascertained:

$$\bar{m}_i = [\mathbf{L} \ \mathbf{0}] \left[\begin{pmatrix} \mathbf{0} & -\mathbf{K} \\ -\mathbf{K} & -\mathbf{D} \end{pmatrix}^{-1} \begin{pmatrix} -\mathbf{K} & \mathbf{0} \\ \mathbf{0} & \mathbf{M} \end{pmatrix} \right]^i \begin{pmatrix} \mathbf{0} & -\mathbf{K} \\ -\mathbf{K} & -\mathbf{D} \end{pmatrix}^{-1} \begin{pmatrix} \mathbf{0} \\ \mathbf{Q} \end{pmatrix} \quad (2.163)$$

$$= [\mathbf{L} \ \mathbf{0}] \begin{pmatrix} -\mathbf{K}^{-1}\mathbf{D} & -\mathbf{K}^{-1}\mathbf{M} \\ \mathbf{I} & \mathbf{0} \end{pmatrix}^i \begin{pmatrix} -\mathbf{K}^{-1}\mathbf{Q} \\ \mathbf{0} \end{pmatrix}, \quad (2.164)$$

where in Eq. (2.163) the matrix inverse \mathbf{A}^{-1} is computed with the help of the relationship:

$$\mathbf{A}^{-1} = \begin{pmatrix} \mathbf{0} & -\mathbf{K} \\ -\mathbf{K} & -\mathbf{D} \end{pmatrix}^{-1} = \begin{pmatrix} \mathbf{K}^{-1}\mathbf{D}\mathbf{K}^{-1} & -\mathbf{K}^{-1} \\ -\mathbf{K}^{-1} & \mathbf{0} \end{pmatrix}. \quad (2.165)$$

In Eq. (2.128) the necessary condition for the definition of the system's moments is the non-singularity of the system matrix \mathbf{A} . In view of the \mathbf{A}^{-1} definition in Eq. (2.165), the analogous necessary condition for the system in Eq. (2.160) - (2.161) is the non-singularity of the \mathbf{K} stiffness matrix.

The system information of the ROM is obtained in the same way as presented in Eq. (2.38) - (2.39) and Eq. (2.131) - (2.132). Once more, the general two-sided MOR approach is regarded, i.e. the definition of two coordinate transformation matrices is necessary. On that basis, the ROM can be written in the realization form of Eq. (2.160) - (2.161), i.e.

$$\underbrace{\begin{pmatrix} -\mathbf{K}_R & \mathbf{0} \\ \mathbf{0} & \mathbf{M}_R \end{pmatrix}}_{\mathbf{E}_R} \underbrace{\begin{pmatrix} \dot{\mathbf{z}} \\ \ddot{\mathbf{z}} \end{pmatrix}}_{\dot{\mathbf{x}}_R} = \underbrace{\begin{pmatrix} \mathbf{0} & -\mathbf{K}_R \\ -\mathbf{K}_R & -\mathbf{D}_R \end{pmatrix}}_{\mathbf{A}_R} \underbrace{\begin{pmatrix} \mathbf{z} \\ \dot{\mathbf{z}} \end{pmatrix}}_{\mathbf{x}_R} + \underbrace{\begin{pmatrix} \mathbf{0} \\ \mathbf{Q}_R \end{pmatrix}}_{\mathbf{B}_R} \mathbf{u} \quad (2.166)$$

$$\mathbf{y} = \underbrace{[\mathbf{L}_R \ \mathbf{0}]}_{\mathbf{C}_R} \begin{pmatrix} \mathbf{z} \\ \dot{\mathbf{z}} \end{pmatrix}, \quad (2.167)$$

with the second-order system matrices and vectors being defined as given in the following relationships:

$$[]_R = \mathbf{T}_l^T \cdot [] \cdot \mathbf{T}_r, \quad [] := \{\mathbf{M}, \ \mathbf{D}, \ \mathbf{K}\} \quad \text{and} \quad \mathbf{Q}_R = \mathbf{T}_l^T \mathbf{Q}, \quad \mathbf{L}_R = \mathbf{L} \mathbf{T}_r. \quad (2.168)$$

The expansion of the system matrices in Eq. (2.166) - (2.167) with the help of the ROM data in Eq. (2.168) results in the calculation of the projection matrices, which are suitable for directly reducing the order of the realization system in Eq. (2.160) - (2.161), i.e.

$$\overline{\mathbf{T}}_r = \begin{pmatrix} \mathbf{T}_r & \mathbf{0} \\ \mathbf{0} & \mathbf{T}_r \end{pmatrix} \in \mathbb{R}^{N \times 2q} \quad \text{and} \quad \overline{\mathbf{T}}_l = \begin{pmatrix} \mathbf{T}_l & \mathbf{0} \\ \mathbf{0} & \mathbf{T}_l \end{pmatrix} \in \mathbb{R}^{N \times 2q} \quad (2.169)$$

The aim of the second-order KSM algorithm is to match a certain number of moments for the original and the reduced realization. This moment-matching procedure is feasible due to the introduction of the, so called, second-order Krylov subspaces [107, 4], the definition of which is given below:

$$K_{q,2} := K_q(\mathbf{A}_1, \mathbf{A}_2, \mathbf{B}_1) = \text{span} \{ \mathbf{P}_0, \mathbf{P}_1, \dots, \mathbf{P}_{q-1} \}. \quad (2.170)$$

Here, $\{\mathbf{A}_1, \mathbf{A}_2\} \in \mathbb{R}^{n \times n}$ and $\mathbf{B}_1 \in \mathbb{R}^{n \times k}$ are constant matrices with the columns of the latter being referred to as the starting vectors, and \mathbf{P}_i are the basic blocks, for which it

holds:

$$\mathbf{P}_0 = \mathbf{B}_1, \quad \mathbf{P}_1 = \mathbf{A}_1 \mathbf{P}_0, \quad \mathbf{P}_i = \mathbf{A}_1 \mathbf{P}_{i-1} + \mathbf{A}_2 \mathbf{P}_{i-2}, \quad i = 2, 3, \dots, q. \quad (2.171)$$

Thus, the second order input $K_{q,2}^{\text{input}} := K_q(-\mathbf{K}^{-1}\mathbf{D}, -\mathbf{K}^{-1}\mathbf{M}, -\mathbf{K}^{-1}\mathbf{Q})$ and output $K_{q,2}^{\text{output}} := K_q(-\mathbf{K}^{-T}\mathbf{D}^T, -\mathbf{K}^{-T}\mathbf{M}^T, -\mathbf{K}^{-T}\mathbf{L}^T)$ Krylov subspaces are introduced, the basic blocks \mathbf{P}_i of which are directly connected to the definition of moments (Eq. (2.164)) via the relationship:

$$\underbrace{[\mathbf{L} \ \mathbf{0}] \begin{pmatrix} -\mathbf{K}^{-1}\mathbf{D} & -\mathbf{K}^{-1}\mathbf{M} \\ \mathbf{I} & \mathbf{0} \end{pmatrix}}_{\bar{m}_i}^i \begin{pmatrix} -\mathbf{K}^{-1}\mathbf{Q} \\ \mathbf{0} \end{pmatrix} = \underbrace{[\mathbf{L} \ \mathbf{0}] \begin{pmatrix} \mathbf{P}_i \\ \mathbf{P}_{i-1} \end{pmatrix}}_{\mathbf{LP}_i}, \quad \forall i \in [1, q]. \quad (2.172)$$

According to the procedure of the first-order KSM MOR, a statement analogous to the **Theorem 2.1** follows as given in SALIMBAHRAWI [107], which shows that the basis vectors of the $K_{q,2}^{\text{input}}$ and $K_{q,2}^{\text{output}}$ subspaces can be utilized in the MOR scheme of Eq. (2.160) - (2.161).

Theorem 2.2 *If the columns of the matrices \mathbf{T}_l and \mathbf{T}_r constitute the basis vectors of the Krylov subspaces $K_{q,2}^{\text{input}} := K_q(-\mathbf{K}^{-1}\mathbf{D}, -\mathbf{K}^{-1}\mathbf{M}, -\mathbf{K}^{-1}\mathbf{Q})$ and $K_{q,2}^{\text{output}} := K_q(-\mathbf{K}^{-T}\mathbf{D}^T, -\mathbf{K}^{-T}\mathbf{M}^T, -\mathbf{K}^{-T}\mathbf{L}^T)$, respectively, then the first $2q$ moments of the original and the ROM match, i.e. $\bar{m}_{R,i} = \bar{m}_i$, $\forall i \in [0, 2q-1]$. Herein, it is assumed that \mathbf{K} and \mathbf{K}_R are non singular matrices.*

The proof of **Theorem 2.2** is conducted accordingly to the proof of **Theorem 2.1**. Firstly, it is proved that the first q moments of both the original and the ROM match in case of the second-order input Krylov subspace $K_{q,2}^{\text{input}}$ and a random projection matrix \mathbf{T}_l , which fulfills the non singularity conditions of \mathbf{K} and \mathbf{K}_R . Secondly, the analogous proof is regarded for the associated second-order output Krylov subspace $K_{q,2}^{\text{output}}$ and an equivalent projection matrix \mathbf{T}_r under the same \mathbf{K} and \mathbf{K}_R inversion assumptions. Finally, both outcomes are combined for the total moment matching properties.

Regarding the first part, the validity of the following relationship should be proved:

$$\bar{m}_i = \bar{m}_{R,i} \stackrel{(2.172)}{\Leftrightarrow} \mathbf{LP}_i = \mathbf{L}_R \mathbf{P}_{R,i} \stackrel{(2.168)}{\Leftrightarrow} \mathbf{P}_i = \mathbf{T}_r \mathbf{P}_{R,i}, \quad \forall i \in [0, q-1], \quad (2.173)$$

which should hold for the three basic block types defined in Eq. (2.171). Therefore, the definition of the basic blocks \mathbf{P}_i for the ROM are taken into consideration, i.e.

$$\mathbf{P}_{R,0} = -\mathbf{K}_R^{-1}\mathbf{Q}_R \quad (2.174)$$

$$\mathbf{P}_{R,1} = -\mathbf{K}_R^{-1}\mathbf{D}_R \mathbf{P}_{R,0} = \mathbf{K}_R^{-1}\mathbf{D}_R \mathbf{K}_R^{-1}\mathbf{Q}_R \quad (2.175)$$

$$\mathbf{P}_{R,i} = -\mathbf{K}_R^{-1}\mathbf{D}_R \mathbf{P}_{R,i-1} - \mathbf{K}_R^{-1}\mathbf{M}_R \mathbf{P}_{R,i-2}, \quad i = 2, 3, \dots, q-1. \quad (2.176)$$

On this account, Eq. (2.173) is reformulated in terms of the first basic block $\mathbf{P}_{R,0}$ of

the ROM as follows:

$$\mathbf{T}_r \mathbf{P}_{R,0} \stackrel{(2.174)}{=} -\mathbf{T}_r \mathbf{K}_R^{-1} \mathbf{Q}_R \stackrel{(2.168)}{=} -\mathbf{T}_r (\mathbf{T}_l^T \mathbf{K} \mathbf{T}_r)^{-1} \mathbf{T}_l^T \mathbf{Q} \quad (2.177)$$

$$= \mathbf{T}_r (\mathbf{T}_l^T \mathbf{K} \mathbf{T}_r)^{-1} \mathbf{T}_l^T \mathbf{K} \underbrace{(\mathbf{K}^{-1} \mathbf{Q})}_{\mathbf{P}_0} \quad (2.178)$$

$$= \mathbf{T}_r (\mathbf{T}_l^T \mathbf{K} \mathbf{T}_r)^{-1} \mathbf{T}_l^T \mathbf{K} \underbrace{\mathbf{P}_0}_{\in K_{0,2}^{\text{input}}} \quad (2.179)$$

$$= \mathbf{T}_r (\mathbf{T}_l^T \mathbf{K} \mathbf{T}_r)^{-1} \mathbf{T}_l^T \mathbf{K} \mathbf{T}_r \mathbf{R}_0 = \mathbf{T}_r \mathbf{R}_0 \stackrel{(2.181)}{=} \mathbf{P}_0, \quad (2.180)$$

where in Eq. (2.179) the under braced vector \mathbf{P}_0 belongs to the $K_{0,2}^{\text{input}}$ subspace and thus, it can be written as a linear combination of the columns of \mathbf{T}_r , i.e.

$$\exists \mathbf{R}_0 \in \mathbb{R}^{q \times k} : \mathbf{P}_0 = \mathbf{T}_r \mathbf{R}_0. \quad (2.181)$$

The validity of Eq. (2.173) regarding the second basic block \mathbf{P}_1 is proved analogously, i.e.

$$\mathbf{T}_r \mathbf{P}_{R,1} \stackrel{(2.174)}{=} -\mathbf{T}_r \mathbf{K}_R^{-1} \mathbf{D}_R \mathbf{P}_{R,0} \stackrel{(2.168)}{=} -\mathbf{T}_r (\mathbf{T}_l^T \mathbf{K} \mathbf{T}_r)^{-1} \mathbf{T}_l^T \mathbf{D} \mathbf{T}_r \mathbf{P}_{R,0} \quad (2.182)$$

$$\stackrel{(2.180)}{=} -\mathbf{T}_r (\mathbf{T}_l^T \mathbf{K} \mathbf{T}_r)^{-1} \mathbf{T}_l^T \mathbf{D} \mathbf{P}_0 \quad (2.183)$$

$$= \mathbf{T}_r (\mathbf{T}_l^T \mathbf{K} \mathbf{T}_r)^{-1} \mathbf{T}_l^T \mathbf{K} \underbrace{(-\mathbf{K}^{-1} \mathbf{D} \mathbf{P}_0)}_{\mathbf{P}_1} \quad (2.184)$$

$$= \mathbf{T}_r (\mathbf{T}_l^T \mathbf{K} \mathbf{T}_r)^{-1} \mathbf{T}_l^T \mathbf{K} \underbrace{\mathbf{P}_1}_{\in K_{1,2}^{\text{input}}} \quad (2.185)$$

$$= \mathbf{T}_r (\mathbf{T}_l^T \mathbf{K} \mathbf{T}_r)^{-1} \mathbf{T}_l^T \mathbf{K} \mathbf{T}_r \mathbf{R}_1 \stackrel{(2.187)}{=} \mathbf{P}_1, \quad (2.186)$$

where in Eq. (2.185) the under braced vector \mathbf{P}_1 belongs to the $K_{1,2}^{\text{input}}$ subspace and is defined analogously to the term in Eq. (2.181):

$$\exists \mathbf{R}_1 \in \mathbb{R}^{q \times k} : \mathbf{P}_1 = \mathbf{T}_r \mathbf{R}_1. \quad (2.187)$$

At this point, the induction algorithm is invoked and it is assumed that Eq. (2.173) holds for $i = k$, i.e.

$$\mathbf{P}_k = \mathbf{T}_r \mathbf{P}_{R,k}, \quad \forall i \in [0, k]. \quad (2.188)$$

Furthermore, the equivalent definition of the basic blocks \mathbf{P}_i for the original model gives

$$\mathbf{P}_0 = -\mathbf{K}^{-1} \mathbf{Q} \quad (2.189)$$

$$\mathbf{P}_1 = -\mathbf{K}^{-1} \mathbf{D} \mathbf{P}_0 = \mathbf{K}^{-1} \mathbf{D} \mathbf{K}^{-1} \mathbf{Q} \quad (2.190)$$

$$\mathbf{P}_{k+1} = -\mathbf{K}^{-1} \mathbf{D} \mathbf{P}_k - \mathbf{K}^{-1} \mathbf{M} \mathbf{P}_{k-1}, \quad i = 2, 3, \dots, q-1. \quad (2.191)$$

If it is proved that Eq. (2.173) holds for $i = k + 1$, then the first part of **Theorem 2.2**

is proved. On that basis, the following relationships are obtained for $i = k + 1$:

$$\mathbf{T}_r \mathbf{P}_{R,k+1} \stackrel{(2.191)}{=} \mathbf{T}_r (-\mathbf{K}_R^{-1} \mathbf{D}_R \mathbf{P}_{R,k} - \mathbf{K}_R^{-1} \mathbf{M}_R \mathbf{P}_{R,k-1}) \quad (2.192)$$

$$\stackrel{(2.180)}{=} \mathbf{T}_r \left(-(\mathbf{T}_l^T \mathbf{K} \mathbf{T}_r)^{-1} \mathbf{T}_l^T \mathbf{D} \mathbf{T}_r \mathbf{P}_{R,k} - (\mathbf{T}_l^T \mathbf{K} \mathbf{T}_r)^{-1} \mathbf{T}_l^T \mathbf{M} \mathbf{T}_r \mathbf{P}_{R,k-1} \right) \quad (2.193)$$

$$\stackrel{(2.188)}{=} \mathbf{T}_r \left(-(\mathbf{T}_l^T \mathbf{K} \mathbf{T}_r)^{-1} \mathbf{T}_l^T \mathbf{D} \mathbf{P}_k - (\mathbf{T}_l^T \mathbf{K} \mathbf{T}_r)^{-1} \mathbf{T}_l^T \mathbf{M} \mathbf{P}_{k-1} \right) \quad (2.194)$$

$$= \mathbf{T}_r (\mathbf{T}_l^T \mathbf{K} \mathbf{T}_r)^{-1} \mathbf{T}_l^T \mathbf{K} (-\mathbf{K}^{-1} \mathbf{D} \mathbf{P}_k - \mathbf{K}^{-1} \mathbf{M} \mathbf{P}_{k-1}) \quad (2.195)$$

$$\stackrel{(2.191)}{=} \mathbf{T}_r (\mathbf{T}_l^T \mathbf{K} \mathbf{T}_r)^{-1} \mathbf{T}_l^T \mathbf{K} \underbrace{\mathbf{P}_{k+1}}_{K_{k+1,2}^{\text{input}}} \quad (2.196)$$

$$= \mathbf{T}_r (\mathbf{T}_l^T \mathbf{K} \mathbf{T}_r)^{-1} \mathbf{T}_l^T \mathbf{K} \mathbf{T}_r \mathbf{R}_k = \mathbf{T}_r \mathbf{R}_{k+1} = \mathbf{P}_{k+1} \quad (2.197)$$

The second part of the proof is conducted in the same way, since it can be regarded as the dual formulation of the first part. The proof of **Theorem 2.2** is completed by combining the moment matching relationships for both the input and output second-order Krylov subspaces. It is accomplished by following exactly the same scheme presented in Eq. (2.148) - (2.151). The ROM data therefor, i.e. the reduced system matrices \mathbf{E}_R , \mathbf{A}_R and \mathbf{C}_R are defined in Eq. (2.166) - (2.169).

The characteristic of symmetry for the system matrices in Eq. (2.158) - (2.159), i.e.

$$[]^T = [], [] = \{\mathbf{M}, \mathbf{K}, \mathbf{D}\} \quad (2.198)$$

allows the application of the one-sided MOR version, i.e. $\mathbf{T}_l \equiv \mathbf{T}_r \in K_{q,2}^{\text{input}}$. On this account, an extension of the classical ARNOLDI algorithm is utilized, namely, the second-order ARNOLDI method, with which the basis vectors $\mathbf{V}_q = [\mathbf{v}_1 \ \mathbf{v}_2 \ \dots \ \mathbf{v}_q] \in K_{q,2}^{\text{input}}$ of the second-order input Krylov subspace are computed. For simplicity, the following notation for the basic blocks of $K_{q,2}^{\text{input}}$ is adopted:

$$\overline{[]] := -\mathbf{K}^{-1} \cdot [], [] = \{\mathbf{M}, \mathbf{D}, \mathbf{Q}\} \quad (2.199)$$

and under this consideration the second-order ARNOLDI algorithm [107] is given below:

1. $i = 1$: Set $\mathbf{g}_1 = \mathbf{0}$ and normalize the starting vector \mathbf{q} , i.e.

$$\mathbf{v}_1 = \frac{\mathbf{q}}{\sqrt{\mathbf{q}^T \mathbf{q}}} = \frac{\mathbf{q}}{\|\mathbf{q}\|_2} \quad (2.200)$$

2. *FOR* $i = 2, 3, \dots, q$ *DO*

- (a) Calculate the next basis vector, i.e.

$$\hat{\mathbf{v}}_i = \overline{\mathbf{D} \mathbf{v}_{i-1} + \overline{\mathbf{M}} \mathbf{g}_{i-1}}, \quad \hat{\mathbf{g}}_i = \mathbf{v}_{i-1} \quad (2.201)$$

(b) Gram-Schmidt orthogonalization: *FOR* $j = 1$ to $i - 1$

$$\mathbf{h}_{j,i-1} = \hat{\mathbf{v}}_i^T \mathbf{v}_j \quad (2.202)$$

$$\hat{\mathbf{v}}_i = \hat{\mathbf{v}}_i - \mathbf{h}_{j,i-1} \mathbf{v}_j, \quad \hat{\mathbf{g}}_i = \hat{\mathbf{g}}_i - \mathbf{h}_{j,i-1} \mathbf{g}_j \quad (2.203)$$

(c) Normalization: *BREAK* the loop *IF* $\hat{\mathbf{v}}_i = \mathbf{0}$ *ELSE*

$$\mathbf{v}_i = \frac{\hat{\mathbf{v}}_i}{\sqrt{\hat{\mathbf{v}}_i^T \hat{\mathbf{v}}_i}}, \quad \mathbf{g}_i = \frac{\hat{\mathbf{g}}_i}{\sqrt{\hat{\mathbf{v}}_i^T \hat{\mathbf{v}}_i}} \quad (2.204)$$

(d) *END IF* $i = q$ *ELSE* go to step (a) and increase i .

As in the first-order ARNOLDI method the generated basis vectors are normalized and orthogonal to each other (Eq. (2.157)). Furthermore, the same deflation techniques can be implemented in order to stepwise delete the linear dependent vectors.

In case of proportionally damped FE structures, i.e. $\mathbf{D} = \alpha \mathbf{M} + \beta \mathbf{K}$, $\{\alpha, \beta\} = \text{const.}$, two important relationships regarding the computation of the projection matrices $\mathbf{T}_l \equiv \mathbf{T}_r$ are derived (Eq. (2.205) - (2.206)). In [103, 42] it is proved that for such systems the damping matrix does not contribute to the derivation of the basis vectors for the projection matrices. Instead of calculating the second-order Krylov subspaces and thus, utilizing the second-order ARNOLDI algorithm, it suffices to compute the associated first-order subspaces via the application of the classical ARNOLDI scheme (Eq. (2.152) - (2.156)), since it holds:

$$K_q(-\mathbf{K}^{-1}\mathbf{D}, -\mathbf{K}^{-1}\mathbf{M}, -\mathbf{K}^{-1}\mathbf{Q}) = K_q(-\mathbf{K}^{-1}\mathbf{M}, -\mathbf{K}^{-1}\mathbf{Q}) \quad (2.205)$$

$$K_q(-\mathbf{K}^{-T}\mathbf{D}^T, -\mathbf{K}^{-T}\mathbf{M}^T, -\mathbf{K}^{-T}\mathbf{L}^T) = K_q(-\mathbf{K}^{-T}\mathbf{M}^T, -\mathbf{K}^{-T}\mathbf{Q}^T) \quad (2.206)$$

The above results (Eq. (2.205) - (2.206)) contribute to a simpler and computationally less expensive application of the KSM MOR method for second-order systems.

The case of undamped structures is also examined in [103, 42] and a similar relationship is derived, i.e.

$$K_q(\mathbf{0}, -\mathbf{K}^{-1}\mathbf{M}, -\mathbf{K}^{-1}\mathbf{Q}) = K_q(-\mathbf{K}^{-1}\mathbf{M}, -\mathbf{K}^{-1}\mathbf{Q}) \quad (2.207)$$

$$K_q(\mathbf{0}, -\mathbf{K}^{-T}\mathbf{M}^T, -\mathbf{K}^{-T}\mathbf{L}^T) = K_q(-\mathbf{K}^{-T}\mathbf{M}^T, -\mathbf{K}^{-T}\mathbf{Q}^T). \quad (2.208)$$

The first-order Krylov subspace in Eq (2.207) constitutes the classical choice for the definition of the \mathbf{T}_{KSM} coordinate transformation matrix when dealing with undamped systems (Eq. (2.50)), i.e.

$$\mathbf{M}\ddot{\mathbf{z}} + \mathbf{K}\mathbf{z} = \mathbf{F} \Rightarrow \mathbf{T}_{\text{KSM}} \in K_q(\mathbf{K}^{-1}\mathbf{M}, \mathbf{K}^{-1}\mathbf{F}) \quad (2.209)$$

$$K_q(\mathbf{K}^{-1}\mathbf{M}, \mathbf{K}^{-1}\mathbf{F}) = \text{span} \left\{ \underbrace{\mathbf{K}^{-1}\mathbf{F}}_{\text{static}}, \underbrace{(\mathbf{K}^{-1}\mathbf{M})\mathbf{K}^{-1}\mathbf{F}, \dots, (\mathbf{K}^{-1}\mathbf{M})^{q-1}\mathbf{K}^{-1}\mathbf{F}}_{\text{dynamic}} \right\} \quad (2.210)$$

The expansion of the Krylov subspace in Eq. (2.210) allows the interpretation of the basis vectors w.r.t the FE theory. It consists of the vector part, which gives the displacement vectors during a static analysis (static modes), and the matrix part, which contributes in capturing the inertia terms of the original model (dynamic modes). Thereafter, the system matrices and the vector of applied forces for the KMS-ROM are computed according to the relationship in Eq. (2.109).

The KSM MOR constitutes a powerful method for reducing the dimension of second-order systems of the form Eq. (2.158) - (2.159). The associated ROMs preserve the structure and the stability properties of the original model. Moreover, they capture the dynamics of the original model better than the so far analyzed MOR approaches. The KSM algorithmic scheme is independent of the position of the master and slave DoF (master DoF free) and thus, this method is highly appropriate for reducing the order of FE structures, where an inappropriate DoF allocation is compulsory.

Nevertheless, the dependence of the ARNOLDI method on the definition of a certain starting vector (Eq. (2.152) and Eq. (2.200)) leads to the derivation of different projection matrices when different starting vectors are applied. Although the impact on the ROM's quality is minor, a specific algorithm for obtaining a suitable starting vector is essential.

Herewith, the Subsection referring to the KSM MOR method is completed and the second reduction algorithm belonging to the category of *Non physical subspace reduction-expansion methods* is presented.

2.6.3 First order Balanced Truncation

The Balanced Truncation (BT) method constitutes an interesting energetic approach, which has been widely used for reducing the dimension of first-order LTI systems. For the purpose of this Subsection the following reformulation of the classical mathematical description given in Eq. (2.124) - (2.125) is considered:

$$\dot{\mathbf{z}}(t) = \mathbf{A}\mathbf{z}(t) + \mathbf{B}\mathbf{u}(t) \quad (2.211)$$

$$\mathbf{y}(t) = \mathbf{C}\mathbf{z}(t) + \mathbf{D}^{\text{LTI}}\mathbf{u}(t). \quad (2.212)$$

Here, the system matrix $\mathbf{D}^{\text{LTI}} \in \mathbb{R}^{p \times k}$ is used instead of the common $\mathbf{D} \in \mathbb{R}^{p \times k}$ in order to differentiate it from the classical damping matrix.

As the previously introduced MOR methods, BT aims in reducing the dimension of the original system and generating a ROM according to the scheme presented in Eq. (2.131) - (2.133).

The BT algorithm is based on the definition of two important control-theory quantities, which relate the controllability and observability nature [62] of the system's states $\mathbf{x}(t)$ and $\mathbf{y}(t)$, namely, the controllability \mathbf{W}_c and the observability \mathbf{W}_o Gramians, i.e.

$$\mathbf{W}_c = \int_0^\infty e^{t\mathbf{A}} \mathbf{B} \mathbf{B}^T e^{t\mathbf{A}^T} dt \quad \text{and} \quad \mathbf{W}_o = \int_0^\infty e^{t\mathbf{A}^T} \mathbf{C}^T \mathbf{C} e^{t\mathbf{A}} dt. \quad (2.213)$$

The \mathbf{W}_c and \mathbf{W}_o Gramians are closely related to the two Lyapunov equations [17], which can be regarded as an alternative formulation of the system in Eq. (2.211) - (2.212):

$$\mathbf{A}\mathbf{W}_c + \mathbf{W}_c\mathbf{A}^T + \mathbf{B}\mathbf{B}^T = \mathbf{0} \quad \text{and} \quad \mathbf{A}^T\mathbf{W}_o + \mathbf{W}_o\mathbf{A} + \mathbf{C}^T\mathbf{C} = \mathbf{0}. \quad (2.214)$$

Under the assumption of both the system matrix \mathbf{A} being asymptotically stable, i.e.

$$\mathbf{A} \text{ is stable} \Leftrightarrow \lambda(\mathbf{A}) \in \mathbb{C}^-, \quad (2.215)$$

and the matrix pairs (\mathbf{A}, \mathbf{B}) and (\mathbf{C}, \mathbf{A}) being controllable and observable [62], respectively, the \mathbf{W}_c and \mathbf{W}_o Gramians are the unique Hermitian and positive definite solutions of the above stated Lyapunov equations (Eq. (2.214)).

The importance of the Gramians in the algorithmic scheme of BT is ascertained with the help of the system's energy definition, which can be described in terms of the following functionals [17]:

$$E_c = \min_{\mathbf{z}(-\infty)=\mathbf{0}, \mathbf{z}(0)=\mathbf{z}} \|\mathbf{u}(t)\|^2, \quad t \leq 0 \quad (2.216)$$

$$E_o = \|\mathbf{y}(t)\|^2, \quad \mathbf{z}(0) = \mathbf{z}_0, \quad \mathbf{u}(t) = \mathbf{0}, \quad t \geq 0. \quad (2.217)$$

Herein, E_c annotates the minimal energy required in order to drive the system from the state $\mathbf{z}_0 = \mathbf{0}$ at $t = -\infty$ to the state \mathbf{z} at $t = 0$, whereas the functional E_o represents the energy obtained by the observation of the output due to the initial state \mathbf{z}_0 and without input.

The energy functionals E_c and E_o can be described in terms of the Gramians (Eq. (2.213)) and thus, the latter directly contribute to the characterization of the system's energetic state:

$$E_c = \mathbf{z}^T \mathbf{W}_c^{-1} \mathbf{z} \quad \text{and} \quad E_o = \mathbf{z}^T \mathbf{W}_o \mathbf{z}. \quad (2.218)$$

The states, which are difficult to control, require a large amount of control energy E_c and equivalently, the states that are difficult to observe yield a small amount of observation energy E_o . According to Eq. (2.218), the first type of states are spanned by the eigenvectors of \mathbf{W}_c corresponding to small eigenvalues and the second type are spanned by the eigenvectors of \mathbf{W}_o corresponding to small eigenvalues, respectively.

The kernel of the BT MOR resides on the energetic relationships in Eq. (2.218), namely, the BT-ROM can be generated by eliminating the system's states, which are both difficult to control and observe. The decision of which state variables to eliminate is not a trivial task. There might exist states, which are easy to control and at the same time difficult to observe. Therefore, a certain basis has to be ascertained, which should allow the computation of the states with the desired properties.

A change of the state-space realization in the LTI system (Eq. (2.211) - (2.212)) leads to the derivation of sufficient conclusions regarding the common basis. The introduction of the state-space matrix $\mathbf{T} \in \mathbb{R}^{N \times N}$ allows the realization $(\hat{\mathbf{A}}, \hat{\mathbf{B}}, \hat{\mathbf{C}}, \hat{\mathbf{D}}^{\text{LTI}})$ of the system $(\mathbf{A}, \mathbf{B}, \mathbf{C}, \mathbf{D}^{\text{LTI}})$ as given below:

$$(\hat{\mathbf{A}}, \hat{\mathbf{B}}, \hat{\mathbf{C}}, \hat{\mathbf{D}}^{\text{LTI}}) = (\mathbf{T}\mathbf{A}\mathbf{T}^{-1}, \mathbf{T}\mathbf{B}, \mathbf{C}\mathbf{T}^{-1}, \mathbf{D}^{\text{LTI}}). \quad (2.219)$$

By simple vector-matrix multiplications it can be proved that the transfer matrix (Eq. (2.126)) $\mathbf{H}(s)$ is invariant under such state-space transformations, whereas the associated Gramians are not, i.e.

$$\hat{\mathbf{H}}(s) = \mathbf{H}(s), \quad (2.220)$$

$$\hat{\mathbf{W}}_c = \mathbf{T} \mathbf{W}_c \mathbf{T}^T \quad \text{and} \quad \hat{\mathbf{W}}_o = \mathbf{T}^{-T} \mathbf{W}_o \mathbf{T}^{-1}. \quad (2.221)$$

In other words, while the eigenvalues of $(\mathbf{A}, \mathbf{B}, \mathbf{C}, \mathbf{D}^{\text{LTI}})$ are invariant under any state-space transformation, the eigenvalues of the associated Gramians are not. Nevertheless, the invariance properties are preserved, if the product of the Gramians is considered, i.e.

$$\hat{\mathbf{W}}_c \hat{\mathbf{W}}_o \stackrel{(2.221)}{=} (\mathbf{T} \mathbf{W}_c \mathbf{T}^T) (\mathbf{T}^{-T} \mathbf{W}_o \mathbf{T}^{-1}) = \mathbf{T} \mathbf{W}_c \mathbf{W}_o \mathbf{T}^{-1}, \quad (2.222)$$

the square-rooted eigenvalues of which are the, so called, Hankel Singular Values (HSVs) $\underline{\Sigma}$ of the LTI system $(\mathbf{A}, \mathbf{B}, \mathbf{C}, \mathbf{D}^{\text{LTI}})$:

$$\Lambda(\hat{\mathbf{W}}_c \hat{\mathbf{W}}_o) = \Lambda(\mathbf{W}_c \mathbf{W}_o) = \{\sigma_1^2, \sigma_2^2, \dots, \sigma_N^2\} = \underline{\Sigma}^2. \quad (2.223)$$

Eq. (2.223) allows the derivation of the common basis such that the Gramians $\hat{\mathbf{W}}_c$ and $\hat{\mathbf{W}}_o$ are equal constituting thus, the, so called, balanced realization. Precisely, a realization of a reachable, observable, and stable system $\Sigma := (\mathbf{A}, \mathbf{B}, \mathbf{C}, \mathbf{D}^{\text{LTI}})$ is balanced, if the associated Gramians are equal and diagonal with decreasingly sorted HSV, i.e.

$$\mathbf{W}_c = \mathbf{W}_o = \text{diag}\{\sigma_1, \sigma_2, \dots, \sigma_N\} = \boldsymbol{\sigma}(\mathbf{W}_c \mathbf{W}_o) = \underline{\Sigma} \quad \text{with} \quad \sigma_1 > \sigma_2 > \dots > \sigma_N. \quad (2.224)$$

Based on Eq. (2.224), the definition of the energetic functionals in Eq. (2.218) can be expressed in terms of the HSVs as follows:

$$E_c = \sum_{k=1}^N \frac{1}{\sigma_k} \mathbf{z}_k^2 \quad \text{and} \quad E_o = \sum_{k=1}^N \sigma_k \mathbf{z}_k^2. \quad (2.225)$$

The interpretation of Eq. (2.225) ascertains the retrieval of the common basis, which simultaneously permits the isolation of the states difficult to control and observe. Small HSVs correspond to the system states, which are difficult to control, whereas large HSVs correspond to states, which contain a large amount of energy. On this account, a methodology is required, which contributes to computing the balanced realization transformation matrix \mathbf{T}_{BR} . It is accomplished by the, so called, state-space balancing algorithm (SSB).

As given in Eq. (2.224), the calculation of the HSV is necessary for defining the balanced basis \mathbf{T}_{BR} . It can be done either by directly computing the Gramians or their Cholesky factors (Eq. (2.226)):

$$\mathbf{W}_c = \mathbf{L}_c \mathbf{L}_c^T \quad \text{and} \quad \mathbf{W}_o = \mathbf{L}_o \mathbf{L}_o^T, \quad (2.226)$$

$$\underline{\Sigma} = \boldsymbol{\sigma}(\mathbf{W}_c \mathbf{W}_o) = \Lambda^{1/2}(\mathbf{W}_c \mathbf{W}_o) \quad (2.227)$$

$$= \Lambda^{1/2} \left((\mathbf{L}_c^T \mathbf{L}_o) (\mathbf{L}_c^T \mathbf{L}_o)^T \right) = \boldsymbol{\sigma}(\mathbf{L}_c^T \mathbf{L}_o) \quad (2.228)$$

In fact, specific algorithms exist, e.g. the HAMMARLING algorithm [56], which allow the direct computation of the Gramian's Cholesky factors during the solution of the Lyapunov equations without having to explicitly compute the Gramians themselves.

At this point, the SSB algorithm is invoked, the process of which is presented in the following:

- (1) Compute the SVD of the matrix product $\mathbf{L}_o^T \mathbf{L}_c$, i.e.

$$\mathbf{L}_o^T \mathbf{L}_c = \mathbf{U} \underline{\Sigma} \mathbf{V}^T. \quad (2.229)$$

- (2) Formulate the \mathbf{T}_{BR} transformation matrix, i.e.

$$\mathbf{T}_{\text{BR}} = \mathbf{L}_c \underline{\Sigma}^{-1/2} \quad \text{and} \quad \mathbf{T}_{\text{BR}}^{-1} = \underline{\Sigma}^{-1/2} \mathbf{U}^T \mathbf{L}_o^T. \quad (2.230)$$

- (3) Formulate the balanced realization system matrices, i.e.

$$\hat{\mathbf{A}} = \mathbf{T}_{\text{BR}}^{-1} \mathbf{A} \mathbf{T}_{\text{BR}} \stackrel{(2.227)}{=} \underline{\Sigma}^{-1/2} \mathbf{U}^T \mathbf{L}_o^T \mathbf{A} \mathbf{L}_c \mathbf{V} \underline{\Sigma}^{-1/2}, \quad (2.231)$$

$$\hat{\mathbf{B}} = \mathbf{T}_{\text{BR}}^{-1} \mathbf{B} \stackrel{(2.227)}{=} \underline{\Sigma}^{-1/2} \mathbf{U}^T \mathbf{L}_o^T \mathbf{B}, \quad (2.232)$$

$$\hat{\mathbf{C}} = \mathbf{C} \mathbf{T}_{\text{BR}} \stackrel{(2.227)}{=} \mathbf{C} \mathbf{L}_c \mathbf{V} \underline{\Sigma}^{-1/2}. \quad (2.233)$$

The second step of the SSB algorithm in combination with Eq. (2.221) validates the requirement of the Gramians to be equal and diagonal, since the following relationship holds:

$$(2.221), (2.230) \Rightarrow \mathbf{T}_{\text{BR}}^{-1} \mathbf{W}_c \mathbf{T}_{\text{BR}}^{-T} = \mathbf{T}_{\text{BR}}^T \mathbf{W}_o \mathbf{T}_{\text{BR}} = \underline{\Sigma} = \mathbf{\Lambda}^{1/2}. \quad (2.234)$$

The ROM is obtained by truncating the smallest HSVs, which are of less importance to the balanced-realization system (Eq. (2.231) - (2.233)). The following block partition of the balanced system matrices helps visualize the ROM matrices, i.e.

$$\mathbf{A} = \begin{pmatrix} \mathbf{A}_{11}^{q \times q} & \mathbf{A}_{12}^{q \times (N-q)} \\ \mathbf{A}_{21}^{(N-q) \times q} & \mathbf{A}_{22}^{(N-q) \times (N-q)} \end{pmatrix}, \quad \mathbf{B} = \begin{pmatrix} \mathbf{B}_1^{q \times k} \\ \mathbf{B}_2^{(N-q) \times k} \end{pmatrix} \quad (2.235)$$

$$\underline{\Sigma} = \begin{pmatrix} \underline{\Sigma}_{11}^{q \times q} & \mathbf{0} \\ \mathbf{0} & \underline{\Sigma}_{22}^{(N-q) \times (N-q)} \end{pmatrix}, \quad \mathbf{C} = \begin{bmatrix} \mathbf{C}_1^{k \times q} & \mathbf{C}_2^{k \times (N-q)} \end{bmatrix}, \quad (2.236)$$

and thereof, the asymptotically stable and minimal BT-ROM $\mathbf{\Sigma}_{\text{BT}} := (\mathbf{A}_{11}, \mathbf{B}_{11}, \mathbf{C}_{11}, \mathbf{D}^{\text{LTI}})$ is obtained. The decision to truncate the states can be driven according to the fundamental error-bound condition [17, 5], which computes the H_∞ -normed error between the original $\mathbf{\Sigma}$ and the ROM $\mathbf{\Sigma}_{\text{BT}}$, i.e.

$$\|\mathbf{\Sigma} - \mathbf{\Sigma}_{\text{BT}}\|_{H_\infty} \leq 2(\sigma_{q+1}, \dots, \sigma_N). \quad (2.237)$$

The presented BT algorithmic scheme (Eq. (2.229) - (2.233)) can be robustly implemented by requiring the utilization of the largest HSVs Σ_{11} , already from the second step. Thus, the transformation matrices are written as follows:

$$\mathbf{T}_{\text{BR}} = \mathbf{L}_c \mathbf{V}_1 \Sigma_1^{-1/2} \quad \text{and} \quad \mathbf{T}_{\text{BR}}^{-1} = \Sigma_1^{-1/2} \mathbf{U}_1^T \mathbf{L}_o^T \quad (2.238)$$

and thereafter the SSB algorithm proceeds with the direct computation of the ROM data.

The classical first-order BT method is a very efficient MOR approach when dealing with small to medium size models. The existence of the error bound in Eq. (2.237) constitutes BT a powerful method. Herewith, according to a user defined error tolerance, the quality of the ROM is obtained prior to the reduction process.

Nevertheless, BT suffers from computational problems in case of large dimension models, since the whole algorithmic scheme is based on the computation of the Gramian's Cholesky factors. In order to cope with such problems various iterative methods have been proposed, e.g. the Smith method or the Alternating Direction Implicit (ADI) approach [17, 5], which utilize the sparsity pattern of the system matrices during the solution of the Lyapunov equations. Furthermore, the low numerical rank of the Gramians, which is due to their rapidly decaying eigenvalues could be regarded both as a positive and negative aspect. On one hand, the computation of the, so called, approximate low rank Cholesky factors is feasible [17, 5], which contributes in reducing the computational problems. On the other hand, it is suggested to avoid utilizing formulations, which include the inversion of either the Gramians or their Cholesky factors, since these matrices are typically ill-conditioned.

On the basis of the first-order BT reduction scheme the necessary adaptation steps are presented in the next Subsection, according to which the BT MOR can be applied for reducing the dimension of second-order LTI systems.

2.6.4 Second order Balanced Truncation

The BT MOR for second-order systems is developed similarly to the second-order KSM scheme. Therefore, a realization of the second-order system in Eq. (2.158) - (2.159) is required, with which the second-order ODE is transformed into a set of first-order ODE, i.e.

$$\underbrace{\begin{pmatrix} \dot{\mathbf{z}} \\ \ddot{\mathbf{z}} \end{pmatrix}}_{\dot{\mathbf{x}}} = \underbrace{\begin{pmatrix} \mathbf{0} & \mathbf{I} \\ -\mathbf{M}^{-1}\mathbf{K} & -\mathbf{M}^{-1}\mathbf{D} \end{pmatrix}}_{\mathbf{A}} \underbrace{\begin{pmatrix} \mathbf{z} \\ \dot{\mathbf{z}} \end{pmatrix}}_{\mathbf{x}} + \underbrace{\begin{pmatrix} \mathbf{0} \\ \mathbf{M}^{-1}\mathbf{Q} \end{pmatrix}}_{\mathbf{B}} \mathbf{u} \quad (2.239)$$

$$\mathbf{y} = \underbrace{[\mathbf{L} \quad \mathbf{0}]}_{\mathbf{C}} \begin{pmatrix} \mathbf{z} \\ \dot{\mathbf{z}} \end{pmatrix}. \quad (2.240)$$

The dimension of the system matrices in Eq. (2.239) - (2.240) is, as in the case of Eq. (2.160) - (2.161), twice as large (Eq. (2.162)) compared to the dimension of the

associated system matrices in the second-order form.

The nature of the state vector \mathbf{x} , which depends both on \mathbf{z} and $\dot{\mathbf{z}}$, i.e. $\mathbf{x} = [\mathbf{z} \ \dot{\mathbf{z}}]^T$ leads to the definition of the energy functionals associated to the second-order form in Eq. (2.158) - (2.159). Considering, for example, the control energy E_c (Eq. (2.217)), the following relationships are obtained:

$$E_{c,1} = \min_{\dot{\mathbf{z}}(-\infty)=0, \mathbf{z}(0)=\mathbf{z}} \|\mathbf{u}(t)\|^2, \quad t \leq 0 \text{ and } \dot{\mathbf{z}}(0) \text{ is free,} \quad (2.241)$$

$$E_{c,2} = \min_{\dot{\mathbf{z}}(-\infty)=0, \mathbf{z}(0)=\mathbf{z}} \|\mathbf{u}(t)\|^2, \quad t \leq 0 \text{ and } \dot{\mathbf{z}}(0) = \mathbf{0}. \quad (2.242)$$

By partitioning the \mathbf{W}_c and \mathbf{W}_o Gramians into the following block matrices, i.e.

$$\mathbf{W}_c = \begin{pmatrix} \mathbf{R} & \mathbf{S} \\ \mathbf{S}^T & \mathbf{T} \end{pmatrix} \quad \text{and} \quad \mathbf{W}_o = \begin{pmatrix} \mathbf{U} & \mathbf{V} \\ \mathbf{V}^T & \mathbf{N} \end{pmatrix}, \quad (2.243)$$

the optimum solution of the above stated optimization problems is derived:

$$(2.241) \Rightarrow E_{c,1} = \mathbf{z}^T \mathbf{R}^{-1} \mathbf{z}, \quad (2.244)$$

$$(2.242) \stackrel{(2.218)}{\Rightarrow} E_{c,2} = \mathbf{z}^T (\mathbf{R} - \mathbf{S} \mathbf{T}^{-1} \mathbf{S}^T)^{-1} \mathbf{z}. \quad (2.245)$$

On this account, the definition of the second-order free-velocity (FV) and zero-velocity (ZV) Gramians is derived [87], which holds for the standard first-order realization $\{\mathbf{A}, \mathbf{B}, \mathbf{C}\}$ of the second-order dynamical system given in Eq. (2.158) - (2.159). Their definition is based on the block partition of the standard Gramians (Eq. (2.43)), i.e.

$$\mathbf{W}_{c,FV} = \mathbf{R} \quad \text{and} \quad \mathbf{W}_{o,FV} = \mathbf{U} \quad (2.246)$$

$$\mathbf{W}_{c,ZV} = \mathbf{R} - \mathbf{S} \mathbf{T}^{-1} \mathbf{S}^T \quad \text{and} \quad \mathbf{W}_{o,ZV} = \mathbf{U} - \mathbf{V} \mathbf{N}^{-1} \mathbf{V}^T \quad (2.247)$$

Both the FV- and ZV-Gramians are symmetric and positive definite, since they constitute the block parts of the standard symmetric and positive definite Gramians.

In accordance with the HSV definition in the previous Subsection the second-order FV- and ZV-HSV are ascertained, as given below:

$$\underline{\Sigma}_{FV} = \mathbf{\Lambda}^{1/2} (\mathbf{W}_{c,FV} \mathbf{W}_{o,FV}) \quad (2.248)$$

$$\underline{\Sigma}_{ZV} = \mathbf{\Lambda}^{1/2} (\mathbf{W}_{c,ZV} \mathbf{W}_{o,ZV}) \quad (2.249)$$

and thus, a second-order realization form (Eq. (2.158) - (2.159)) is referred to as free-velocity or zero-velocity balanced, if and only if the following relationships hold, respectively, i.e.

$$\mathbf{W}_{c,FV} = \mathbf{W}_{o,FV} = \text{diag} \{ \sigma_{FV,1}, \sigma_{FV,1}, \dots, \sigma_{FV,N} \} = \underline{\Sigma}_{FV} \quad (2.250)$$

$$\mathbf{W}_{c,ZV} = \mathbf{W}_{o,ZV} = \text{diag} \{ \sigma_{ZV,1}, \sigma_{ZV,1}, \dots, \sigma_{ZV,N} \} = \underline{\Sigma}_{ZV}. \quad (2.251)$$

The calculation of the second-order BT-ROM is accomplished with the help of the second-order state-space balancing algorithm (SOSSB) [87], which is accompanied by a

new state-space realization (Step 2) for the original second-order ODEs [87]:

- (1) Start with Eq. (2.158) - (2.159) and perform a SVD on the mass matrix \mathbf{M} , i.e.

$$\mathbf{M} = \mathbf{Z}_1 \boldsymbol{\Lambda}_{\mathbf{M}} \mathbf{Z}_2 \quad (2.252)$$

and define the following transformation matrices:

$$\mathbf{T}_1 = \boldsymbol{\Lambda}_{\mathbf{M}}^{-1/2} \mathbf{Z}_1 \quad \text{and} \quad \mathbf{T}_2 = \mathbf{Z}_2 \boldsymbol{\Lambda}_{\mathbf{M}}^{-1/2}. \quad (2.253)$$

- (2) Generate the system's realization by utilizing \mathbf{T}_1 and \mathbf{T}_2 , i.e.

$$\hat{\boldsymbol{\Sigma}} := \{\hat{\mathbf{M}}, \hat{\mathbf{D}}, \hat{\mathbf{K}}, \hat{\mathbf{B}}, \hat{\mathbf{L}}\} = \{\mathbf{I}, \mathbf{T}_1 \mathbf{D} \mathbf{T}_2, \mathbf{T}_1 \mathbf{K} \mathbf{T}_2, \mathbf{T}_1 \mathbf{B}, \mathbf{L} \mathbf{T}_2\}. \quad (2.254)$$

- (3) Compute either the FV- or the ZV-balancing transformation matrix \mathbf{T}_{BR} of $\hat{\boldsymbol{\Sigma}}$, as given in Eq. (2.229) - (2.233).
- (4) Project the \mathbf{T}_{BR} -coordinate-transformed dynamic system on the space spanned by \mathbf{T}_{BR} , i.e. left multiply by \mathbf{T}_{BR}^T and the final balanced realization is obtained. Herewith, the ROM data is ascertained by utilizing the relationships in Eq. (2.235) - (2.236).

As observed, the above algorithmic scheme is independent of the master DoF choice. Thus, the second-order BT comprises the advantages of this type of MOR methods, such as SEREP and KSM. Despite this fact, the second-order BT is accompanied by a series of non-positive aspects, which concern on one hand the disability to utilize the advantages of its first-order variant, and on the other hand the applicability range in structural mechanics.

Generally, the second-order BT method, as well as several of its variants [29, 118, 98], constitutes an area of current research. In contrast to the classical first-order BT MOR, no error-bound exists (Eq. (2.237)), which could be utilized prior the reduction procedure and thus, the powerful aspect of the classical first-order BT is no longer valid. Furthermore, for several of its variants, e.g. the Second Order Balanced Truncation (SOBT) [29], there is no guarantee that the ROM preserves the stability. Thence, the consideration of this MOR for the FEM-MBS coupling procedure is not appropriate.

The second-order BT can be directly applied to reducing the dimension of small to medium sized mechanical models. The direct application, though, can be forestalled in case of dealing with ill-conditioned system matrices. The Gramians of the associated first-order realization system are rank deficient and thus, the Cholesky factors cannot be computed. This problem is overcome either by transforming the state-space realization of the original system (Step 2 of the SOSSB algorithm) or by utilizing the two-step MOR methodology (Section 2.7).

The controllability and observability Gramians are defined as the unique, symmetric, positive definite solutions of the Lyapunov equations (Eq. (2.214)) provided that the pencil $\lambda \mathbf{I} - \mathbf{A}$ of $\{\mathbf{A}, \mathbf{B}, \mathbf{C}\}$ (Eq.(2.239)) is stable, i.e. all eigenvalues of $\lambda \mathbf{I} - \mathbf{A}$ have negative real parts. In case of free-vibrated mechanical MBS this stability condition is

damaged, since the matrix polynomial $\mathbf{P}(\lambda) = \lambda^2\mathbf{M} + \lambda\mathbf{D} + \mathbf{K}$ is unstable. Thus, the BT scheme is no longer applicable unless the undesirable eigenvalues are deflated.

On the basis of the aforesaid, the second-order BT will be used for examining several interesting academic aspects, which occur during the MOR in structural mechanics. Nevertheless, in view of the numerous mentioned disadvantages regarding its practical applicability during the FEM-MBS procedure, it will not constitute the kernel of this Thesis.

The cycle of *Non physical subspace reduction-expansion methods* is completed with the introduction of the Second Order Modal Truncation method in the next Subsection.

2.6.5 Second Order Modal Truncation

The SOMT method follows the exact algorithmic scheme presented, so far, in the previous two Sections. Thus, a coordinate transformation matrix is required, with which the ROM is generated (Eq. (2.56)). It is acquired based on the state-space realization of the basic dynamic equation for FE discretized structures (Eq. (2.37)), which describes the state of the system in the space spanned by its own eigenvectors Φ , i.e.

$$\mathbf{T}_{\text{SOMT}} = \Phi \in \mathbb{R}^{n \times p}. \quad (2.255)$$

According to the general projection scheme (Eq. (2.38)) the ROM dynamic equation is obtained, i.e.

$$\mathbf{M}\ddot{\mathbf{z}} + \mathbf{D}\dot{\mathbf{z}} + \mathbf{K}\mathbf{z} = \mathbf{F} \quad (2.256)$$

$$\mathbf{z} = \Phi\mathbf{q} \quad (2.257)$$

$$\underbrace{\Phi^T \mathbf{M} \Phi}_{\mathbf{M}_{\text{SOMT}}} \underbrace{\ddot{\mathbf{q}}}_{\mathbf{q}} + \underbrace{\Phi^T \mathbf{D} \Phi}_{\mathbf{D}_{\text{SOMT}}} \underbrace{\dot{\mathbf{q}}}_{\mathbf{q}} + \underbrace{\Phi^T \mathbf{K} \Phi}_{\mathbf{K}_{\text{SOMT}}} \underbrace{\mathbf{q}}_{\mathbf{q}} = \underbrace{\Phi^T \mathbf{F}}_{\mathbf{F}_{\text{SOMT}}}. \quad (2.258)$$

Here, the dimension of the ROM system matrices depends on the number of the computed eigenvalues p , i.e.

$$[]_{\text{SOMT}}^{p \times p}, [] := \{\mathbf{M}, \mathbf{D}, \mathbf{K}\} \text{ and } \mathbf{F}_{\text{SOMT}}^{p \times 1}. \quad (2.259)$$

Based on the scaling properties of the eigenvalues, e.g. mass normalized or maximum value the reduced system matrices possess a specific structure (Chapter 3), which can be effectively utilized for further simulation processes.

The SOMT MOR can be regarded as the first part of the SEREP reduction method, since in both approaches the modal matrix is utilized for defining the associated coordinate transformation matrix. SEREP proceeds one step further by projecting the ROM's dynamic information back onto the physical configuration space. As shown, this occurs within the computation procedure of the $\mathbf{T}_{\text{SEREP}}$ subspace (Eq. (2.97)). The importance of such back-transformation approaches w.r.t the FEM-MBS coupling process will be analyzed in Chapter 5.

2.7 Two-step reduction-expansion methods

This Section copes with FE discretized mechanical structures, which result in large dimension systems of ODEs. Such systems occur either due to the requirement of high accuracy during the discretization procedure or because of the geometry's complexity, which imposes the generation of a smoother mesh. In this case, the application of a MOR approach is a rather difficult task, since the efficiency of the MOR scheme is affected by the system's large dimension.

The efficiency of a reduction method is a relative issue and is actually application dependent. Nevertheless, in almost all cases the efficiency factor is measured based on two aspects. Firstly, the ROM should be able to capture the dynamics of the original model as well as possible, and secondly, the computation time required therefor should not be vast. Thence, MOR methods, which succeed in generating dynamically accurate ROMs, but exceeding a certain user defined computation time limit are practically useless.

In order to cope with this problem the two-step MOR scheme is introduced. Herewith, the dimension reduction of the original model is stepwise completed in two stages (Fig. 2.8). During the first stage a MOR method is applied generating a fairly large ROM, which is computed relatively fast and captures well the dynamics of the original model up to a predefined frequency range. Thereafter, the second stage is invoked and the dimension of the ROM is further reduced by applying the second MOR scheme and thus, generating the final ROM. The efficiency of the two-step MOR depends on the

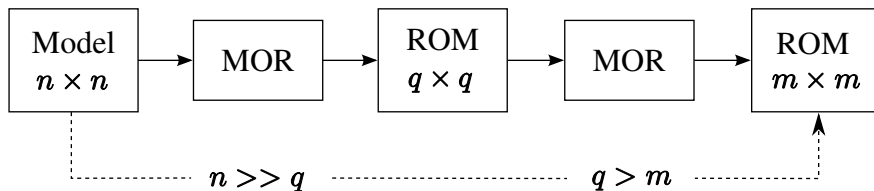


Fig. 2.8: Two-step MOR algorithmic scheme

choice of the algorithm for the generation of the first ROM. The applied MOR algorithm should be in the position of generating a stable and dynamically accurate ROM under the assumption of a fairly low computation time.

The master and slave DoF allocation constitutes an essential aspect during the first MOR stage. The reduction method to be applied should belong to the m -free MOR algorithms, but simultaneously both the number and position of the master DoF set must be included in the total q set of the first ROM (Fig. 2.8), i.e.

$$m < q \ll n \quad \text{with} \quad M \subset Q \subset N, \quad (2.260)$$

where M , Q and N annotate the sets of master, first-reduced and total DoF, respectively.

The reason therefor resides on the aim of eventually coupling the final ROM into a MBS code. According to the master DoF selection criteria (Section 2.2) certain DoF must be *de facto* appointed to the m set in order for the coupling procedure to be feasible. If no FEM-MBS coupling is required, then the condition of Eq. (2.260) is redundant.

The global applicability of the two-step MOR scheme requires the first stage MOR to belong to the m -free MOR category. Herewith, it is assured that an inadequate choice of the m set would have no effect on the quality of the first ROM. Under this consideration the following Table 2.1 is created, which appoints the applicability of each MOR method presented in the previous Sections based on three aspects, namely, the accuracy of the ROM, the computation time required and the algorithm's dependence on the master DoF set. All three aspects are evaluated for each MOR approach under the assumption of an awkward choice for the m set fulfilling thus, the global condition of the two-step MOR scheme.

Table 2.1: MOR quality comparison under inadequate m selection

MOR	Accurate ROM	Fast computation	m -free
Guyan	✗	✗	✗
g-Guyan	✗	✗	✗
Dynamic	✗	✗	✗
IRS	✗	✗	✗
DIRS	✗	✗	✗
iter-IRS	✗	✗	✗
iter-DIRS	✗	✗	✗
SEREP	✓	✓	✓
CMS	✗	✗	✗
KCMS	✗	✗	✗
ICMS	✗	✗	✗
iter-ICMS	✓	✗	✗
IKCMS	✗	✗	✗
iter-IKCMS	✓	✗	✗
KSM	✓	✓	✓
BT	✓	✗	✓
SOMT	✓	✓	✓

As observed, the reduction algorithms, which correspond to the above stated requirements are three, namely, the SEREP, the KSM, and the SOMT MOR methods. Thence, one of these three methods could be appointed as the first stage MOR of the two-step scheme. Thereafter, the selection of which MOR approach to apply is both user and model dependent. Nevertheless, the consideration of the accuracy aspect for the listed methods (Table 2.1) indicates the suitable methods to apply. According to the MOR

categories of the previous Sections, some of the two-step MOR methods are gathered in Table 2.2:

Table 2.2: Sample of two-step MOR methods

Physical space MOR	Semi physical space MOR	Non physical space MOR
SEREP-Guyan	SEREP-CMS	SEREP-KSM
SEREP-IRS	SEREP-KCMS	SEREP-ICMS
	SEREP-ICMS	KSM-BT
	SEREP-IKCMS	SOMT-KSM
		SOMT-BT

The accuracy of the MOR methods is the topic of Chapter 3 and is ascertained by utilizing the, so called, Model Correlation Criteria (MCC). Various FE discretized mechanical structures undergo dimension reduction with the help of the above listed MOR algorithms and the quality of the associated ROMs is compared. It can be regarded as the controlling step during the FEM-MBS coupling process.

3 Validation of reduced order models

In Chapter 2 several MOR schemes were introduced, based on which the generation of ROMs for usage in the field of structural mechanics is feasible. Although in certain cases the theory of the applied MOR approach indicates the quality of the dynamic properties for the associated ROM, the methodical application of certain correlation criteria is compulsory. Herewith, it can be assured that the ROM's dynamics sufficiently capture the properties of the original model. Regarding the coupling procedure of elastic and rigid MBS dynamics, it is essential for the consistency of the ROM to be verified prior to the elastic data transfer into the MBS code.

As mentioned in the Introduction, the FEM-MBS coupling is supported by commercial software packages, which are developed either as FEM tools, e.g. ANSYS, Msc Nastran, etc., or as MBS codes, e.g. SIMPACK, ADAMS, etc., or as the necessary interfaces for coping with the elastic data transfer into MBS codes, e.g. FEMBS. All three disciplines are affiliated to two aspects, the existence of which restricts both the application of alternative MOR procedures and the efficient verification of the ROM's elastic properties. On one hand, the sole choice between the classical Guyan or CMS MOR methods does not allow the application of the MOR schemes presented in the previous Chapter, which could offer qualitatively better ROMs at a reduced cost. On the other hand, the application of a rather simple eigenfrequency comparison between the original and the ROM cannot give sufficient information regarding the ROM's dynamic properties. Especially in case of complex structures, using only the eigenfrequency consideration could point to misleading conclusions unless either perfect correlation or advanced engineering experience is at hand.

On this account, the structure of this Chapter is comprised of three Sections. Firstly, in Section 3.1 the modal analysis theory of FE discretized mechanical structures is shortly outlined. The introduction of various Model Correlation Criteria (MCC) is the kernel of Section 3.2, with which the dynamic properties of FE models can be well ascertained. Finally, in Section 3.3 the MCC are utilized in comparing the MOR methods of Chapter 2 applied to four different mechanical models, namely, the 3D solid bar structure, the UIC60 elastic rail, the elastic rod, and the elastic crankshaft.

3.1 Eigenvalue analysis in structural mechanics

3.1.1 Undamped free vibrated systems

Let us consider the undamped free vibrated version of Eq. (2.37), i.e.

$$(2.37) \text{ with } \mathbf{D} = \mathbf{0}, \mathbf{F} = \mathbf{0} \Rightarrow \mathbf{M}\ddot{\mathbf{z}} + \mathbf{K}\mathbf{z} = \mathbf{0}. \quad (3.1)$$

In general, the solution of such homogeneous sets of ODEs has the form

$$\mathbf{z} = \underline{\Phi} e^{j\omega t}, \quad (3.2)$$

where $\underline{\Phi}$ is a $n \times 1$ vector of time-independent amplitudes and ω is the angular frequency of harmonic response. The solution type in Eq. (3.2) imposes the system to be capable of vibrating in simple harmonic motion at a single frequency ω .

The double differentiation of Eq. (3.2) w.r.t time and the substitution of the resulting equation in Eq. (3.1) leads to

$$(3.2) \Rightarrow \ddot{\mathbf{z}} = -\omega^2 \underline{\Phi} e^{j\omega t} \quad (3.3)$$

$$(3.1) \stackrel{(3.3)}{\Rightarrow} (\mathbf{K} - \omega^2 \mathbf{M}) \underline{\Phi} = \mathbf{0}. \quad (3.4)$$

The n homogeneous algebraic equations of Eq. (3.4) constitute the, so called, generalized eigenvalue or modal analysis problem. Non trivial solutions exist only if the determinant of the coefficient matrix is zero, i.e.

$$\det |(\mathbf{K} - \omega^2 \mathbf{M})| = 0 \quad (3.5)$$

and thereof, the n values of ω^2 : $\{\omega_1^2, \omega_2^2, \dots, \omega_n^2\}$ can be found, which are the distinct roots of the n -th order polynomial. The solutions are called frequencies and their square root are the, so called, natural frequencies or eigen angular frequencies. Substituting any of these back into Eq. (3.4) yields a corresponding set of relative values $\underline{\Phi}$, which is the associated eigenvector, or eigenmode, or mode shape.

The complete solution of Eq. (3.4) can be expressed in the form of two $n \times n$ matrices, namely, the modal matrix Φ and the spectral matrix Λ , i.e.

$$\Phi = [\underline{\Phi}_1 \ \underline{\Phi}_2 \ \dots \ \underline{\Phi}_n] = \begin{pmatrix} \Phi_{11} & \Phi_{21} & \dots & \Phi_{n1} \\ \Phi_{12} & \Phi_{22} & \dots & \Phi_{n2} \\ \vdots & \vdots & \vdots & \vdots \\ \Phi_{1n} & \Phi_{2n} & \dots & \Phi_{nn} \end{pmatrix} \quad (3.6)$$

$$\Lambda = \text{diag} [\omega_i^2] = \begin{pmatrix} \omega_1^2 & & \mathbf{0} \\ & \omega_2^2 & \\ & & \ddots \\ \mathbf{0} & & \omega_n^2 \end{pmatrix} \quad (3.7)$$

As observed, the eigenvectors are column-wise sorted in the modal matrix and the non-diagonal elements of the spectral matrix are zero entries.

An important characteristic regarding both quantities copes with the property of uniqueness. While the spectral matrix Λ is a fixed quantity, the modal matrix Φ is subject to indeterminate scaling factors, which do not affect the shape of the vibration modes, but their amplitude.

3.1.2 Orthogonality properties

The modal model, i.e. the model, which is described in the space spanned by its own eigenvectors features certain properties known as orthogonality or normalization properties. The analytical derivation of these properties constitutes the necessary basis, with which several MCC are generated.

Considering two distinct roots ω_r and ω_s and therefore, the associated eigenvectors $\underline{\Phi}_r$ and $\underline{\Phi}_s$ of the eigenvalue problem in Eq. (3.4), the following is obtained:

$$(\mathbf{K} - \omega_r^2 \mathbf{M}) \underline{\Phi}_r = \mathbf{0} \quad (3.8)$$

$$(\mathbf{K} - \omega_s^2 \mathbf{M}) \underline{\Phi}_s = \mathbf{0}. \quad (3.9)$$

The left multiplication of Eq. (3.8) by $\underline{\Phi}_s^T$, the right multiplication of the transposed Eq. (3.9) by $\underline{\Phi}_r$ and the subtraction of the resulting equations ascertains the following system of equations, i.e.

$$(3.8) \xrightarrow{\underline{\Phi}_s^T} \underline{\Phi}_s^T (\mathbf{K} - \omega_r^2 \mathbf{M}) \underline{\Phi}_r = \mathbf{0} \quad (3.10)$$

$$(3.9) \xrightarrow{\underline{\Phi}_r} ((\mathbf{K} - \omega_s^2 \mathbf{M}) \underline{\Phi}_s)^T \underline{\Phi}_r = \underline{\Phi}_s^T (\mathbf{K} - \omega_s^2 \mathbf{M}) \underline{\Phi}_r = \mathbf{0} \quad (3.11)$$

$$(3.10) - (3.11) \Rightarrow (\omega_r^2 - \omega_s^2) \underline{\Phi}_s^T \mathbf{M} \underline{\Phi}_r = \mathbf{0}. \quad (3.12)$$

Under the assumption of non-repeated roots, i.e. $\omega_r \neq \omega_s, \forall r \neq s$, Eq. (3.12) is valid if and only if

$$\underline{\Phi}_s^T \mathbf{M} \underline{\Phi}_r = \underline{\Phi}_r^T \mathbf{M} \underline{\Phi}_s = \mathbf{0}, \quad r \neq s. \quad (3.13)$$

By introducing Eq. (3.13) in Eq. (3.10) - (3.11) an equivalent expression is obtained in terms of the stiffness matrix \mathbf{K} , i.e.

$$\underline{\Phi}_s^T \mathbf{K} \underline{\Phi}_r = \underline{\Phi}_r^T \mathbf{K} \underline{\Phi}_s = \mathbf{0}, \quad r \neq s. \quad (3.14)$$

For the special case, where $r = s$, i.e. $\omega_r = \omega_s$, Eq. (3.13) and Eq. (3.14) do not apply, but an interesting relationship is ascertained if Eq. (3.10) or Eq. (3.12) is used, i.e.

$$\underbrace{\underline{\Phi}_r^T \mathbf{K} \underline{\Phi}_r}_{\tilde{k}_r} = \omega_r^2 \underbrace{\underline{\Phi}_r^T \mathbf{M} \underline{\Phi}_r}_{\tilde{m}_r}. \quad (3.15)$$

Here, the terms \tilde{m}_r and \tilde{k}_r refer to the modal mass and stiffness matrices, respectively. The orthogonality conditions given throughout the Eq. (3.13) - (3.15) indicate the linear independence of the system's mode shapes. Since the eigenvectors are subject to arbitrary scaling factors, the definition of both \tilde{m}_r and \tilde{k}_r is not unique. Hence, the reference to as the modal system matrices w.r.t a particular mode. Nevertheless, Eq. (3.15) allows the introduction of a unique quantity, namely, the ratio \tilde{k}_r/\tilde{m}_r , which equals the eigenvalue ω_r^2 . Based on this observation several scaling methodologies exist, the most popular of which are the largest magnitude and the mass normalization procedures. While the first scales the eigenvectors such that its largest element has unit magnitude, the latter reduces the corresponding modal mass matrix to the unity matrix. In this

In this Thesis the mass normalization scaling methodology is adopted, because of its practical relevance to modal testing and therefore, it is shortly outlined.

The eigenvector $\underline{\Phi}_{r,m}$, which is scaled w.r.t the mass matrix is defined as follows:

$$\underline{\Phi}_{r,m} = \frac{\underline{\Phi}_r}{\sqrt{\tilde{m}_r}} = \frac{\underline{\Phi}_r}{\sqrt{\underline{\Phi}_r^T \mathbf{M} \underline{\Phi}_r}} \quad (3.16)$$

and is usually referred to as the normal mode. The column wise sorting of the normal modes leads to the definition of the normal modal matrix $\underline{\Phi}_m$, which is ascertained analogously to Eq. (3.6). On this basis the orthogonality conditions (Eq. (3.13) - (3.15)) w.r.t the mass and stiffness matrices are obtained:

$$\underline{\Phi}_m^T \mathbf{M} \underline{\Phi}_m = \mathbf{I} \quad (3.17)$$

$$\underline{\Phi}_m^T \mathbf{K} \underline{\Phi}_m = \mathbf{\Lambda}, \quad (3.18)$$

where \mathbf{I} annotates the $n \times n$ unity matrix and the spectral matrix $\mathbf{\Lambda}$ is defined as given in Eq. (3.7).

The properties of the relationships in Eq. (3.17) - (3.18) will be later utilized for appointing certain MCC. The analogous condition should also be derived in case of damped mechanical systems, which is handled in the following Subsection.

3.1.3 Proportionally damped free vibrated systems

The modelling of the damping parameter in mechanical systems contributes to a more generalized observation of systems in structural mechanics. Thus, the free vibrated version of Eq. (2.38) is considered, i.e.

$$\mathbf{M}\ddot{\mathbf{z}} + \mathbf{D}\dot{\mathbf{z}} + \mathbf{K}\mathbf{z} = \mathbf{0}. \quad (3.19)$$

There exist several methodologies on how to include the damping effect in a mechanical system, i.e. on how define the damping matrix \mathbf{D} in Eq. (3.19). The most popular approach, which will be considered in this Thesis refers to as the proportional damping assumption.

The particular advantage of using proportionally damped models resides on the modal analysis properties of such structures. While the natural frequencies of the proportionally damped model are similar to the frequencies of the undamped system, the associated eigenvectors are linearly identical. Consequently, it is feasible to derive the modal properties of a proportionally damped system by invoking the modal analysis procedure of the associated undamped system and thereafter to apply the required correction terms due to the consideration of the damping effect. On this account, the most commonly used definition \mathbf{D} for proportionally damped models is given below:

$$\mathbf{D} = \alpha \mathbf{M} + \beta \mathbf{K} \quad \text{with} \quad \alpha, \beta = \text{const.} \quad (3.20)$$

The left and right multiplication of the damping matrix in Eq. (3.20) by the mass normalized modal matrix Φ_m and the combination of the relationships in Eq. (3.17) - (3.18) ascertains the definition of the normal modal damping matrix \tilde{c}_r , i.e.

$$(3.20) \Rightarrow \tilde{c}_r = \Phi_m^T (\alpha \mathbf{M} + \beta \mathbf{K}) \Phi_m \quad (3.21)$$

$$(3.17), (3.18) \stackrel{(3.21)}{\Rightarrow} \tilde{c}_r = \alpha \mathbf{I} + \beta \Lambda. \quad (3.22)$$

The substitution of Eq. (3.17) - (3.18) and Eq. (3.22) in the dynamic system of Eq. (2.258), delivers a system of n uncoupled ODEs, which describe the motion of FE discretized mechanical structures in the, so called, principle space:

$$(3.17), (3.18), (3.22) \stackrel{(2.258)}{\Rightarrow} \ddot{\mathbf{q}} + \tilde{c}_r \dot{\mathbf{q}} + \Lambda \mathbf{q} = \Phi_m^T \mathbf{F}, \quad (3.23)$$

with the modal damping \tilde{c}_{ri} for the i -th normal mode being defined as follows:

$$\tilde{c}_{ri} = 2\omega_i \xi_i = \alpha + \beta \omega_i^2. \quad (3.24)$$

Apart from the derivation of the MCC in the subsequent Section, the interesting orthogonality relationships regarding the modal damping matrix have an important influence on the algorithmic scheme for several of the previously analyzed MOR methods. A particular emphasis is given to the derivation of the first-order Krylov subspace within the second-order KSM reduction approach (Eq. (2.205) - (2.206)).

3.1.4 Practical implementation for mechanical structures

Numerous methods exist [51], which allow the fast computation of the generalized eigenvalue problem (Eq. (3.4)). In case of mechanical structures, though, it is essential to apply an algorithmic scheme, which additionally validates the preservation of the model's structural properties. Herewith, it can be ascertained if the structural properties of a ROM are damaged during the MOR. Therefore, the mass matrix Cholesky based (Eq. (3.26)) eigenvalue approach is suggested and is conducted as given below:

$$(3.4) \Rightarrow \mathbf{0} = \mathbf{K}\Phi - \omega^2 \mathbf{M}\Phi \quad (3.25)$$

$$\mathbf{M} = \mathbf{L}^T \mathbf{L} \quad (3.26)$$

$$(3.25) \stackrel{(3.26)}{\Rightarrow} \mathbf{0} = \mathbf{K}\Phi - \omega^2 \mathbf{L}^T \mathbf{L}\Phi \quad (3.27)$$

$$\mathbf{0} = \underbrace{(\mathbf{L}^{-T} \mathbf{K} \mathbf{L}^{-1})}_{\mathbf{A}} \underbrace{\mathbf{L}\Phi}_{\mathbf{Y}} - \omega^2 \underbrace{\mathbf{L}\Phi}_{\mathbf{Y}}. \quad (3.28)$$

The generalized eigenvalue problem is reduced to the, so called, special eigenvalue problem $\mathbf{AY} - \omega^2 \mathbf{Y} = \mathbf{0}$, the solution of which is conducted by choosing an adequate numerical scheme. Thereafter, the ROM's eigenvectors have to be computed based on the relationship in Eq. (3.28), i.e. $\Phi = \mathbf{L}^{-1} \mathbf{Y}$.

The direct utilization of the special eigenvalue problem with $\mathbf{A} = \mathbf{M}^{-1} \mathbf{K}$ should be avoided in general unless engineering experience is at hand.

3.2 Model Correlation Criteria

As mentioned in the introductory part of the Chapter the only available comparison method within commercial FEM software packages relies on the eigenfrequency information. Additional to this restriction, the application of other criteria regarding, e.g. the eigenvector correlation, is forestalled due to the non-direct availability of the associated coordinate transformation matrix (Eq. (2.38)). Herewith, eigenvectors of the same dimension can be compared, namely, either by expanding the $m \times q$ ROM's modal matrix Φ_{ROM} to the $n \times q$ dimension of the original model's modal matrix Φ or the opposite (q annotates the number of the computed eigenvectors). The first case would lead to the definition of the expanded modal matrix Ψ , which is given as follows:

$$\underbrace{\Psi}_{n \times q}^{(2.38)} = \underbrace{\mathbf{T}_{\text{MOR}}}_{n \times m} \underbrace{\Phi_{\text{ROM}}}_{m \times q}. \quad (3.29)$$

On the basis of the aforesaid, two general categories of correlation criteria are introduced, namely, the eigenfrequency and eigenvector related MCC [50, 13, 64, 65, 70, 67, 72, 2]. The first category consists of the:

- Normalized Relative Frequency Difference (NRFD),
- Natural Frequency Difference (NFD),
- Stiffness Normalized Vector Difference (SNVD),

whereas the second category includes the:

- Modal Assurance Criterion (MAC),
- Modified Modal Assurance Criterion (modMAC),
- Modal Comparison Criteria Matrix (MCCM),
- Coordinate Modal Assurance Criterion (COMAC),
- Normalized Modal Difference (NMD),
- Mass Normalized Vector Difference (MNVD).

The theoretical part of certain MCC will be accompanied by the analogous visualization in order to demonstrate the plausibility of the results. Therefore, the figures that follow are created according to a randomly generated FE discretized structure.

3.2.1 Eigenfrequency related criteria

1. *Normalized Relative Frequency Difference (NRFD)*. Generally, the MOR scheme implies the eigenfrequencies of the ROM f_{ROM} to be higher than the eigenfrequencies of the original (full) model f_{Full} . The reason therefor resides on the higher stiffness properties of the ROM model. On this account, the NRFD criterion is formulated, i.e.

$$f_{\text{NRFD}}(i) = \left| 1 - \frac{f_{\text{Full}}(i)}{f_{\text{ROM}}(i)} \right| \cdot 100\%, \quad i = 1, 2, \dots, q. \quad (3.30)$$

Herein, q annotates the number of the computed eigenfrequencies. The lower the value of f_{NRFD} is, the better the ROM captures the dynamic properties of the original model at the predefined frequency range.

2. *Natural Frequency Difference (NFD)*. The NRFD criterion constitutes the first step in indicating the potential Correlated Modal Pairs (CMPs) for both the original and the ROM. Nevertheless, there is always the possibility of existing CMPs, which do not belong to related frequency ranges. Thence, the NFD is utilized, the mathematical formulation of which is given below:

$$f_{\text{NFD}}(i, j) = \frac{|f_{\text{Full}}(i) - f_{\text{ROM}}(j)|}{\min(f_{\text{Full}}(i), f_{\text{ROM}}(j))} \cdot 100\%, \quad i, j = 1, 2, \dots, q. \quad (3.31)$$

Herewith, a two dimensional matrix is obtained, which gives a general assessment of the differences between all possible combinations of the eigenfrequencies, i.e. all potential CMPs (Fig. 3.1).

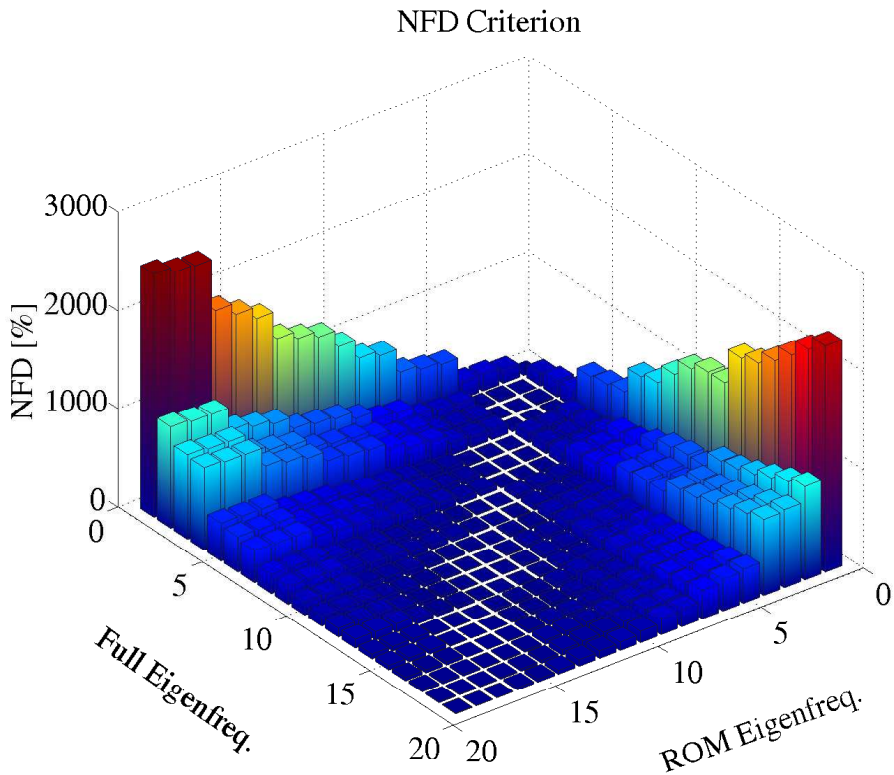


Fig. 3.1: Natural Frequency Difference - 3D view

The NFD criterion combined with the associated modMAC correlation coefficient delivers important information, which can be utilized for updating the ROM's modal matrices by the, so called, switching process methodology (Section 3.2.3).

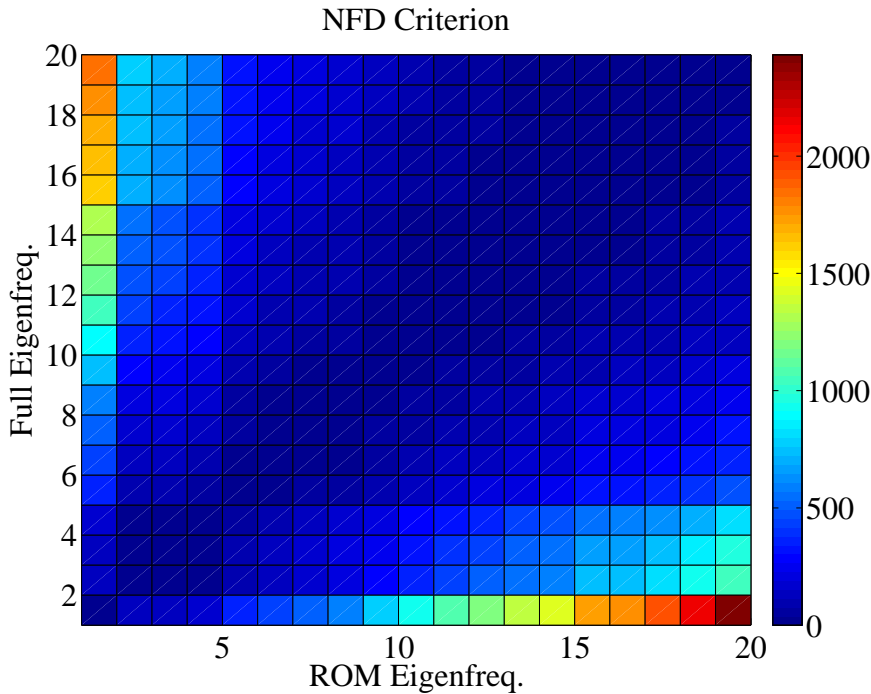


Fig. 3.2: Natural Frequency Difference - top view

3. *Stiffness Normalized Vector Difference (SNVD)*. SNVD gives the information about the relative vector difference of the stiffness modal matrices (Eq. (3.18)) for both the original and the ROM model, i.e.

$$SNVD_{(k,l)} = \frac{\left\| \tilde{\mathbf{k}}_{ROM} - \tilde{\mathbf{k}}_{Full} \right\|_2}{\left\| \tilde{\mathbf{k}}_{ROM} \right\|_2} \cdot 100\% = \frac{\sqrt{\sum_r (\tilde{\mathbf{k}}_{ROM}(r) - \tilde{\mathbf{k}}_{Full}(r))^2}}{\sqrt{\sum_r (\tilde{\mathbf{k}}_{ROM}(r))^2}} \cdot 100\%. \quad (3.32)$$

The SNVD coefficient resembles the NRFD criterion, if the relationship in Eq. (3.18) is taken into consideration. As in the previous case, the smallest SNVD value depicts the best result. Based on the typical SNVD plot (Fig. 3.3) no sufficient conclusion can be derived about the CMP, unless a bad correlation is at hand. Therefore, the main diagonal isolation of the SNVD matrix is suggested, which ultimately delivers the dynamic information obtained by the NRFD criterion.

3.2.2 Eigenvector related criteria

1. *Modal Assurance Criterion (MAC)*. The MAC approach copes with the information regarding the angle of compared eigenvectors in space as well as their orthogonal coherence. It is based on the dimension expansion of the ROM's modal matrix according to the relationship given in Eq. (3.29), i.e.

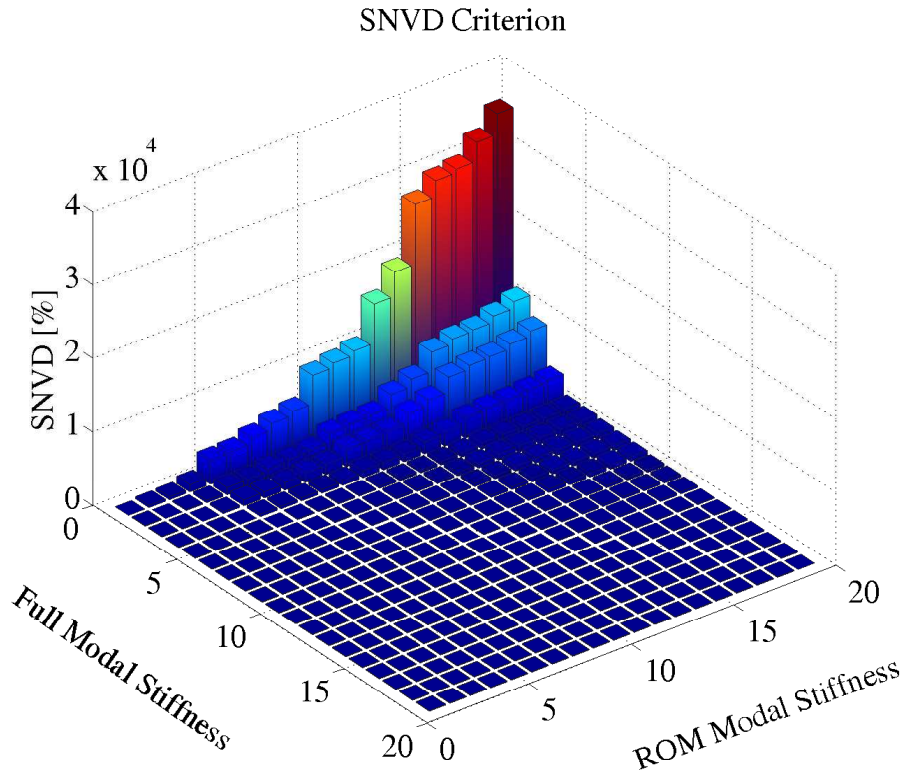


Fig. 3.3: Stiffness Normalized Vector Difference - 3D view

$$MAC_{(k,l)} = \frac{(\Phi_k^T \Psi_l)^2}{(\Phi_k^T \Phi_k)(\Psi_l^T \Psi_l)} \cdot 100\%. \quad (3.33)$$

The value ‘ $MAC = 100\%$ ’ corresponds to absolute correlation and therefore, the less this value becomes, the worse the eigenvector correlation is. A thumb-rule assures that a MAC coefficient of a magnitude larger or equal than 80%, i.e. $MAC \geq 80\%$ implies a satisfactory correlation.

Fig. 3.4 and Fig. 3.5 constitute the representative plots for the MAC coefficient matrix. As observed, the well CMPs occupy the main diagonal of the MAC matrix with decreasing MAC values. Herein, the correlation of the first 6 pairs is rather bad. This set of eigenvectors, though, has no influence on the dynamic behavior of the FE structure, since they are the, so called, rigid eigenvectors and therefore will not be considered in the succeeding comparisons.

The utilization of the information obtained both from the MAC and the frequency related criteria contributes to a more efficient understanding concerning the dynamic properties of a ROM. Nevertheless, MAC lacks in delivering sufficient information in case of damped FE structures. As mentioned in Subsection 3.1.3, the eigenvectors of proportionally damped structures are linearly identical to the eigenvectors of the associated undamped systems. The only difference resides on the magnitude, which is affected by the presence of the damping terms. This information is not included in the MAC definition (Eq. (3.33)).

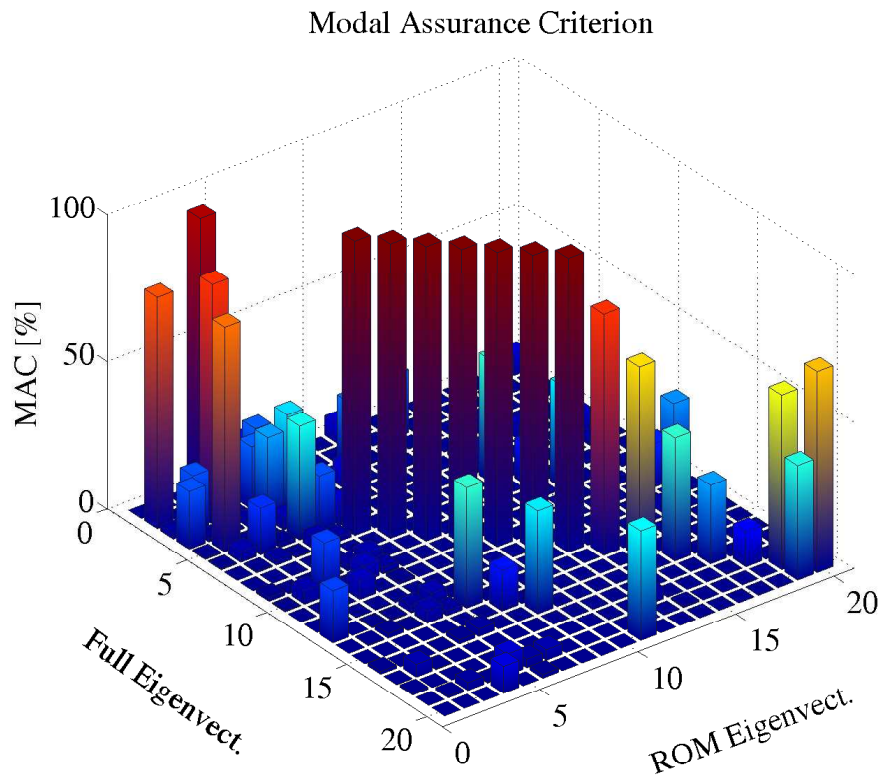


Fig. 3.4: Modal Assurance Criterion - 3D view

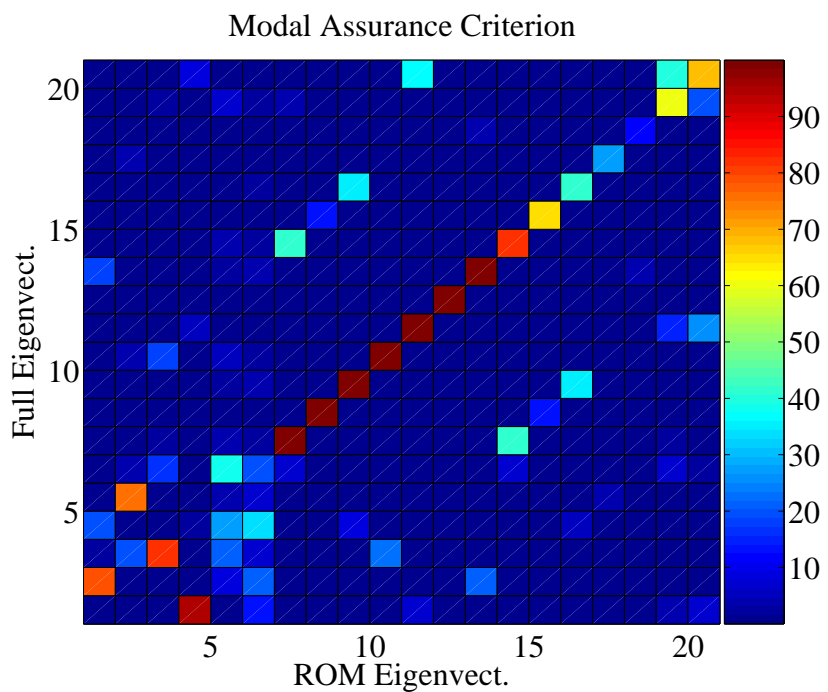


Fig. 3.5: Modal Assurance Criterion - top view

2. *Modified Modal Assurance Criterion (modMAC)*. modMAC utilizes the orthogonality properties regarding the mass normalized eigenvectors of a FE structure (Eq. (3.17) - (3.18)). On this account, the mathematical formulation of this criterion is given below:

$$\text{modMAC}_{(k,l)} = \frac{(\Phi_k^T \mathbf{M} \Psi_l)^2}{(\Phi_k^T \mathbf{M} \Phi_k)(\Psi_l^T \mathbf{M} \Psi_l)} \cdot 100\%. \quad (3.34)$$

Analogously to the MAC case, the value ‘ $\text{modMAC} = 100\%$ ’ corresponds to absolute correlation and therefore, the less this value becomes, the worse the eigenvector correlation is (Fig. 3.6 and Fig. 3.7).

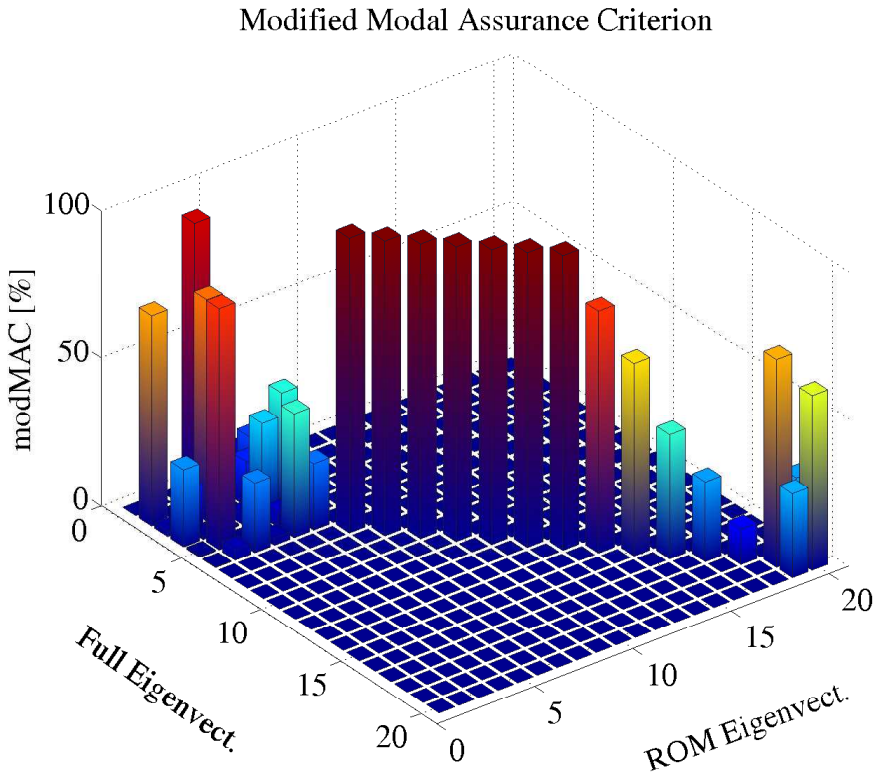


Fig. 3.6: Modified Modal Assurance Criterion - 3D view

The consideration of the mode shapes being orthogonal w.r.t the mass matrix contributes in the computation of zero elements for the non diagonal entries. Based on the relationship in Eq. (3.17) a perfect modMAC correlation would result in generating the unity matrix. As in the MAC case, whenever the dimension of non-fixed structures is reduced, a 6×6 block matrix with badly CMPs is generated, which corresponds to the rigid modes.

3. *Modal Comparison Criteria Matrix (MCCM)*. MCCM can be regarded as the criterion complementary to modMAC, since it measures the deviation of the modMAC coefficient matrix from the unity matrix or, equivalently, it generates the

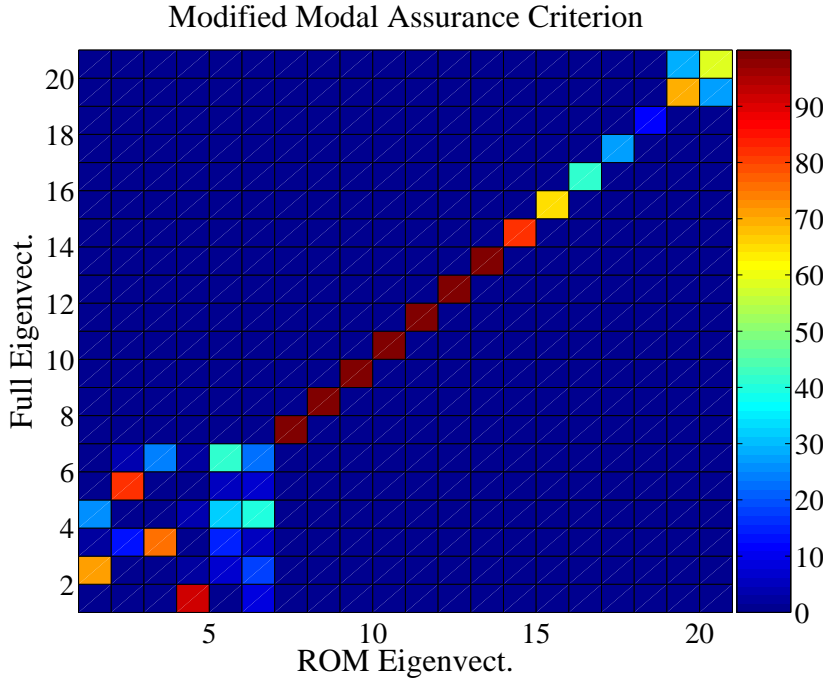


Fig. 3.7: Modified Modal Assurance Criterion - top view

magnitude of the badly CMPs, i.e.

$$MCCM_{(k,l)} = \left(\delta_{kl} - \frac{\Phi_k^T \mathbf{M} \Psi_l}{\sqrt{(\Phi_k^T \mathbf{M} \Phi_k)(\Psi_l^T \mathbf{M} \Psi_l)}} \right) \cdot 100\%, \quad \delta_{kl} = \begin{cases} 1, & k = l \\ 0, & k \neq l \end{cases} \quad (3.35)$$

In Fig. 3.8 the MCCM coefficient corresponds to the complementary modMAC case of Fig. 3.6.

4. *Coordinate Modal Assurance Criterion (COMAC).* While the MAC and modMAC coefficient matrices give the information regarding the CMPs, the COMAC approach delivers the correlation information for the individual DoF of each CMP, i.e.

$$COMAC_{(r)} = \frac{\left\{ \sum_r (\Phi(r) \Psi(r)) \right\}^2}{\left\{ \sum_r \Phi(r)^2 \right\} \left\{ \sum_r \Psi(r)^2 \right\}} \cdot 100\%. \quad (3.36)$$

[]: eigenvector's r-th coordinate, [] = { Φ, Ψ }.

The COMAC application is more suitable for small to medium size systems, which undergo dimension reduction. Herewith, the DoF, which are responsible for dynamic inconsistencies in the ROM can be identified and isolated. Thereafter, the MOR procedure can be restarted excluding the problematic DoF and defining others instead of them.

5. *Normalized Modal Difference (NMD).* The NMD criterion is similar to COMAC

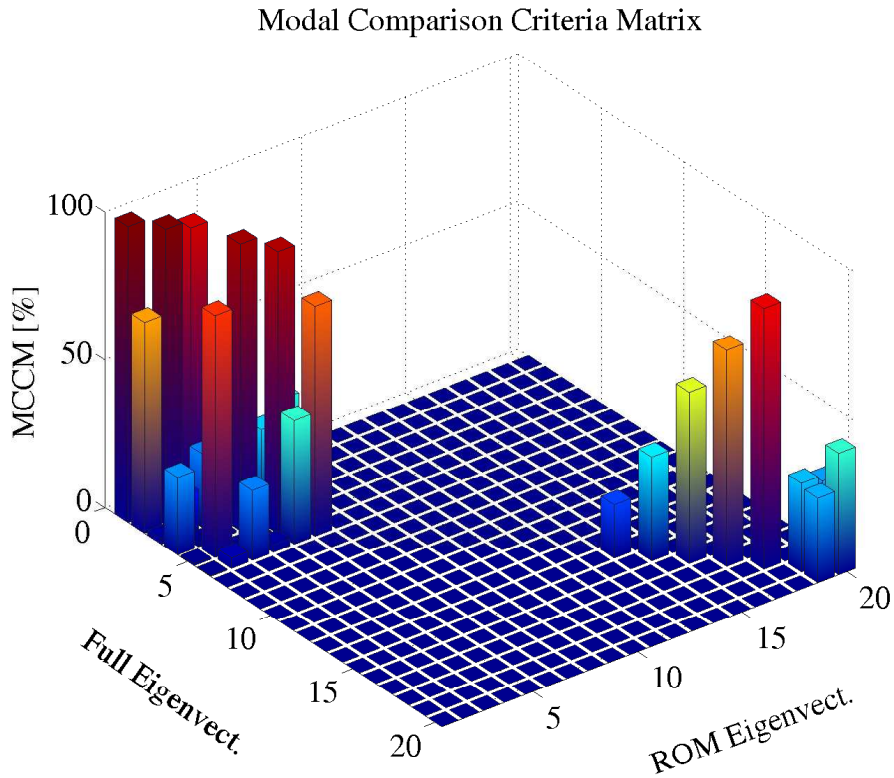


Fig. 3.8: Modal Comparison Criteria Matrix - 3D view

and it is based on the Modal Scale Factor (MSF), which is a scale factor according to the principle of least-square error, i.e.

$$NMD_{(k, r)} = \frac{|\Psi_k(r) - MSF \cdot \Phi_k(r)|_2}{\Psi_k(r)} \quad (3.37)$$

$$MSF_{(i, j)} = \frac{\Psi_i^T \Phi_j}{\Psi_i^T \Psi_i}, \quad i, j = 1, 2, \dots, q. \quad (3.38)$$

As in the COMAC case the objective of NMD is clearer for smaller dimension models, where the DoF are easier to isolate and better to visualize.

6. *Mass Normalized Vector Difference (MNVD).* The MNVD comparison corresponds to the relative vector difference of the modal mass matrices (Eq. (3.17)) for both the original and the ROM model, i.e.

$$MNVD_{(k, l)} = \frac{|\tilde{\mathbf{m}}_{\text{Expanded}} - \tilde{\mathbf{m}}_{\text{Full}}|_2}{\|\tilde{\mathbf{m}}_{\text{Expanded}}\|_2} \cdot 100\% = \frac{\sqrt{\sum_r (\tilde{\mathbf{m}}_{\text{Expanded}}(r) - \tilde{\mathbf{m}}_{\text{Full}}(r))^2}}{\sqrt{\sum_r (\tilde{\mathbf{m}}_{\text{Expanded}}(r))^2}} \cdot 100\%. \quad (3.39)$$

Fig. 3.9 is a typical representation of the MNVD correlation coefficient. This representation does not help in deriving sufficient conclusions regarding the com-

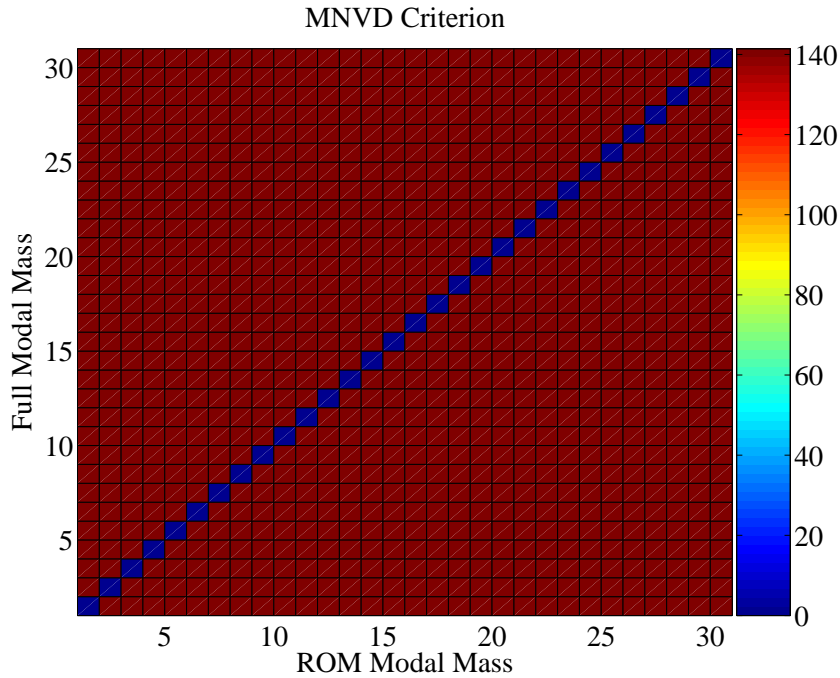


Fig. 3.9: Mass Normalized Vector Difference - top view

parison of the original and the ROM. Based on the relationship of Eq. (3.17) the correlation is reduced in comparing only the diagonal entries of the MNVD matrix. Herewith, the smaller the values of the diagonal entries are, the better ROM is.

3.2.3 Switching process updating methodology

As mentioned in Subsection 3.2.1, the combination of both the eigenfrequency and eigenvector MCC contributes to the derivation of sufficient conclusions regarding the dynamic properties of the ROM. Up to this point, only the case of CMPs was examined, which occupy the main diagonal of the associated eigenvector criteria (Fig. 3.4 - 3.7). It is quite often, though, that CMPs exist, which do not belong to the associated frequency ranges of the compared models.

In terms of the NFD criterion, the well correlated eigenfrequency pairs deviate from the band diagonal structure (Fig. 3.10). Regarding the correlation example of Fig. 3.10, the associated modMAC coefficient matrix is given in Fig. 3.11. As observed, at the positions indicated by the NFD criterion the eigenvectors correlation is high. The non diagonal CMPs with high modMAC values, i.e. $modMAC \geq 80\%$ are gathered in Table 3.1.

The FEMBS interface [114] utilizes the ROM data generated within a FEM software program and activates certain modules (Chapter 5), with which the FE-data representation is ascertained in the MBS formalism. During this procedure the ROM data cannot be

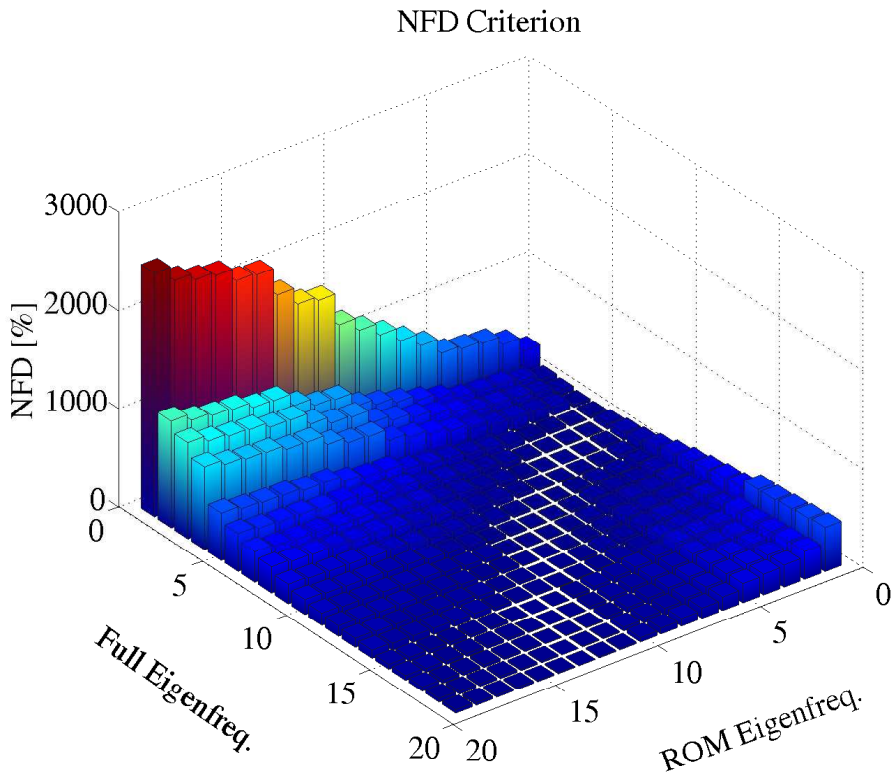


Fig. 3.10: Switching process - Natural Frequency Difference

Table 3.1: Switching process - modMAC matrix - non diagonal CMPs

Non diagonal CMPs	Full-eigenvector Nr.	ROM-eigenvector Nr.
1	13	14
2	14	13
3	19	15
4	16	19

altered, unless the MOR is restarted. In this regard, the correlation order in Fig. 3.11 can only be improved by indicating a larger set of master DoF or Craig-Bampton modes for the case of either the Guyan or the CMS MOR, respectively.

Still, such a procedure is not obligatory during the application of the FEMBS interface aiming at a rigid-elastic coupling. The dynamics of the imported structure, which might be given for example based on Fig. 3.10 - 3.11 are retained and therefore are not false. Thus, a bending or a torsional excitation within the MBS environment would invoke the correct system response based on the adequate bending or torsional mode, respectively. Consequently, the analogous modMAC correlation magnitude is of great importance.

The MORPACK toolbox includes, among other features, the switching process updating methodology. Herewith, the modMAC correlation matrix and therefore the modal

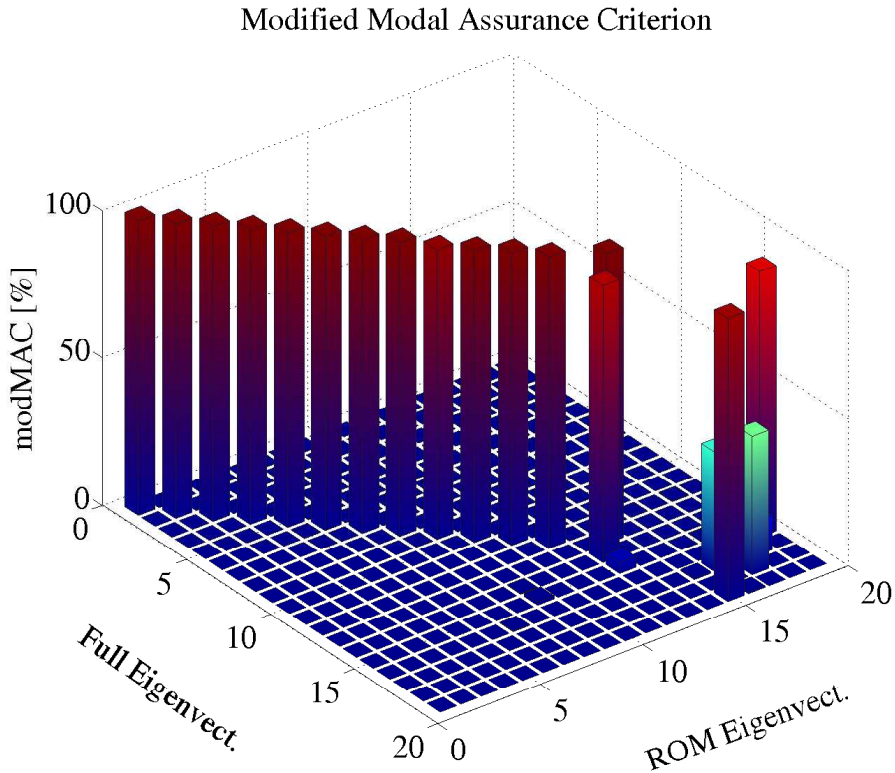


Fig. 3.11: Switching process - Modified Modal Assurance Criterion

matrix of the ROM can be updated. It is accomplished by switching the interchanged eigenvectors, which are identified by their associated modMAC values, since they symmetrically occupy the modMAC secondary diagonal. Such CMPs occur, when the sequential eigenvectors of a model correspond to closely vicinal eigenfrequencies.

On this account, the number of the well CMPs in the main modMAC-diagonal is increased. Regarding the case in Fig. 3.11 and Table 3.1, the updated ROM's modal matrix is given in Eq. (3.40) and the associated modMAC matrix in Fig. 3.12, i.e.

$$\Phi_{\text{updated}} = \begin{bmatrix} \Phi_1 & \Phi_2 & \dots & \underbrace{\Phi_{14} & \Phi_{13}}_{\text{switched vectors}} & \dots & \Phi_{20} \end{bmatrix}. \quad (3.40)$$

The switching process can be conducted for more than one CMPs, which occupy the secondary diagonal of the modMAC matrix (Fig. 3.13 - 3.14). Such dynamic behavior is quite often, especially in case of coping with fixed FE structures (Section 3.3), and the standardized MOR methods are utilized. Therefore, unless better reduction schemes are available, which avoid such kind of minor order inconsistencies but not directly affect the model's dynamics during the FEM-MBS coupling, the application of the switching process updating methodology is rather favored.

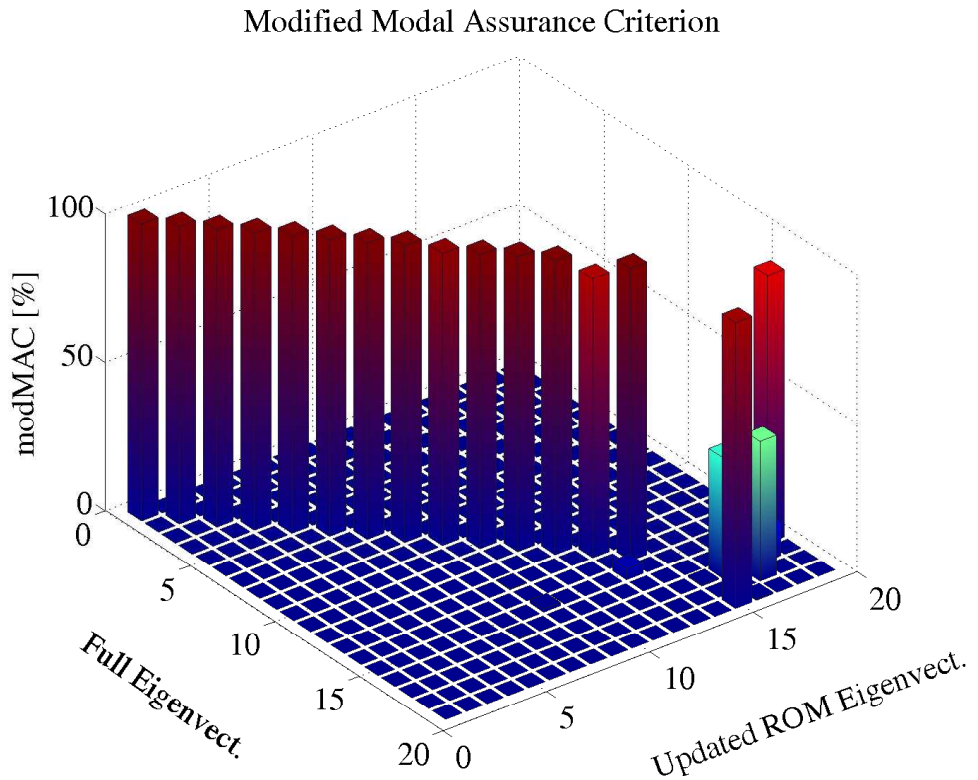


Fig. 3.12: Switching process - Updated modMAC coefficient matrix

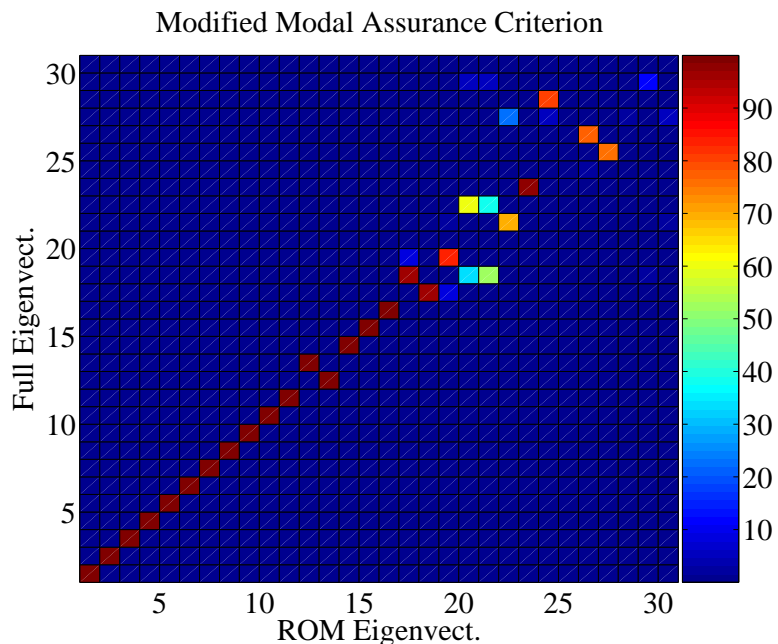


Fig. 3.13: Switching process - Secondary diagonal CMP - original modMAC

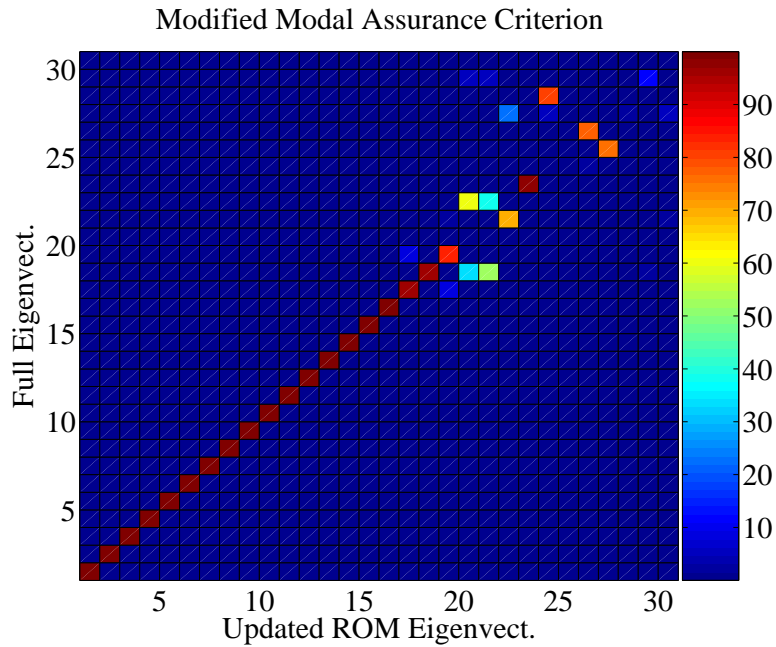


Fig. 3.14: Switching process - Secondary diagonal CMP - updated modMAC

3.3 Application examples

In this Section certain FE discretized structures are used in order to compare the effectiveness of the MOR schemes presented in Chapter 2. Several master DoF constellations are chosen such that both the advantages and disadvantages of each MOR approach can be illustrated. For the first two mechanical structures, i.e. the 3D solid bar and the UIC60 rail, numerous reduction methods are applied, whereas for the last two examples, i.e. the elastic rod and crankshaft, only the dominant MOR methods are used.

The ROM's dynamic properties are validated with the help of the MCC. A particular emphasis is placed on the modMAC coefficient matrix. The eigenvector information is a prerequisite aspect during the FEM-MBS coupling procedure and therefore, the modMAC assessment is compulsory.

3.3.1 3D solid bar structure - Case 1

The first case concerns an undamped 3D solid bar structure, which is discretized with FE in ANSYS (Fig. 3.15). The number of elements (tetrahedron *SOLID95*) and nodes generated is $n_{elem} = 60$ and $n_{node} = 471$, respectively. Each node is appointed with 3 translational DoF (UX, UY, UZ). On this account the dimension of the model's system matrices is computed as given in Eq. (2.32) - (2.33), i.e.

$$\dim(\mathbf{M}) = \dim(\mathbf{K}) = (1413, 1413). \quad (3.41)$$

The master DoF set is selected according to the criteria presented in Section 2.2 and is depicted in Fig. 3.15. Thus, the dimension of the ROM system matrices is:

$$\dim(\mathbf{M}_{\text{ROM}}) = \dim(\mathbf{K}_{\text{ROM}}) = (72, 72). \quad (3.42)$$

The purpose of this first application example is to test the validity range of each of the applied MOR methods. In this regard, the consideration of a rather large eigenvalue (eigenfrequency and eigenvector) range is required. Thus, in the MCC figures that follow, the first 36 eigenvalues for both the original and the associated ROM are compared. The rigid body eigenvalues are disregarded for the case of coping with the unconstrained version of the structure.

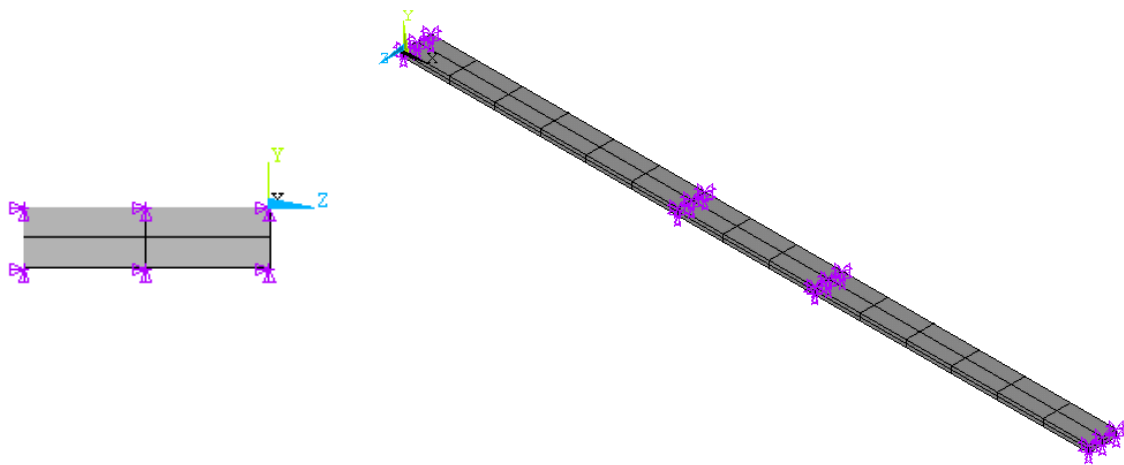


Fig. 3.15: 3D solid bar structure - Case 1 - master DoF

Firstly, the non constrained case is examined and the associated MCC coefficient matrices are depicted throughout the Fig. 3.16 - 3.19. As expected, both the Guyan and the dynamic ROM fail to sufficiently capture the dynamics of the original model. The important inertia effect is neglected and thence, the correlation of medium to high eigenvalues is rather unsuccessful. Isolating the MNVD coefficient matrix (Fig. 3.19a), it is observed that the above mentioned reduction schemes end up with the best possible correlation results. The y-axis is logarithmically scaled indicating thus, all applied MOR schemes to be delivering sufficiently accurate results regarding this criterion.

The SEREP as well as the KSM ROM capture best the dynamics of the original model, namely, for the whole eigenvalue comparison range. The algorithm of the SEREP method indicates the procedure to be exact. Therefore, for the rest of the master DoF constellations to be formulated in this first application example, the SEREP ROM will not be further considered.

The ROM generated by the standardized CMS method with 10 CB modes appears to be capturing the original model's dynamics up to the mid-end of the chosen frequency range and its dynamic quality is overwhelmed by both the generalized Guyan and the IRS ROM. As expected, the ICMS reduction scheme succeeds in generating a better correlated ROM. A plausible outcome, since the algorithm takes into consideration the

information loss due to the part-static nature of both the IRS and the CMS MOR. The IKCMS ROM is slightly worse than the equivalent ICMS ROM, i.e. the effect of the slave structure's Krylov modes is less effective than the equivalent CB modes. Finally, the KCMS method marginally improves the Guyan ROM due to the consideration of the Krylov modes in the algorithm's superposition principle.

In Fig. 3.20 the NRFD and the modMAC coefficient matrices depict the results of the restarted CMS, ICMS, IKCMS, and IRS methods. It is conducted by indicating a larger CB modes set for the first three methods, i.e. $CB = 20$, and by applying the iterated version of the IRS algorithm for the latter method, i.e. $n_{\text{IRS}}^{\text{iter}} = 2$. The quality of the resulted ROM's dynamics is substantially improved, but is accompanied by a 27% matrix dimension increase (CMS, ICMS, IKCMS), which can only be negatively regarded in case of importing the ROM into a MBS code. The CMS MOR is the less efficient method, since inconsistencies occur with a consequence of zero modMAC correlation (eigenvectors 23, 24 and 33, 34 in Fig. 3.20b). The NRFD values of the associated eigenfrequencies (Fig. 3.20b) fail in delivering sufficient conclusions for the poorly correlated eigenvectors. Hence, the sole utilization of eigenfrequency MCC should be avoided. The answer for this occurrence is depicted in Fig. 3.21 and concerns the case of perfectly CMP, which symmetrically occupy the modMAC secondary diagonal. The application of the switching process updating methodology (Subsection 3.2.3) could improve the order properties of the associated modal matrix.

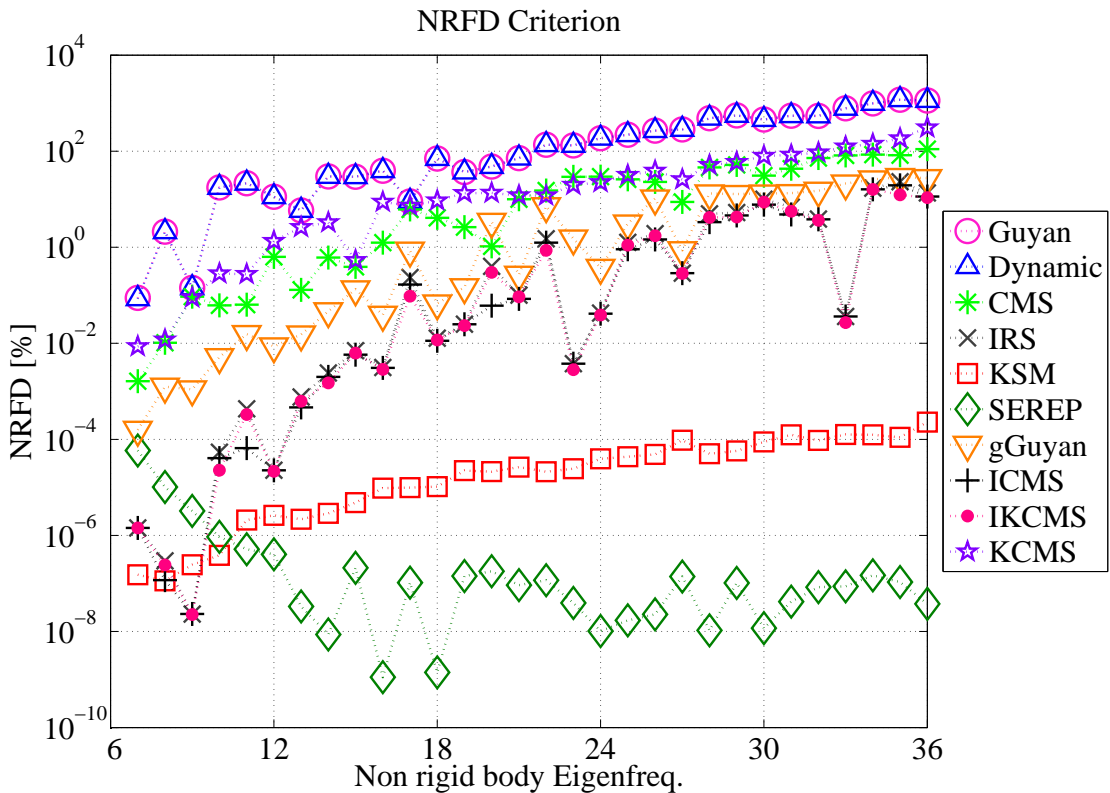


Fig. 3.16: Free 3D solid bar - NRFD criterion

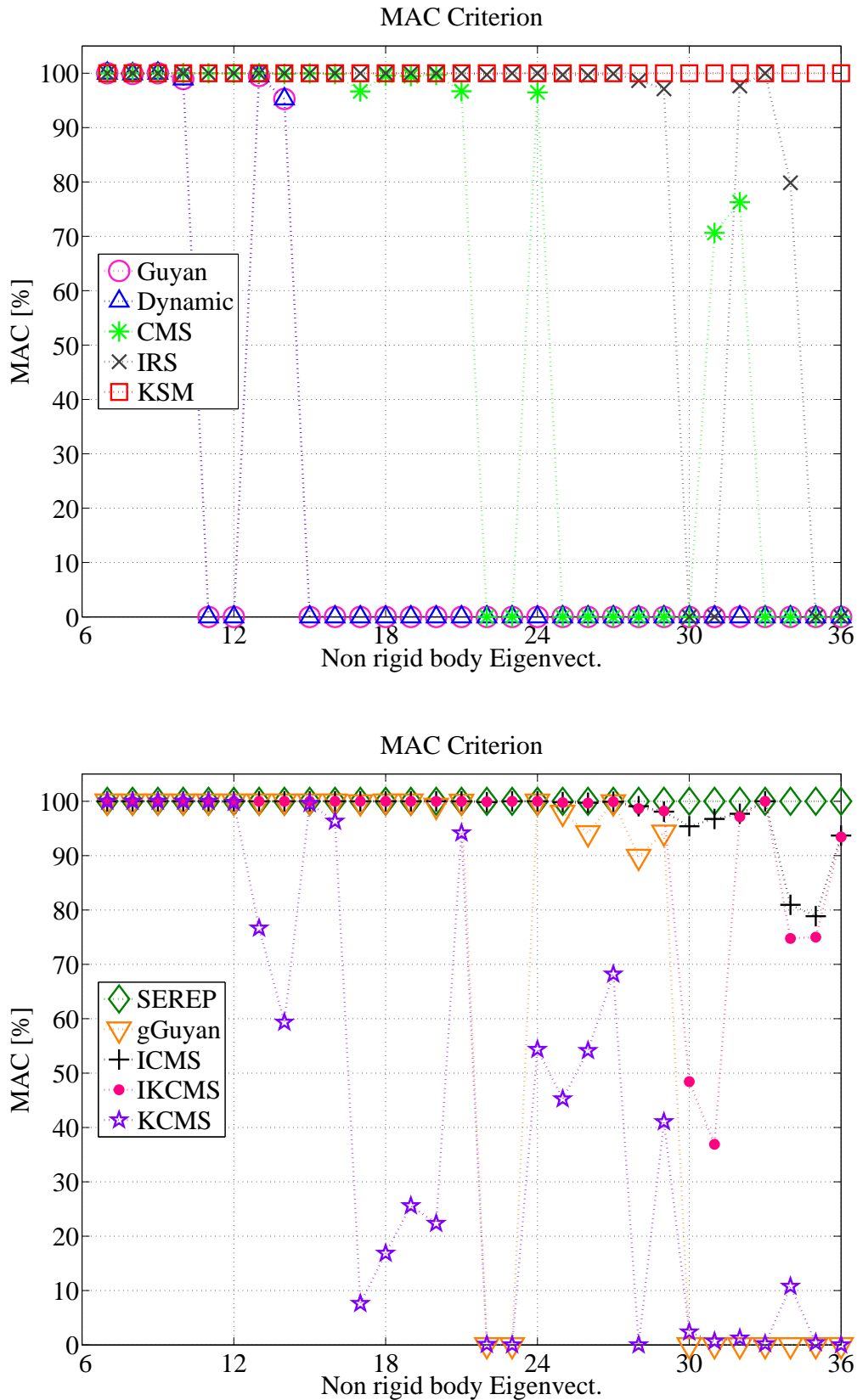


Fig. 3.17: Free 3D solid bar - MAC criterion

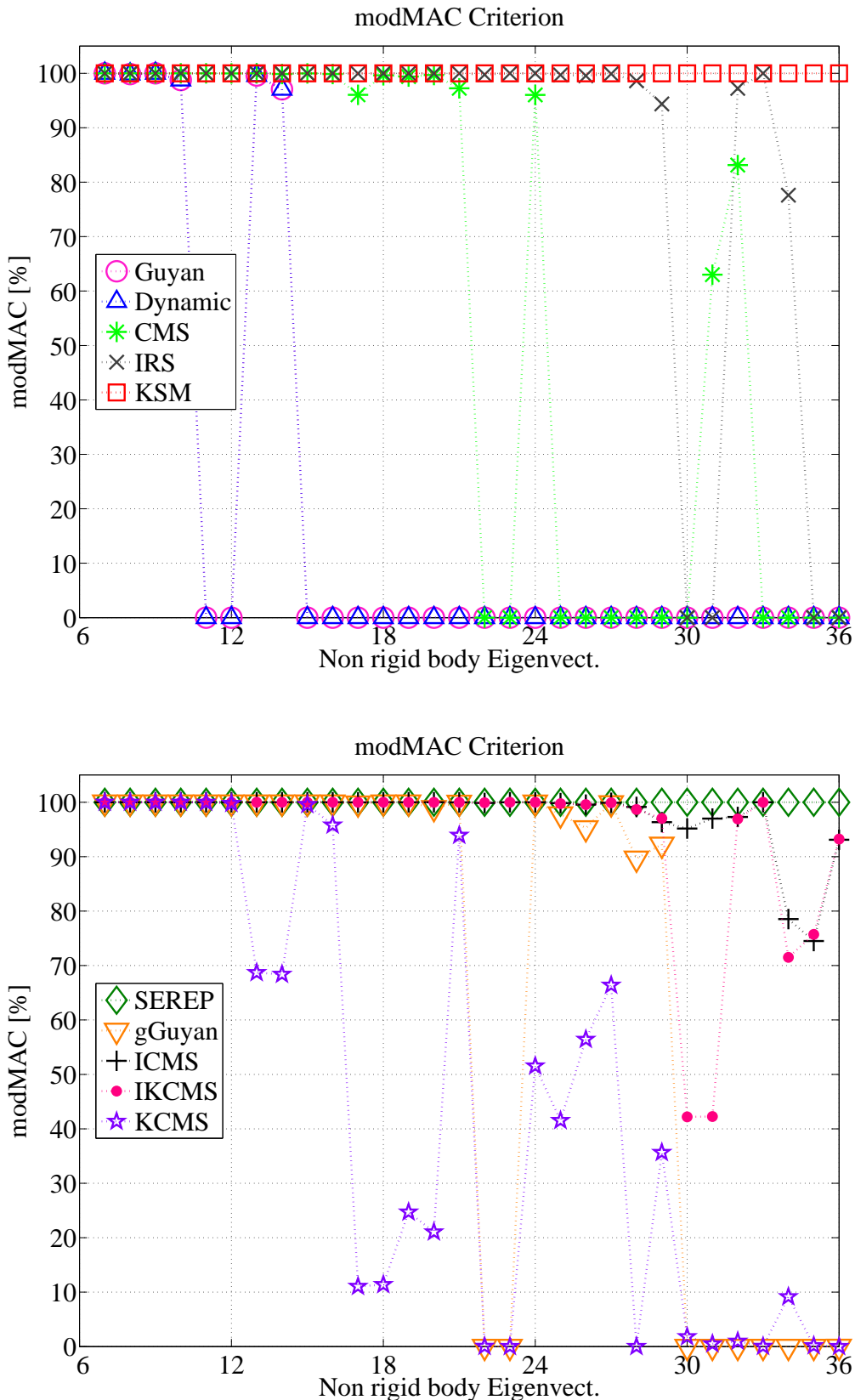


Fig. 3.18: Free 3D solid bar - modMAC criterion

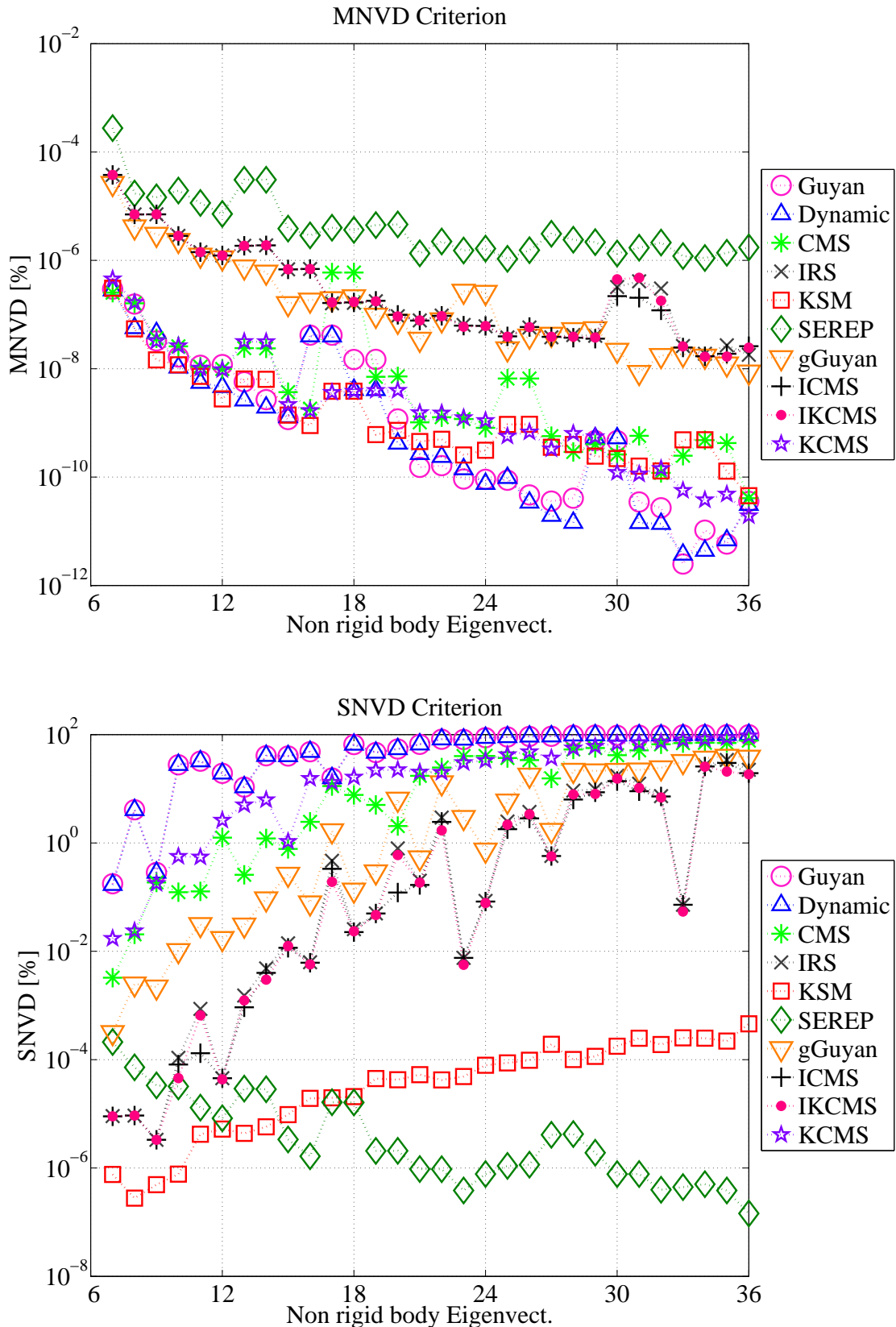


Fig. 3.19: Free 3D solid bar - MNVD & SNVD criterion

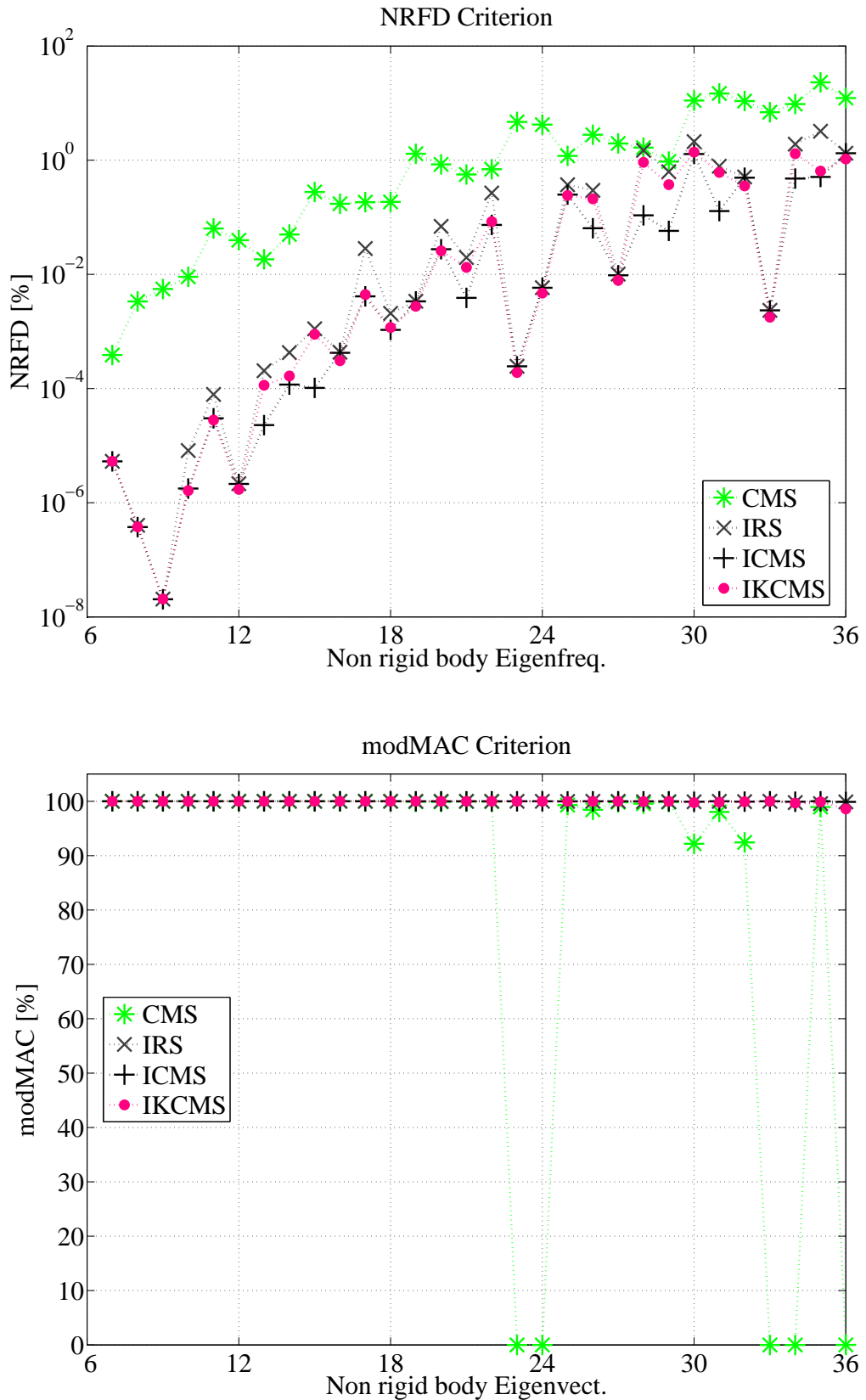


Fig. 3.20: Free 3D solid bar - NRFD & modMAC - 2 IRS iter. & 20 CB

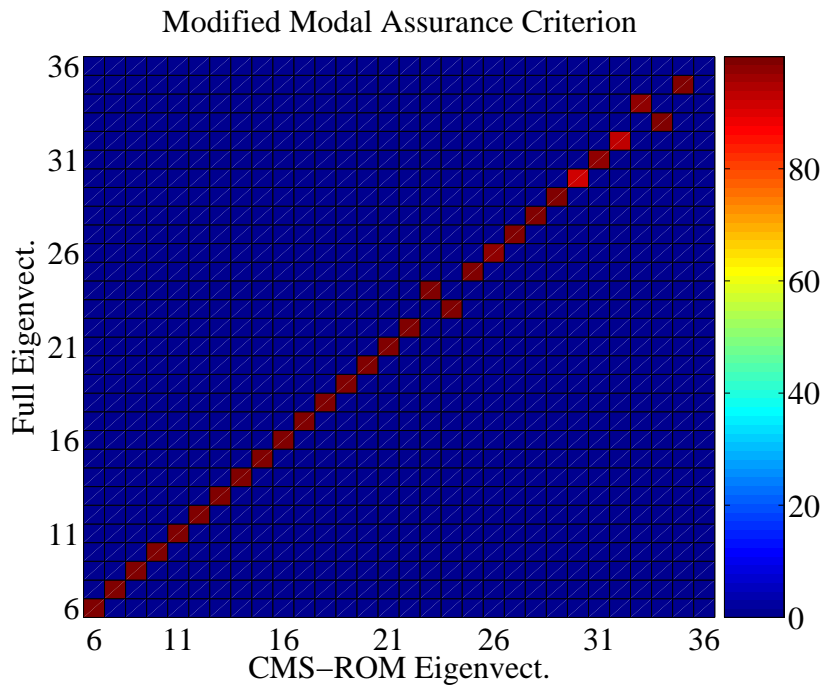


Fig. 3.21: Free 3D solid bar - CMS - modMAC top view

The consideration of the 3D solid bar with certain DoF being fixed is the content of Fig. 3.22 - 3.27. Here, two different constrained models are utilized, namely, the one-end and the two-end fixed 3D solid bar structure. In general, constrained structures are of particular interest if, ultimately, the FEM-MBS coupling is intended. Firstly, the task of every MOR scheme is aggravated, since the required correlated eigenvalue range is higher and secondly, the dimension of the ROM's system matrices is always smaller than the dimension of the associated non-constrained ROM, i.e. the information gathered into the reduced system is minimized (Eq. (2.35)):

$$\text{One-end fixed: } n_{\text{DoF}}^{\text{fixed}} = 18 \Rightarrow \dim(\mathbf{M}_{\text{ROM}}) = \dim(\mathbf{K}_{\text{ROM}}) = (54, 54) \quad (3.43)$$

$$\text{Two-end fixed: } n_{\text{DoF}}^{\text{fixed}} = 36 \Rightarrow \dim(\mathbf{M}_{\text{ROM}}) = \dim(\mathbf{K}_{\text{ROM}}) = (36, 36). \quad (3.44)$$

The larger the constrained DoF set is, the less effective the MOR scheme under the consideration of a certain ROM dimension is, an outcome depicted throughout the Fig. 3.22 - 3.27. The KSM MOR scheme offers qualitatively the best ROM with a number of perfectly CMPs, which reduces along with the increase of the constrained DoF. The rest of the reduction schemes provide ROM, which satisfy the dynamic requirements up to the medium frequency range with the best in this category being the ICMS ROM.

An improvement of the ROM's quality takes place by increasing the CB modes set or applying the iteration scheme for the CMS, ICMS, IKCMS, or the IRS methods (Fig. 3.25 and 3.27). Here, the same dimension disadvantage occurs as in the non-constrained case and as observed, only the ICMS MOR succeeds in well capturing the required eigenvalue range. For the two-end fixed case further improvement is possible by applying the switching process updating methodology (Fig. 3.27).

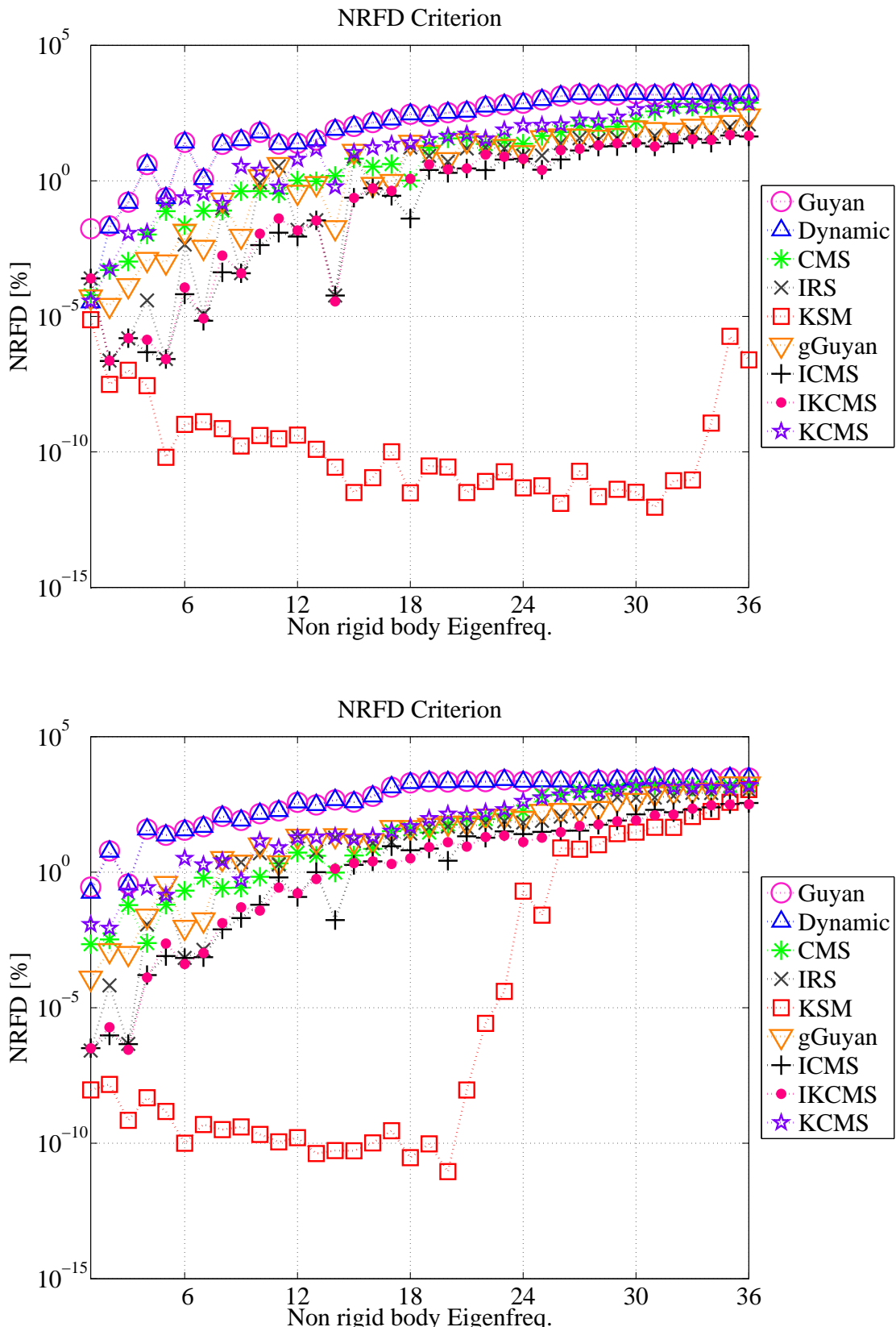


Fig. 3.22: One-end (top) & two-end (bottom) fixed 3D solid bar - NRFD

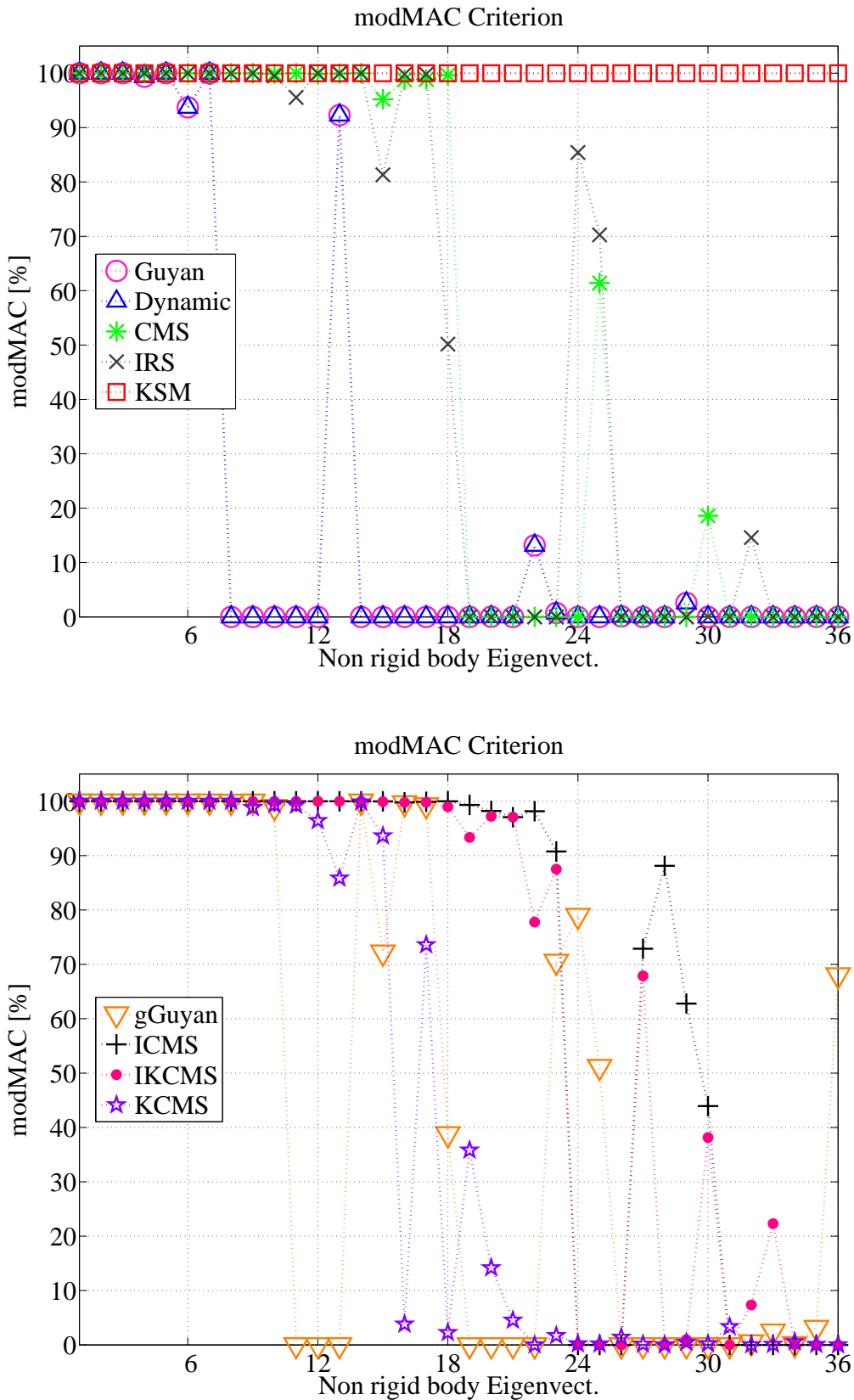


Fig. 3.23: One-end fixed 3D solid bar - modMAC criterion

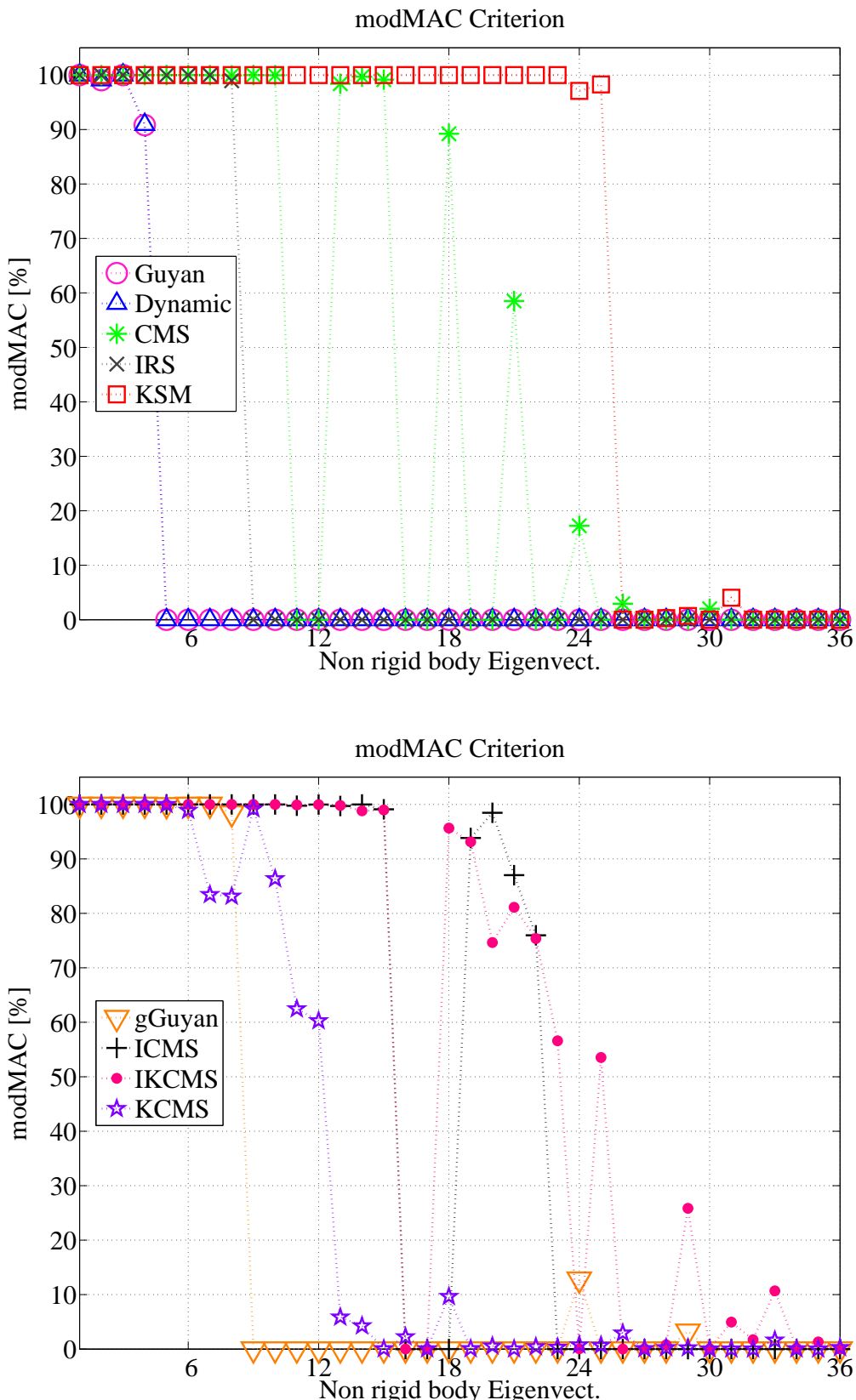


Fig. 3.24: Two-end fixed 3D solid bar - modMAC criterion

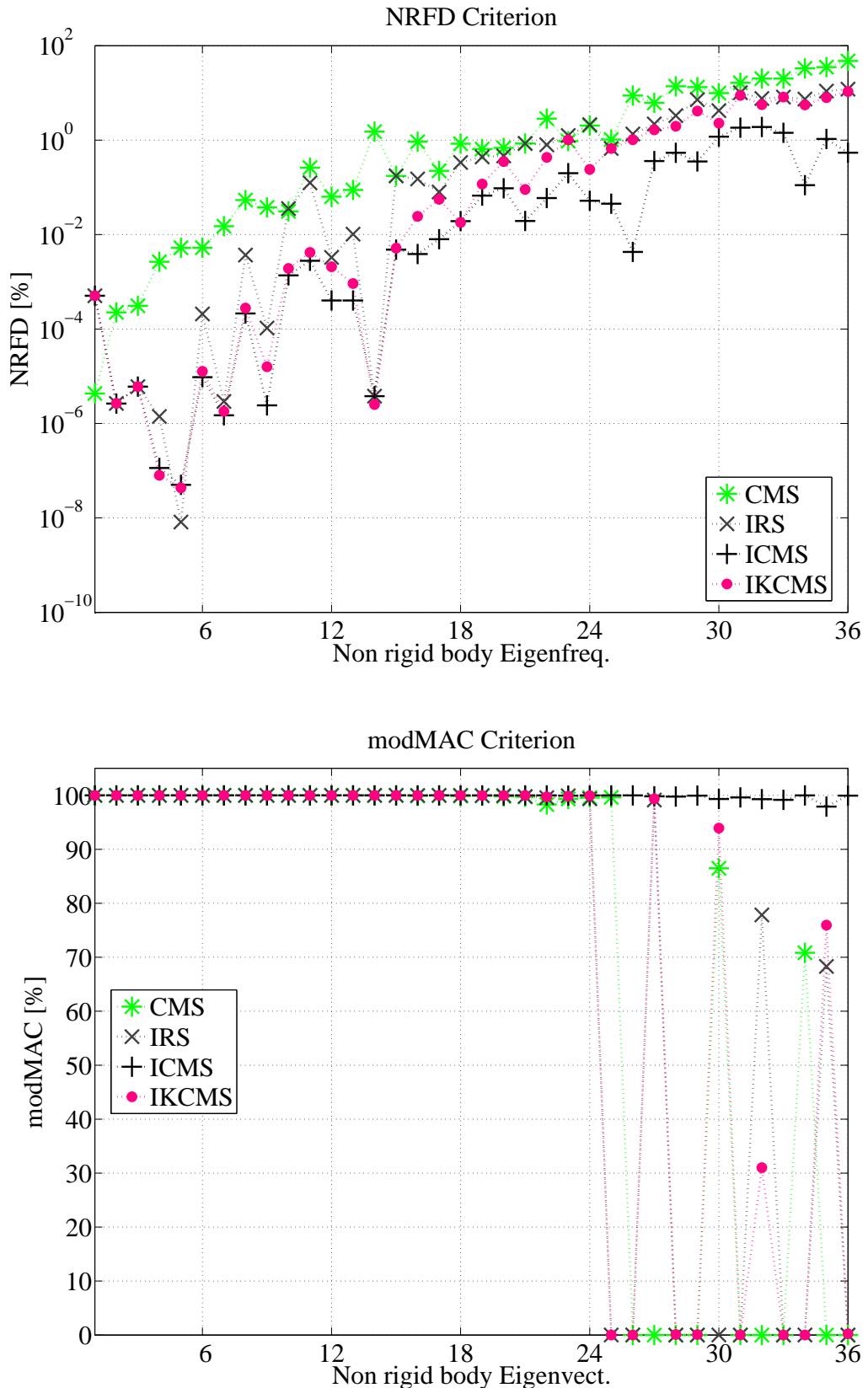


Fig. 3.25: One-end fixed 3D solid bar - NRFD & modMAC- 2 IRS iter. & 20 CB

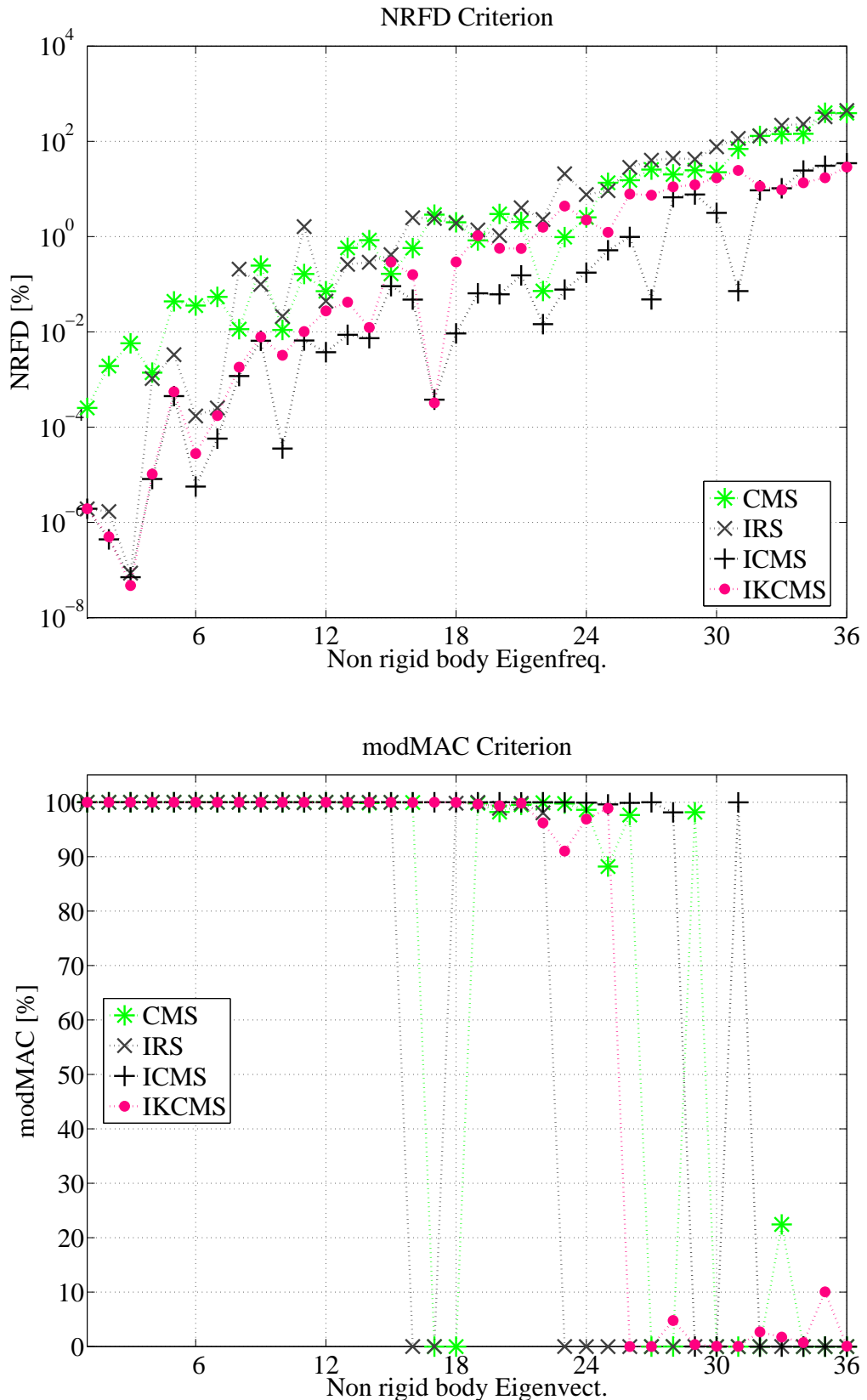


Fig. 3.26: Two-end fixed 3D solid bar - NRFD & modMAC- 2 IRS iter. & 20 CB

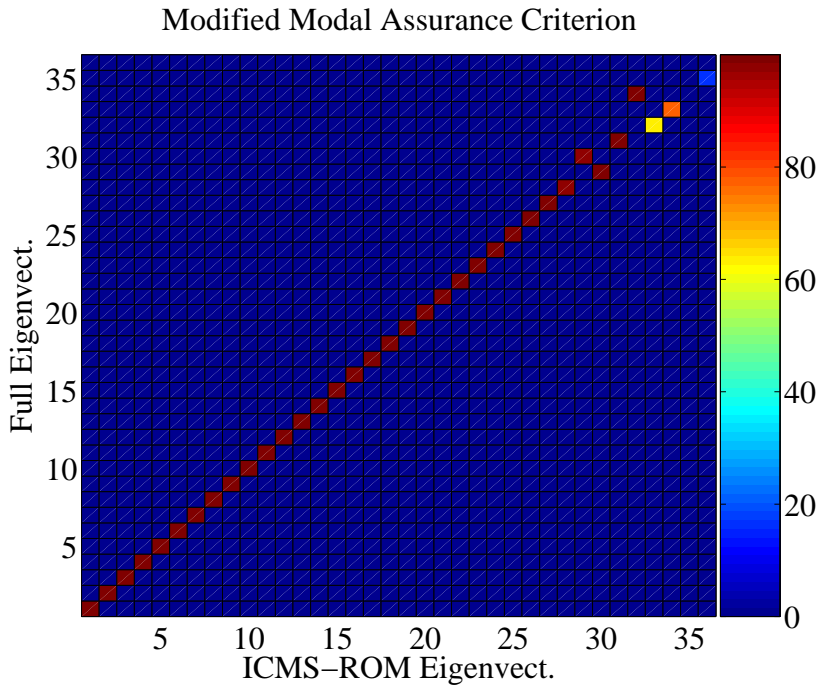


Fig. 3.27: Two-end fixed 3D solid bar - ICMS - modMAC top view

3.3.2 3D solid bar structure - Case 2

This case copes with the aspect of the symmetric master DoF allocation and its effect on the dynamic properties of the ROM. According to the m -set selection guidelines (Section 2.2), it is advised for the master DoF to be symmetrically selected along the structure and thus, generating a slave-model with plausible structural properties. Therefore, the same 3D solid bar model is utilized, but a different master DoF constellation is chosen as depicted in Fig. 3.28. The structure is fixed at both ends and thus, the dimension of the ROM's system matrices are given as follows:

$$n_{\text{DoF}}^{\text{fixed}} = 18 \Rightarrow \dim(\mathbf{M}_{\text{ROM}}) = \dim(\mathbf{K}_{\text{ROM}}) = (36, 36) \quad (3.45)$$

The dimension of the ROM's system matrices equals the dimension of the equivalent system matrices in the previous two-end fixed case (Eq. (3.44)). Due to its algorithmic scheme, the KSM MOR approach should be to a larger extend invariant to such master DoF variations, which result in ROMs of the same dimension. The only drawback would refer to a degradation of the condition properties of the constrained sorted stiffness matrix, which could affect the ARNOLDI algorithm during the necessary stiffness inversion step.

Here, only the dominant MOR methods are considered, namely, the CMS, IRS, ICMS, and KSM. While the KSM ROM is almost identical to its equivalent of the previous two-end fixed case (the last three eigenvalues are affected), the IRS ROM shows no substantial improvement. On the contrary, the CMS ROM is satisfactorily improved,

whereas the ICMS ROM stands as the best choice. Thence, apart from the KSM scheme and according to all the previous MCC results, the ICMS MOR method constitutes an interesting candidate competing the standardized CMS.

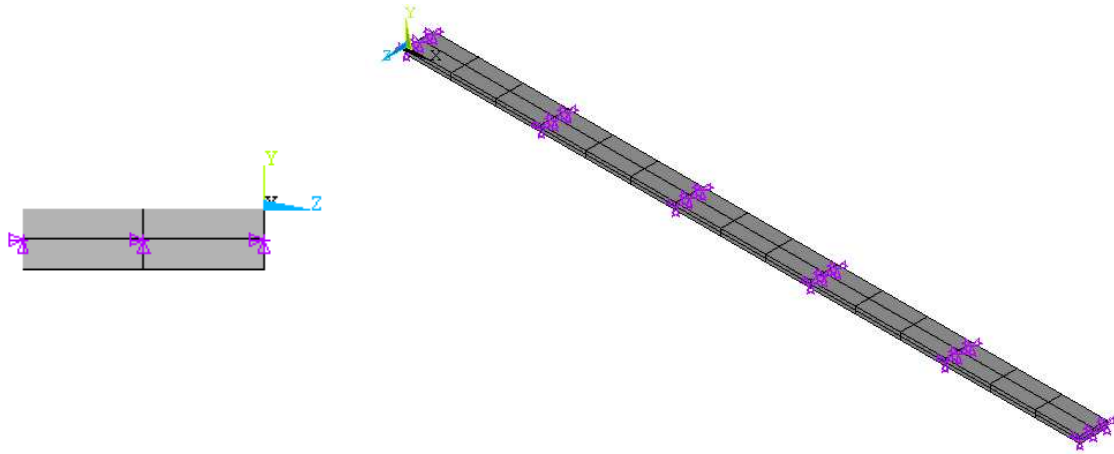


Fig. 3.28: 3D solid bar structure - Case 2 - master DoF

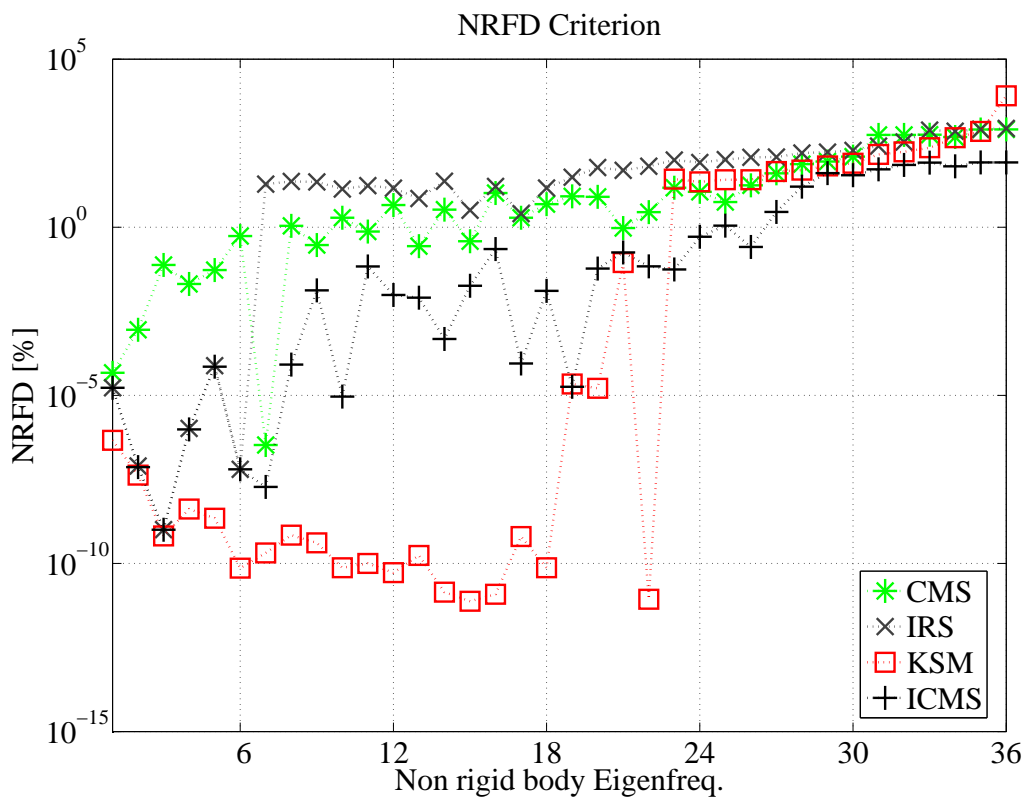


Fig. 3.29: Two-end fixed 3D solid bar - Case 2 - NRFD

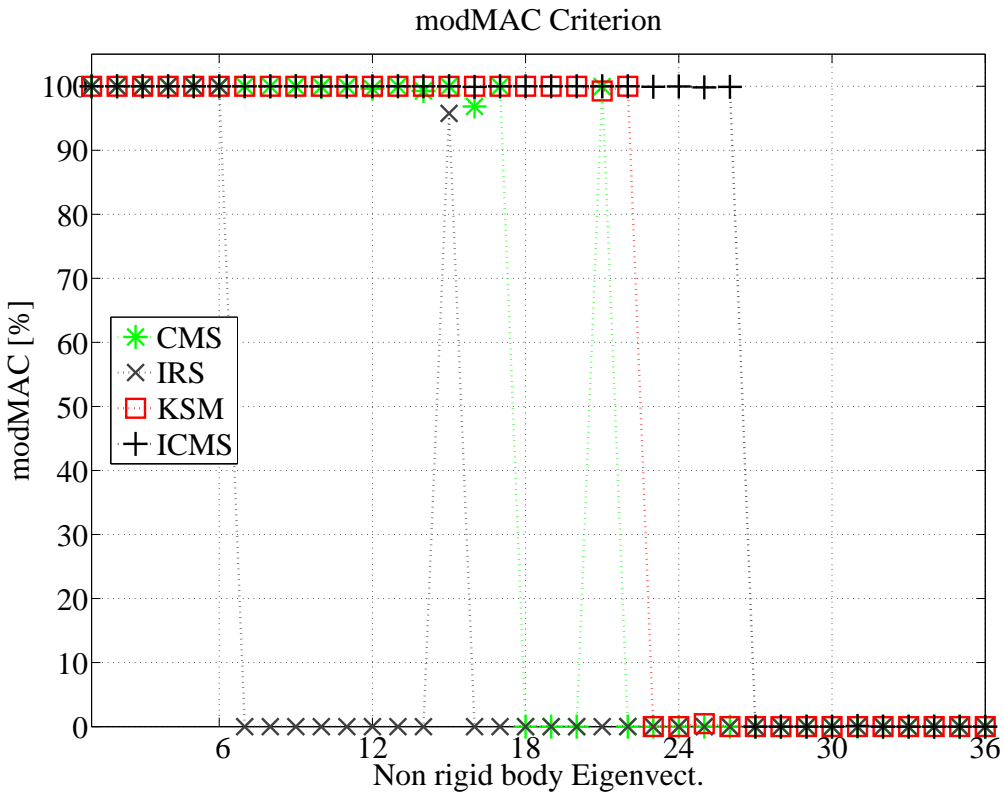


Fig. 3.30: Two-end fixed 3D solid bar - Case 2 - modMAC

3.3.3 UIC60 elastic rail - Case 1

The structure depicted in Fig. 3.31 concerns a 1.2 meter long and 144 kilogram heavy UIC60 rail. It is modeled and discretized in ANSYS and consists of $n_{elem} = 576$ elements (hexahedron *SOLID45*) and $n_{node} = 1054$ nodes. Each node is appointed with 3 translational DoF (UX, UY, UZ). Thence, the dimension of the model's system matrices is computed as given in Eq. (2.32) - (2.33), i.e.

$$\dim(\mathbf{M}) = \dim(\mathbf{K}) = (3162, 3162). \quad (3.46)$$

In order to initialize the MOR schemes, a total of $m = 105$ master DoF are selected (Fig. 3.31). The nature of the structure requires the selected m DoF, which are situated at the bottom of the model, to be grounded. Therefore, the dimension of the ROM's system matrices is:

$$n_{\text{DoF}}^{\text{fixed}} = 45 \Rightarrow \dim(\mathbf{M}_{\text{ROM}}) = \dim(\mathbf{K}_{\text{ROM}}) = (60, 60) \quad (3.47)$$

The m selection is conducted according to the criteria presented in Section 2.2 and therefore, it is expected from the MOR schemes, which depend upon this aspect, to generate ROM of high accuracy. Still, as depicted in Fig. 3.32 - 3.34, this is not the

case, since the existence of constraints implies a higher eigenvalue spectrum requirement for both the original and the ROM models. On this account, the standardized CMS MOR (10 CB modes) succeeds well in capturing the dynamics of the original model up to the beginning of the mid-ranged eigenvalues. SEREP, KSM, and ICMS ($n_{\text{IRS}}^{\text{iter}} = 0$ and 10 CB modes) constitute the best choices. The consideration of Fig. 3.35 suggests a further correlation improvement for the ICMS-ROM via the application of the switching process updating methodology.

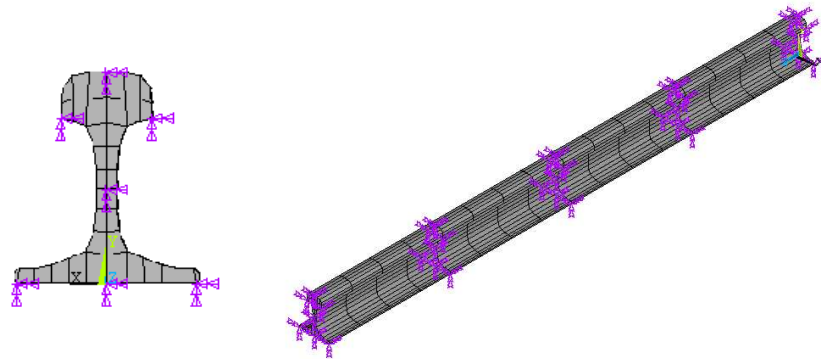


Fig. 3.31: UIC60 rail - bottom grounded - master DoF

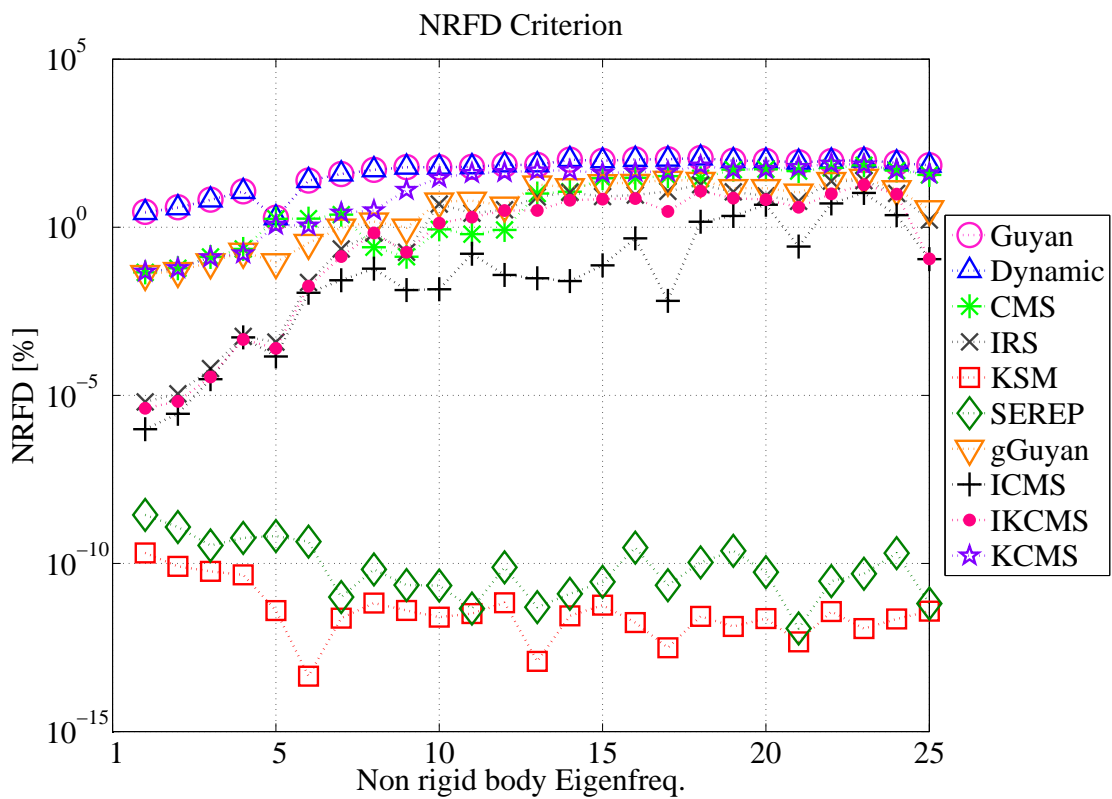


Fig. 3.32: UIC60 rail - bottom grounded - NRFD criterion

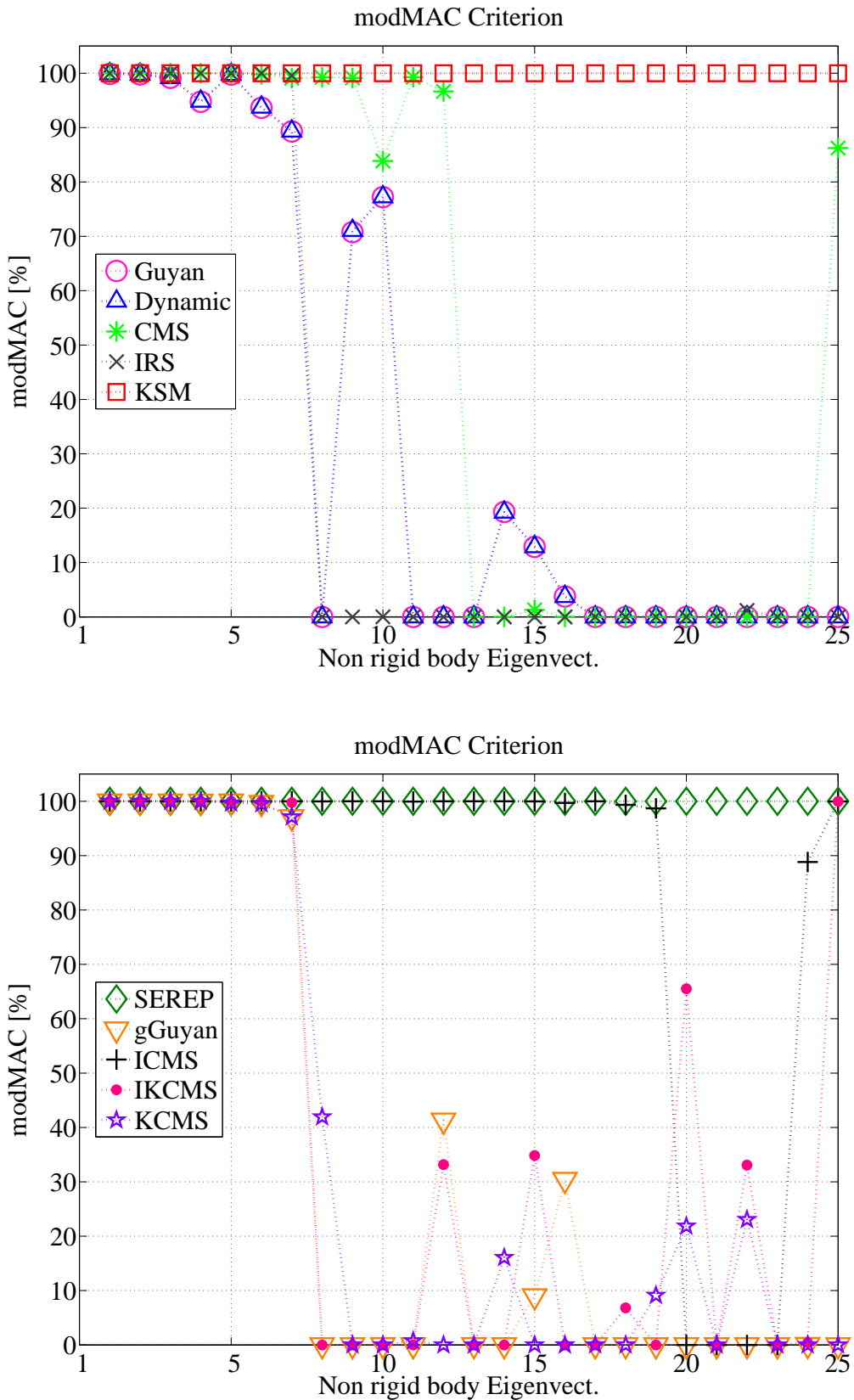


Fig. 3.33: UIC60 rail - bottom grounded - modMAC criterion

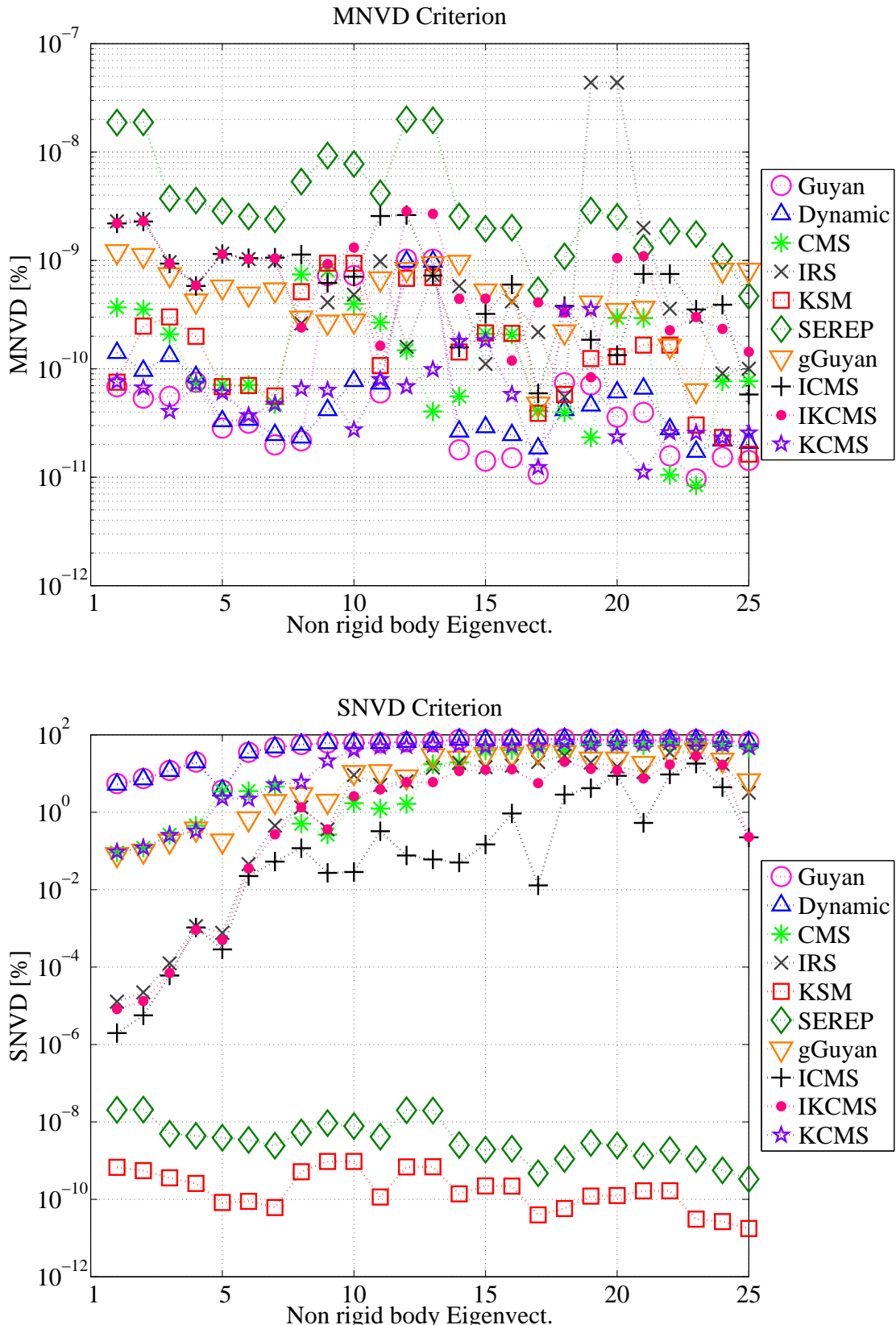


Fig. 3.34: UIC60 rail - bottom grounded - MNVD & SNVD

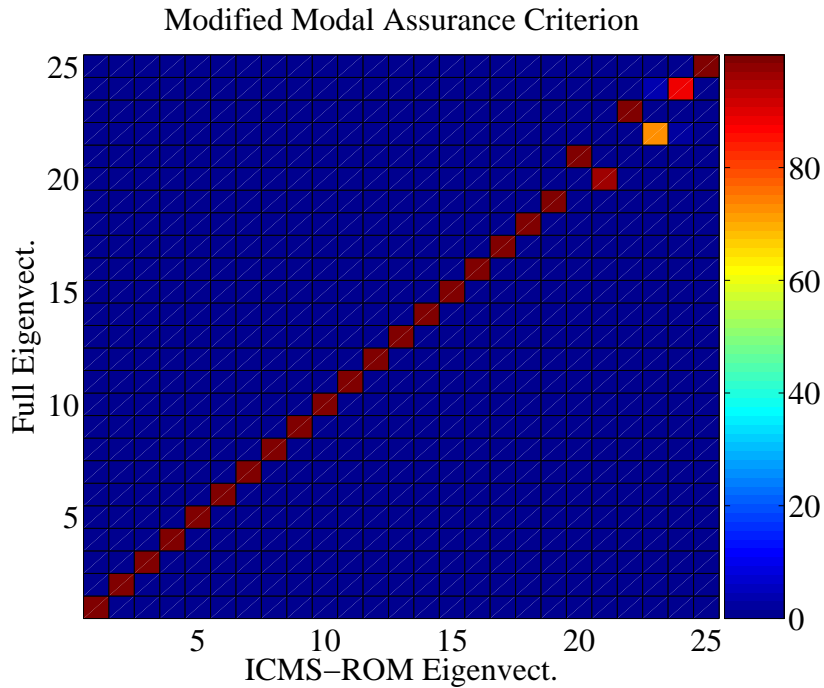


Fig. 3.35: UIC60 rail - bottom grounded - modMAC ICMS top view

3.3.4 UIC60 elastic rail - Case 2

In this example the dependency of the MOR algorithms on the master DoF choice is demonstrated. Therefore, two different master ($m = 48$) sets are chosen, namely, the normal and the clumsy master DoF sets (Fig. 3.36). While the normal set consists of master DoF equally and symmetrically distributed along the unconstrained UIC60 structure, the clumsy set constitutes the case of inappropriately concentrating the master DoF at one end of the model. The correlation results throughout the Fig. 3.37 - 3.39 plausibly depict the SEREP and KSM superiority (m -free MOR) under such conditions.

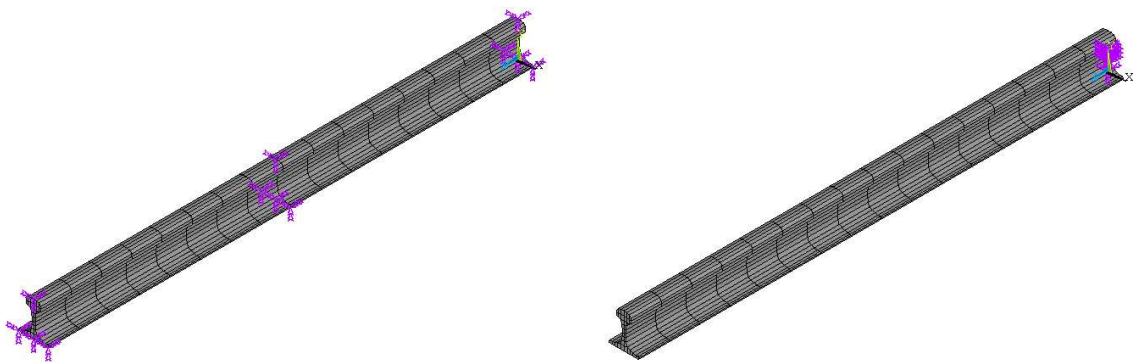


Fig. 3.36: UIC60 rail - Normal (left) & Clumsy (right) m -set

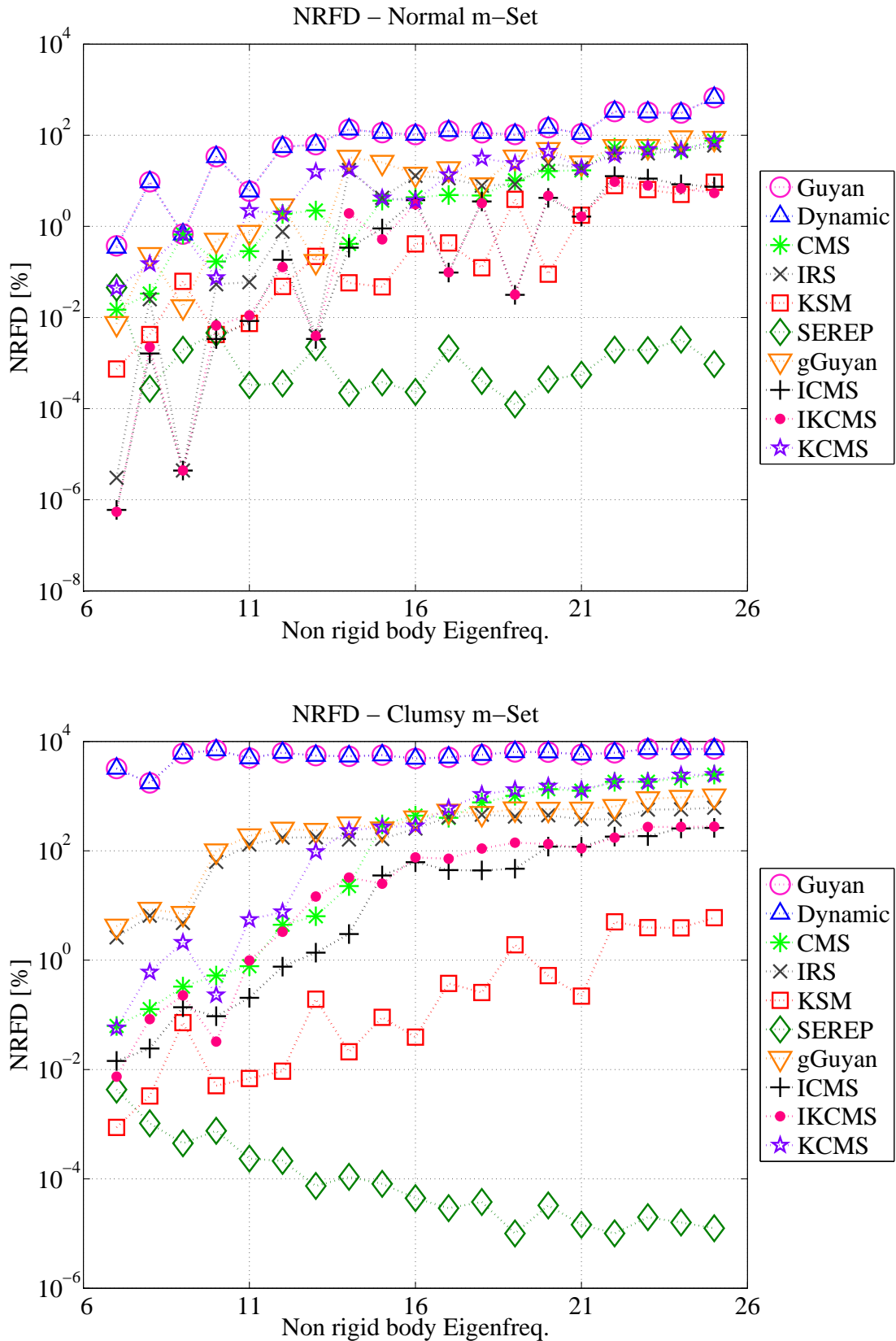
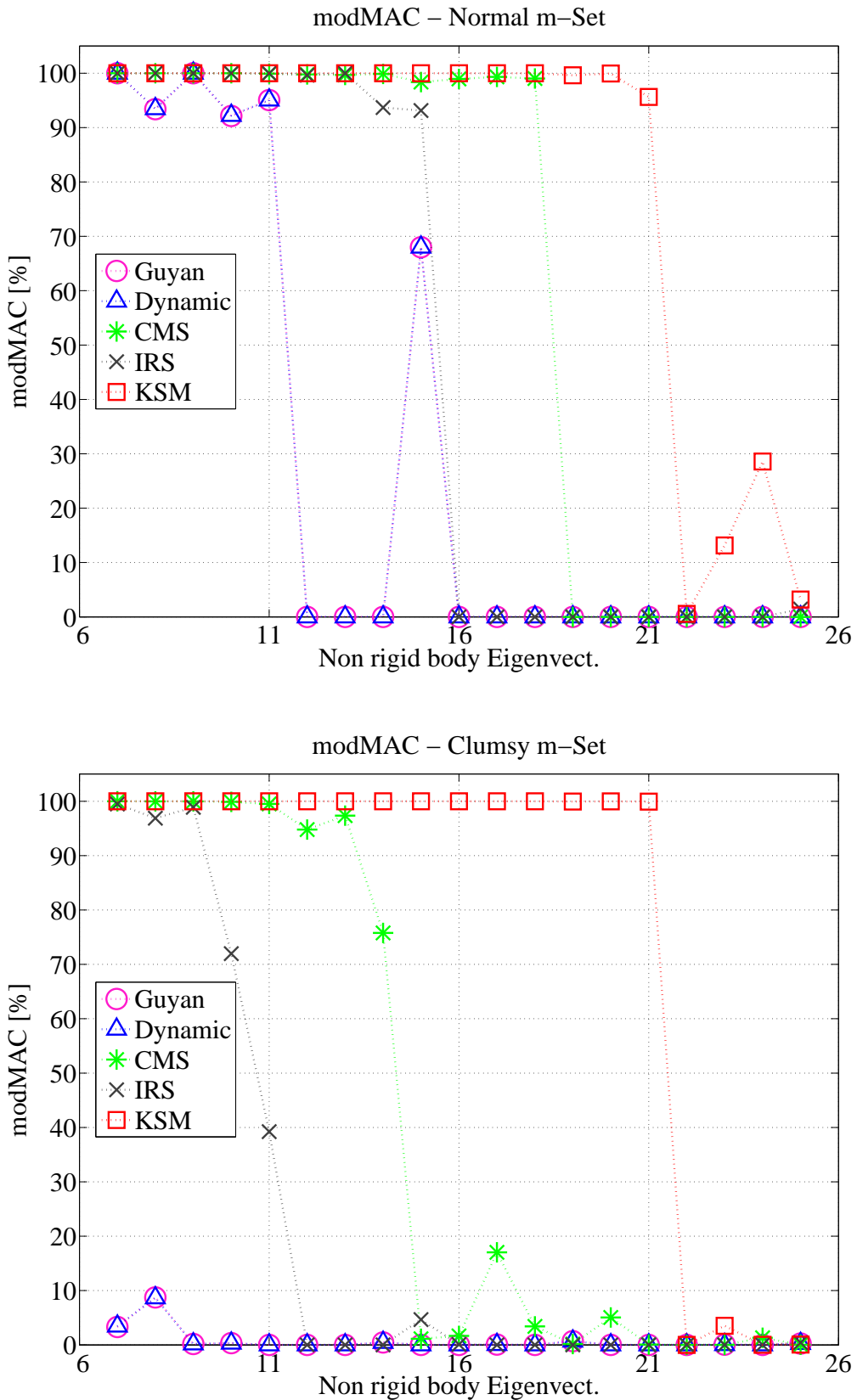


Fig. 3.37: UIC60 rail - NRFD - Normal & Clumsy m -set

Fig. 3.38: UIC60 rail - modMAC - Normal & Clumsy *m*-set

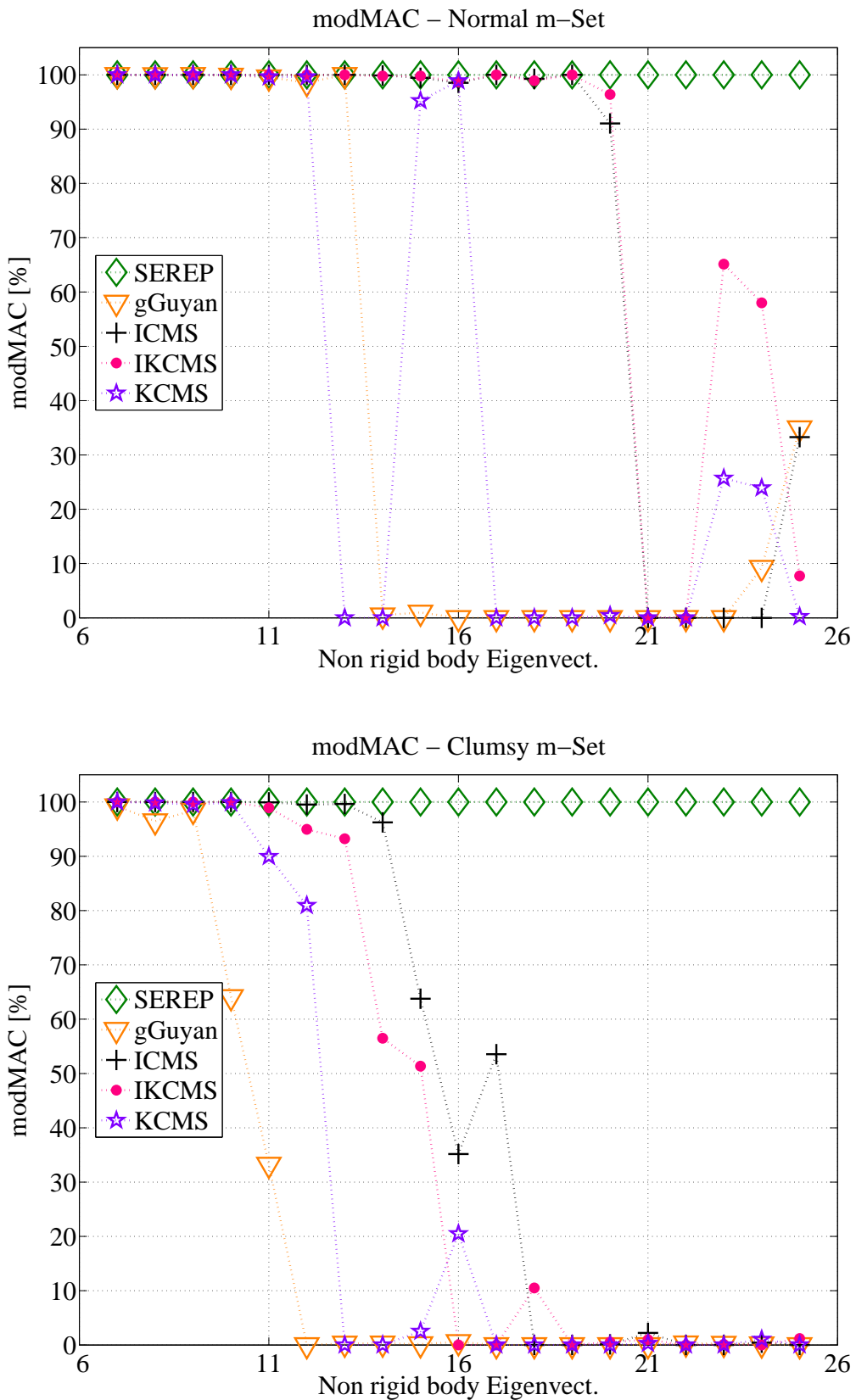


Fig. 3.39: UIC60 rail - modMAC - Normal & Clumsy *m*-set

3.3.5 Elastic rod

The comparison of various reduction schemes is a procedure, the nature of which is twofold. So far, two application examples were utilized in order to validate the dynamics of the associated ROM under several master DoF constellations. It was accomplished with the help of the previously presented MCC.

The second important aspect regarding the twofold nature of the MOR comparison is the computation time. On one hand, the ROM is by all means desired to be able to capture the dynamics of the original structure up to the user's predefined eigenvalue spectrum. On the other hand, the generation of perfectly correlated ROMs, which is accompanied by vast computation times, can only be negatively regarded. Thence, the conclusion of a MOR being successful or not resides on both the dynamic properties of the ROM and the computation time required for the procedure to be completed.

In case of coping with very large structures, the application of direct methods [51, 36] for computing the coordinate transformation matrix (Eq. (2.38)) fails due to increased storage requirements. Hence, iterative approaches are advised [102]. The efficiency of the iterative algorithm is measured by the convergence rate at each iteration step, an aspect which can be vastly affected by the common ill-conditioned properties of a FE structure's stiffness matrix (Chapter 4). On this account, the elastic rod (Fig. 3.40) is chosen to constitute the third application example for the iterative application of various MOR schemes. It belongs to the category of medium sized models, since it consists

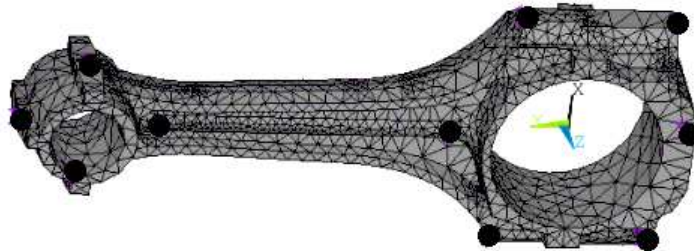


Fig. 3.40: Elastic rod - master DoF (black points) - Unconstrained

of $n_{elem} = 13868$ elements (tetrahedron *SOLID95*) and $n_{node} = 23835$ nodes. Each node is appointed with 3 translational DoF (UX, UY, UZ). The dimension of the model's system matrices is computed as given in Eq. (2.32) - (2.33), i.e.

$$\dim(\mathbf{M}) = \dim(\mathbf{K}) = (71505, 71505). \quad (3.48)$$

Here, only the dominant MOR methods are utilized, i.e. CMS, ICMS, KSM and SEREP, and the dynamic properties of the associated ROM are compared by means of the NRFD and the modMAC criterion. Additionally, two types of the two-step MOR approaches are applied, namely, the SEREP-KSM, and SEREP-ICMS methods. Based on the two-step MOR algorithmic procedure (Fig. 2.8), the original model is firstly reduced

generating thus, a fairly large dimensioned ROM and thereafter, the second reduction scheme is applied in order to compute the final ROM.

On the basis of the aforesaid, the master DoF set is selected, as depicted in Fig. 3.40 and the dimension of the sequentially generated ROM is given below:

$$\text{First MOR: } q_{\text{node}} = 90 \Rightarrow \dim(\mathbf{M}_{\text{ROM}}) = \dim(\mathbf{K}_{\text{ROM}}) = (270, 270) \quad (3.49)$$

$$\text{Second MOR: } m_{\text{node}} = 10 \Rightarrow \dim(\mathbf{M}_{\text{ROM}}) = \dim(\mathbf{K}_{\text{ROM}}) = (30, 30). \quad (3.50)$$

The SEREP MOR method constitutes the best possible choice regarding both the quality of the ROM and the computation time required therefor (Fig. 3.41 - 3.44 and Table 3.2). Although the standardized CMS MOR is the second fastest algorithm, it generates the worst quality ROM. The utilization of the switching process updating methodology could improve the ICMS-ROM's correlation properties and consequently designate it as a marginally better ROM than the KSM-ROM. Concerning the computational time aspect though, the KSM MOR seems to be a better candidate than the ICMS approach.

The application of the two-step MOR methods could be regarded as a compulsory methodology in cases where either the computation time of one-step MOR schemes is vast or specifically, when the direct utilization of SEREP fails (Section 2.4.4). As depicted in Fig. 3.44 such reduction schemes can be very efficient with minor computation time requirements (Table 3.2).

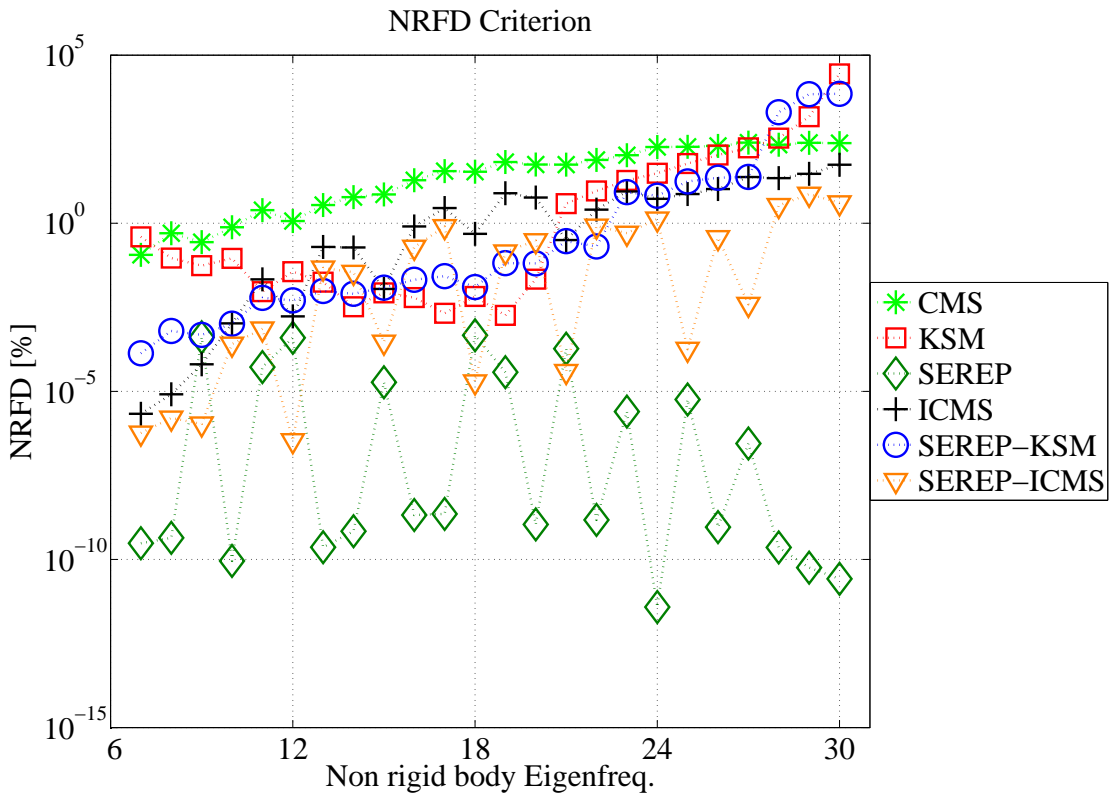


Fig. 3.41: Elastic rod - NRFD criterion

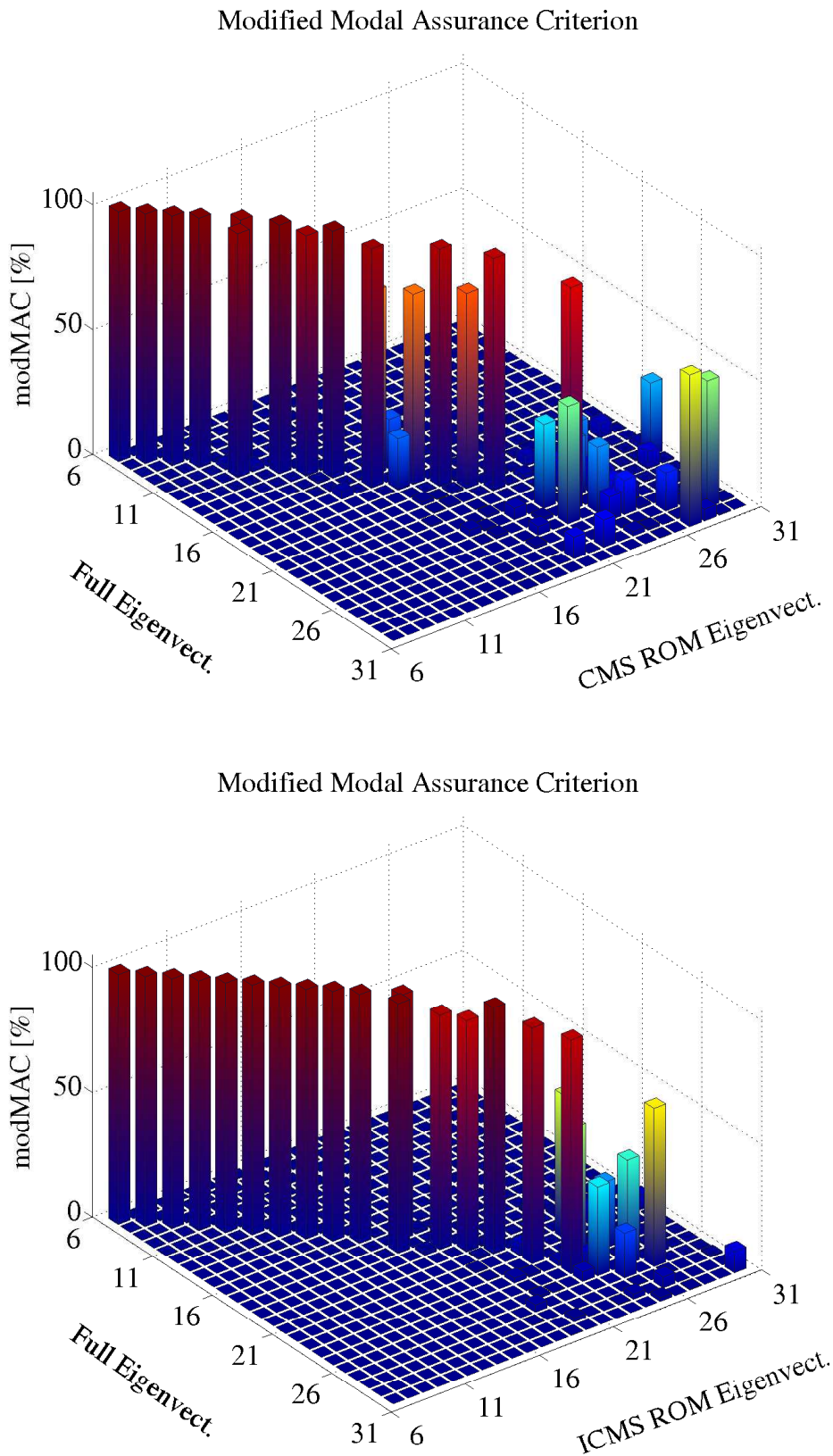


Fig. 3.42: Elastic rod - CMS & ICMS MOR - modMAC

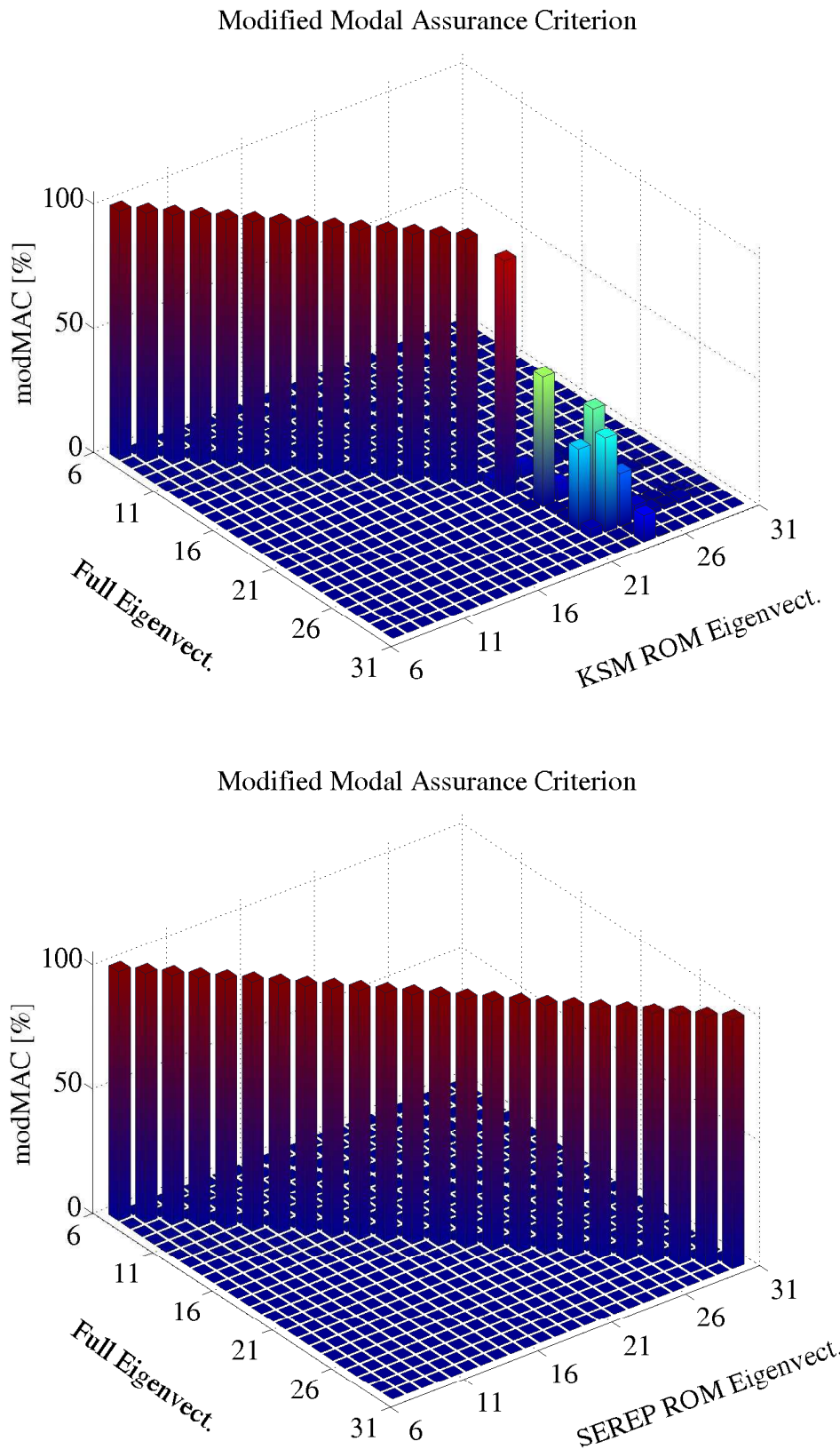


Fig. 3.43: Elastic rod - KSM & SEREP MOR - modMAC

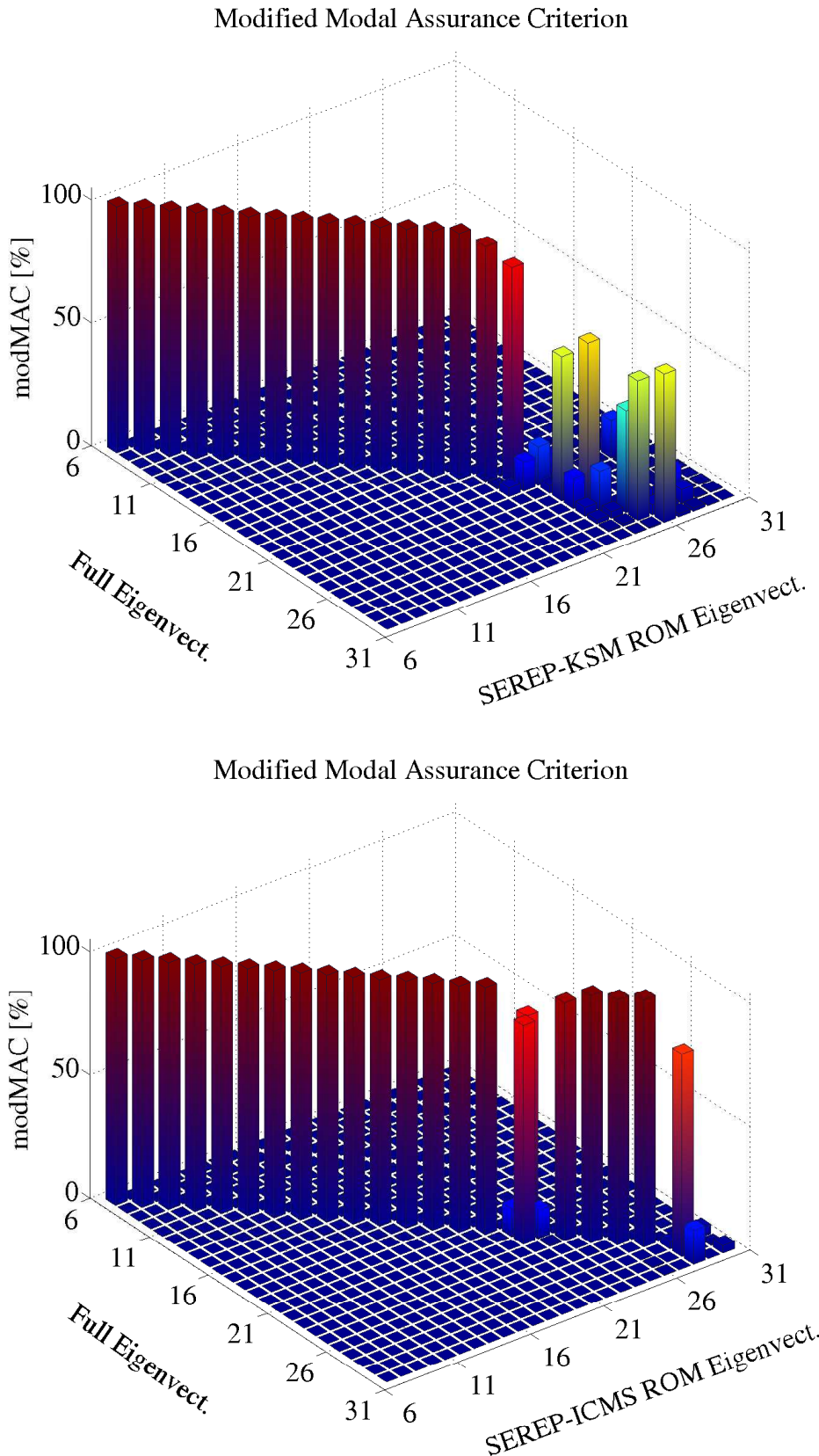


Fig. 3.44: Elastic rod - SEREP-KSM & SEREP-ICMS MOR - modMAC

Table 3.2: Elastic rod - MOR Comparison - Quality Computation Time

MOR	Computation time [min]	$modMAC \geq 90\%$
CMS	18.6	9
ICMS	37.8	13
KSM	32.3	14
SEREP	2.1	24
SEREP-KSM	2.3	15
SEREP-ICMS	2.2	19

Finally, the matter of the obligatory utilization of both the eigenfrequency and eigenvector criteria when validating the dynamic properties of a ROM is demonstrated in this Subsection. Therefore, Table 3.3 is comprised of some additional information regarding the quality of the ICMS and CMS ROM. As observed, a simple comparison of the eigenfrequency spectrum for the original and the ROM results in very well eigenfrequency-CMPs, e.g. 11 and 12, or 17 and 18 for the CMS or the ICMS ROM, respectively. In both cases the relative eigenfrequency comparison is small, i.e. $NRFD < 3\%$ and consequently, the analogous correlation is expected for the associated eigenvectors. Nevertheless, the $modMAC$ criterion (Fig. 3.42) gives a zero percent correlation, i.e. $modMAC = 0\%$ (Table 3.3).

Table 3.3: Elastic rod - CMS & ICMS - NRFD & modMAC

MOR	Eigenvect. Nr.	NRFD [%]	modMAC [%]
CMS	11	2.45	0
	12	1.16	0
ICMS	17	2.84	0
	18	0.48	0

The initialization of the switching process updating methodology could improve the order of the eigenvector correlating discrepancies.

3.3.6 Elastic crankshaft

The elastic crankshaft (Fig. 3.45) completes the series of application examples for this Chapter. It is selected under the same assumptions and conditions as the elastic rod model (Subsection 3.3.5) and is discretized in ANSYS with tetrahedron *SOLID95* elements, each one being appointed with three translational DoF (UX, UY, UZ). It belongs to the category of large FE models, since it consists of $n_{elem} = 73141$ elements (tetrahedron *SOLID95*) and $n_{node} = 114608$ nodes. In this regard, the dimension of the

model's system matrices (Eq. (2.32) - (2.33)) is ascertained as shown below:

$$\dim(\mathbf{M}) = \dim(\mathbf{K}) = (343824, 343824). \quad (3.51)$$

In order to initialize the reduction procedure the master DoF are selected in the middle of each bearing as depicted in Fig. 3.45. Thence, the designated dimension of the ROM is:

$$\dim(\mathbf{M}_{\text{ROM}}) = \dim(\mathbf{K}_{\text{ROM}}) = (33, 33). \quad (3.52)$$

The large dimension of the system matrices (Eq. (3.51)) indicates the application of an iterative approach for the MOR scheme to be rather compulsory. Nevertheless, the direct solution appears to be feasible in case of invoking special software packages and libraries for sparse linear systems, e.g. CSparse [36], TAUCS [121] or the, so called, Multifrontal Massively Parallel Solver [91]. On this account, the computation time is comparable to the time required for a static-analysis solution by commercial FEM software packages. Here, the iterative approach is adopted and four different ROM are computed, namely, by utilizing both the one- and two-step MOR algorithms. The CMS and KSM schemes are chosen for the purpose of the first category, whereas the SEREP-CMS and SEREP-ICMS constitute the methods of the latter category.

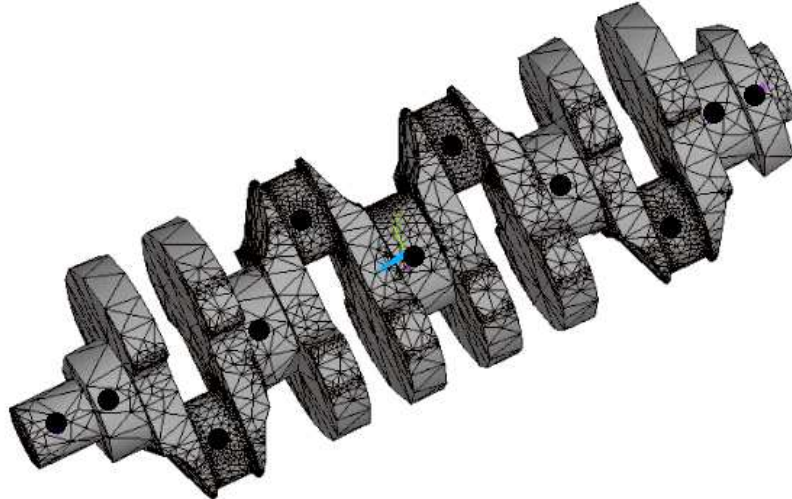


Fig. 3.45: Elastic crankshaft - Unconstrained

In Fig. 3.46 - 3.48 and Tables 3.5 - 3.6 the lack of efficiency regarding the one-step algorithmic schemes is demonstrated. Although the well CMPs cover a fairly large eigenvalue range, the required computation time is vast and thus, such MOR methods are inappropriate for large dimensioned models. In contrast to the one-step methods the applied two-step algorithms overcome this problem and moreover, the generated ROM are more accurate. Therefore, the fast SEREP algorithmic scheme is utilized and a fairly

large dimensioned first-ROM is computed, i.e.

$$\text{First MOR: } \Rightarrow \dim(\mathbf{M}_{\text{ROM}}) = \dim(\mathbf{K}_{\text{ROM}}) = (450, 450). \quad (3.53)$$

The large dimension number in Eq. (3.53) assures the computation of a first-ROM, which captures perfectly the dynamics of the original model up to the predefined limit. The SEREP MOR is completed within 2 hours (Table 3.5) with approximately 77% thereof being utilized for the formulation of the associated ROM matrices (Table 3.4).

Table 3.4: Elastic crankshaft - SEREP - CPU Time

SEREP MOR	CPU Time [min]	CPU Time [%]	Algorithm
Modal analysis	22.93	19.6	Lumped mass
$\mathbf{T}_{\text{SEREP}}$	4.15	3.6	PCG Lanczos
$\{\mathbf{M}, \mathbf{D}, \mathbf{K}\}_{\text{SEREP}}$	89.73	76.8	Sparse SVD
Total	116.8	100	Matrix algebra

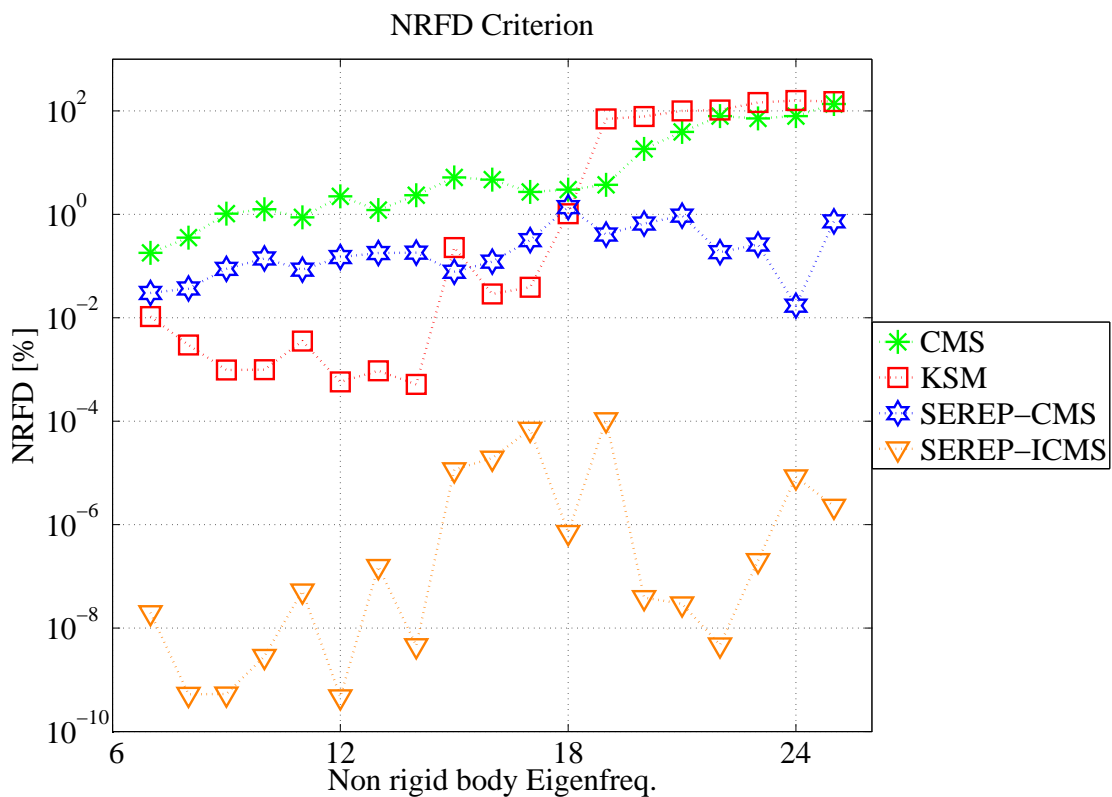


Fig. 3.46: Elastic crankshaft - NRFD criterion

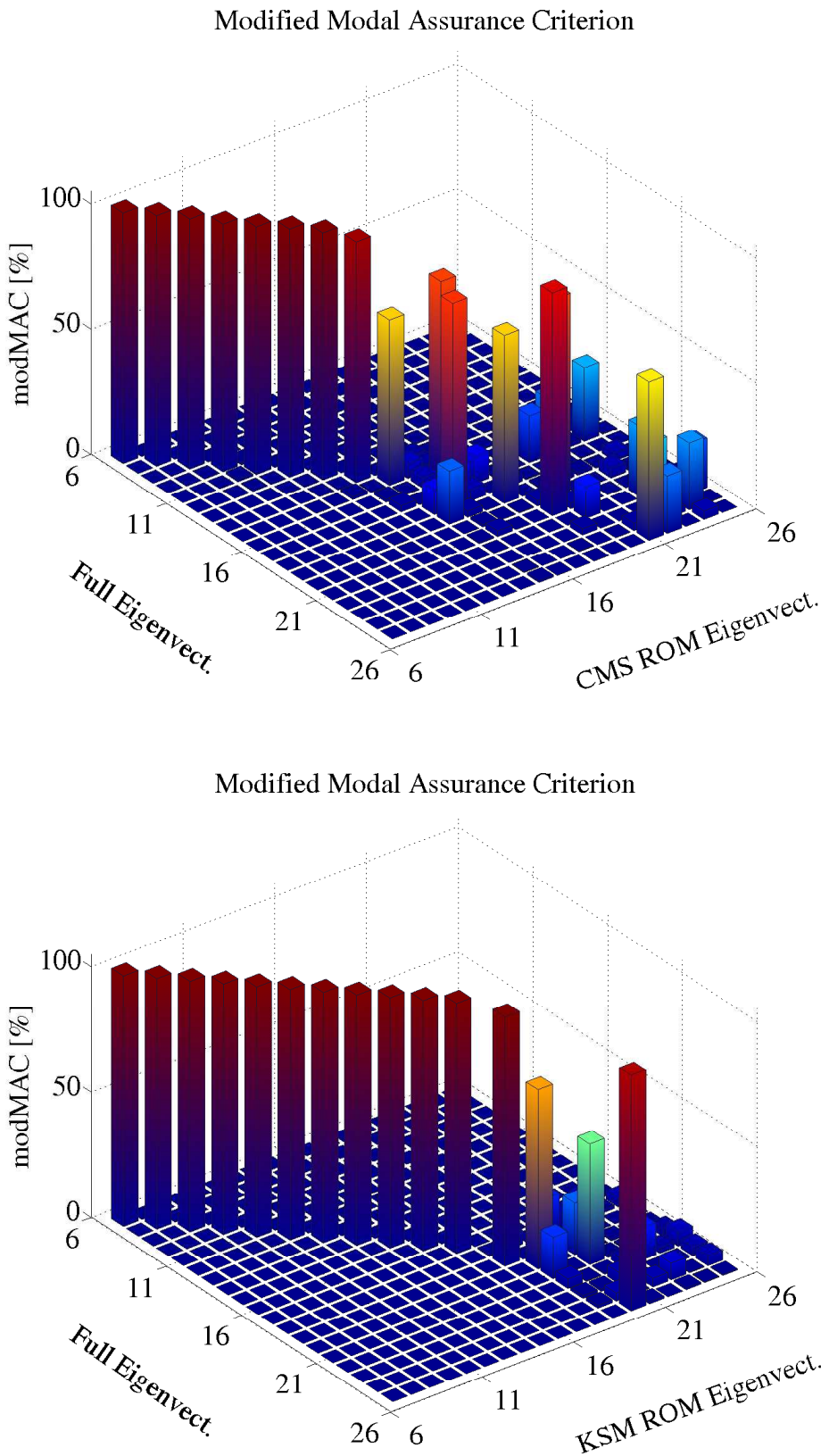


Fig. 3.47: Elastic crankshaft - CMS & KSM MOR - modMAC

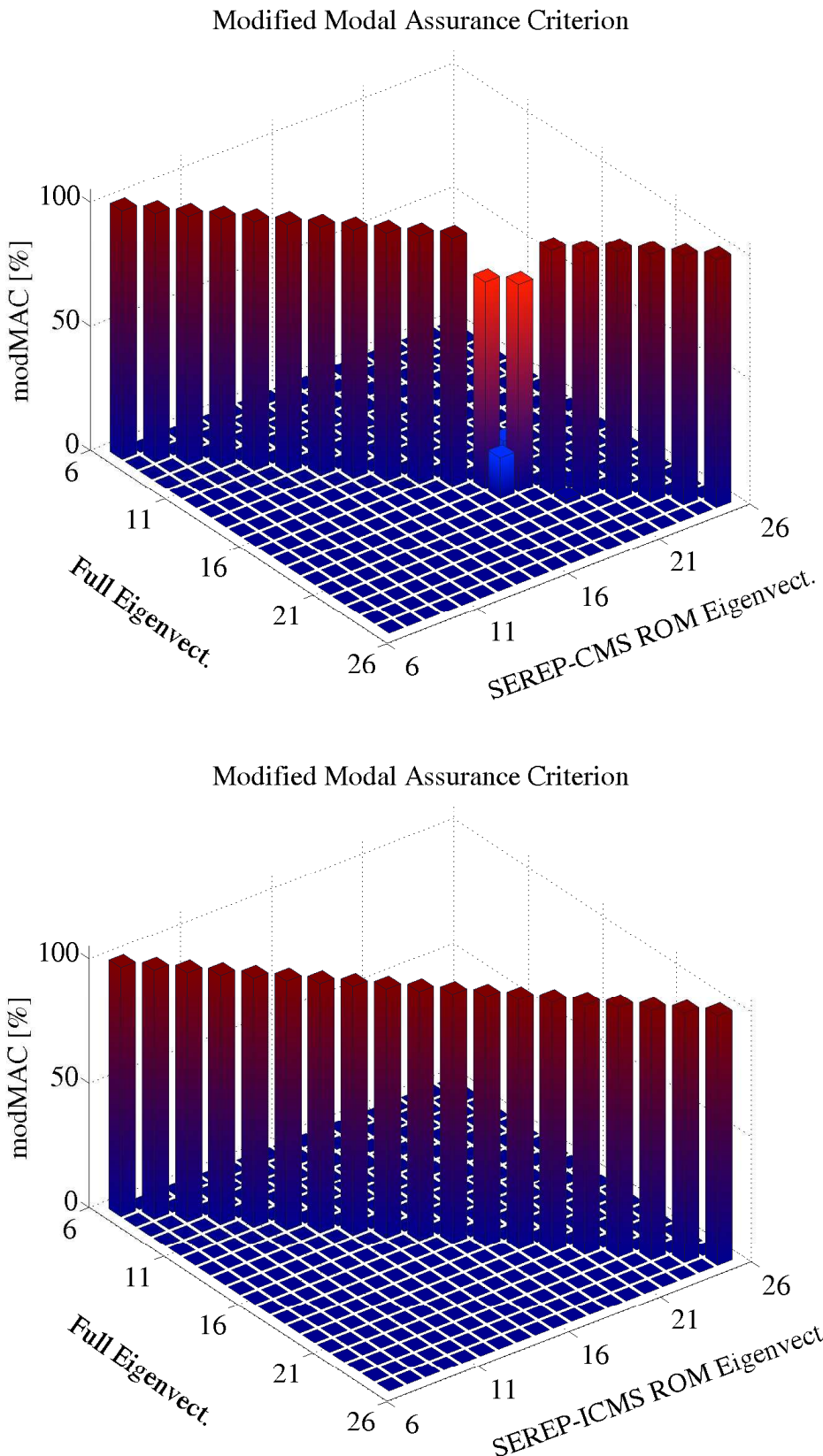


Fig. 3.48: Elastic crankshaft - SEREP-CMS & SEREP-ICMS MOR - modMAC

Table 3.5: Elastic crankshaft - MOR Comparison - Quality Computation Time

MOR	Computation time [hrs]	$modMAC \geq 90\%$
CMS	≈ 18	8
KSM	≈ 40	11
SEREP-CMS	≈ 2	17
SEREP-ICMS	≈ 2	19

Finally, the importance of utilizing both the eigenfrequency and eigenvector MCC is given in Table 3.6. Here, as in the case of the elastic rod (Table 3.3), a simple eigenfrequency comparison ascertains insufficient conclusions regarding the dynamic properties of the ROM - in this case the CMS-ROM, since the associated eigenvectors correlate either poorly ($modMAC(15) = 65\%$) or not at all.

Table 3.6: Elastic crankshaft - CMS - NRFD & modMAC

MOR	Eigenvect. Nr.	NRFD [%]	modMAC [%]
CMS	15	5.15	65
	16	4.67	4
	17	2.7	9
	18	3	0
	19	3.71	0

The calculations for both the elastic piston rod and crankshaft models were conducted within the Matlab environment [59] under Microsoft Windows XP installed on a personal computer with the following configuration: Dual Core AMD Opteron(tm) Processor 246, 1.99 GHz, 3.25 GB RAM.

With the elastic crankshaft model being the last application example of this Chapter, the cycle of comparing several MOR schemes by use of eigenvalue correlation criteria is completed. The utilization of either direct or iterative methods for reducing the dimension of several FE model types under various master DoF constellations has shown that alternative MOR algorithms exist, which could offer qualitatively better results at a reduced computation time cost than the standardized Guyan or CMS schemes.

4 Numerical issues in model order reduction

In Chapters 2 and 3 the algorithmic scheme of numerous MOR methods was presented and their practical application along with a comparison based on four types of FE models was exemplified, respectively. As indicated, the successful application of a MOR procedure relies both on the quality of the computed ROM, i.e. the range of the well CMPS between the original and the associated ROM, and on the computation time required therefor. While the first aspect depends on the applied MOR approach and the appropriate master DoF selection and allocation, the latter is vastly affected on one hand by the dimension size of the FE model to be reduced, and on the other hand by the condition properties of the model's system matrices.

The general scheme for the practical implementation of all the previously presented MOR methods, apart from SEREP and BT, leads to the formulation of a linear system of equations, which must be solved in order to compute the associated coordinate transformation matrix (Eq. (2.38)). Considering, for instance, the Guyan MOR method and the derivation of the Guyan transformation matrix in Eq. (2.55), the following system of equations is acquired:

$$(2.55) \Rightarrow \mathbf{z} = \mathbf{T}_{\text{static}} \cdot \mathbf{z}_m = \begin{pmatrix} \mathbf{I}_m \\ -\mathbf{K}_{ss}^{-1} \mathbf{K}_{sm} \end{pmatrix} \cdot \mathbf{z}_m = \begin{pmatrix} \mathbf{I}_m \\ \mathbf{T} \end{pmatrix} \cdot \mathbf{z}_m \quad (4.1)$$

$$\Rightarrow \mathbf{T} = -\mathbf{K}_{ss}^{-1} \mathbf{K}_{sm} \quad (4.2)$$

$$\Leftrightarrow \mathbf{A}\mathbf{X} = \mathbf{B}, \quad \mathbf{A} := \mathbf{K}_{ss}, \quad \mathbf{X} := \mathbf{T}, \quad \mathbf{B} := -\mathbf{K}_{sm} \quad (4.3)$$

Thus, in order to compute the Guyan coordinate transformation matrix, the linear system in Eq. (4.3) must be solved. Based on the hardware profile as well as the CPU power two different approaches could be adopted:

- *Direct calculation.* This methodology copes with the factorization of the matrix \mathbf{A} . It is conducted by invoking certain decomposition methods [51, 36], e.g. Cholesky, QR, LU, ILU, Dulmage-Mendelsohn, etc., and thereafter by solving the decomposed sub-systems, e.g. with the help of the back-substitution method. As already mentioned in Subsection 3.3.6, the utilization of specialized libraries for the solution of large sparse linear systems, e.g. CSparse [36], TAUCS [121], MUMPS [91], etc., allows the non-problematic application of a factorization procedure, which could actually be completed within an acceptable range of computation time. Nevertheless, the direct calculation is highly dependent on the CPU power and thus, for constantly increasing FE models several memory capacity problems occur.
- *Iterative calculation.* The application of iterative algorithms [102], e.g. the Conjugate Gradient method (CG) and its variants, the Generalized Minimal Residual

method (GMRES), etc., is always feasible and moreover compulsory in cases where any direct approach fails. Several preconditioning techniques exist [102], the utilization of which accelerates the convergence rate of the iterative approach under the assumption of a predefined residuum limit. Nevertheless, the acceleration rate of any iterative procedure is highly related to a specific matrix property referred to as the condition number [51, 5] $k(\mathbf{A})$, which is defined as the ratio of the largest to the smallest singular values of \mathbf{A} , i.e.

$$k(\mathbf{A}) = \|\mathbf{A}\| \|\mathbf{A}^{-1}\| = \frac{\sigma_1(\mathbf{A})}{\sigma_n(\mathbf{A})}. \quad (4.4)$$

Regarding, for example, the CG method, the number of iteration steps N_{CG} depends on the condition number $k(\mathbf{A})$ and is approximated [102] via the relationship:

$$N_{CG} \approx \sqrt{k(\mathbf{A})}. \quad (4.5)$$

According to the MOR algorithms presented in Chapter 2, the calculation of each coordinate transformation matrix requires the inversion of either the entire stiffness matrix \mathbf{K} , e.g. as in the KSM case (Eq. (2.210)), or a part of it, namely, the sub-block matrix \mathbf{K}_{ss} defined by the slave structure, e.g. as in Guyan, IRS, CMS, ICMS, etc. The finer the original structure is discretized, the larger the dimension of the resulting system of ODEs is and consequently the more difficult it is to apply a factorization method for the inversion of \mathbf{K} or \mathbf{K}_{ss} . On this account, a general thumb rule regarding large structures implies for systems with dimension $n_{dim} \geq 5 \cdot 10^5$ the application of direct methods to be rather inadequate.

The initiation of iterative procedures is accompanied by a common negative aspect of FE discretized structures, namely, the ill-condition properties of the stiffness matrix. It is regarded as a natural property of the stiffness matrix in the FE theory, which is amplified in case of tolerance failures during the discretization process. Based on the definition in Eq. (4.4) an ill-conditioned matrix \mathbf{A} corresponds to a large $k(\mathbf{A})$ value, which automatically reduces the effectiveness of the applied iterative algorithm, since the number of required convergence steps are increased, e.g. as given in Eq. (4.5) for the CG case. Thence, the application of the MOR algorithm for large dimensioned models is restrained in both levels of direct and iterative calculation, with the latter being qualitatively inappropriate to conduct due to vast computation times.

The side-effect of the ill-condition properties is not only restricted to large dimensioned models during the iterative MOR solution. The direct MOR methodology for small or medium sized models might also suffer from inaccurate calculations during the solution of the linear systems of equations (Eq. (4.3)). According to [5], if in Eq. (4.3) the terms \mathbf{A} and \mathbf{B} are perturbed to the equivalent terms $\tilde{\mathbf{A}}$ and $\tilde{\mathbf{B}}$ with the associated norms $\|\mathbf{A} - \tilde{\mathbf{A}}\|$ and $\|\mathbf{B} - \tilde{\mathbf{B}}\|$ being small, then it holds:

$$\frac{\|\mathbf{x} - \tilde{\mathbf{x}}\|}{\|\mathbf{x}\|} \leq k(\mathbf{A}) \cdot \left(\frac{\|\mathbf{A} - \tilde{\mathbf{A}}\|}{\|\mathbf{A}\|} + \frac{\|\mathbf{B} - \tilde{\mathbf{B}}\|}{\|\mathbf{B}\|} \right). \quad (4.6)$$

Hence, the relative error in the solution can be amplified up to $k(\mathbf{A})$ -times w.r.t the relative error in the data.

The practical interpretation of the conclusion in Eq. (4.6) can be easily understood, if for example, the KSM MOR is considered. As described in Eq. (2.210) the \mathbf{T}_{KSM} subspace depends on the definition of the starting vector \mathbf{F} , which might not necessarily coincide with the vector of applied forces acting on the structure, since it can be arbitrarily chosen. In case of the stiffness matrix being ill-conditioned and based on the above equation (Eq. (4.6)) with $\mathbf{A} \equiv \tilde{\mathbf{A}} = \mathbf{K}$, the utilization of different starting vectors would lead to the computation of different coordinate transformation matrices and therefore, different - in terms of the dynamic properties - ROMs. A fact, which can only be regarded as unacceptable, since the KSM algorithmic approach should not be vastly affected by the choice of the starting vector during the application of the ARNOLDI algorithm.

On the basis of the aforesaid, the diagonal perturbation methodology is proposed [67, 64] in the following Section 4.1. It is developed in view of improving the condition properties of the matrix \mathbf{A} for linear equation systems, as given in Eq. (4.3), which are explicitly formulated during the application of a MOR algorithm.

4.1 Diagonal perturbation methodology

Instead of solving the original linear system (Eq. (4.3)), the matrix \mathbf{A} is perturbed into the matrix term $\tilde{\mathbf{A}}$ and thereafter, the perturbed system is solved:

$$\tilde{\mathbf{A}}\mathbf{x} = \mathbf{B} \iff (\mathbf{A} + \alpha\mathbf{A}_d)\mathbf{x} = \mathbf{B}. \quad (4.7)$$

In Eq. (4.7) the term \mathbf{A}_d annotates the diagonal entries of the original matrix \mathbf{A} , i.e.

$$\mathbf{A}_d = [a_{ii}], \quad i = 1, 2, \dots, n, \quad \text{with } \mathbf{A} \in \mathbb{R}^{n \times n}, \quad (4.8)$$

whereas the perturbation parameter α is defined as given below:

$$\alpha = 10^{-(c+k)} \quad (4.9)$$

$$c = \max_{j \in \mathbb{N}} \{f(j, i) := 10^{\pm j} \cdot \hat{a}_{ii}, \quad i = 1, 2, \dots, n\} \quad (4.10)$$

$$k \geq \min(j) - \max(j). \quad (4.11)$$

The perturbation parameter α depends on the definition of the parameters c and k , as given in Eq. (4.9). The first parameter c equals the maximum upper script absolute value j of the matrix's diagonal entries with the latter being annotated as a floating point number, as described in Eq. (4.10). Thus, the term $f(j, i)$ can be regarded as a different annotation for the diagonal entries defined in Eq. (4.8). Let us consider the following example:

$$a[1\dots 5, 1\dots 5] = \left\{ 4.9 \cdot 10^5, 5.4 \cdot 10^5, 1.2 \cdot 10^6, 1.8 \cdot 10^6, 1.7 \cdot 10^7 \right\} \quad (4.12)$$

Here, the diagonal entries of a 5×5 matrix are depicted. According to Eq. (4.10) in order to define the parameter c , the maximum of the five diagonal entries should be located and the absolute upper script value of its floating point number representation should be isolated: the fifth entry $a[5,5] = 1.7 \cdot 10^7$ constitutes the maximum value and thus, $c = 7$.

The definition of the α perturbation parameter is completed by allocating the value for the parameter k (Eq. (4.9)), which is derived based on Eq. (4.11). On this account, the k value for the example in Eq. (4.12) should be always larger or equal than -2 , i.e. $k \geq -2$, since $\min(j) = 5$ and $\max(j) = 7$. The choice of the k -value is user dependent and as shown in the following Section 4.2, the more the value reaches the lower permitted limit (Eq. (4.11)), the faster the iterative solution converges, but simultaneously the larger the produced numeric error is. Thence, the limit expressed in Eq. (4.11) assures the determination of a global perturbation parameter α , such that the solution of the perturbed system (Eq. (4.7)) is not erroneous.

In this regard, the diagonal perturbation methodology is applied on one hand to the iterative solution of the elastic rod and crankshaft models (Subsections 3.3.5 and 3.3.6, respectively) and on the other hand to the direct solution of a small dimension 3D solid bar structure. The purpose in the first case is to demonstrate the effect of the method in accelerating the iterative solution within acceptable error bounds. The second case copes with the improvement of the dynamic properties of the resulting ROM through the application of the diagonal perturbation, which is due to the improvement of the condition properties for the stiffness matrix. In both cases, the numeric error is measured based on the NRFD and modMAC MCC for the original and the associated ROM.

4.2 Diagonal perturbation - application examples

4.2.1 Iterative model order reduction

The results depicted in the following Fig. 4.1 - 4.4 concern the iterative application of the KSM MOR approach for the dimension reduction of the elastic rod (Fig. 4.1 - 4.2) and the elastic crankshaft (Fig. 4.3 - 4.4), respectively.

In both cases the computation of the associated Krylov subspaces (Eq. (2.210)) fails, since the iterative algorithm - Preconditioned Conjugate Gradient method (PCG) with an incomplete Cholesky factor being defined as a preconditioner - cannot converge. Therefore, the application of the diagonal perturbation methodology is compulsory. According to its algorithmic scheme (Eq. (4.7) - (4.11)), the user can choose to vary the values of the k -parameter as long as the condition in Eq. (4.11) is satisfied. On this account, the following choices for the k -parameter have been made for both of the aforementioned elastic structures, respectively, i.e.:

$$\text{KSM-Rod: } \Rightarrow k = \{-2, -1, 0, 1, 2\} \quad (4.13)$$

$$\text{KSM-Crankshaft: } \Rightarrow k = \{0, 1, 2\} \quad (4.14)$$

The value $k = 2$ represents a small perturbation for the diagonal entries of the stiffness matrices of both models. The associated condition number remains almost unaffected and thus, the simulation time required for the completion of the iterative procedure is vast. Nevertheless, the PCG algorithm does not fail to converge as in the previous case (Fig. 4.1 - 4.3). However, for the crankshaft example, as observed in Fig. 4.3, the iteration-steps upper limit ($n_{iter}^{lim} = 5000$) is reached and the solution does not converge according to the applied tolerance (10^{-3}). By reducing the values of k a faster convergence rate is achieved. A thumb rule of $0 \leq k \leq 2$ assures a satisfactory convergence rate keeping intact the dynamic properties of the models.

Table 4.1 gathers the information for two major aspects regarding the effectiveness of the diagonal perturbation methodology, namely, the computation time reduction and the amount of the dynamics' damage caused by its application. Considering the elastic rod, it is observed that the system's $k = -1$ perturbation reduces the computation time by 48.3% without negatively affecting the quality of results (0% modMAC damage), whereas the choice $k = -2$ accelerates the solution, which in comparison to the $k = 2$ case is reduced by 82.6%, but the dynamics of the model are damaged (42.8% modMAC damage, depicted also in Fig. 4.2).

An analogous outcome is derived for the KSM-ROM in case of the elastic crankshaft and under the influence of the diagonal perturbation method. Here, the parameter choices $k = 0$ and $k = 1$ drastically reduce the computation time by 13.2% and 61.5%, respectively, while keeping intact the dynamics of the original model up to a certain limit. The percentage of the damaged dynamics depicted in Table 4.1 are due to the KSM algorithm and not because of the diagonal perturbation. Therefore, the percentage rate is the same for all of the applied perturbation parameters. This outcome could only be improved by applying either a different MOR approach or denoting a larger dimension for the ROM.

Table 4.1: Diagonal perturbation - Computation time - Quality of results

Elastic structure	k parameter	Time reduction [%]	Damaged Eigenvect. [%]
Rod	2	0	0
	1	11.46	0
	0	33.5	0
	-1	48.3	0
	-2	82.6	42.8
Crankshaft	2	0	42.1
	1	13.2	42.1
	0	61.5	42.1

The diagonal perturbation method is both independent of the MOR algorithm applied and the preconditioning technique utilized for the iterative procedure. Additionally, it is highly advised for MOR approaches, which require the inversion of the entire stiffness matrix \mathbf{K} . In such cases the associated condition number (Eq. (4.4)) is high due

to almost zero (numerically) eigenfrequencies, which are a common characteristic of non-fixed matrices in structural mechanics.

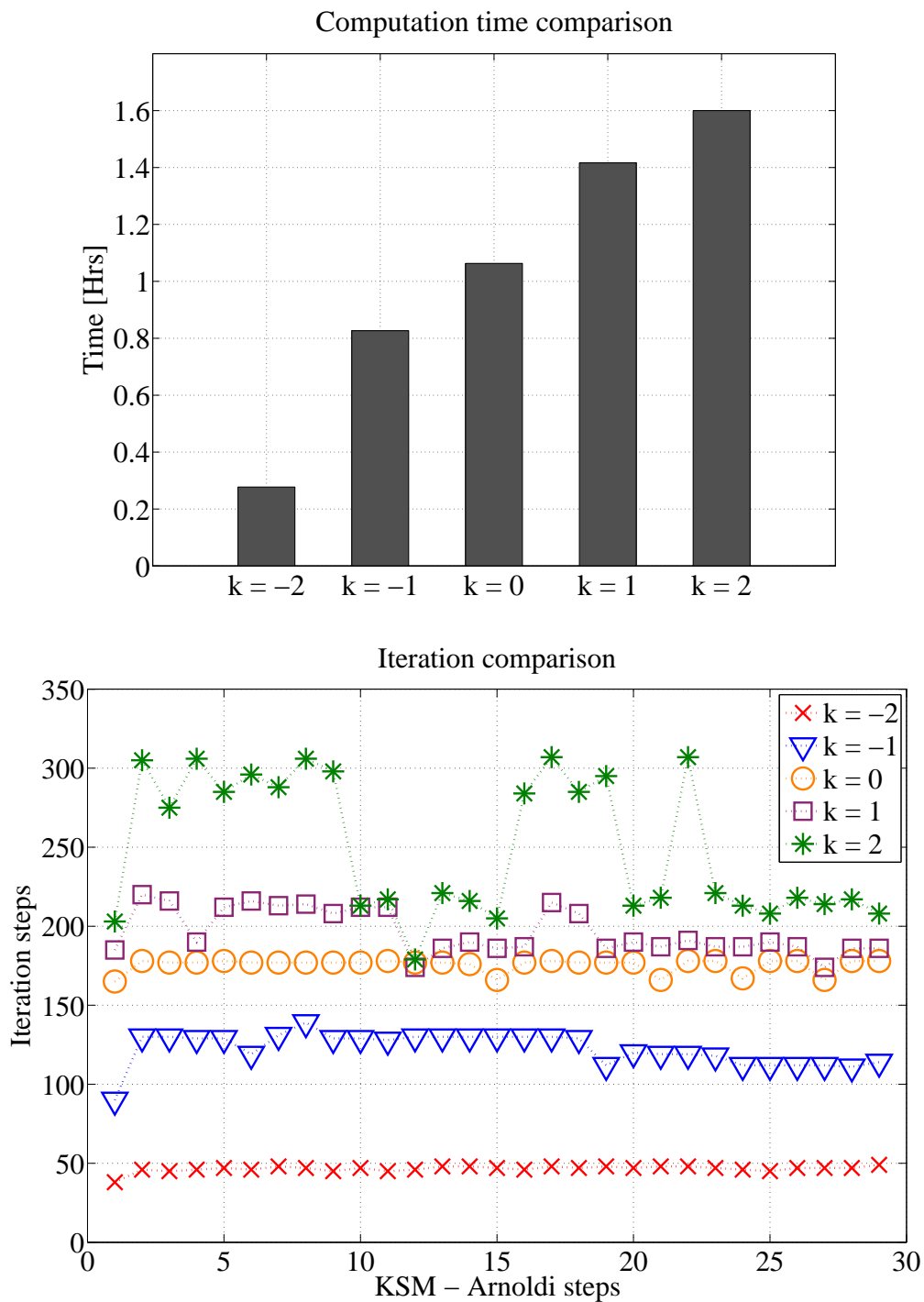


Fig. 4.1: Diagonal perturbation - elastic rod - comp. time & conv. rate

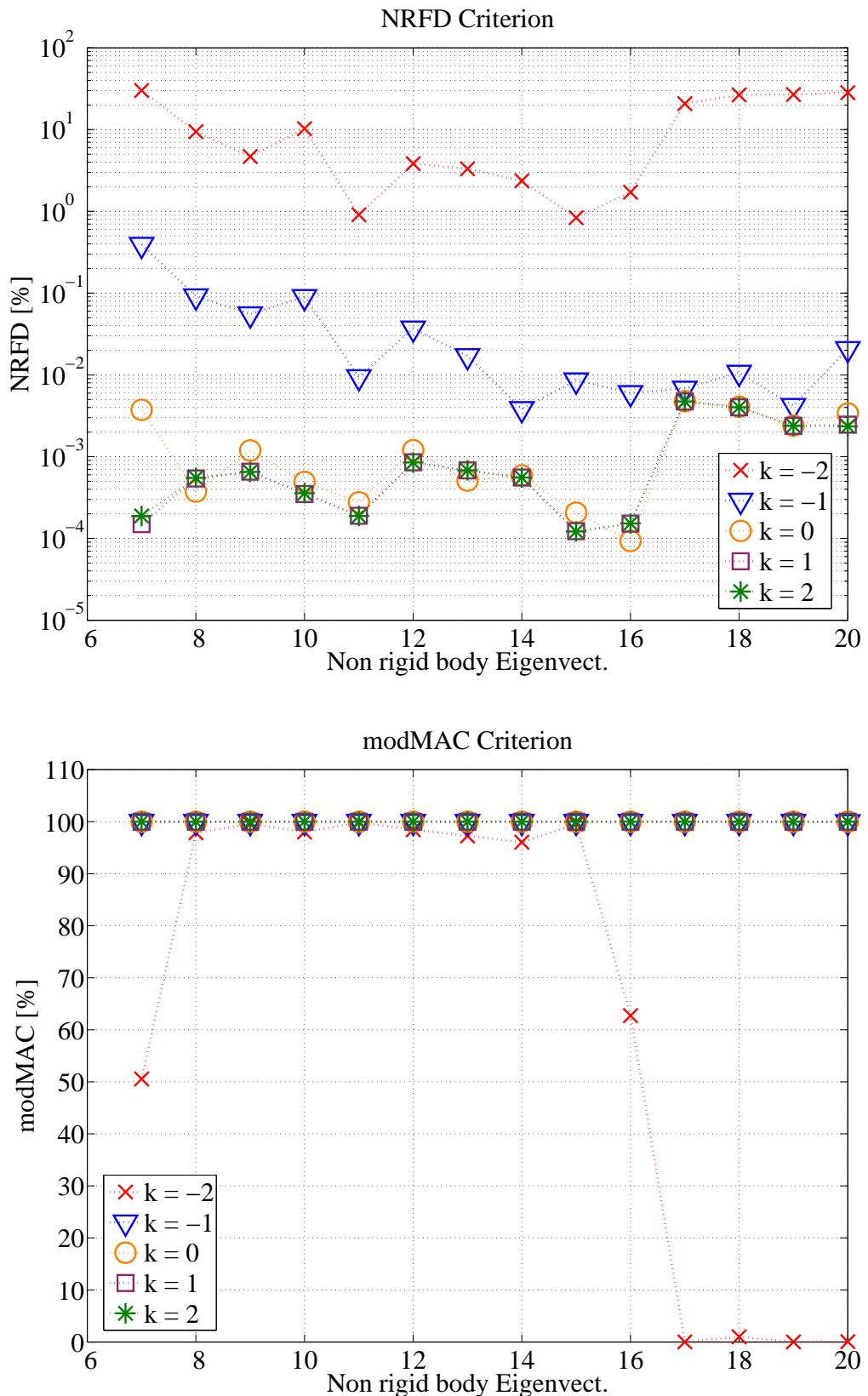


Fig. 4.2: Diagonal perturbation - elastic rod - NRFD & modMAC

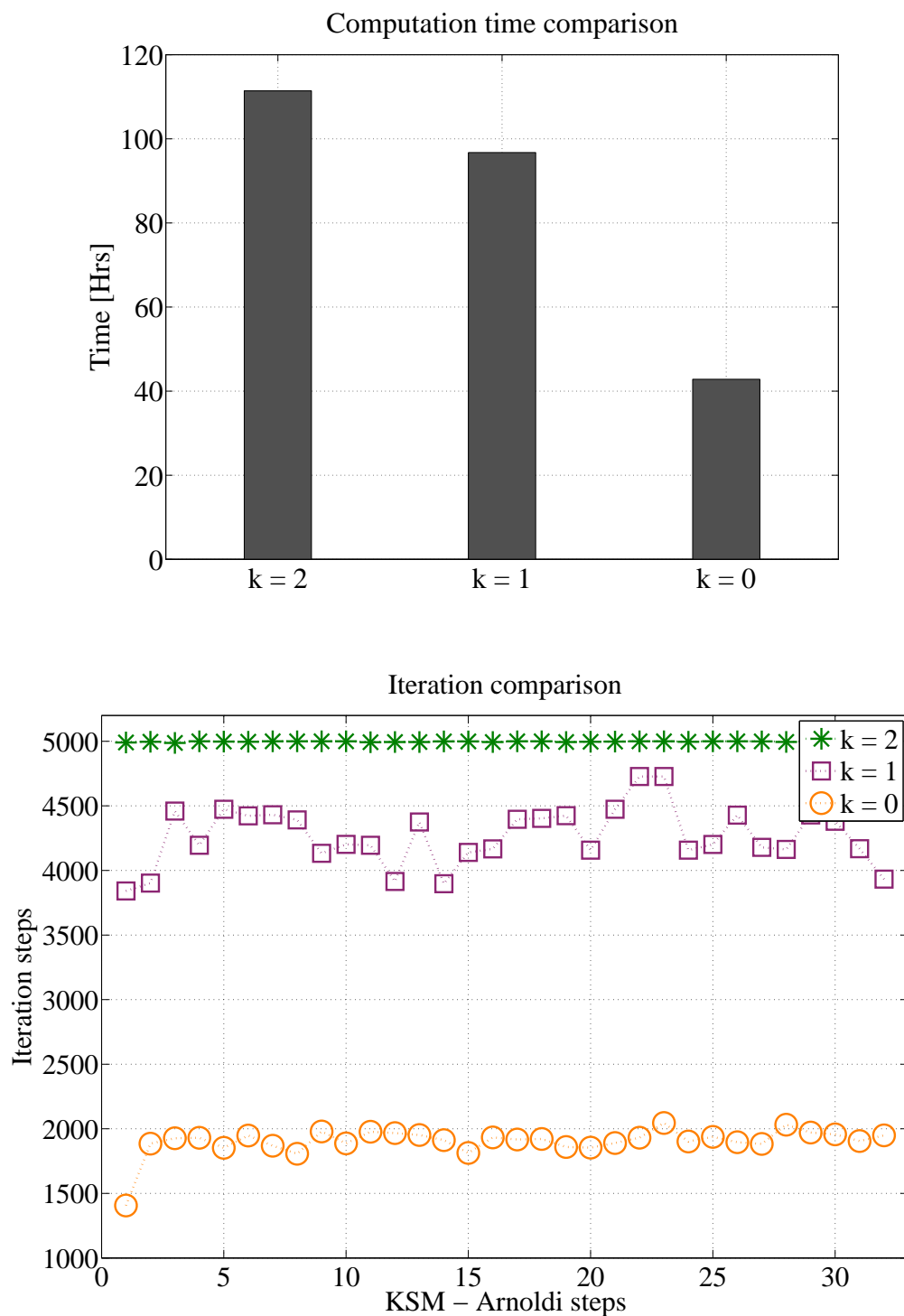


Fig. 4.3: Diagonal perturbation - elastic crankshaft - comp. time & conv. rate

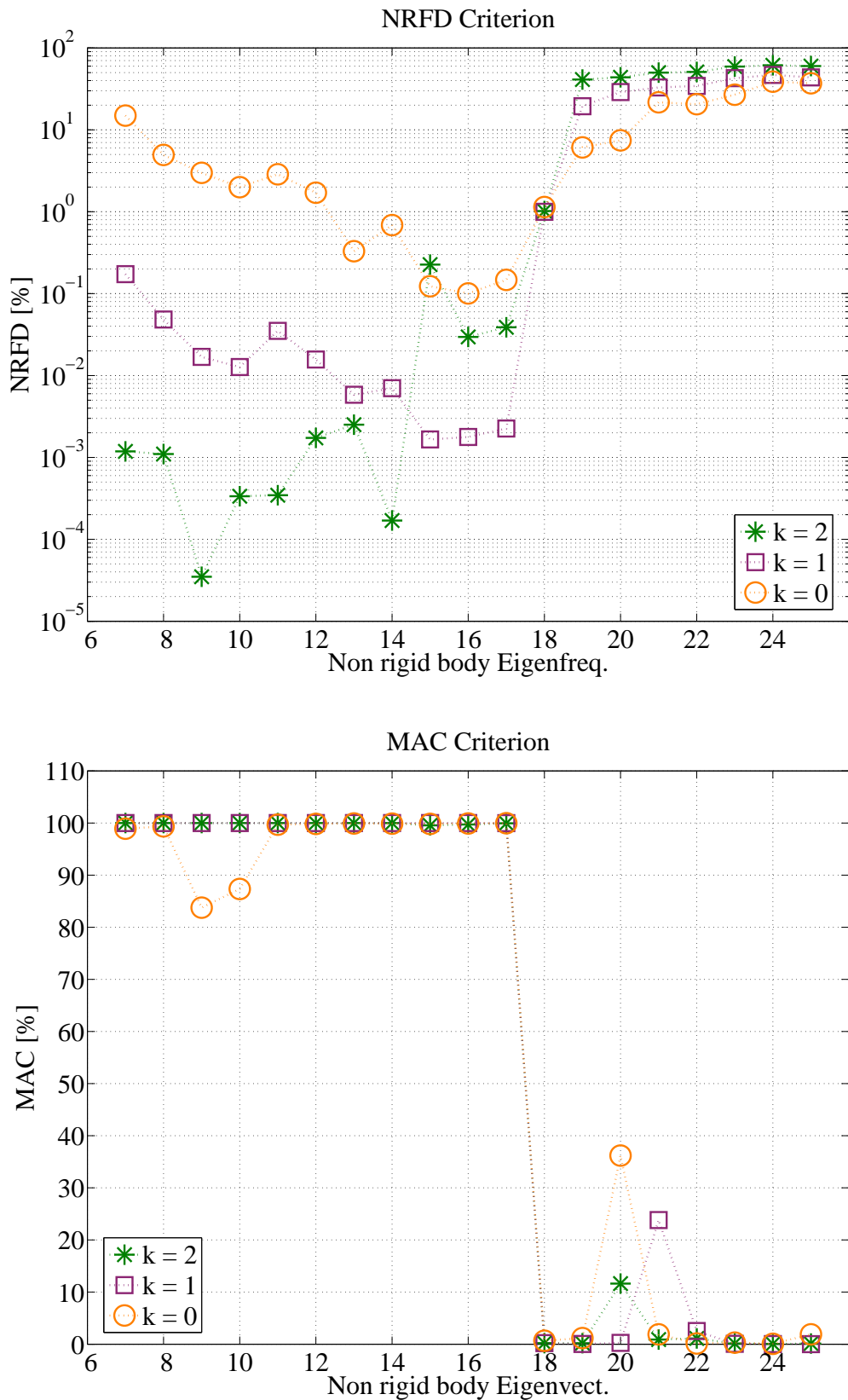


Fig. 4.4: Diagonal perturbation - elastic crankshaft - NRFD & MAC

4.2.2 Direct model order reduction

In this Subsection, the example of a 3D solid bar structure is considered (Fig. 4.5), the dimension of which is directly reduced with the help of the KSM method. The immediate consequence of present ill-conditioned matrices is depicted throughout the Fig. 4.6 - 4.8, the nature of which is twofold.

The first aspect concerns the application of non-adequate direct methods for the solution of the MOR problem. As observed in Fig. 4.6 the utilization of such inappropriate methodologies might lead to the generation of ROM with severely damaged dynamics in comparison to the original model. Thence, the computed results are erroneous. On the other hand, the application of the same direct numeric approaches combined with the diagonal perturbation methodology contributes in minimizing the numeric error due to the high condition number of the stiffness matrix and thus, generating a ROM (annotated as DP ROM in Fig. 4.6), which perfectly captures the dynamics of the original model. Of course, the generation of erroneous results is avoided if appropriate numeric methods are selected. Nevertheless, the diagonal perturbation methodology is independent of the chosen direct numeric scheme and in case of ill-conditioned systems the quality of the generated ROM is good (as long as the condition in Eq. (4.11) is fulfilled).

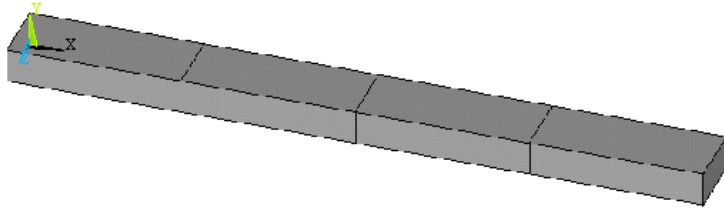


Fig. 4.5: 3D solid bar structure - 60 DoF

The second aspect regarding the presence of ill-conditioned matrices during the direct MOR is restricted to the special KSM MOR case. Here, the influence of different starting vectors for the initialization of the ARNOLDI algorithm is investigated. On this account, two different KSM ROM are generated and for both cases the eigenvector correlation w.r.t the dynamics of the original model is depicted in Fig. 4.7 - 4.8. As observed, the dynamics of the ROM I & II suffer from correlation discrepancies, which is an immediate consequence of the relationship given in Eq. 4.6. In view of coupling the FEM ROM into a MBS code, such results cannot be accepted and therefore, either a different MOR scheme or a special type of deflation technique [86, 24] should be applied. On the other hand, the ROM generated with the help of the diagonal perturbation methodology, i.e. DP ROM I & II, undergo no correlation-discrepancies, which proves that in case of the KSM MOR for ill-conditioned systems the diagonal perturbation methodology is independent of the chosen starting vector for the initialization of the ARNOLDI scheme.

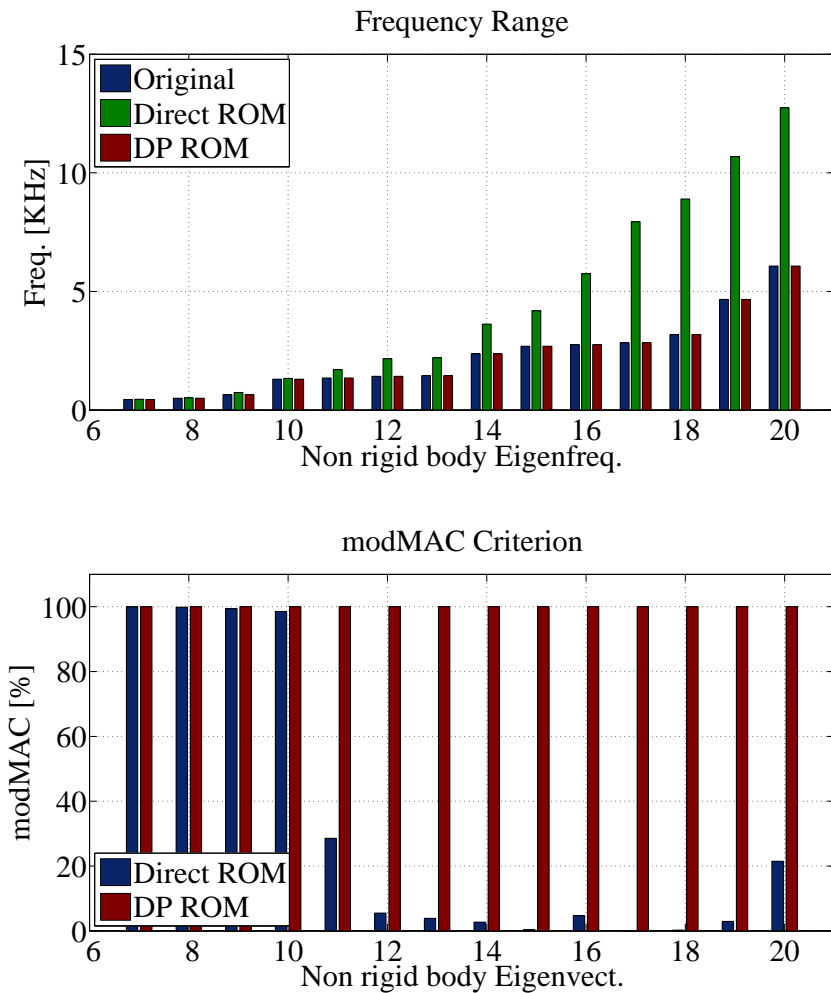


Fig. 4.6: ROM comparison - direct & diagonal perturbation solution

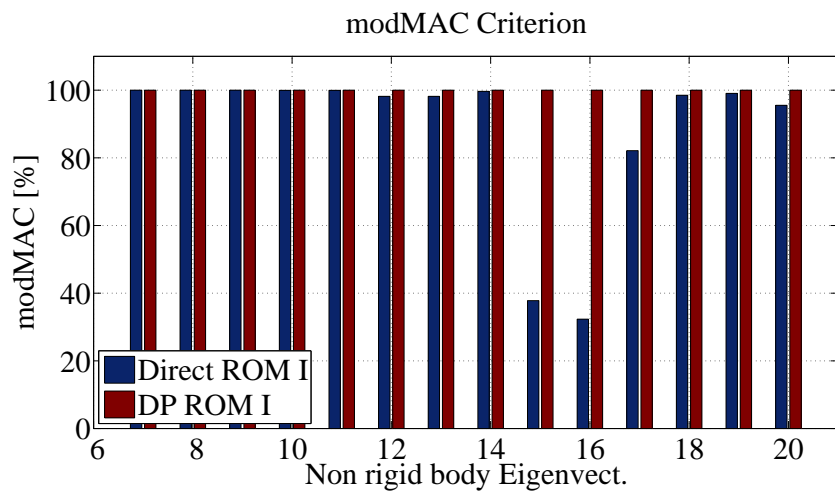


Fig. 4.7: KSM ROM - Starting vector effect I

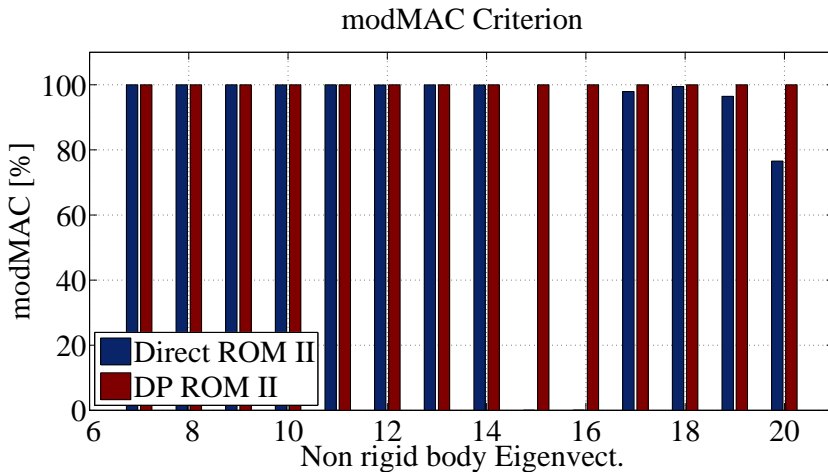


Fig. 4.8: KSM ROM - Starting vector effect II

4.3 Stabilization of the matrix polynomial in structural mechanics

The application of balancing related truncation techniques in the area of structural mechanics (Section 2.6.4) depends on the stability properties of the, so called, matrix polynomial, i.e.

$$\mathbf{P}(\lambda) = \lambda^2 \mathbf{M} + \lambda \mathbf{D} + \mathbf{K}, \quad (4.15)$$

the definition of which was given in Section 2.6.4, p. 57. On this account, the controllability and observability Gramians are defined as the unique, symmetric and positive definite solutions of the Lyapunov equations (Eq. (2.214)), provided that the pencil $\mathbf{P}(\lambda)$ in Eq (4.15) possesses eigenvalues with only negative real parts. In case of free vibrated MBS, though, this condition is damaged and therefore, the BT MOR is no longer applicable. When coping with first-order systems the decomposition of the n $\mathbf{P}(\lambda)$ -poles into a stable and unstable part [93] is feasible and the BT MOR proceeds without problems. Unfortunately, this approach is no longer valid for the $2n$ -poles of the matrix polynomial in Eq (4.15).

The problem regarding the non-stability of $\mathbf{P}(\lambda)$ in structural mechanics resides on the rigid body eigenvalues. In terms of the modal analysis process the $\mathbf{P}(\lambda)$ unstable part can be located to the rigid body eigenfrequencies (numerically absolute zero valued eigenfrequencies) of the equivalent undamped structure. Since the isolation or decomposition of this part is not feasible for the second-order $\mathbf{P}(\lambda)$, a modification of the original matrix pencil according to the properties of the diagonal perturbation methodology is proposed, based on which the undesired eigenvalues are shifted, enabling thus, the application of BT MOR methods.

According to the Diagonal Perturbation (DP) algorithm (Eq. (4.7) - (4.11)) and based on the application examples of the previous Section, the convergence acceleration for iterative MOR methods is due to the better conditioned properties of the perturbed

system in comparison to the associated original system. The definition of a matrix's \mathbf{A} condition number in Eq. (4.4) indicates that $k(\mathbf{A})$ can be drastically reduced, if the smallest eigenvalues of \mathbf{A} are marginally increased. The utilization of the DP method before the initialization of a BT MOR process contributes to decreasing the system's stiffness matrix condition number by increasing the zero - w.r.t machine precision - rigid body eigenfrequencies and thus, the stability condition $Re(\mathbf{P}(\lambda) < 0)$ is fulfilled. By dividing the structure's eigenfrequency spectrum into two parts, namely, the rigid ω_{rigid} and the flexible body ω_{flex} part the DP application (Eq. (4.7) - (4.11)) leads to the following relationship:

$$|\omega_{\text{rigid}}^{\text{DP}} - \omega_{\text{rigid}}| \leq \varepsilon_1 \quad \text{and} \quad |\omega_{\text{flex}}^{\text{DP}} - \omega_{\text{flex}}| \leq \varepsilon_2 \quad \text{with} \quad \varepsilon_2 \ll \varepsilon_1. \quad (4.16)$$

The statement $\varepsilon_2 \ll \varepsilon_1$ (Eq. (4.16)) annotates that when the DP scheme is applied according to the condition in Eq. (4.11), the rigid eigenfrequency difference between the original and the DP model might be large, e.g. $10^{-2} < \varepsilon_1 < 10^4$, whereas the analogous flexible eigenfrequency difference is small, e.g. $10^{-15} < \varepsilon_2 < 10^{-3}$. The consistency of the latter flexible region is of importance, since it constitutes the basis during the FEM-MBS coupling procedure.

On the basis of the aforesaid, the 3D solid bar (Section 3.3.1) and the UIC60 rail (Section 3.3.3) non-grounded elastic structures are considered and the SOMT-BT two-step MOR scheme is applied. At first, a medium sized ROM is generated (240 DoF) for both structures and thereafter, the zero velocity BT scheme is applied. The dimension of the final ROM is computed based on the requirements presented in the above mentioned Sections for each of the models.

Tables 4.2 and 4.3 gather the rigid body eigenfrequencies for both elastic structures prior to the initialization of the BT scheme. As observed, the non utilization of the DP algorithm leads to the derivation of zero eigenfrequencies and thence, the polynomial matrix is non stable, i.e. real positive eigenvalues exist (Fig. 4.9 and Fig. 4.11).

The application of the DP algorithm succeeds in increasing the undesired zero eigenfrequencies and thus, stabilizing the polynomial matrix. Nevertheless, the selection of the DP k -parameter should be conducted according to the condition in Eq. (4.11), otherwise the resulting ROM might not accurately represent the original model. Therefore, the permitted k -values are ascertained as given below, i.e.

$$\text{3D solid bar: } k \geq -1 \quad (4.17)$$

$$\text{UIC60 rail: } k \geq -1. \quad (4.18)$$

The immediate consequence of violated conditions in Eq. (4.17) - (4.18) is, on one hand, the generation of extremely high rigid body eigenfrequencies for the associated perturbed systems ($k = -2$ and $k = -4$ as depicted in Tables 4.2 and 4.3, respectively), and on the other hand the computation of ROMs, which are characterized by correlation discrepancies (Fig. 4.10 - 4.12) w.r.t the dynamics of the original model. The correlation damage can only be effectively ascertained with the help of eigenvector criteria and not by a simple eigenfrequency comparison. For example, in Fig. 4.10 the eigenfrequency

spectrum of the case $k = -4$ ROM is almost identical to the spectrum of the original model, whereas the associated eigenvector correlation shows severe discrepancies.

Table 4.2: 3D solid bar- diagonal perturbation - ω -shifting

ω_{rigid}	no DP	$k = 5$	$k = 3$	$k = -4$
1	0	0	$4.294 \cdot 10^{-3}$	15.221
2	0	0	$5.071 \cdot 10^{-3}$	16.190
3	0	0	$5.280 \cdot 10^{-3}$	16.251
4	$2.257 \cdot 10^{-3}$	$2.329 \cdot 10^{-3}$	$8.679 \cdot 10^{-3}$	27.635
5	$2.587 \cdot 10^{-3}$	$2.688 \cdot 10^{-3}$	$8.768 \cdot 10^{-3}$	27.728
6	$3.260 \cdot 10^{-3}$	$3.350 \cdot 10^{-2}$	$1.010 \cdot 10^{-2}$	29.806

Table 4.3: UIC60 rail - diagonal perturbation - ω -shifting

ω_{rigid}	no DP	$k = 5$	$k = 2$	$k = -2$
1	0	$4.564 \cdot 10^{-2}$	1.443	$1.443 \cdot 10^2$
2	0	$6.259 \cdot 10^{-2}$	1.979	$1.979 \cdot 10^2$
3	0	$6.271 \cdot 10^{-2}$	1.983	$1.983 \cdot 10^2$
4	0	$7.732 \cdot 10^{-2}$	2.445	$2.444 \cdot 10^2$
5	$1.310 \cdot 10^{-3}$	$8.013 \cdot 10^{-2}$	2.533	$2.529 \cdot 10^2$
6	$2.209 \cdot 10^{-3}$	$8.065 \cdot 10^{-2}$	2.549	$2.549 \cdot 10^2$

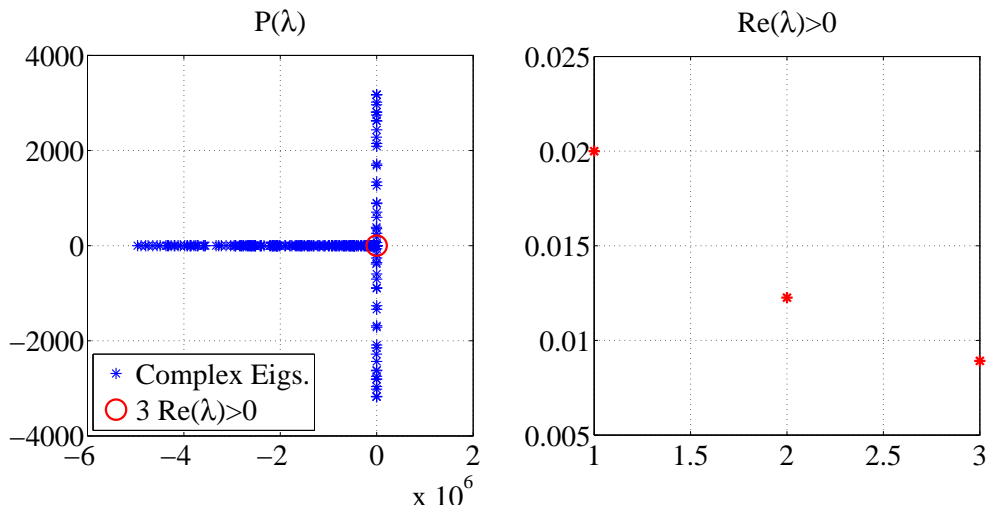


Fig. 4.9: 3D solid bar - unstable $\mathbf{P}(\lambda)$

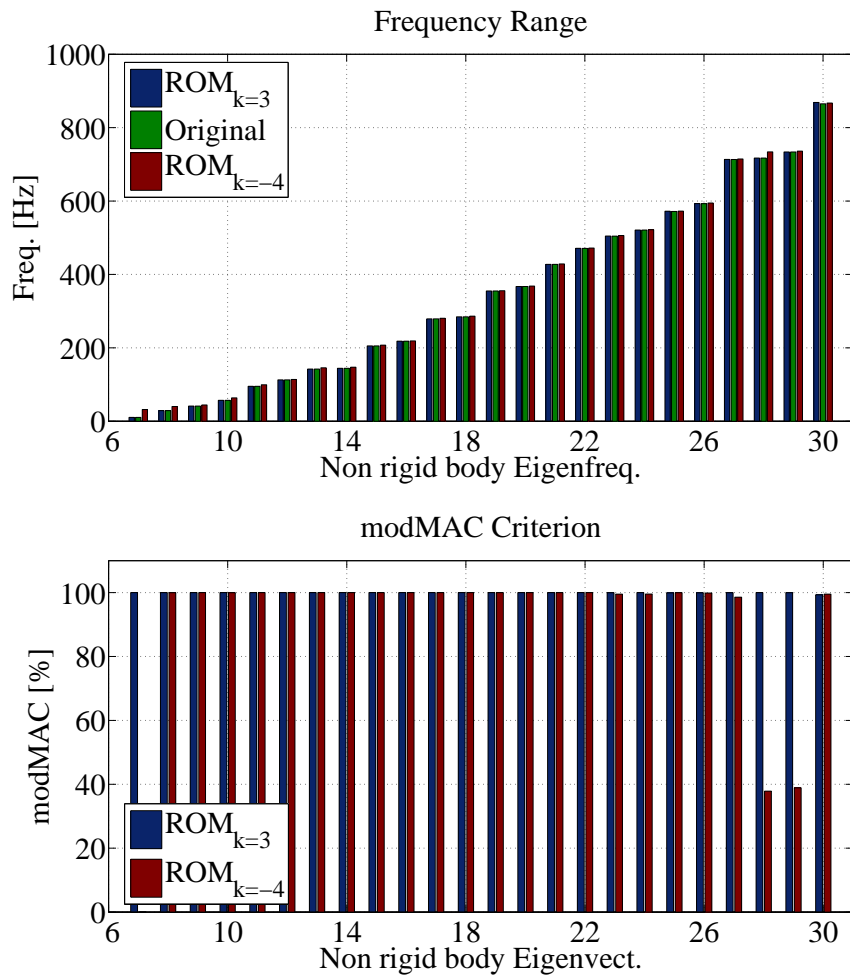
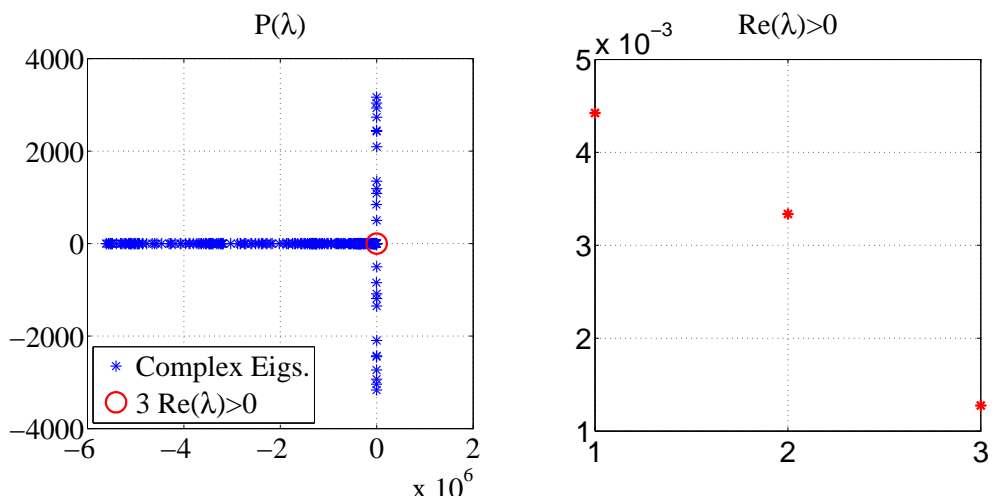


Fig. 4.10: 3D solid bar - BT ROM correlation - DP

Fig. 4.11: UIC60 rail - unstable $\mathbf{P}(\lambda)$

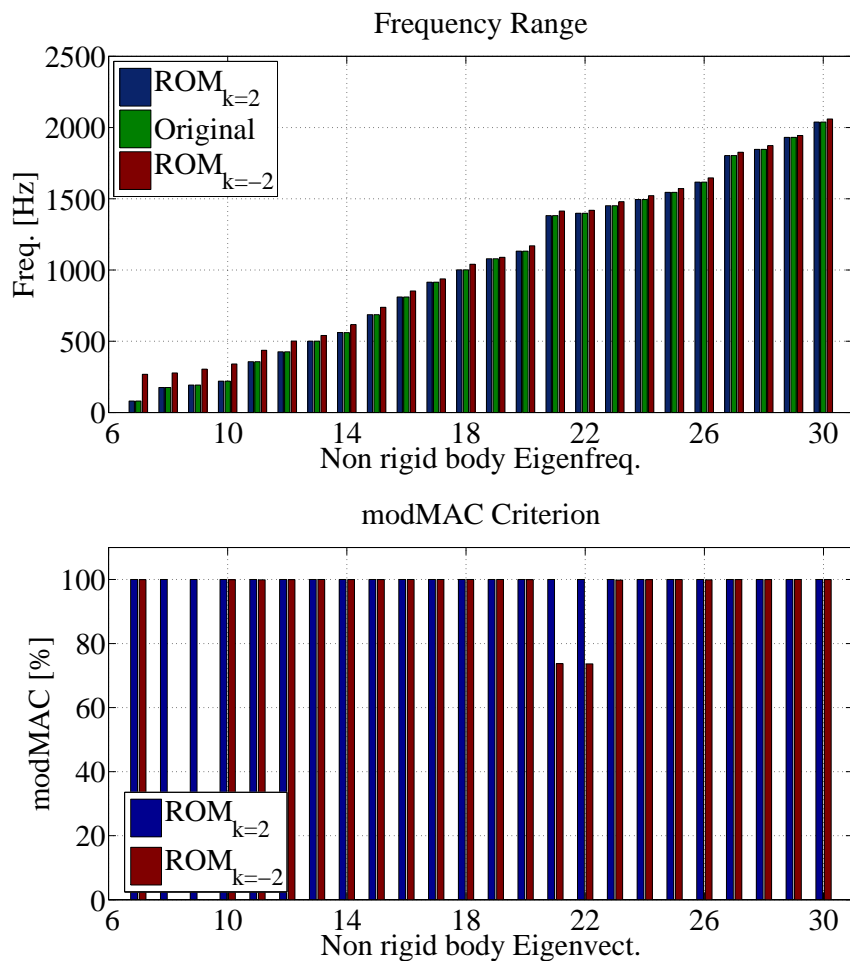


Fig. 4.12: UIC60 rail - BT ROM correlation - DP

5 Flexible body dynamics in multi body systems

The contents of the previously presented Chapters cover important aspects regarding the adaptation of various MOR methods to the requirements of the discipline referred to as elastic body dynamics. The theoretical background (Chapter 2), the level of application (Chapter 3), and the effective implementation with the help of numeric enhancements (Chapter 4) have shown the application of certain MOR schemes to be more accurate and therefore more adequate to use than the already standardized (Fig. 1.1) Guyan or CMS algorithms. In view of generating mechanical MBS based on such alternative MOR methods, the utilization of the existing rigid-flexible body dynamics theory (FEM-MBS coupling) is rather compulsory. Herewith, the system's rigid and elastic information is formulated according to the MBS formalism into the, so called, descriptor form.

The descriptor form's evaluation is conducted based on the category to which the applied MOR scheme belongs (Section 2.3). In case of *Non physical subspace reduction-expansion methods* (Section 2.3) several adaptation steps (back-projection approach [71, 72]) are necessary in order for the physical properties of the final MBS to be adequately defined during the FEM-MBS coupling. For the rest of the MOR methods presented in this Thesis such intervention is not necessary. Nevertheless, for all the MOR approaches, excluding the previously mentioned standardized Guyan and CMS methods, the appropriate interface must be provided in order for the coupling process to be realizable between commercial FEM and MBS software packages. In terms of the requirements in this Thesis the software availability is restricted to two tools (Fig. 1.1), namely, ANSYS [3] and SIMPACK [115].

On this account, the generalized equations of motion for mechanical MBS are shortly derived in Section 5.1. Based on the floating frame of reference formulation and the Ritz approximation for deformations [110, 112], the symmetric system matrices are partitioned into specific sub-parts according to the rigid and elastic contribution for both the translational and rotational coordinates. The system's integrals are given, namely, the generalized mass and forces. Their evaluation is derived in Section 5.2 under consideration of several approximating assumptions [123] and the final equation of motion for the coupled FEM-MBS formulation is presented as a set of generalized Differential and Algebraic Equations (DAEs).

In Section 5.3 the back-projection approach is introduced, the application of which enables the import of ROM belonging to the *Non physical subspace reduction-expansion methods* category into SIMPACK . Finally, Section 5.4 copes with the structure of the SID file.

5.1 Floating frame of reference formulation

A mechanical MBS is defined as an assembly of arbitrary rigid and flexible bodies, which interact with each other due to the presence of joints and force elements. The latter are defined either among bodies only or between certain bodies and a predefined inertial frame [125, 110, 112].

In the following Subsections the equations of motion for an arbitrary elastic body i will be derived under the modelling assumption of the, so called, floating frame of reference formulation. The description of such an elastic body is conducted based on Fig. 5.1, which is introduced in SCHWERTASSEK and WALLRAPP [110].

According to the floating frame of reference formulation, it is assumed the deformation of the elastic body i to be described w.r.t a selected body reference, e.g. $\{O^i, \mathbf{e}^i\}$ as depicted in Fig. 5.1. Thence, the total displacement of the material points P of an arbitrary elastic body i (linear material properties are assumed) is a superposition of the motion of the reference frame $\{O^i, \mathbf{e}^i\}$ and the associated displacement due to deformation. Finally, it is assumed the deformation to be small, but without excluding

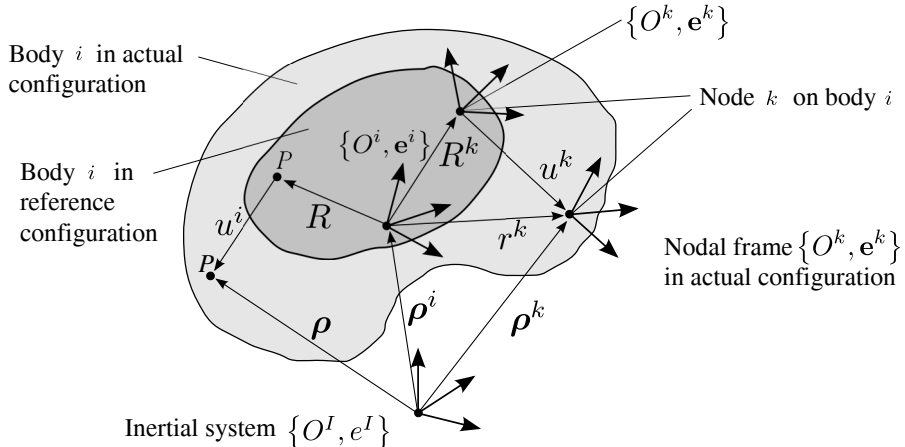


Fig. 5.1: Floating frame of reference formulation

the consideration of pre-stresses. Herewith, the equations of motion can be linearized w.r.t the deformation coordinates even in case of large overall - reference - motion.

5.1.1 Kinematics of flexible multi body systems

According to Fig. 5.1, the orientation of the body reference frame $\{O^i, \mathbf{e}^i\}$ w.r.t to the inertial system $\{O^I, \mathbf{e}^I\}$ is ascertained with the help of the rotation matrix \mathbf{A}^i , i.e.

$$\mathbf{e}^i = \mathbf{A}^i(t)\mathbf{e}^I, \quad \mathbf{A}^i(t) = [A_{\alpha\beta}^i(t)], \quad \{\alpha, \beta\} = 1, 2, 3. \quad (5.1)$$

Eq. (5.1) constitutes the necessary information for describing the motion of an arbitrary material point P within an elastic body i w.r.t either $\{O^i, \mathbf{e}^i\}$ or $\{O^I, \mathbf{e}^I\}$. In this regard, the translational equations of motion of such a point P w.r.t the body reference frame $\{O^i, \mathbf{e}^i\}$ are given in compact form as follows [110]:

$$\boldsymbol{\rho}(\mathbf{R}, t) = \boldsymbol{\rho}^i(t) + \mathbf{R} + \mathbf{u}^i(\mathbf{R}, t) \quad (5.2)$$

$$\mathbf{v}(\mathbf{R}, t) = \mathbf{v}^i(t) + \dot{\mathbf{u}}^i(\mathbf{R}, t) + \tilde{\boldsymbol{\omega}}^i(t)(\mathbf{R} + \mathbf{u}^i(\mathbf{R}, t)) \quad (5.3)$$

$$\mathbf{a}(\mathbf{R}, t) = \mathbf{a}^i(t) + \ddot{\mathbf{u}}^i(\mathbf{R}, t) + 2\tilde{\boldsymbol{\omega}}^i\dot{\mathbf{u}}^i(\mathbf{R}, t) + (\dot{\tilde{\boldsymbol{\omega}}}^i(t) + \tilde{\boldsymbol{\omega}}^i(t)\tilde{\boldsymbol{\omega}}^i(t))(\mathbf{R} + \mathbf{u}^i(\mathbf{R}, t)). \quad (5.4)$$

Here, $\boldsymbol{\rho}(\mathbf{R}, t)$, $\mathbf{v}(\mathbf{R}, t)$ and $\mathbf{a}(\mathbf{R}, t)$ annotate the position, linear velocity, and linear acceleration, respectively. Furthermore, $\tilde{\boldsymbol{\omega}}^i$ is the skew-symmetric angular velocity matrix and $\mathbf{u}^i(\mathbf{R}, t)$ the vector representing the inner displacement of the point P due to deformation.

The kinematic description of the point P is completed by including the rotational information of the body reference frame w.r.t to a specific coordinate system of the flexible body. In case of FE structures such a coordinate system is given by the, so called, nodal frame, e.g. $\{O^k, \mathbf{e}^k\} \equiv \{O, \mathbf{e}\}$ as depicted in Fig. 5.1. Thus, for small rotational motion of $\{O, \mathbf{e}\}$ w.r.t $\{O^i, \mathbf{e}^i\}$ the analogous vectors of position, angular velocity, and angular acceleration are obtained [110]:

$$\mathbf{A}(\mathbf{R}, t) = \left(\mathbf{I} - \tilde{\boldsymbol{\vartheta}}^i(\mathbf{R}, t) \right) \boldsymbol{\Gamma}^i(\mathbf{R}) \mathbf{A}^i(t), \quad \mathbf{A}(\mathbf{R}, t) = \boldsymbol{\Theta}^i(\mathbf{R}, t) \mathbf{A}^i(t) \quad (5.5)$$

$$\boldsymbol{\omega}(\mathbf{R}, t) = \boldsymbol{\omega}^i(t) + \dot{\boldsymbol{\vartheta}}^i(\mathbf{R}, t) \quad (5.6)$$

$$\mathbf{b}(\mathbf{R}, t) = \dot{\boldsymbol{\omega}}^i(t) + \ddot{\boldsymbol{\vartheta}}^i(\mathbf{R}, t) + \tilde{\boldsymbol{\omega}}^i(t)\dot{\boldsymbol{\vartheta}}^i(\mathbf{R}, t), \quad (5.7)$$

where $\boldsymbol{\Theta}^i(\mathbf{R}, t)$ is the local orientation due to deformation parametrized by $\boldsymbol{\vartheta}^i(\mathbf{R}, t)$, $\boldsymbol{\Gamma}^i(\mathbf{R}) := [\Gamma_{\alpha\beta}^i]$ the analog of the matrix $\boldsymbol{\Gamma}^e$ defined in Eq. (2.2) - (2.3), and $\boldsymbol{\vartheta}^i(\mathbf{R}, t)$ the deformation vector due to rotation.

According to Eq. (5.2) - (5.7) the motion of an arbitrary point P of an elastic body i w.r.t the inertial system is a superposition of the motion of $\{O^i, \mathbf{e}^i\}$ given by the time dependent terms $\boldsymbol{\rho}^i(t)$, $\mathbf{a}^i(t)$, $\mathbf{v}^i(t)$, and $\boldsymbol{\omega}^i(t)$, and the motion of the $\{O, \mathbf{e}\}$ w.r.t $\{O^i, \mathbf{e}^i\}$. The latter motion is ascertained by the time and space dependent functions $\mathbf{u}^i(\mathbf{R}, t)$ and $\boldsymbol{\vartheta}^i(\mathbf{R}, t)$, respectively, the approximation of which is conducted with the help of the Ritz method.

5.1.2 Ritz approximation for deformations

The mathematical theory of variable separation leads to the description of the displacement fields $\mathbf{u}^i(\mathbf{R}, t)$ and $\boldsymbol{\vartheta}^i(\mathbf{R}, t)$ in terms of infinite series as given in Eq. (5.8):

$$\mathbf{u}^i(\mathbf{R}, t) = \sum_{k=1}^{\infty} \Phi_{\alpha k}^i q_k^i(t) \quad \text{and} \quad \boldsymbol{\vartheta}^i(\mathbf{R}, t) = \sum_{k=1}^{\infty} \Psi_{\alpha k}^i q_k^i(t). \quad (5.8)$$

Here, the time dependent terms $\mathbf{q}^i(t)$ are the, so called, generalized coordinates and the space dependent functions $\Phi^i(\mathbf{R})$ and $\Psi^i(\mathbf{R})$ constitute the, so called, basis functions. The deformation shape is then exactly captured, if and only if, the infinite series converge to the limit functions $\mathbf{u}^i(\mathbf{R}, t)$ and $\tilde{\boldsymbol{\vartheta}}^i(\mathbf{R}, t)$, respectively.

The Ritz method approximates the deformation field by truncating the infinite series of Eq. (5.8) and thus, leading to the following relationship

$$\tilde{\mathbf{u}}^i(\mathbf{R}, t) \approx \sum_{k=1}^{n_q} \Phi_{\alpha k}^i q_k^i(t) = \Phi^i(\mathbf{R}) \mathbf{q}^i(t) \quad (5.9)$$

$$\tilde{\boldsymbol{\vartheta}}^i(\mathbf{R}, t) \approx \sum_{k=1}^{n_q} \Psi_{\alpha k}^i q_k^i(t) = \Psi^i(\mathbf{R}) \mathbf{q}^i(t) \quad (5.10)$$

with the prerequisite of $\tilde{\mathbf{u}}^i(\mathbf{R}, t)$ and $\tilde{\boldsymbol{\vartheta}}^i(\mathbf{R}, t)$ being Cauchy sequences [128, 112], i.e. converging to the limit functions of Eq. (5.8). Hence, the basis functions have to satisfy the geometric boundary conditions induced by the floating frame of reference formulation.

On the basis of Eq. (5.9) - (5.10), the equations of motion given in Eq. (5.2) - (5.7) can be expressed in terms of the generalized coordinates and the associated basis functions. Therefore, according to [110] the following is obtained:

$$\mathbf{v}(\mathbf{R}, t) = \underbrace{[\mathbf{I} \quad (\mathbf{R} + \Phi^i(\mathbf{R}) \mathbf{q}^i) \quad \Phi^i(\mathbf{R})]}_{\mathbf{T}_t^i(\mathbf{R}, \mathbf{q}^i)} \underbrace{[\mathbf{v}^i(t) \quad \boldsymbol{\omega}^i(t) \quad \dot{\mathbf{q}}^i]^T}_{\mathbf{z}^i(t)} \quad (5.11)$$

$$= \mathbf{T}_t^i(\mathbf{R}, \mathbf{q}^i) \mathbf{z}^i(t) \quad (5.12)$$

$$\mathbf{a}(\mathbf{R}, t) = \mathbf{T}_t^i \dot{\mathbf{z}}^i(t) + \underbrace{\tilde{\boldsymbol{\omega}}^i \left(\mathbf{v}^i + 2\Phi^i(\mathbf{R}) \dot{\mathbf{q}}^i + \tilde{\boldsymbol{\omega}}^i (\mathbf{R} + \Phi^i(\mathbf{R}) \mathbf{q}^i) \right)}_{\boldsymbol{\zeta}_t^i} \quad (5.13)$$

$$= \mathbf{T}_t^i \dot{\mathbf{z}}^i(t) + \boldsymbol{\zeta}_t^i \quad (5.14)$$

$$\boldsymbol{\omega}(\mathbf{R}, t) = \underbrace{[\mathbf{0} \quad \mathbf{I} \quad \Psi^i(\mathbf{R})]}_{\mathbf{T}_r^i(\mathbf{R})} \mathbf{z}^i(t) = \mathbf{T}_r^i(\mathbf{R}) \mathbf{z}^i(t) \quad (5.15)$$

$$\mathbf{b}(\mathbf{R}, t) = \mathbf{T}_r^i(\mathbf{R}) \mathbf{z}^i(t) + \underbrace{\tilde{\boldsymbol{\omega}} \Psi^i(\mathbf{R}) \dot{\mathbf{q}}^i}_{\boldsymbol{\zeta}_r^i} = \mathbf{T}_r^i(\mathbf{R}) \mathbf{z}^i(t) + \boldsymbol{\zeta}_r^i. \quad (5.16)$$

According to the relationships in Eq. (5.11) - (5.16) the complete kinetic description of the elastic body i is outlined in the next Subsection 5.1.3.

5.1.3 Kinetics of flexible multi body systems

The derivation of the elastic body's kinetic information is straightforward based on the principle of virtual power - JOURDAIN's principle [61] -, the analogon of which is already introduced in Eq. (2.13) - (2.14) with the associated terms being defined in

Section 2.1.2. In this regard, the inertia as well as the internal and external forces of the elastic body i are shortly derived in the following.

- *Inertia of the deformed body.* According to the virtual work for infinitesimal volume elements the virtual power of the inertia forces is given as follows:

$$\int_{V_0^i} \delta \mathbf{v}^T \mathbf{a}_{dm} = \delta \mathbf{z}^{iT} \left(\int_{V_0^i} \mathbf{T}_t^{iT} \mathbf{T}_t^i dm \dot{\mathbf{z}}^i + \int_{V_0^i} \mathbf{T}_t^{iT} \boldsymbol{\zeta}_t^i dm \right) = \delta \mathbf{z}^{iT} (\mathbf{M}^i \dot{\mathbf{z}}^i - \mathbf{h}_\omega^i) \quad (5.17)$$

Thus, the generalized mass matrix is given by:

$$\mathbf{M}^i = \int_{V_0^i} \mathbf{T}_t^{iT} (\mathbf{R}, \mathbf{q}^i) \mathbf{T}_t^i (\mathbf{R}, \mathbf{q}^i) dm = \int_{V_0^i} \begin{bmatrix} \mathbf{I} \\ (\mathbf{R} + \boldsymbol{\Phi}^i \mathbf{q}^i) \\ \boldsymbol{\Phi}^{iT} \end{bmatrix} \begin{bmatrix} \mathbf{I} \\ -(\mathbf{R} + \boldsymbol{\Phi}^i \mathbf{q}^i) \\ \boldsymbol{\Phi}^{iT} \end{bmatrix}^T dm \quad (5.18)$$

which is symmetric and can be partitioned into the following parts:

- Rigid body
 - (i) pure translational (index tt) and rotational motion (index rr)
 - (ii) contribution (indexes rt, tr)
- Elastic body
 - (i) pure elastic influence (index ee)
 - (ii) rigid-elastic contribution (indexes er, et, te, re)

$$\mathbf{M}^i = \begin{bmatrix} \mathbf{M}_{tt}^i & & \text{sym.} \\ \mathbf{M}_{rt}^i & \mathbf{M}_{rr}^i & \\ \mathbf{M}_{et}^i & \mathbf{M}_{er}^i & \mathbf{M}_{ee}^i \end{bmatrix} = \begin{bmatrix} m^i \mathbf{I} & & \text{sym.} \\ m^i \tilde{\mathbf{c}}^i & \mathbf{I}_O^i & \\ \mathbf{C}_t^i & \mathbf{C}_r^i & \mathbf{M}_e^i \end{bmatrix}, \quad (5.19)$$

with $m^i = \int_{V_0^i} dm = \int_{V_0^i} \rho_0^i(\mathbf{R}) dV$ being the body mass, \mathbf{c}^i the center of mass, $\mathbf{M}_{rr} \equiv \mathbf{I}_O^i$ the matrix of mass moment of inertia w.r.t $\{O^i, \mathbf{e}^i\}$, $\mathbf{M}_{et} \equiv \mathbf{C}_t^i$ the matrix coupling the translational motion and deformation, $\mathbf{M}_{er} \equiv \mathbf{C}_r^i$ the matrix coupling the angular motion and deformation, and \mathbf{M}_{ee} the generalized mass due to the deformation coordinates.

The acceleration and gyroscopic load term \mathbf{h}_ω^i is written in compact form as shown below, i.e.

$$\mathbf{h}_\omega^i = \int_{V_0^i} \mathbf{T}_t^{iT} \boldsymbol{\zeta}_t^i dm = \begin{bmatrix} \mathbf{h}_{\omega t}^i \\ \mathbf{h}_{\omega r}^i \\ \mathbf{h}_{\omega e}^i \end{bmatrix} = \begin{bmatrix} -m^i \tilde{\omega}^i \mathbf{v}^i - 2\omega \mathbf{C}_t^{iT} \dot{\mathbf{q}}^i - m^i \tilde{\omega}^i \tilde{\omega}^i \mathbf{c}^i \\ -m^i \tilde{\mathbf{c}}^i \tilde{\omega}^i \mathbf{v}^i - \sum_{l=1}^{n_q^i} \mathbf{G}_{rl}^i \dot{q}_l^i \omega^i - \tilde{\omega}^i \mathbf{I}_O^i \omega^i \\ -\mathbf{C}_t^i \tilde{\omega}^i \mathbf{v}^i - \sum_{l=1}^{n_q^i} \mathbf{G}_{el}^i \dot{q}_l^i \omega^i - \mathbf{O}_e^i \omega_q^i, \end{bmatrix}. \quad (5.20)$$

and the matrices required for its complete definition, i.e. \mathbf{G}_{rl}^i , \mathbf{G}_{el}^i , and $\mathbf{O}_e^i \omega_q^i$, are calculated according to the following relationships with n_q referring to the number

of elastic coordinates:

$$\mathbf{G}_{rl}^i = -2 \int_{V_0^i} (\mathbf{R} + \boldsymbol{\Phi}^i \mathbf{q}^i) \tilde{\boldsymbol{\Phi}}_{*l}^i \rho_0 dV, \quad (5.21)$$

$$\mathbf{G}_{el}^i = -2 \int_{V_0^i} \boldsymbol{\Phi}^{iT} \tilde{\boldsymbol{\Phi}}_{*l}^i \rho_0 dV, \quad (5.22)$$

$$\mathbf{O}_e^i \omega_q^i = \int_{V_0^i} \boldsymbol{\Phi}^{iT} \tilde{\boldsymbol{\omega}}^i \tilde{\boldsymbol{\omega}}^i \mathbf{r}^i \rho_0 dV. \quad (5.23)$$

- *Internal forces.* The tensor of generalized internal forces is a nonlinear function of the coordinates \mathbf{q}^i , as shown in Eq. (5.24), which is introduced based on the relationship in Eq. (2.13). Here, pre-stresses $\boldsymbol{\sigma}_0$ due to reference loads might be considered:

$$\int_{V_0^i} \delta \dot{\boldsymbol{\epsilon}}^{iT} \boldsymbol{\sigma}^i dV = \delta \dot{\mathbf{q}}^{iT} \int_{V_0^i} \mathbf{B}^{iT} \boldsymbol{\epsilon}^i dV = \delta \mathbf{z}^{iT} \mathbf{h}_e^i = \begin{bmatrix} \mathbf{0} \\ \mathbf{0} \\ \mathbf{K}_{ee}^i \end{bmatrix} \quad (5.24)$$

with the terms $\boldsymbol{\epsilon}$ and \mathbf{B} being defined in Eq. (2.15) and Eq. (2.20), respectively (linear case). The final calculation of the stiffness matrix \mathbf{K}_{ee}^i in Eq. (5.24) is conducted based on three modeling approaches depending on the application area [112, 128, 110, 111, 126, 125]:

- (i) Assumption of linear displacement functions and deformations (Ritz approximation (Eq. (5.9))), which consequently lead to the definition of a linear stiffness matrix.
- (ii) Assumption of (i), but considering pre-stresses leading thus, to geometric stiffening matrices.
- (iii) Assumption of (ii), but considering quadratic displacement functions, which ultimately contribute to generating quadratic mode shape terms.
- *External forces.* As external forces are considered to be all surface forces applied on the body i . They are divided into two categories according to the nature of their existence:
 - (a) Imposed (user defined) forces and
 - (b) forces $\mathbf{F}^{k,i}$ and $\mathbf{L}^{k,i}$ resulting from force elements (e.g. springs) and joints at the nodes k of the i -th body.

The virtual power conducted due to the above mentioned forces is given below:

$$\int_{A_{p_0}^i} \delta \mathbf{v}^T \bar{\mathbf{p}}_0^i dA + \sum_{k:i=i(k)} \left(\delta \mathbf{v}^{k,iT} \mathbf{F}^{k,i} + \delta \boldsymbol{\omega}^{k,iT} \mathbf{L}^{k,i} \right) = \delta \mathbf{z}^{iT} (\mathbf{h}_p^i + \mathbf{h}_d^i). \quad (5.25)$$

Herein, $A_{p_0}^i$ annotates the infinitesimal surface where the loads are applied and $\bar{\mathbf{p}}_0^i$ is the density vector of all imposed forces. Finally, the vectors \mathbf{h}_p^i , \mathbf{h}_d^i denote the continuous imposed and the discrete joint forces, respectively.

The application of the Ritz method leads to the derivation of the following integrals, i.e.

$$\mathbf{h}_p^i = \begin{bmatrix} \mathbf{h}_{pt}^i \\ \mathbf{h}_{pr}^i \\ \mathbf{h}_{pe}^i \end{bmatrix} = \begin{bmatrix} \int_{A_{p_0}^i} \bar{\mathbf{p}}_0^i dA \\ \int_{A_{p_0}^i} (\mathbf{R} + \boldsymbol{\Phi}(\mathbf{R})\mathbf{q}^i) \tilde{\bar{\mathbf{p}}}_0^i(\mathbf{R}, t) dA \\ \int_{A_{p_0}^i} \boldsymbol{\Phi}^{iT}(\mathbf{R}) \bar{\mathbf{p}}_0^i(\mathbf{R}, t) dA \end{bmatrix} \quad (5.26)$$

$$\mathbf{h}_d^i = \begin{bmatrix} \mathbf{h}_{dt}^i \\ \mathbf{h}_{dr}^i \\ \mathbf{h}_{de}^i \end{bmatrix} = \sum_{k:i=i(k)} \left(\mathbf{T}_t^{k,iT} \mathbf{F}^{k,i} + \mathbf{T}_r^{k,iT} \mathbf{L}^{k,i} \right). \quad (5.27)$$

The introduction of the state vector $\tilde{\mathbf{z}}^i = [\rho^i \ \boldsymbol{\alpha}^i \ \mathbf{q}^i]$ with the coordinates ρ^i and $\boldsymbol{\alpha}^i$ annotating the state variables of position (Eq. (5.2)) and velocity (Eq. (5.5)), respectively, enables the formulation of the general motion equations for the elastic body i . The assembly of n_b bodies of this type, the motion of which can be imposed to certain constraints due to their interconnection (joints) or ground conditions w.r.t the inertial frame, leads to the derivation of the generalized index-3 DAE for mechanical MBS, i.e.

$$\mathbf{M}^i \ddot{\tilde{\mathbf{z}}}^i + \mathbf{K}^i \tilde{\mathbf{z}}^i + \mathbf{G}_{\tilde{\mathbf{z}}^i}^T \boldsymbol{\lambda} = \mathbf{h}_p^i + \mathbf{h}_d^i + \mathbf{h}_\omega^i \quad (5.28)$$

$$\dot{\tilde{\mathbf{z}}}^i \stackrel{(5.11)}{=} \mathbf{Z}(\tilde{\mathbf{z}}^i) \mathbf{z}^i, \quad i = 1, 2, \dots, n_b \quad (5.29)$$

$$\mathbf{g}(\mathbf{z}, \tilde{\mathbf{z}}, t) = \mathbf{0} \quad (5.30)$$

Herein, the term $\mathbf{G}_{\tilde{\mathbf{z}}^i}^T$ refers to as the constraint Jacobian matrix, $\boldsymbol{\lambda}$ denotes the associated Lagrange multipliers [6, 7, 66] and the term $\mathbf{Z}(\tilde{\mathbf{z}}^i)$ is defined as given in [110, p. 382].

5.2 Evaluation of the elastic body information

This Section constitutes the kernel of the FEM-MBS coupling procedure, which is conducted by means of commercial software tools. The integral representation of the elastic body information given throughout the Eq. (5.17) - (5.27) should be approximated in order to be importable into MBS codes. As already mentioned, in this Thesis the coupling of rigid and flexible body dynamics is realized with the help of two specific commercial software tools, namely, the ANSYS FE and the SIMPACK MBS program. Therefore, according to Fig. 1.1, the coupling process is conducted in two steps.

Firstly, the flexible structure is modelled with the help of the FEM and the associated ROM is generated using a certain MOR approach. The direct utilization of a non-reduced FE structure is not advised, since any kind of DAE numeric approach [21, 6, 66, 101] for the solution of the large time-continuous system in Eq. (5.28) - (5.30) results in definite failure. The efficiency of the mentioned solvers is highly dependent on the dimension n_{dim}^{DAE} of the DAE system. A thumb rule of $n_{dim}^{DAE} \leq 500$ ascertains

the derivation of a solution with no computation burden. The more this boundary is exceeded, the more likely it is for a failure or vast computation times to occur.

Secondly, the ROM's information, the dynamic properties of which are expressed via the kinetic integrals of Eq. (5.17) - (5.27) is evaluated such that it is applicable for the MBS code import. In case of ANSYS and SIMPACK, the first step is restricted to the application of only two specific condensation methods, namely, either the Guyan or the CMS MOR and the second step is realizable, only if the ROM's evaluated data is transferred into the SIMPACK code by means of the SID file format (Section 5.4).

The allocation of the $\Phi^i(\mathbf{R})$ and $\Psi^i(\mathbf{R})$ basis functions defined in Eq. (5.9) - (5.10) constitutes the initial step during the activation of the elastic body's evaluation procedure. In case of FE models these functions are defined as the structure's mode displacement matrices, i.e. the eigenmodes and static modes. Nevertheless, higher order polynomials or frequency response modes may be utilized instead [37].

In this regard, the evaluation is conducted based on simple vector-matrix calculations of the ROM's system matrices $\{\mathbf{M}_F, \mathbf{D}_F, \mathbf{K}_F, \mathbf{K}_{F,geo}\} \in \mathbb{R}^{n_F \times n_F}$ annotating the mass, damping, stiffness, and geometric stiffness matrix, respectively, the deformation mode matrix $\mathbf{S}_e^i \in \mathbb{R}^{n_F \times n_{mode}}$ with n_{mode} representing the number of computed modes, and the translational and rotational rigid body modes $\{\mathbf{S}_t^i, \mathbf{S}_r^i\} \in \mathbb{R}^{n_F \times 3}$. The latter are defined as given below:

$$\mathbf{S}_e^i = \begin{bmatrix} \vdots \\ \left[\begin{array}{c} \Phi^i \\ \Psi^i \end{array} \right]^k \\ \vdots \end{bmatrix}, \quad \mathbf{S}_t^i = \begin{bmatrix} \vdots \\ \left[\begin{array}{c} \mathbf{I} \\ \mathbf{0} \end{array} \right]^k \\ \vdots \end{bmatrix}, \quad \mathbf{S}_r^i = \begin{bmatrix} \vdots \\ \left[\begin{array}{c} -\tilde{\mathbf{R}}^k \\ \mathbf{I} \end{array} \right]^k \\ \vdots \end{bmatrix}, \quad k = 1, 2, \dots, n_{\text{master}}. \quad (5.31)$$

The term \mathbf{R}^k gives the position of the k -th node of the reduced FE discretized elastic body i and consequently $\tilde{\mathbf{R}}^k$ annotates the associated skew symmetric matrix. Finally, n_{master} denotes the total number of nodes in the ROM.

The integral sub-matrices of the generalized mass matrix in Eq. (5.19) are evaluated by the use of Taylor expansion up to first-order Taylor terms [110]. Therefore, in the following, the subscript indexes 0 and 1 represent the zero- and the first-order Taylor terms, respectively.

- Mass sub-matrices

$$\mathbf{M}_{tt}^i = \mathbf{S}_t^i{}^T \mathbf{M}^i \mathbf{S}_t^i, \quad \mathbf{M}_{rr0}^i = \mathbf{S}_r^i{}^T \mathbf{M}^i \mathbf{S}_r^i, \quad \mathbf{M}_{ee0}^i = \mathbf{S}_e^i{}^T \mathbf{M}^i \mathbf{S}_e^i, \quad (5.32)$$

$$\mathbf{M}_{rt0}^i = \mathbf{S}_r^i{}^T \mathbf{M}^i \mathbf{S}_t^i, \quad \mathbf{M}_{et0}^i = \mathbf{S}_e^i{}^T \mathbf{M}^i \mathbf{S}_t^i, \quad \mathbf{M}_{er0}^i = \mathbf{S}_e^i{}^T \mathbf{M}^i \mathbf{S}_r^i, \quad (5.33)$$

$$\mathbf{M}_{er1}^i = [\mathbf{K}_{r1}^i \mathbf{q}^i \quad \mathbf{K}_{r2}^i \mathbf{q}^i \quad \mathbf{K}_{r3}^i \mathbf{q}^i], \quad \mathbf{M}_{rr1}^i = - \sum_{l=1}^{n_{\text{master}}} (\mathbf{C4}_l^i + \mathbf{C4}_l^{iT}) q_l^i, \quad (5.34)$$

where for the computation of the first order matrices in Eq. (5.34) the calculation

of the following matrices is necessary based on the approximations introduced in LOVE [85]:

$$\mathbf{K}_{r\alpha}^i \approx \frac{1}{2} \left(\mathbf{M}^i \widehat{\boldsymbol{\omega}}_{\alpha}^i + \widehat{\boldsymbol{\omega}}_{\alpha}^i \mathbf{M}^i \right), \quad \widehat{\boldsymbol{\omega}}_{\alpha}^i = \frac{\partial}{\partial \omega_{\alpha}^i} \text{diag} \begin{bmatrix} \widetilde{\boldsymbol{\omega}}^i & \mathbf{0} \\ \mathbf{0} & \widetilde{\boldsymbol{\omega}}^i \end{bmatrix}^k \quad (5.35)$$

$$\mathbf{C4}_l^i = \begin{bmatrix} C4_{l\alpha\beta}^i \end{bmatrix} = -\mathbf{S}_{r*\alpha}^{iT} \mathbf{K}_{r\beta}^i \mathbf{S}_{e*l}^i, \quad \alpha, \beta = \{1, 2, 3\}, \quad l = 1, \dots, n_{\text{master}}. \quad (5.36)$$

- Matrices of gyroscopic and acceleration forces

$$\mathbf{G}_{rl}^i = -2\mathbf{C4}_l^i, \quad \sum_{l=1}^{n_{\text{nodes}}^i} \mathbf{G}_{el}^i \dot{q}_l^i = 2 [\mathbf{K}_{r1}^i \dot{\mathbf{q}}^i \quad \mathbf{K}_{r2}^i \dot{\mathbf{q}}^i \quad \mathbf{K}_{r3}^i \dot{\mathbf{q}}^i] \quad (5.37)$$

$$\mathbf{O}_{e1}^i \boldsymbol{\omega}_q^i = \sum_{\alpha,\beta=1}^3 \mathbf{K}_{\omega\alpha\beta}^i \mathbf{q}^i \omega_{\alpha}^i \omega_{\beta}^i, \quad \mathbf{K}_{\omega\alpha\beta}^i \approx \mathbf{S}_e^{iT} \widehat{\boldsymbol{\omega}}_{\alpha}^i \mathbf{M}^i \widehat{\boldsymbol{\omega}}_{\beta}^i \mathbf{S}_e^i. \quad (5.38)$$

- Internal forces

$$\mathbf{K}_e^i = \mathbf{S}_e^{iT} \mathbf{K} \mathbf{S}_e^i, \quad \mathbf{K}_{e_{\text{geo}}}^i = \mathbf{S}_e^{iT} \mathbf{K}_{\text{geo}} \mathbf{S}_e^i, \quad \mathbf{D}_e^i = \mathbf{S}_e^{iT} \mathbf{D} \mathbf{S}_e^i. \quad (5.39)$$

5.3 Back-projection approach

The information gathered in Eq. (5.31) - (5.39) ascertains the evaluated form of the generalized DAE of Eq. (5.28) - (5.30), which should always be valid independent of the MOR scheme applied. In view of utilizing a MOR method, which belongs to the *Non physical subspace reduction-expansion methods* category, the properties of the aforementioned DAE system are defined in a non-physical space $\mathfrak{X}^n := \{\mathbf{z} : \{\mathbf{z} \in \mathfrak{X}^n\} \cap \{\mathbf{z} \notin \mathbb{R}^n\}\}$, e.g. $\mathfrak{X} = \mathbb{K}$ the Krylov subspace in case of the KSM method.

The FE data required in order for the FEM-MBS coupling process to be realizable in terms of the ANSYS and SIMPACK software packages are shortly listed below:

1. System matrices (damping and geometric stiffness matrices if required).
2. Mode displacement matrices (static and modal analysis).
3. Geometry information of the nodes.
4. DoF information (free or fixed).
5. Stress matrices of the body at nodes.
6. Load vectors due to reference unit loads.

In case, for example, of a KSM ROM and based on the relationships provided throughout the Eq. (5.31) - (5.39) the mechanical properties of the generated MBS, e.g. the mass, center of mass, mass moments of inertia, etc., possess no direct physical

interpretation (Table 5.1), since they are not defined on the physical configuration space (Euclidean space) $\{\mathbb{R}^n, n = 1, 2, 3\}$. Herewith, the practical data transfer into SIMPACK is forestalled, since the basic model properties [115] are inadequately defined.

On this account, an extra subspace is required, with which the ROM's dynamic information is projected back onto the Euclidean space. This methodology is referred to as the back-projection approach (Fig. 5.2) and is introduced in KOUTSOVASILIS, QUARZ and BEITELSCHMIDT [71, 72].

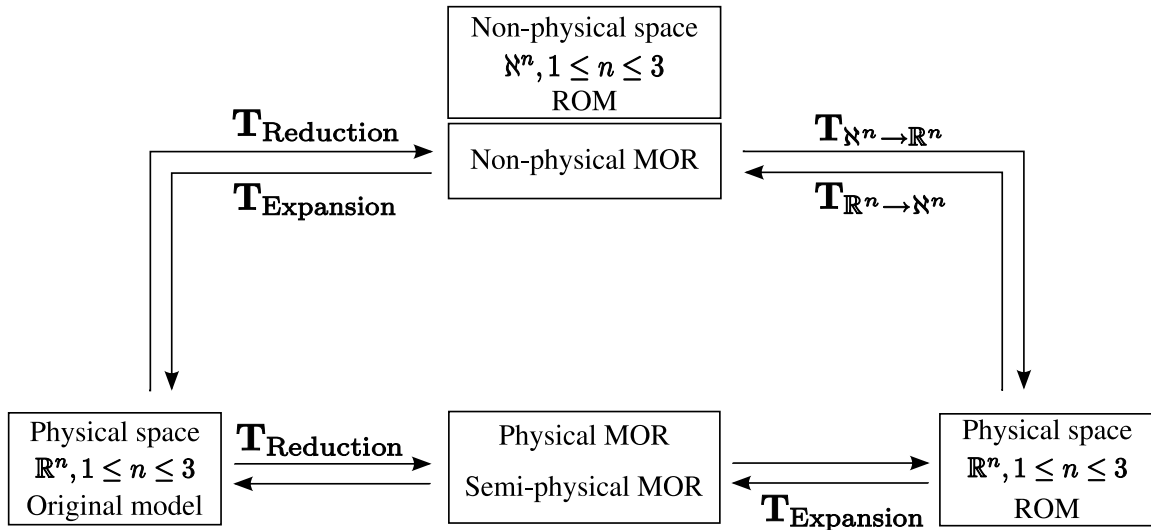


Fig. 5.2: Back-projection approach: reduction-expansion subspace

Without loss of generality, let us consider the undamped version of the master and slave DoF sorted dynamical system of Eq. (2.43), i.e.

$$\begin{bmatrix} \mathbf{M}_{mm} & \mathbf{M}_{ms} \\ \mathbf{M}_{sm} & \mathbf{M}_{ss} \end{bmatrix} \begin{bmatrix} \ddot{\mathbf{z}}_m \\ \ddot{\mathbf{z}}_s \end{bmatrix} + \begin{bmatrix} \mathbf{K}_{mm} & \mathbf{K}_{ms} \\ \mathbf{K}_{sm} & \mathbf{K}_{ss} \end{bmatrix} \begin{bmatrix} \mathbf{z}_m \\ \mathbf{z}_s \end{bmatrix} = \begin{bmatrix} \mathbf{F}_m \\ \mathbf{F}_s \end{bmatrix}. \quad (5.40)$$

According to the space reduction-expansion work flow in Fig. 5.2, let $\mathbf{T}_{N^n \rightarrow R^n}$ denote the transformation matrix required for projecting the non-physical ROM onto the physical configuration space and $\mathbf{T}_{R^n \rightarrow N^n}$ the equivalent reverse projection matrix.

The original model's state vector \mathbf{z} is approximated by \mathbf{z}_R with help of the lower dimension subspace \mathbf{T}_{N^n} , as already defined in Eq. (2.38). The annotation \mathbf{T}_{N^n} corresponds to the coordinate transformation matrix for MOR schemes, which belong to the *Non physical subspace reduction-expansion methods* category and therefore, the ROM resides on the non-physical space N^n . The vector of master DoF \mathbf{z}_m can be

formulated as a part of \mathbf{z} , as given in the following Eq. (5.41):

$$\mathbf{z} = \begin{bmatrix} \mathbf{z}_m \\ \mathbf{z}_s \end{bmatrix} = \mathbf{T}_{\aleph^n} \cdot \mathbf{z}_R \quad (5.41)$$

$$\mathbf{z}_m = [\mathbf{I}_{(m,m)} \mid \mathbf{0}_{(m,(s-m))}] \mathbf{z} = \hat{\mathbf{A}} \cdot \mathbf{z} \quad (5.42)$$

$$(5.41), (5.42) \Rightarrow \mathbf{z}_m = \hat{\mathbf{A}} \cdot \mathbf{T}_{\aleph^n} \cdot \mathbf{z}_R, \quad (5.43)$$

Here, $\mathbf{I}_{(m,m)}$ annotates the identity matrix of dimension $m \times m$ and $\mathbf{0}_{(m,(s-m))}$ the zero matrix of dimension $m \times (s-m)$.

Eq. (5.43) gives the relationship between the ROM's DoF defined on the non-physical subspace \aleph^n and the physical space \mathbb{R}^n . Thus, the computation of the matrix product $\hat{\mathbf{A}} \cdot \mathbf{T}_{\aleph^n}$ would ascertain the subspace $\mathbf{T}_{\mathbb{R}^n \rightarrow \aleph^n}$:

$$\hat{\mathbf{A}} \cdot \mathbf{T}_{\aleph^n} = [\mathbf{I}_{(m,m)} \mid \mathbf{0}_{(m,(s-m))}] \begin{bmatrix} \mathbf{T}_{\aleph^n(m,m)} \\ \hline \mathbf{T}_{\aleph^n((s-m),m)} \end{bmatrix} = \mathbf{I}_{(m,m)} \cdot \mathbf{T}_{\aleph^n(m,m)} \quad (5.44)$$

$$\Rightarrow \mathbf{T}_{\mathbb{R}^n \rightarrow \aleph^n} := \mathbf{T}_{\aleph^n(m,m)} \quad \text{and} \quad \mathbf{T}_{\aleph^n \rightarrow \mathbb{R}^n} := (\mathbf{T}_{\aleph^n(m,m)})^{-1}, \quad (5.45)$$

with $\mathbf{T}_{\aleph^n(m,m)}$ and $\mathbf{T}_{\aleph^n((s-m),m)}$ being the block parts of the transformation matrix for the associated non-physical space MOR scheme with dimensions $\mathbb{R}^{m \times m}$ and $\mathbb{R}^{(s-m) \times m}$, respectively. On that basis the following relationships are obtained regarding the state space vectors \mathbf{z}_m and \mathbf{z}_R , i.e.

$$\mathbb{R}^n \ni \mathbf{z}_m = \mathbf{T}_{\aleph^n \rightarrow \mathbb{R}^n} \cdot \mathbf{z}_R \quad \text{and} \quad \aleph^n \ni \mathbf{z}_R = \mathbf{T}_{\mathbb{R}^n \rightarrow \aleph^n} \cdot \mathbf{z}_m. \quad (5.46)$$

Herewith, the ROM, which is defined on \aleph^n , is projected onto the subspace $\mathbf{T}_{\mathbb{R}^n \rightarrow \mathbb{R}^n}$ and with help of (5.46) the system's information is defined on the physical configuration space \mathbb{R}^n (Fig. 5.2), as given in the following for the general damped version of Eq. (2.43):

$$\hat{\mathbf{M}}_m \ddot{\mathbf{z}}_m + \hat{\mathbf{D}}_m \dot{\mathbf{z}}_m + \hat{\mathbf{K}}_m \mathbf{z}_m = \hat{\mathbf{F}}_m, \quad (5.47)$$

$$[\hat{\mathbf{]}}_m = (\mathbf{T}_{\aleph^n \rightarrow \mathbb{R}^n})^T []_R \mathbf{T}_{\mathbb{R}^n \rightarrow \aleph^n}, \quad [] := \{\mathbf{M}, \mathbf{D}, \mathbf{K}\}.$$

In case of directly coping with Eq. (2.37), the back-projection approach proof is similar with the sole difference of having to take into account the automatic DoF reordering of FEM programs - due to the integrated wavefront solver [3]. Thereafter, an extra vector should be defined, which would allocate the master DoF \mathbf{z}_m out of the \mathbf{z} set.

Finally, an eigenvalue analysis of (5.47) ascertains the required input data (Table 5.1) for the evaluation of the elastic body's kinetic information (Eq. (5.31) - (5.39)) and therefore enabling it for further processing in a MBS code. As mentioned in Chapter 3, during the modal analysis of second-order mechanical systems the eigenfrequencies (and not the eigenvectors) are invariant to any kind of coordinate transformation, which does not affect their dimension, as in the back-projection case. Thence, as verification

criterion the eigenfrequencies of the non-physical space and the back-projected space ROM ought to be compared (NRFD). Herewith, it is assured that the structural properties of the model are preserved, e.g. the property of the mass matrix being positive definite. This observation is important, since according to Eq. (5.45) the definition of $\mathbf{T}_{\mathbb{X}^n \rightarrow \mathbb{R}^n}$ depends on the inversion of $\mathbf{T}_{\mathbb{X}^n(m,m)}$. In almost all cases $m \ll 10^3$ and the inversion is computationally inexpensive. Nevertheless, the properties of the subspace $\mathbf{T}_{\mathbb{X}^n(m,m)}$ might be ill-conditioned. Therefore, adequate direct or iterative inversion algorithms [51, 102, 36] should be applied in order to avoid numeric discrepancies caused by ill-conditioned matrices, several consequences of which were exemplified in Subsection 4.2.2.

Table 5.1: Back-projection - UIC60 rail - physical properties validation

ROM	Back-projection	Mass [Kg]	Center of mass $[x, y, z]^T$
CMS (FEMBS)	-	144.3	0
KSM I	no	3.035	11.65
			173.1
			-0.01459
KSM II	yes	144.3	0.2223
			3.371
			0
			11.65
			173.1

At this point, it should be mentioned that during the FEM-MBS coupling procedure, the mechanical properties of ROMs belonging to the *Non physical subspace reduction-expansion methods* category without applying the back-projection approach are retained. This is for example the case of the KSM I ROM in Table 5.1. The different values for the mass and the center of mass for this model do not indicate any damaged properties during the MOR application, but simply express these properties in a different configuration space.

5.4 Standard Input Data file

The introduction of the back-projection approach in Subsection 5.3 enables the import of MOR schemes of all three categories, as defined in Subsection 2.3, into MBS codes. Hence, qualitatively better ROM - in terms of the required computation time as well as the dimension size - can be ascertained. Both aspects were thoroughly analyzed in Chapter 3.

The importance of the latter aspect is now easier to comprehend, since it is directly connected to the dimension of the generalized mechanical DAE system in Eq. (5.28)

- (5.30). With the CMS method being the standardized MOR scheme any eigenvalue discrepancy regarding the quality of the ROM could be resolved only by the increase of its dimension, which immediately affects any further MBS simulation (Section 5.2). Of course, a selection of master DoFs according to the criteria in Subsection 2.2 is assumed. On the other hand, the utilization of alternative reduction schemes, e.g. ICMS, KSM, SEREP, SEREP-ICMS, SEREP-KSM, etc., overcomes the aforementioned problem, as presented in Subsection 3.3 and a better correlated ROM is generated for the FEM-MBS coupling process without having to increase the dimension requirements.

The last step, with which the FEM-MBS coupling process is completed, concerns the data transfer between the FEM and MBS software packages - in this case ANSYS and SIMPACK. As depicted in Fig. 5.3, four data types are required in order for the process to be successful when using the commercial tools. Two ANSYS FE output data are generated (*.rst, *.sub), which contain the ROM's information, as listed in Subsection 5.3. Thereafter, a SIMPACK integrated toolbox, namely, FEMBS [114] is activated, the purpose of which is twofold. Firstly, the Flexible Body Input file (FBI) is computed, which contains the ROM's information given throughout the Eq. (5.31) - (5.39), and secondly, the Standard Input Data file (SID) is generated, which constitutes a specially formatted MBS importable file.

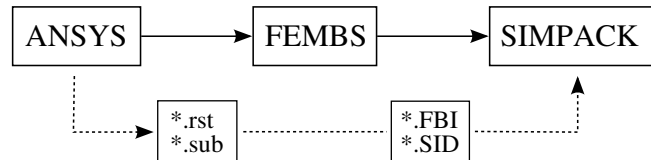


Fig. 5.3: FEM-MBS coupling - ANSYS & SIMPACK - file-type work flow

The SID file was proposed by WALLRAPP [123] and it is actually compatible for any kind of MBS code, which is based on linear or non linear equations of motion. It is an ASCII file, the structure of which is developed according to the object oriented techniques firstly introduced in OTTER, HOCKE, DABERKOW, and LEISTER [94]. The aforementioned references provide an extensive description of the file and therefore, it is not further analyzed in this Subsection.

With the SID file being introduced, the theoretical part of the FEM-MBS coupling process along with the necessary adaptation steps (back-projection approach) is completed. As already mentioned, the realization based on the commercial ANSYS and SIMPACK tools is feasible only for the Guyan and CMS MOR methods. On this account, the Model Order Reduction PACKAGE (MORPACK) [71, 68] has been created (Chapter 6), which enables the ANSYS-SIMPACK coupling via alternative MOR methods.

6 Model Order Reduction Package

The Matlab based [59] MORPACK toolbox [71, 68] is the topic of this Chapter. Its functionality is outlined and concluded by the Graphical User Interface (GUI) (Appendix A).

MORPACK consists of two inner interfaces (Fig. 6.1), namely, the MOR and the SID interface and combines all necessary procedures presented throughout the Chapters 2-5 for the automatic import of ANSYS FE structures into the SIMPACK MBS code. Firstly, the FE discretized model's information is converted into the, so called, Matrix Market file format. Thereafter, the MOR inner-interface is activated and the ROM is generated based on a user selected variety of physical, semi-physical or non-physical space MOR methods, which belong either to the one-step or the two-step general MOR algorithmic scheme. The ROM's dynamic properties and the preservation of its mechanical properties are validated with the help of certain Model Correlation Criteria (MCC). Finally, the SID inner-interface is activated, which copes with the necessary SID file generation for further usage of the ROM in SIMPACK.

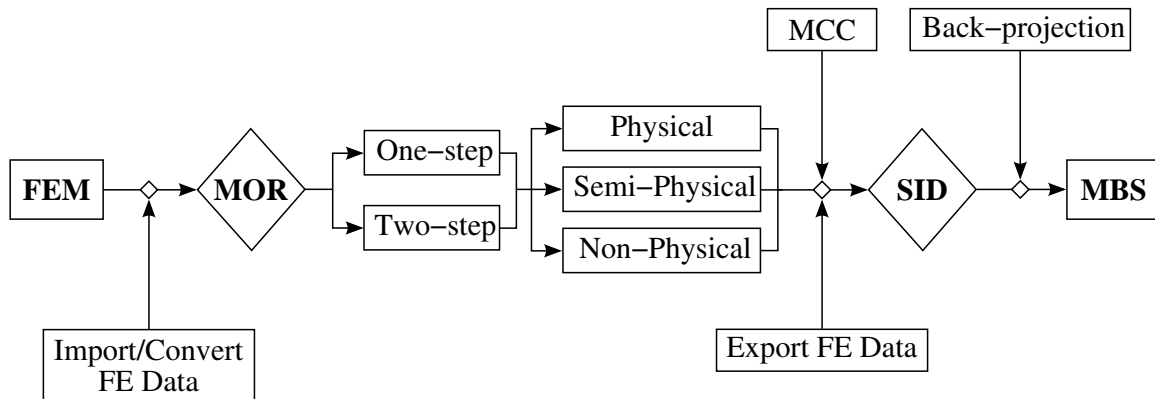


Fig. 6.1: MORPACK toolbox - work flow

In all the above mentioned levels the numeric and modelling schemes introduced in Chapters 4 and 5, are integrated within MORPACK, e.g. the diagonal perturbation methodology and the back-projection approach. While the first numeric method copes with the solution (either direct or iterative) of ill-conditioned systems (Section 4.2) and the stabilization of the, so called, matrix polynomial (Section 4.3) regarding the BT MOR techniques, the latter modelling approach (Section 5.3) enables the import into SIMPACK, or a general MBS code based on linear or non linear systems of equations, of MOR algorithms belonging to the *Non physical subspace reduction-expansion methods* category (Section 2.3). The switching process updating methodology will be included (Subsection 3.2.3) for maximizing the correlation order of the ROM's modal matrix.

The structure of Chapter 6 is divided into four Sections. Firstly, in Section 6.1 the functionality of both the MORPACK's inner interfaces is outlined and the application levels are analyzed in terms of the data required or generated during or after their operation, respectively. The two implemented algorithmic procedures are the topic of Section 6.2. Depending on the procedure's selection, the MORPACK work flow is automatically generated with the required options being highlighted thus, avoiding possible user mistakes or misunderstandings. All categories are valid for both free and grounded FE structures. In Section 6.3 the MORPACK toolbox is tested on two application examples of Chapters 3 and 4, namely, the 3D solid bar structure (Subsection 4.2.2) and the UIC60 rail (Subsections 3.3.3 - 3.3.4). Finally, the case of non successful SID generation is discussed in Section 6.4.

6.1 Functionality of the MORPACK toolbox

As depicted in Fig. 6.1, MORPACK consists of two interfaces, namely, the MOR and the SID interface and four application levels. The application levels operate either as data transfer or as functions, which validate the model's dynamics or transform their state-space definition in order to import and export compatible models for the aforementioned interfaces.

6.1.1 Inner interfaces

The MOR inner interface of MORPACK integrates the majority of the MOR schemes gathered in Table 2.1, the categorization of which is given in Section 2.3 and depicted in Fig. 6.1.

Particularly, the MOR interface integrates and utilizes sparse solvers for the direct or iterative solution of the selected MOR method. The diagonal perturbation methodology (Section 4.1) constitutes a valid alternative for accelerating the included numeric algorithm, which is the Preconditioned Conjugate Gradient method [51, 59]. The possibility of a model dependent pre-conditioner is given, namely, an incomplete Cholesky factor [51, 59] of the FE structure's stiffness matrix types \mathbf{K} or \mathbf{K}_{ss} depending on the applied MOR scheme (Chapter 2). The level of the pre-conditioner's fill-in is user-dependent to be chosen out of a given list. The valid spectrum for the initial perturbation parameter α (Eq. (4.9)) is partially predefined. The user need only to designate the value of the k parameter, the selection of which is accomplished based on MORPACK's predefined k -spectrum.

Furthermore, the two-step algorithmic schemes are integrated (Table 2.2) utilizing the above mentioned numeric schemes for the associated one-step methods. Special emphasis is given to the following MOR approaches, i.e. SEREP-KSM, SEREP-ICMS, KSM-ICMS, SOMT-ICMS and SOMT-KSM, which are powerful tools for accurately reducing the dimension of very large dimensioned FE structures within acceptable computation time limits (Section 3.3.5 and 3.3.6). Nevertheless, the conditions for safely applying the

SEREP MOR scheme (Section 2.4.4, p. 32) should always be taken into consideration. Finally, a matrix polynomial validation algorithm (Section 4.3) is activated whenever a BT MOR is selected.

The SID inner interface retrieves the ROM data and activates the elastic body evaluation procedure (Section 5.2). The ASCII object oriented structured SID file is generated under certain user-defined modelling parameters, e.g. the free or fixed nature of the structure, the FE units, the extra mass-scaling of the ROM's eigenvectors in case of changing the FE units, etc. The SID interface is considered to be the exact analogon to the commercial FEMBS interface. The sole difference resides on the calculation of the data, which is completed in two steps within FEMBS - first the FBI and then the SID file is generated -, whereas MORPACK's SID interface completes both tasks in one step.

6.1.2 Application levels

The two inner MOR and SID interfaces of MORPACK operate with data provided by four application functions (Fig. 6.1), which operate as follows.

Firstly, the application referred to as the *Import/Convert FE data* is activated aiming at converting the FE information provided within the ANSYS environment (Appendix A) as ASCII files. The FE system matrices are treated separately, since they constitute ASCII files, the contents of which are written in the, so called, Harwell-Boeing file format [39]. The aforementioned data is utilized for the applied MOR scheme and thereafter, the *Export FE data* second application level is activated, which gathers all ROM's information required for the initialization of the SID interface. The general specifications for both levels are gathered in Table 6.1, i.e.

Table 6.1: Application level I-II: Import-convert FE data & Export FE data

Model	Application level I	Application level II
Free	1. – 6., p. 137	1. – 6., p. 137
Fixed	1. – 6., p. 137 and 1. – 6., p. 137 for the associated free case	1. – 6., p. 137 and 1. – 6., p. 137 for the associated free case

As given in Table 6.1, the data computation for fixed FE ROM also requires the data of the associated free ROM. Herewith, the correct computation of the system's physical properties is ascertained, e.g. the mass, center of mass and mass moments of inertia.

Prior to the SID interface activation, the third application is invoked. It consists of various Model Correlation Criteria (Section 3.2), with which the dynamic properties of the ROM are validated (Table 6.2). Thus, the SID file is generated upon successful fulfillment of the MCC's requirements. Otherwise, the MOR scheme should be repeated. In case, though, of MCC discrepancies due to interchange of eigenvalues, which

constitutes a rather common phenomenon in the discipline of structural mechanics, the switching process updating methodology (Subsection 3.2.3) could be applied (not yet fully integrated in Version 1.0 MORPACK).

Table 6.2: Application level III: MCC

Level III	Model Correlation Criteria	Validated dynamic properties
NRFD		
MAC		1. Matrix definiteness
modMAC		
MNVD		2. Structure preservation
SNVD		

The fourth application level concerns the ROMs, which are computed with the help of the back-projection approach (Section 5.3). Thence, it copes with the MOR schemes of the *Non physical subspace reduction-expansion methods* category (Section 2.3). The *Back-projection control* application level verifies whether or not the ROM's structure properties are preserved (Table 6.3). If not, the ROM under this specific configuration is not importable into any MBS code, i.e. in this case SIMPACK.

Table 6.3: Application level IV: Back-projection control

Level IV	Criterion	Validated dynamic properties
NRFD		Structure preservation

6.2 Algorithmic procedures for free and fixed structures

The general work flow of MORPACK (Fig. 6.1) can be accessed based on two different types of algorithmic procedures, namely, the procedures I and II (Appendix A). The procedure's selection is conducted during the initiation of the MORPACK package and herewith, the aforementioned application levels are automatically adapted to the associated input data requirements. On this account, the MORPACK toolbox operates efficiently according to the user's requirements as well as the model's specifications.

The first procedure copes with structures, which are fully modelled within the ANSYS environment. Therefore, the FE information required for the initiation of the first application level (*Import-convert FE data*) concerns the following data: system matrices, eigenvectors, eigenfrequencies, DoF ordering due to the ANSYS implemented wavefront solver (Appendix A), full DoF set, and master DoF set. In case of FE structures with fixed DoF, the associated fixed information of the previously listed data should be acquired as well as the information for the fixed DoF.

The second procedure is slightly more independent from ANSYS, since the information required as input data for the first MORPACK application level are only the system matrices of the FE discretized structure and the DoF ordering. The rest is conducted within the MORPACK environment. In case of structures with fixed DoF, the additional information for the fixed DoF set should be ascertained, i.e. for fixed FE structures the system matrices and the DoF ordering of the associated free structure are used plus the fixed DoF information.

6.3 Application examples

The application examples presented in this Section, namely, the 3D solid bar structure (Section 4.2.2) and the elastic UIC60 rail (Sections 3.3.3 - 3.3.4), serve in demonstrating that the MORPACK toolbox is operational in the practical sense of coupling FE models generated in ANSYS into the SIMPACK MBS code. In this regard, both the aforementioned models are randomly chosen out of the FE models utilized so far in this Thesis (Chapters 3 and 4) and the KSM MOR scheme is selected for comparing the analogous CMS ROM imported into the SIMPACK code.

6.3.1 3D solid bar structure

The one-end fixed version of the 3D solid bar structure presented in Subsection 4.2.2 (Fig. 4.5) is reduced on one hand within the ANSYS environment with the help of the integrated CMS method and on the other hand within the MORPACK toolbox by use of the KSM reduction scheme. For the first case the FEMBS interface has been activated in order to transfer the elastic body data into SIMPACK, whereas for the second reduction scheme the SID inner-interface of the MORPACK toolbox is used.

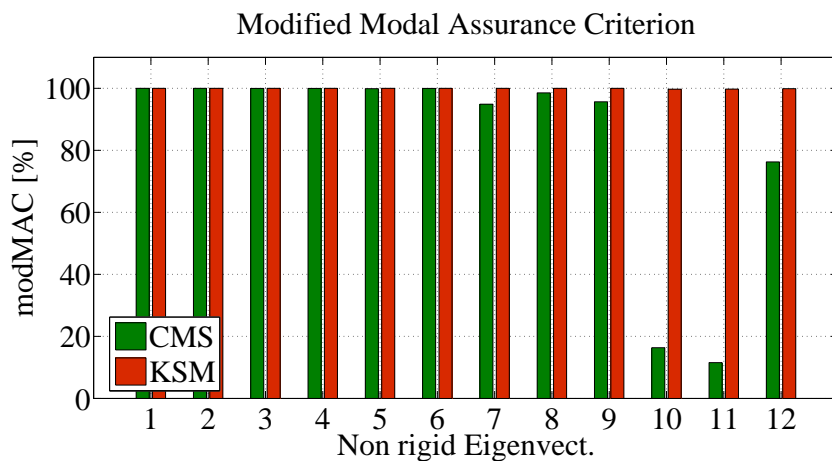


Fig. 6.2: 3D solid bar - modMAC - CMS & KSM

As expected, the KSM ROM captures the dynamic properties of the original model

better than the equivalent CMS ROM. This is to be visualized both in Fig. 6.2, where the eigenvector correlation for both of the aforementioned models is depicted, and in Fig. 6.6 within the SIMPACK Graphical User Interface (GUI) environment.

In Fig. 6.6 the 10th eigenvector of the original and the associated CMS and KSM models is depicted in SIMPACK. An eigenvector correlation of the order $modMAC_{10} \approx 20\%$ (Fig. 6.2) has an immediate effect on the associated SIMPACK model. The CMS ROM has the qualitative tendency of capturing the dynamics of the original model, still it fails to do so compared to both the original and the KSM ROM. Hence, the SIMPACK KSM ROM imported with the help of the MORPACK toolbox ascertains better dynamic properties than the equivalent ANSYS CMS ROM. An increase in the dimension requirements would improve the ANSYS CMS ROM, but would also aggravate any further simulation task in SIMPACK.

6.3.2 UIC60 rail

The free-version of the UIC60 rail model given in Subsection 3.3.3 (Fig. 3.31) is utilized for the purpose of demonstrating the functionality of the MORPACK toolbox over the classical coupling methodology, which is conducted by generating the ANSYS CMS model and transferring the elastic body data into SIMPACK by use of FEMBS.

According to the master DoF constellation in Fig 3.31 (here no DoF is grounded), it concerns a fairly large ROM and thus, a good correlation of dynamics is expected. Within the ANSYS environment, the analogon of the NRFD criterion for the CMS ROM depicted in Fig. 6.3 is producible. On that basis, the user would be satisfied up to the 23rd eigenfrequency, where the associated correlation is always smaller than 10%, i.e. $NRFD(i) \leq 10\%$, $i = 1, 2, \dots, 23$ and therefore, the next step would be to transfer the CMS ROM's information into the SIMPACK code.

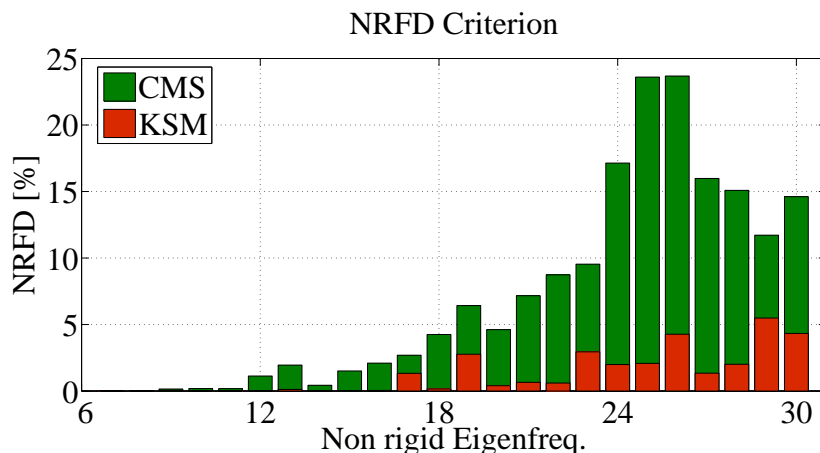


Fig. 6.3: UIC60 free - NRFD - CMS & KSM ROM

The visualization of the eigenvectors in SIMPACK would result with serious discrepancies from the 18th eigenvector and above, i.e. the first assumption based on the eigenfrequency

correlation is false. The visualization of the 20th eigenvector in SIMPACK (Fig. 6.7) shows zero correlation, although the associated eigenfrequency correlation is less than 5%, i.e. $NRFD(5) \leq 5\%$.

The application of the MORPACK toolbox overcomes the aforementioned problems. In case of the CMS ROM being an obligatory choice, the MCC application level of MORPACK allows the visualization of the eigenvector correlation for the original and the associated CMS ROM (Fig. 6.5). Therefore, the user is in the position to identify the level of perfect correlation and actually to improve the associated modal matrix in case of the eigenvector-interchange phenomenon (19th and 20th eigenvectors in Fig. 6.5 and eventually Fig. 6.7) by using the switching process updating methodology (Subsection 3.2.3). Of course, the possibility of applying a different MOR scheme is also given and in this case the KSM MOR method results with a perfectly correlated ROM in SIMPACK (Fig. 6.5 and Fig. 6.7) under the same master DoF requirements as for the CMS case.

Again, the same master DoF constellation is considered as for the UIC60 rail model given in Subsection 3.3.3 (Fig. 3.31), but in this case with one-end of the structure being grounded. This last example is similar to the 3D solid bar case (Subsection 6.3.1) and serves in demonstrating certain eigenvector discrepancies within the SIMPACK environment when comparing the ANSYS full with the ANSYS CMS and MORPACK KSM ROM, respectively. It is accomplished by visualizing the 22nd eigenvector of the aforementioned models in SIMPACK, as depicted in Fig. 6.8. Utilizing the modMAC information generated in MORPACK (Fig. 6.4) a perfect correlation is ascertained for the KSM ROM, whereas a correlation of the order $modMAC \approx 40\%$ is acquired for the ANSYS CMS ROM. The discrepancy is visualized in Fig. 6.8 and undergoes the same dynamic behavior as the 3D solid bar structure (Subsection 6.3.1), i.e. the SIMPACK CMS model tends qualitatively to similar eigenvector behavior compared to the associated eigenvector of the original model, but the MOR's information loss does not allow to perfectly capture its dynamics.

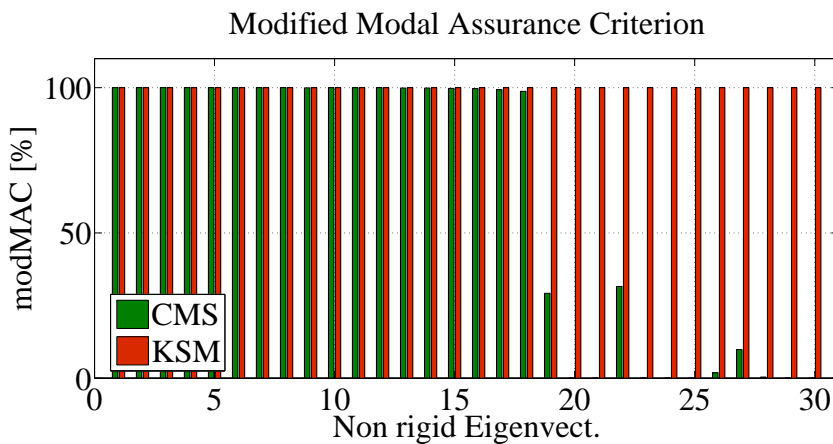


Fig. 6.4: UIC60 one-end fixed - modMAC - CMS & KSM ROM

Herewith, the MORPACK functionality realized with the help of both the ANSYS

and SIMPACK software tools has been demonstrated and the cycle of this Chapter is completed with the last Section 6.4, which copes with the case of non-successful SID generation within the MORPACK environment

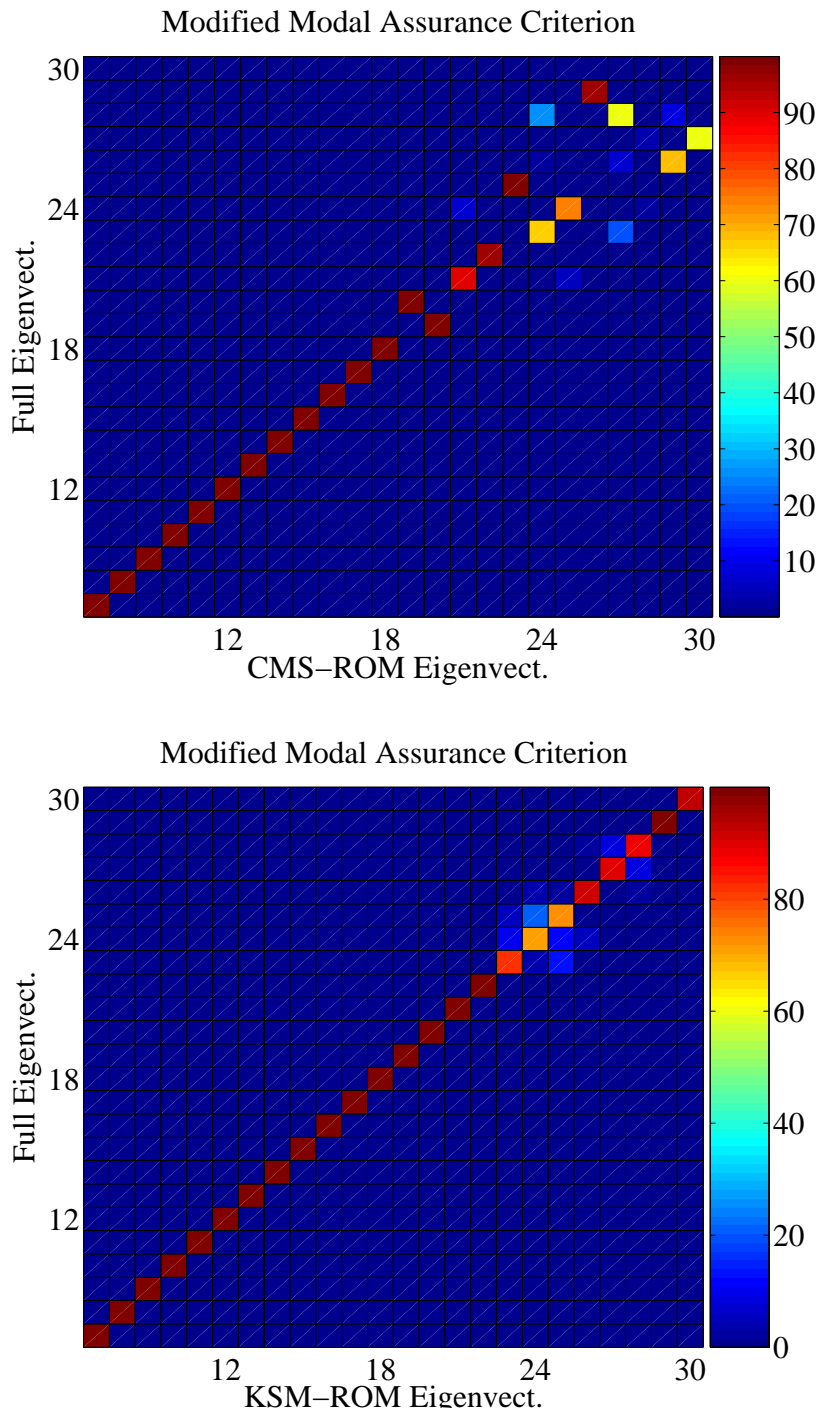


Fig. 6.5: UIC60 free - modMAC - CMS & KSM ROM

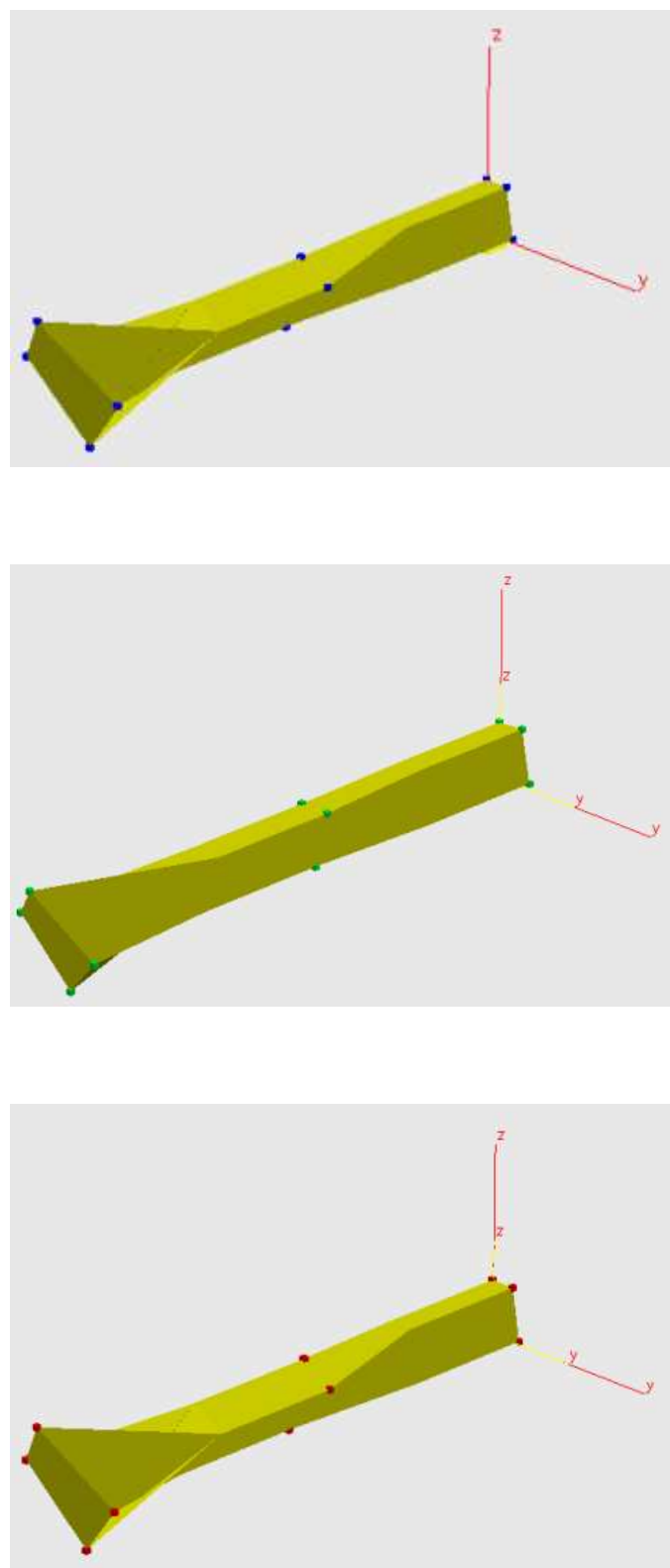


Fig. 6.6: 3D solid bar - Top to bottom: Full_{ANSYS}, CMS_{FEMBS} and KSM_{MORPACK}

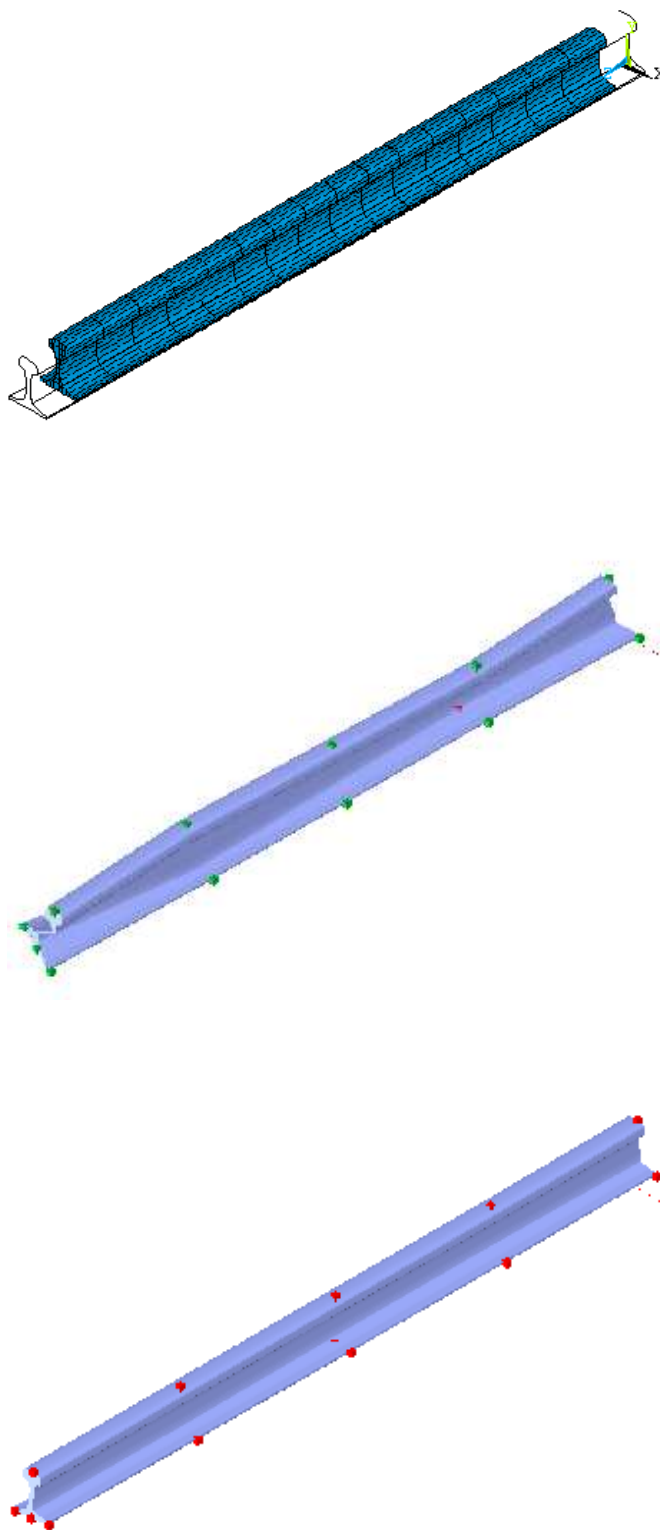


Fig. 6.7: UIC60 rail free - Top to bottom: ANSYS, CMS_{FEMBS} and KSM_{MORPACK}

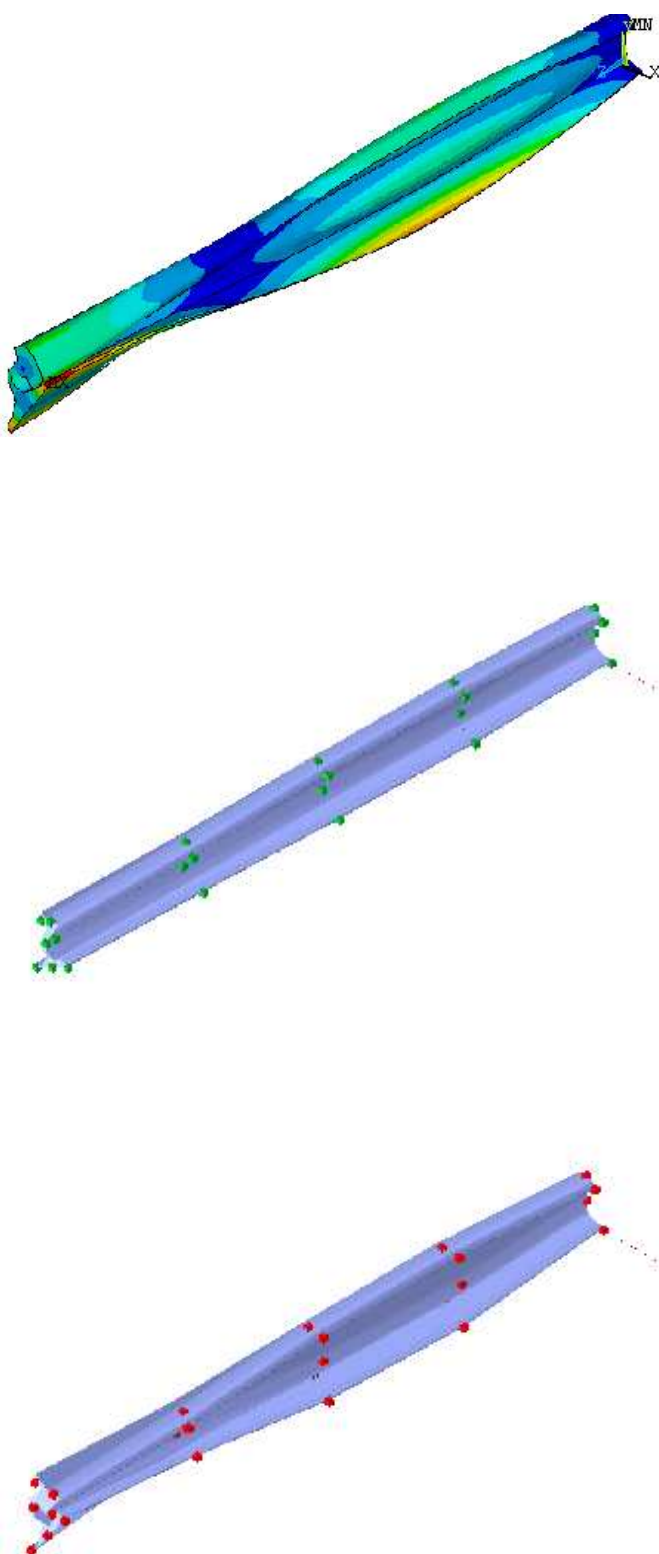


Fig. 6.8: UIC60 rail fixed - Top to bottom: ANSYS, CMS_{FEMBS} and KSM_{MORPACK}

6.4 Non successful SID generation

The SID generation procedure can be regarded as unsuccessful, if and only if the elastic body data evaluation results either in erroneously computed data or in no data at all.

Both aspects are an immediate consequence of the fourth MORPACK application level, namely, the *Back-projection control*. As already mentioned in Section 6.1 this application validates the preservation of the structure properties for the back-projected ROM. Such a validation control is compulsory, since an inversion algorithm is required (Eq. 5.45) for the computation of the associated back-projection matrix $T_{\mathbb{X}^n \rightarrow \mathbb{R}^n}$. The usage of non-adequate machine-precision numeric algorithms therefor might generate back-projected ROMS, the physical properties of which are damaged. The more the $(m \times m)$ block matrix of the associated non-physical-space coordinate transformation matrix $T_{\mathbb{X}^n}$ (Eq. 5.44 - 5.45) is ill-conditioned, the less efficient the inversion algorithms are. Thence, the possibility of generating a back-projected ROM with severely damaged mechanical properties exists, e.g. non-positive definite mass matrix. In such cases, the SID generation cannot be completed and either a different MOR scheme should be utilized instead or a different master DoF constellation should be allocated.

The stability properties of the back-projected ROM constitute an important issue regarding the realization of the FEM-MBS coupling procedure in terms of commercial software packages, in this case ANSYS and SIMPACK. Thence, further research in this area is required.

7 Summary

7.1 Summary in English

The research discipline referred to as the Model Order Reduction in structural mechanics was the topic of this Thesis. Special emphasis was given to the coupling process of rigid and elastic Multi Body Dynamics in terms of both the theoretical aspects and the practical realization within the environment of the commercial Finite Element and the Multi Body Systems software packages, ANSYS and SIMPACK respectively.

In this regard, a variety of structure preserving Model Order Reduction methods was presented in Chapter 2 and a categorization methodology was provided in view of the later FEM-MBS coupling process. The algorithmic scheme of several of the MOR methods, e.g. SEREP, KSM, ICMS, etc., indicated the capability of generating qualitatively better Reduced Order Models than the standardized Guyan and Component Mode Synthesis approaches. Nevertheless, the efficiency of a MOR method is measured in terms of both the quality of the ROM and the associated time required for the computation. Therefore, the general two-step MOR scheme, e.g. SEREP-KSM, SEREP-ICMS, KSM-ICMS, etc., was presented aiming at maximizing the efficiency factor, i.e. maximal quality and minimal computation time, when computing a ROM.

The validation of the ROM's dynamic properties was the topic of Chapter 3. Based on the application of the, so called, Model Correlation Criteria the efficiency of the MOR schemes, presented in Chapter 2, was tested on four application examples originating from the area of structural mechanics, i.e. the 3D elastic solid bar structure, the UIC60 elastic rail, the elastic piston rod, and the elastic crankshaft model. Herewith, the superiority of alternative MOR schemes in comparison to Guyan or CMS methods was demonstrated in terms of the ROM's quality and the computation time by the use of either the one-step or the two-step MOR algorithms. Thence, reduction methods such as the KSM, ICMS, SEREP-KSM, SEREP-ICMS, KSM-ICMS, etc., provide the opportunity of creating a better correlated ROM. The phenomenon regarding the dynamic discrepancies due to eigenvalue interchanges, which constitutes a rather common matter during the application of a MOR approach for mechanical systems was treated with the help of the switching process updating methodology. Herewith, the modal matrix correlation of the compared models is maximized without having to re-apply a MOR algorithm, i.e. indicating neither a different scheme nor a larger dimension number for the ROM.

The diagonal perturbation methodology was the topic of Chapter 4. Numerous of the FE discretized structures suffer from the, so called, ill-conditioned properties regarding the associated stiffness matrix. On one hand, the direct solution of a MOR method might produce erroneous ROMs due to the associated truncation phenomenon and on

the other hand, any kind of iterative approach suffers from vast computation times. The application of the diagonal perturbation methodology improves the condition properties of the model's stiffness matrix and thus, both kinds of the aforementioned solution procedures are affected. This was demonstrated on three mechanical structures, i.e. the 3D solid bar model for the direct MOR solution, and the elastic piston and crankshaft for the convergence acceleration during the iterative computation of the associated ROMs. Finally, with the help of the diagonal perturbation methodology the stabilization of the, so called, matrix polynomial was succeeded enabling thus, the non-problematic application of balancing related techniques in the area of structural mechanics.

In Chapter 5 the necessary theory for realizing the FEM-MBS coupling procedure was shortly outlined. Herewith, the dynamic motion for mechanical MBS was formulated as an index-3 system of generalized Differential and Algebraic Equations, the integrals of which were evaluated based on several approximation procedures. Thereafter, the elastic body information was transferred into the MBS codes in form of the, so called, Standard Input Data format. Nevertheless, the standard procedure is not applicable for MOR methods belonging to the *Non physical subspace reduction-expansion methods* category, since the associated physical properties of the model are inadequately defined. Therefore, the back-projection approach was introduced, which projects the ROM back onto the physical configuration space and thus, enabling its further usage in a MBS code, e.g. SIMPACK.

Chapter 6 summarizes and combines the theoretical, modelling, and numerical advancements of the previous Chapters 2-5 in terms of the Model Order Reduction Package. The Matlab-based MORPACK toolbox enables the FEM-MBS coupling process for the ANSYS-SIMPACK utilization and herewith, several of the aforementioned enhancements are included. With the help of the two integrated inner interfaces, i.e. MOR and SID, as well as the four application levels, the import into SIMPACK of alternatively free or fixed ROMs is enabled. The functionality of MORPACK was demonstrated based on two application examples, namely, the 3D elastic solid bar and the UIC60 elastic rail, the dynamic properties of which were validated prior to their import into SIMPACK. Finally, the case of non-successful SID generation is discussed.

The further development of several modelling and numeric aspects within the MORPACK environment can be regarded as suggestions for future work. On that basis, the thorough examination of the stability properties of the alternatively generated ROMs in SIMPACK is desired. Additionally, the restrictions regarding the non-successful SID generation for certain types of the back-projected ROM should be further examined in an effort to sufficiently categorize the model types, which undergo such damage with respect to their dynamic properties after the application of the back-projection approach. Finally, the expansion of the supported ANSYS FE model types as well as the FE system data obtained from other FEM software tools should constitute a main aspect regarding the later MORPACK versions.

7.2 Summary in German

Gegenstand dieser Arbeit ist die Forschungsdisziplin, welche in der Strukturmechanik als Modellordnungsreduktion bekannt ist. Im Mittelpunkt stehen Kopplungsprozesse von starren und elastischen Mehrkörpersystemen - sowohl in theoretischer Hinsicht als auch bezüglich der praktischen Realisation im Rahmen des Finite-Elemente-Programms ANSYS und des Mehrkörpersimulationsprogramms SIMPACK.

Eine Vielfalt von strukturerhaltenden MOR-Methoden wurde im zweiten Kapitel zum Zwecke des Überblicks dargestellt. Darüber hinaus findet sich hier eine Kategorisierungsmethodik in Hinsicht auf den später beschriebenen FEM-MKS-Kopplungsprozess. Das algorithmische Schema mehrerer MOR-Methoden, beispielsweise SEREP, KSM, ICMS etc., deutet auf die Möglichkeit hin, qualitativ hochwertigere ROM zu generieren als dies mit dem standardisierten Guyan- und Component Mode Synthesis-Ansatz der Fall ist. Trotz alledem wird die Effizienz einer MOR-Methode sowohl hinsichtlich an der Qualität der ROM als auch an der hierfür benötigten Rechenzeit bemessen. Aus diesem Grunde wurde ein allgemeines zweistufiges MOR-Schema dargelegt, z.B SEREP-KSM, SEREP-ICMS, KSM-ICMS, usw., mit dem Ziel, den Effizienzfaktor während der Berechnung eines ROMs zu maximieren, das heißt maximale Qualität und minimale Rechenzeit zu erzielen.

Die Validierung der dynamischen ROM-Eigenschaften war Gegenstand des dritten Kapitels. Basierend auf der Anwendung der sogenannten Modellkorrelationskriterien wurde die Effizienz der MOR-Methoden aus Kapitel 2 an vier Anwendungsbeispielen aus dem Feld der Strukturmechanik getestet: der 3D-Balkenstruktur, der UIC60-Schiene, dem Pleuel und der Kurbelwelle. Hierdurch wurde mit Anwendung des ein- oder zweistufigen MOR-Algorithmus die Überlegenheit der alternativen MOR-Methoden gegenüber der Guyan- oder CMS-Methode hinsichtlich der Qualität und Rechenzeit demonstriert. Folglich bieten Methoden wie KSM, ICMS, SEREP-KSM, SEREP-ICMS, KSM-ICMS, usw., die Möglichkeit, höher korrelierte ROM zu erzeugen. Das bei der Anwendung des MOR-Ansatzes häufig auftauchende Phänomen der dynamischen Diskrepanzen, welches auf dem Vertauschen von Eigenwerten beruht, wurde mit Hilfe der *switching process updating methodology* behandelt. Hierdurch wird die Korrelation der modalen Matrizen der verglichenen Modelle ohne eine wiederholte Anwendung des MOR-Algorithmus maximiert, also ohne eine andere Methode oder eine größere Dimension für die ROM anzuwenden.

Im vierten Kapitel wird die *diagonal perturbation*-Methodik behandelt. Zahlreiche der FE-diskretisierten Strukturen haben schlecht konditionierte Eigenschaften bezüglich der assoziierten Steifigkeitsmatrix. Einerseits könnte die direkte Lösung einer MOR aufgrund von Abrundung ein fehlerhaftes ROM zur Folge haben, andererseits bedeutet jegliche iterative Herangehensweise eine enorme Rechenzeit. Die Anwendung der *diagonal perturbation*-Methodik verbessert die Kondition der Steifigkeitsmatrix eines Modells, wodurch beide der zuvor genannten Lösungsprozeduren betroffen sind. Dies wurde anhand dreier verschiedener mechanischer Modelle demonstriert, des 3D-Balkenmodells und des elastischen Pleuel- bzw. Kurbelwellenmodells. Durch die *diagonal perturbation*-Methodik wurde es so möglich, dass der Stabilisierung des so genannten *matrix*

polynomial die nicht problematische Anwendung der Balanced Truncation-Methode im Umfeld der Strukturmechanik folgte.

Im fünften Kapitel wurde der für das Verständnis der FEM-MKS-Kopplungsprozedur notwendige theoretische Hintergrund erläutert. Es galt die dynamische Bewegung mechanischer MKS als ein Index-3-DAE-System zu formulieren, um die resultierenden Integrale auf Basis verschiedener Näherungsprozeduren zu evaluieren. Daraufhin wurde die Information über die elastischen Körper in Form der sogenannten Standard Input Datei in einen MKS-Code transferiert. Dennoch ist es nicht möglich, die Standardprozedur auch für diejenigen MOR-Methoden zu verwenden, welche zur *Non physical subspace reduction-expansion methods*-Kategorie gehören, da die assoziierten physikalischen Eigenschaften unangemessen definiert werden. Aus diesem Grunde wurde der *Back-projection*-Ansatz eingeführt, welcher die ROM auf den Euklidischen Raum zurückprojiziert und folglich die weitere Verwendung in einem MKS-Code ermöglicht.

Kapitel 6 resümiert und kombiniert gleichermaßen die theoretischen, modellierenden und numerischen Fortschritte der vorhergehenden Kapitel 2-5 im Sinne der Model Order Reduction Package Toolbox. Die Matlab-basierte MORPACK-Toolbox ermöglicht den FEM-MKS-Kopplungsprozess für die Verwendung von ANSYS und SIMPACK. Hierin sind ein Großteil der zuvor erläuterten Erweiterungen eingeschlossen. Mit Hilfe der zwei integrierten inneren MOR- und SID-Schnittstellen als auch der vier Anwendungsebenen wird der Import von freien oder eingespannten ROM in SIMPACK ermöglicht. Die Funktionalität von MORPACK wurde anhand zweier Anwendungsbeispiele, eines 3D-Balkenmodells und einer UIC60-Schiene, demonstriert. Hierbei wurden deren dynamische Eigenschaften vor dem Import in SIMPACK validiert. Am Ende erfolgte ein Abriss der erfolglosen SID-Erzeugungen mit alternativen MOR-Techniken.

Die Entwicklung weiterer Modellierungsaspekte und numerischer Verfahren innerhalb der MORPACK-Umgebung kann als Anregung für künftige Arbeiten verstanden werden. Auf dieser Basis ist die gründliche Untersuchung der Stabilitätseigenschaften für das alternativ entwickelte ROM in SIMPACK erwünscht. Hinzu kommt, dass die Einschränkungen, welche die nicht erfolgreichen SID-Erzeugungen betreffen, genauer beleuchtet werden sollten. Dies ist notwendig, um eine suffiziente Kategorisierung derjenigen Modelle zu erreichen, welche dieser Beschädigung unterliegen. Besonderes Augenmerk gilt hier den dynamischen Eigenschaften nach der Anwendung des *Back-projection*-Ansatzes. Die Ausweitung der unterstützten ANSYS-FE-Typen als auch die Unterstützung der Systemdateien anderer FE-Programme sollten einen Schwerpunkt bei der Entwicklung weiterer MORPACK-Versionen bilden.

Literature

- [1] Oberwolfach Model Reduction Benchmark Collection. Available online at <http://www.imtek.uni-freiburg.de/simulation/benchmark>.
- [2] Allemand, R. J. The Modal Assurance Criterion - Twenty Years of Use and Abuse. In *International Modal Analysis Conference IMACC XX*, Los Angeles, CA, February 2002.
- [3] Ansys. *Guide to Interfacing with ANSYS*, 10.0 edition, August 2005.
- [4] Antoulas, A. C., Sorensen, D. C., Gugercin, S. A survey of model reduction methods for large-scale systems. Technical report, Rice University, Houston, Texas, February 2004.
- [5] Antoulas, C. A. *Approximation of Large-Scale Dynamical Systems*. Advances in Design and Control. SIAM, Philadelphia, 2005.
- [6] Arnold, M. Simulation Algorithms in Vehicle System Dynamics. Technical report, Department of Mathematics and Computer Science, Martin-Luther-Universität Halle, 2004.
- [7] Arnold, M., Carrarini, A., Heckmann, A., Hippmann, G. Modular dynamical simulation of mechatronic and coupled systems. In *MASCI-net Workoshop*, Wuppertal, Germany, February 2004.
- [8] Arnoldi, W. E. The Principle of Minimized Iterations in the Solution of the Matrix Eigenvalue Problem. *Quart. Appl. Math.*, 9:17–29, 1951.
- [9] Bai, Z. Krylov subspace techniques for reduced-order modeling of large-scale dynamical systems. *Applied Numerical Mathematics*, 43:9–44, 2002.
- [10] Bai, Z., Meerbergen, K., Su, Y. Arnoldi Methods for Structure-Preserving Dimension Reduction of Second-Order Dynamical Systems. In *Dimension Reduction of Large-Scale Systems*, Lecture Notes in Computational Science and Engineering, pages 173–189. Springer Verlag Berlin Heidelberg, 2005.
- [11] Bai, Z., Su, Y. Dimension Reduction of Second-Order Dynamical Systems via a Second-Order Arnoldi Method. *SIAM*, 26(5):1692–1709, 2005.
- [12] Bechtold, T. *Model Order Reduction of Electro-Thermal MEMS*. PhD thesis, Albert-Ludwigs Universität Freiburg im Breisgau, 2005.
- [13] Beitelschmidt, M., Koutsovasilis, P., Quarz, V. Zur Modellierung und Simulation der Kolbenmaschinendynamik unter Berücksichtigung von Strukturelastizitäten. In *ANSYS Conference & 24. CADFEM User's Meeting*, Stuttgart, Germany, October 2006.
- [14] Benner, P. Numerical Methods for Model Reduction of Large-Scale Dynamical Systems. In *GAMM Jahrestagung*, Luxembourg, March 2005.

- [15] Benner, P. Numerical Linear Algebra for Model Reduction in Control and Simulation. *GAMM-Mitt.* 29, 2:275 – 296, 2006.
- [16] Benner, P. Balancing-related model reduction for data-sparse systems. In *Computational Methods with Applications*, Harrachov, Czech Republic, August 2007.
- [17] Benner, P., Mehrmann, V., Sorensen, D. C., editor. *Dimension Reduction of Large-Scale Systems*. Lecture Notes in Computational Science and Engineering. Springer Verlag Berlin Heidelberg, 2005.
- [18] Benner, P., Quintana-Ortí, S. Model Reduction Based on Spectral Projection Methods. In *Dimension Reduction of Large-Scale Systems*, Lecture Notes in Computational Science and Engineering, pages 5–48. Springer Verlag Berlin Heidelberg, 2005.
- [19] Blair, M. A., Camino, T. S., Dickens, J. M. An iterative approach to a reduced mass matrix. In *Proc. 9th. Int. Modal Analysis Conference*, pages 621–626, Florence, Italy, 1991.
- [20] Boley, D. L. Krylov Space Methods on State-Space Control Models. *CSSPl*, 13:733–758, 1994.
- [21] Brenan, K. E., Campbell, S. L., Petzold, L. R. *Numerical Solution of Initial-Value Problems in Differential-Algebraic Equations*. Classics in Applied Mathematics. SIAM, 1996.
- [22] Brühls, O. *Integrated Simulation and Reduced-Order Modeling of Controlled Flexible Multibody Systems*. PhD thesis, Université de Liège, 2005.
- [23] Budó, A., editor. *Theoretische Mechanik*. Deutscher Verlag der Wissenschaften, Berlin, 4 edition, 1967.
- [24] Burrage, K., Erhel, J., Pohl, B. A deflation technique for linear systems of equations. Technical Report 94-02, Eidgenössische Technische Hochschule Zürich, 1994.
- [25] Callahan O', J. C. A procedure for an improved reduced system (IRS) model. In *7. International Modal Analysis Conference*, Las Vegas, 1989.
- [26] Callahan O', J. C., Avitabile, P., Riemer, R. System Equivalent Reduction Expansion Process (SEREP). In *7. International Modal Analysis Conference*, Las Vegas, 1989.
- [27] Carney, K. S., Abdallah, A. A, Hucklebridge, A., A. Implementation of the block-Krylov boundary flexibility method of component synthesis. In *MSC World User's Conference*, Arlington, Virginia, May 1993.
- [28] Chahlaoui, Y., Lemonnier, D., Meerbergen, K., Vandendorpe, A., Dooren, P. V. Model reduction of second order systems. In *Math. Th. Netw. Syst. International Symposium*, University Notre Dame, Illinois, August 2006.
- [29] Chahlaoui, Y., Lemonnier, D., Vandendorpe, A., Van Dooren, P. Second-order balanced truncation. *Linear Algebra and its Applications*, 415(3):373–384, 2006.
- [30] Chahlaoui, Y., Van Dooren, P. A collection of Benchmark Examples for Model

- Reduction of Linear Time Invariant Dynamical Systems. Technical report, 2002.
- [31] Chen, S.-H., Pan, H. H. Guyan reduction. *Communications in Applied Numerical Methods*, 4:549–556, 1988.
- [32] Craig, R. R., Jr. A Brief Tutorial on Substructure Analysis and Testing. In *18th International Modal Analysis Conference*, San Antonio, TX, February 2000.
- [33] Craig, R. R. Jr. Coupling of substructures for dynamic analyses: an overview. In *AIAA Dynamics Specialists Conference*, volume 1573, Atlanta, GA, April 2000.
- [34] Craig, R. R. Jr., Bampton, M. C. C. Coupling of Substructures for Dynamic Analysis. *AIAA*, 6(7):1313–1319, 1968.
- [35] Cullum, J., Willoughby, R. Two-sided Arnoldi and Nonsymmetric Lanczos Algorithms. *SIAM Journal on Matrix Analysis and Applications*, 24(3):303–319, 2002.
- [36] Davis, T. A. *Direct Methods for Sparse Linear Systems*. Fundamentals of Algorithms. SIAM, 2006.
- [37] Dietz, S. Vibration and Fatigue Analysis of Vehicle Systems Using Component Modes. *VDI Fortschritt-Berichte*, (401), 1999.
- [38] Dietz, S., Knothe, K. Reduktion der Anzahl der Freiheitsgrade in Finite-Element-Substrukturen. Technical Report 315, Institut für Luft-und Raumfahrt (ILR), Technische Universität Berlin, 1997.
- [39] Duff, I. S., Grimes, R. G., Lewis, J. G. User's Guide for the Harwell-Boeing Sparse Matrix Collection (Release I). Technical report, CERFACS & Boeing Computer Services, October 1992.
- [40] Eich-Soellner, E., Führer, C. *Numerical Methods in Multibody Dynamics*. European Consortium for Mathematics in Industry. B. G. Teubner, Stuttgart, 1998.
- [41] Eid, R., Salimbahrami, B., Lohmann, B. Equivalence of Laguerre-based Order Reduction and Moment Matching. *IEEE Trans. on Automatic Control*, 52(6):1104–1108, 2007.
- [42] Eid, R., Salimbahrami, B., Lohmann, B., Rudnyi, E. B., Korvink, J. G. Parametric Order Reduction of Proportionally Damped Second Order Systems. Technical Report on Automatic Control, Vol. TRAC-1, Technische Universität München, 2006.
- [43] Ewins, D. J. *Modal Testing: theory, practice and application*. Research Studies Press Ltd., second edition, 2000.
- [44] Freund, R. W. Reduced-Order Modeling Techniques Based on Krylov Subspaces and Their Use in Circuit Simulation. Technical Report 98-3-02, Bell Laboratories, Murray Hill, New Jersey, 1998.
- [45] Freund, R. W. Model reduction methods based on Krylov subspaces. *Acta Numerica*, 12:267–319, 2003.
- [46] Friswell, M. I. The convergence of the iterated IRS method. *Journal of Sound and Vibration*, 211(1):123–132, 1998.

- [47] Friswell, M.I., Garvey, S.D., Penny, J. E. T. Model reduction using dynamic and iterated IRS techniques. *Journal of Sound and Vibration*, 186:311–323, 1995.
- [48] Geradin, M., Cardona, A. *Flexible Multibody Dynamics: a finite element approach*. John Wiley & Sons Ltd, 2001.
- [49] Gildin, E. *Model and Controller Reduction of Large-Scale Structures on Projection Methods*. PhD thesis, University of Texas at Austin, 2006.
- [50] Gloth, G. Vergleich zwischen gemessenen und berechneten modalen Parametern. In *Carl-Cranz Gesellschaft e.V*, Oberpfaffenhofen, Germany, 2001.
- [51] Golub, G. H., Van Loan, C. F. *Matrix Computations*. The John Hopkins University Press, Baltimore, Maryland, third edition, 1996.
- [52] Gressick, W., Wen, J. T., Fish, J. Order Reduction for Large-Scale Finite Element Models: A Systems Perspective. *International Journal for Multiscale Computational Engineering*, 3:337–362, 2005.
- [53] Grimme, E. J. *Krylov projection methods for model reduction*. PhD thesis, University of Illinois at Urbana-Champaign, 1997.
- [54] Gugercin, S., Antoulas, A. C., Bedrosian, N. Approximation of the International Space Station 1R and 12A Model. In *Proc. Dec. Contr.*, pages 1515–1516, Orlando, FLorida, 2001.
- [55] Guyan, J. Reduction of stiffness and mass matrices. *AIAA*, 3(380), 1965.
- [56] Hammarling, S. J. Numerical Solution of the Stable, Non-negative Definite Lyapunov Equation. *IMA Journal of Numerical Analysis*, 2:303–323, 1982.
- [57] Hartmann, C., Vulcanov V.-M., Schütte. Balanced truncation of second-order systems: structure-preservation and stability. *SIAM J. Control and Optimization*, (submitted) 2007.
- [58] Imanovic, N. *Validation of large structural dynamics models using modal test data*. PhD thesis, Imperial College of Science, Technology & Medicine, 1998.
- [59] Inc., MathWorks. *Matlab Documentation*, 7.0.4.365 (R14) edition, 2005.
- [60] Irons, B. M. Structural eigenvalue problems - elimination of unwanted variables. *AIAA*, 3(5):961–962, 1965.
- [61] Jourdain, P.E.B. Addition to papers on the equations of mechanics. *Quart. J. Pure Appl. Math.*, (39):241 – 250, 1908.
- [62] Kalman, R.E., Falb, P. L., Arbib, M. A., editor. *Topics in mathematical system theory*. McGraw-Hill, New York, 1969.
- [63] Kammer, D. C. Test-analysis model development using an exact modal reduction. *Int. Journal of Analytical and Experimental Modal Analysis*, 2(3):174–179, 1987.
- [64] Koutsovasilis, P., Beitelschmidt, M. Model Reduction Comparison for the Elastic Crankshaft Mechanism. In *International Operational Modal Analysis Conference, IOMAC*, volume 1, pages 95–106, Copenhagen, Denmark, May 2007.
- [65] Koutsovasilis, P., Beitelschmidt, M. Model Reduction of Large Elastic Systems: A

- Comparison Study on the Elastic Piston Rod. In *XII World Congress in Mechanism and Machine Science, IFTOMM*, Besancon, France, June 2007.
- [66] Koutsovasilis, P., Beitelschmidt, M. Simulation of Constrained Mechanical Systems. In *6th International Congress on Industrial and Applied Mathematics*, Zürich, Switzerland, July 2007.
- [67] Koutsovasilis, P., Beitelschmidt, M. Comparison of Model Reduction Techniques for Large Mechanical Systems; A Study on an Elastic Rod. *Multibody System Dynamics*, 20(2):111–128, 2008.
- [68] Koutsovasilis, P., Beitelschmidt, M. Model Order Reduction Package for Coupling Rigid and Elastic Multibody Dynamics. In *NAFEMS World Congress*, Crete, Greece, June 2009.
- [69] Koutsovasilis, P., Beitelschmidt, M. Model Order Reduction of Finite Element Models: Improved Component Mode Synthesis. *Mathematical and Computer Modelling of Dynamical Systems*, 2009 (accepted).
- [70] Koutsovasilis, P., Quarz, V., Beitelschmidt, M. FEM-MKS Coupling: Transferring Elastic Structures into the SID File-Format by the use of Krylov Subspace Method. In *ANSYS Conference & 25. CADFEM User's Meeting*, Dresden, Germany, October 2007.
- [71] Koutsovasilis, P., Quarz, V., Beitelschmidt, M. MORPACK Interface Functionality for importing FE Structures into MBS-Code via alternative Model Order Reduction Methods. In *SIMVEC Berechnung und Simulation im Fahrzeugbau*, volume 2031 of *VDI Berichte*, pages 259–271, Baden-Baden, Germany, November 2008.
- [72] Koutsovasilis, P., Quarz, V., Beitelschmidt, M. Standard Input Data for FEM-MBS Coupling: Importing Alternative Model Reduction Methods into SIMPACK. *Mathematical and Computer Modelling of Dynamical Systems*, 15(1):51–68, 2009.
- [73] Kraker, A., Campen, D. H. van. Rubin's CMS reduction method for general state-space models. *Computers & Structures*, 58(3):597–606, 1996.
- [74] Krylov, A. N. On the numerical solution of the equation by which in technical questions frequencies of small oscillations of material systems are determined. *Otd. Mat. Estestv. Nauk.*, 2(4):491–539, 1931.
- [75] Lanczos, C. An Iteration Method for the Solution of the Eigenvalue Problem of Linear Differential and Integral Operators. *J. Res. Nat. Bureau Stan.*, 45:255–282, 1950.
- [76] Laub, A. J., Heath, M. T., Paige, C. C., Ward, R. C. Computation of System Balancing Transformations and Other Applications of Simultaneous Diagonalization Algorithms. *IEEE Transactions on Automatic Control*, AC-32(2):115–122, 1987.
- [77] Lehner, M., Eberhard, P. Modellresuktion in elastischen Mehrkörpersystemen. *Automatisierungstechnik*, 54:170–177, 2006.
- [78] Lehner, M., Eberhard, P. A two-step approach for model reduction in flexible multibody dynamics. *Multibody System Dynamics*, 17:157–176, 2007.
- [79] Leung, A. Y. T. An accurate method of dynamic condensation in structural

- analysis. *Int. Journal for Numerical Methods in Engineering*, 12(11):1705–1715, 1978.
- [80] Li, J.-R. *Model Reduction of Large Linear Systems via Low Rank System Gramians*. PhD thesis, Massachusetts Institute of Technology, 2000.
- [81] Li, R.-C., Bai, Z. Structure-preserving model reduction using a Krylov subspace projection formation. *Comm. Math. Sci.*, 13:179–199, 2005.
- [82] Li, R.-C., Bai, Z. Structure-preserving model reduction. *Lecture Notes in Computer Science*, 3732:323–332, 2006.
- [83] Liao, S., Bai, Z., Gao, W. The important modes of subsystems: A moment-matching approach. *Int. J. Numer. Meth. Engng*, 70:1581–1597, 2007.
- [84] Lohmann, B., Salimbahrami, B. Introduction to Krylov-Subspace Methods in Model Order Reduction. In *Methoden und Anwendungen der Automatisierungstechnik. Ausgewählte Beiträge der internat. automatisierungstechnischen Kolloquien Salzhausen 2001 und 2002*, pages 1–13. Shaker-Verlag Aachen, 2003.
- [85] Love, A. E. H. *A treatise on the Mathematical Theory of Elasticity*. First American Printing of the Fourth Edition 1927, Dover Publications, New York, 1944.
- [86] Manteuffel, T. A. An incomplete factorization technique for positive definite linear systems. *Math. Comput.*, 34(150):473–497, 1980.
- [87] Meyer, D. G., Srinivasan, S. Balancing and Model Reduction for Second-Order Form Linear Systems. *IEEE Transactions on Automatic Control*, 41(11):1632–1644, 1996.
- [88] Minnicino, M. A., Hopkins, D. A. Overview of Reduction Methods and Their Implementation Into Finite-Element Local-to-Global Techniques. Technical Report 3340, Army Research Laboratory, Aberdeen Proving Ground, Maryland, 2004.
- [89] Moore, B. C. Principal Component Analysis in Linear Systems: Controllability, Observability, and Model Reduction. *IEEE Trans. on Automatic Control*, AC-26(1):17–32, 1981.
- [90] Mullis, C. T., Roberts, R. A. Synthesis of minimum roundoff noise fixed point digital filters. *Trans. Circuits. Syst.*, 23:551–562, 1976.
- [91] MUMPS. Multifrontal Massively Parallel Solver. Technical report, CERFACS, ENSEEIHT-IRIT, and INRIA, 2006.
- [92] Myklebust, L.I., Skallerud, B. Model reduction methods for flexible structures. In *5th Nordic Seminar on Computational Mechanics*, Aalborg, Denmark, October 2002.
- [93] Nagar, S. K., Singh, S. K. An algorithmic approach for system decomposition and balanced realized model reduction. *Journal of the Franklin Institute*, 341:615–630, 2004.
- [94] Otter, M., Hocke, M., Daberkow, A., Leister, G. An object oriented data model for multibody systems. In W. Schiehlen, editor, *International Symposium on Advanced*

- Multibody System Dynamics*, pages 19–48, Dordrecht, Netherlands, 1993. Kluwer Academic.
- [95] Parisch, H. *Festkörper Kontinuumsmechanik: Von den Grundgleichungen zur Lösung mit Finiten Elementen*. Teubner-Verlag, 2003.
 - [96] Qu, Z.-Q.. *Model order reduction techniques: with application in finite element analysis*. Springer-Verlag, USA, 2004.
 - [97] Reichelt, M. Anwendung neuer Methoden zum Vergleich der Ergebnissen aus rechnerischen und experimentellen Modalanalyseuntersuchungen. *VDI Berichte*, 1550:481–495, 2000.
 - [98] Reis, T., Stykel, T. A survey of model reduction of coupled systems. Technical Report 331, DFG-Forschungszentrum Matheon, 2006.
 - [99] Reis, T., Stykel, T. Balanced truncation model-reduction of second-order systems. Technical Report 376, DFG-Forschungszentrum Matheon, 2007.
 - [100] Rudnyi, E. B., Lienemann, A., Greiner, A., Korvink, J. G. mor4ansys: Generating Compact Models Directly from ANSYS Models. In *Nanotechnology Conference and Trade Show*, volume 2, pages 279–282, Boston, Massachusetts, USA, March 2004.
 - [101] Rulka, W. *Effiziente Simulation der Dynamik mechatronischer Systeme für industrielle Anwendungen*. PhD thesis, Technical University of Vienna, 1998.
 - [102] Saad, Y. *Iterative Methods for Sparse Linear Systems*. SIAM, second edition, 2003.
 - [103] Salimbahrami, B., Eid, R., Lohmann, B. Model Reduction by Second Order Krylov Subspaces: Extensions Stability and Proportional Damping. In *IEEE Conference on Computer Aided Control Systems Design (CACSD)*, October 2006.
 - [104] Salimbahrami, B., Lohmann, B. Krylov Subspace Methods in Linear Model Order Reduction: Introduction and Invariance Properties. Technical report, University of Bremen, 2002.
 - [105] Salimbahrami, B., Lohmann, B. Stopping Criterion in Order Reduction of Large Scale Systems Using Krylov subspace Methods. In *Appl. Math. Mech.*, volume 4, pages 682–683, December 2004.
 - [106] Salimbahrami, B., Lohmann, B. Order reduction of large scale second-order systems using Krylov subspace methods. *Linear Algebra and its Applications*, 415(2-3):385–405, 2005.
 - [107] Salimbahrami, B. S. *Structure Preserving Order Reduction of Large Scale Second Order Models*. PhD thesis, Technische Universität München, 2005.
 - [108] Schiehlen, W., editor. *Advanced Multibody System Dynamics: Simulation and Software Tools*. Kluwer Academic Publishers, Stuttgart, 1992.
 - [109] Schwertassek, R., Dombrowski, S., Wallrapp, O. Modal Representation of Stress in Flexible Multibody Simulation. *Nonlinear Dynamics*, 20:381–399, 1999.
 - [110] Schwertassek, R., Wallrapp, O. *Dynamik flexibler Mehrkörpersysteme*. Grundlagen

- und Fortschritte der Ingenieurwissenschaften. VIEWEG-Verlag, 1999.
- [111] Schwertassek, R., Wallrapp, O., Shabana, A. A. Flexible Multibody Simulation and Choice of Shape Functions. *Nonlinear Dynamics*, 20:361–380, 1999.
- [112] Shabana, A. A. *Dynamics of Multibody Systems*. Cambridge University Press, third edition, 2005.
- [113] Silveira, L. M. Model Order Reduction Techniques for Circuit Simulation. Technical Report 592, The Research Laboratory of Electronics, Massachusetts Institute of Technology, 1995.
- [114] Simpack. *FEMBS*, 8.6 edition, November 2004.
- [115] Simpack. *Simpack Documentation*, 8.6 edition, November 2004.
- [116] Sorensen, D. C. Solvind Large Scale Lyapunov Equations. In *IWASEP VI*, Penn State U., May 2006.
- [117] Srinivasan, R. P. *Krylov Subspace Based Direct Projection Techniques for Low Frequency, Fully Coupled, Structural Acoustic Analysis and Optimization*. PhD thesis, Oxford Brookes University, 2008.
- [118] Stykel, T. *Analysis and Numerical Solution of Generalized Lyapunov Equations*. PhD thesis, Technische Universität Berlin, 2002.
- [119] Stykel, T. Balanced truncation model reduction of second order systems. In *5th MATHMOD*, Vienna, February 2006.
- [120] Su, T. J., Craig, R. R. Model Reduction and Control of Flexible Structures Using Krylov Vectors. *AIAA*, 14:260–267, 1991.
- [121] Toledo, S. TAUCS a library of sparse linear solvers. Technical report, School of Computer Science, Tel-Aviv University, 2003.
- [122] Wallrap, O., Schwertassek, R. Representation of Geometric Stiffening in Multibody System Simulation. *Int. Journal for Numerical Methods in Engineering*, 32:1833–1850, 1991.
- [123] Wallrapp, O. Standardization of Flexible Body Modeling in Multibody System Codes, Part I: Definition of Standard Input Data. *Mech. Struct. & Mach.*, 22:283–304, 1994.
- [124] Wallrapp, O. Nonlinear Beam Theory in Flexible Multibody Dynamics. In *Multibody Dynamics in Sweden II*, Frostavallen, Sweden, November 2001.
- [125] Wallrapp, O. Flexible Multibody Dynamics with Space Flight Applications Using SIMPACK. Technical report, Munich University of Applied Sciences, 2006.
- [126] Wallrapp, O., Wiedemann, S. Comparison of Results in Flexible Multibody Dynamics Using Various Approaches. *Nonlinear Dynamics*, 34:189 – 206, 2003.
- [127] Waltz, M. *Dynamisches Verhalten von gummigefederten Eisenbahnrädern*. PhD thesis, Technische Hochschule Aachen, Fakultät für Maschinenwesen, 2005.
- [128] Zienkiewicz, O. C., Taylor, R. L., Zhu, J. Z., editor. *Finite Element Method: Its Basis & Fundamentals*. Elsevier Butterworth-Heinemann, Oxford, 6 edition, 2005.

List of Figures

1.1	FEM-MBS coupling using ANSYS and SIMPACK	7
2.1	Motion of an element e of a FE structure	11
2.2	Mass matrix of a 3D solid bar before and after the m & s sorting	19
2.3	Mass matrix of an elastic UIC60 rail before and after the m & s sorting	19
2.4	Mass matrix of an elastic rod before and after the m & s sorting	20
2.5	\mathbf{T}_{static} by MOR of a 3D solid bar - $m = 36$	23
2.6	Categorization of the CMS variants	33
2.7	\mathbf{M}_{CMS} of 3D solid bar with $m = 36$ and CB = 15	35
2.8	Two-step MOR algorithmic scheme	58
3.1	Natural Frequency Difference - 3D view	67
3.2	Natural Frequency Difference - top view	68
3.3	Stiffness Normalized Vector Difference - 3D view	69
3.4	Modal Assurance Criterion - 3D view	70
3.5	Modal Assurance Criterion - top view	70
3.6	Modified Modal Assurance Criterion - 3D view	71
3.7	Modified Modal Assurance Criterion - top view	72
3.8	Modal Comparison Criteria Matrix - 3D view	73
3.9	Mass Normalized Vector Difference - top view	74
3.10	Switching process - Natural Frequency Difference	75
3.11	Switching process - Modified Modal Assurance Criterion	76
3.12	Switching process - Updated modMAC coefficient matrix	77
3.13	Switching process - Secondary diagonal CMP - original modMAC	77
3.14	Switching process - Secondary diagonal CMP - updated modMAC	78
3.15	3D solid bar structure - Case 1 - master DoF	79
3.16	Free 3D solid bar - NRFD criterion	80
3.17	Free 3D solid bar - MAC criterion	81
3.18	Free 3D solid bar - modMAC criterion	82
3.19	Free 3D solid bar - MNVD & SNVD criterion	83
3.20	Free 3D solid bar - NRFD & modMAC - 2 IRS iter. & 20 CB	84
3.21	Free 3D solid bar - CMS - modMAC top view	85
3.22	One-end (top) & two-end (bottom) fixed 3D solid bar - NRFD	86
3.23	One-end fixed 3D solid bar - modMAC criterion	87
3.24	Two-end fixed 3D solid bar - modMAC criterion	88
3.25	One-end fixed 3D solid bar - NRFD & modMAC- 2 IRS iter. & 20 CB	89
3.26	Two-end fixed 3D solid bar - NRFD & modMAC- 2 IRS iter. & 20 CB	90
3.27	Two-end fixed 3D solid bar - ICMS - modMAC top view	91
3.28	3D solid bar structure - Case 2 - master DoF	92
3.29	Two-end fixed 3D solid bar - Case 2 - NRFD	92

3.30 Two-end fixed 3D solid bar - Case 2 - modMAC	93
3.31 UIC60 rail - bottom grounded - master DoF	94
3.32 UIC60 rail - bottom grounded - NRFD criterion	94
3.33 UIC60 rail - bottom grounded - modMAC criterion	95
3.34 UIC60 rail - bottom grounded - MNVD & SNVD	96
3.35 UIC60 rail - bottom grounded - modMAC ICMS top view	97
3.36 UIC60 rail - Normal (left) & Clumsy (right) m -set	97
3.37 UIC60 rail - NRFD - Normal & Clumsy m -set	98
3.38 UIC60 rail - modMAC - Normal & Clumsy m -set	99
3.39 UIC60 rail - modMAC - Normal & Clumsy m -set	100
3.40 Elastic rod - master DoF (black points) - Unconstrained	101
3.41 Elastic rod - NRFD criterion	102
3.42 Elastic rod - CMS & ICMS MOR - modMAC	103
3.43 Elastic rod - KSM & SEREP MOR - modMAC	104
3.44 Elastic rod - SEREP-KSM & SEREP-ICMS MOR - modMAC	105
3.45 Elastic crankshaft - Unconstrained	107
3.46 Elastic crankshaft - NRFD criterion	108
3.47 Elastic crankshaft - CMS & KSM MOR - modMAC	109
3.48 Elastic crankshaft - SEREP-CMS & SEREP-ICMS MOR - modMAC	110
4.1 Diagonal perturbation - elastic rod - comp. time & conv. rate	118
4.2 Diagonal perturbation - elastic rod - NRFD & modMAC	119
4.3 Diagonal perturbation - elastic crankshaft - comp. time & conv. rate	120
4.4 Diagonal perturbation - elastic crankshaft - NRFD & MAC	121
4.5 3D solid bar structure - 60 DoF	122
4.6 ROM comparison - direct & diagonal perturbation solution	123
4.7 KSM ROM - Starting vector effect I	123
4.8 KSM ROM - Starting vector effect II	124
4.9 3D solid bar - unstable $\mathbf{P}(\lambda)$	126
4.10 3D solid bar - BT ROM correlation - DP	127
4.11 UIC60 rail - unstable $\mathbf{P}(\lambda)$	127
4.12 UIC60 rail - BT ROM correlation - DP	128
5.1 Floating frame of reference formulation	130
5.2 Back-projection approach: reduction-expansion subspace	138
5.3 FEM-MBS coupling - ANSYS & SIMPACK - file-type work flow	141
6.1 MORPACK toolbox - work flow	143
6.2 3D solid bar - modMAC - CMS & KSM	147
6.3 UIC60 free - NRFD - CMS & KSM ROM	148
6.4 UIC60 one-end fixed - modMAC - CMS & KSM ROM	149
6.5 UIC60 free - modMAC - CMS & KSM ROM	150
6.6 3D solid bar - Top to bottom: Full _{ANSYS} , CMS _{FEMBS} and KSM _{MORPACK}	151
6.7 UIC60 rail free - Top to bottom: ANSYS, CMS _{FEMBS} and KSM _{MORPACK}	152
6.8 UIC60 rail fixed - Top to bottom: ANSYS, CMS _{FEMBS} and KSM _{MORPACK}	153
A.1 MORPACK - Procedure GUI	176

A.2 MORPACK: <i>ANSYS-MATLAB Data Conversion GUI</i>	179
A.3 MORPACK: <i>FE-MATLAB Check GUI</i>	180
A.4 MORPACK: <i>Second Order Model Order Reduction GUI</i>	180
A.5 MORPACK: <i>Model Correlation Criteria GUI</i>	181
A.6 MORPACK: <i>Standard Input Data Properties GUI</i>	181

List of Tables

1.1	Modelling work flow in continuum mechanics	3
1.2	Rigid & elastic MBS: software sample	6
2.1	MOR quality comparison under inadequate m selection	59
2.2	Sample of two-step MOR methods	60
3.1	Switching process - modMAC matrix - non diagonal CMPs	75
3.2	Elastic rod - MOR Comparison - Quality Computation Time	106
3.3	Elastic rod - CMS & ICMS - NRFD & modMAC	106
3.4	Elastic crankshaft - SEREP - CPU Time	108
3.5	Elastic crankshaft - MOR Comparison - Quality Computation Time	111
3.6	Elastic crankshaft - CMS - NRFD & modMAC	111
4.1	Diagonal perturbation - Computation time - Quality of results	117
4.2	3D solid bar- diagonal perturbation - ω -shifting	126
4.3	UIC60 rail - diagonal perturbation - ω -shifting	126
5.1	Back-projection - UIC60 rail - physical properties validation	140
6.1	Application level I-II: Import-convert FE data & Export FE data	145
6.2	Application level III: MCC	146
6.3	Application level IV: Back-projection control	146
A.1	ANSYS FE data required for import into MORPACK	174
A.2	MORPACK: Procedure I & II - Input data from Table A.1	175

A MORPACK User's Guide

A.1 MORPACK version 1.0

MORPACK is a Matlab-based environment, which consists of a total of 120 modules located in 7 different folders. The package is delivered in a root-folder named MORPACK_v1.0 containing the aforementioned modules and folders. The current MORPACK version v1.0 requires the ANSYS FE data to be gathered in a folder created and named by the user and then placed inside the MORPACK_v1.0 root-folder. This procedure can be repeated for arbitrarily many user-created folders containing ANSYS FE data.

The future MORPACK version will have a sub-folder named *Models* within its root-folder, where the user should place the ANSYS FE data.

The MORPACK GUI is started by typing *morpak* in the Matlab command window.

A.2 ANSYS FE data

The MOR and SID inner interfaces as well as the four application levels (Chapter 6) operate only with specifically user-predefined ANSYS FE data. The latter is summarized in Table A.1 along with the description on how to acquire the data within the ANSYS GUI software package. The data has to be saved in the user-created folder as ASCII files (*.txt). The reason therefor resides on the didactic and instructional usage of the FE information during the FEM-MBS coupling process. Later MORPACK versions should not be bounded by such file type restrictions.

The utilization of the ANSYS GUI command for listing an eigenvector (5. in Table A.1) is repeated such that the required number of eigenvectors forming the FE structure's modal matrix is ascertained. The ASCII eigenvector files are saved in a increasing order, e.g. *eig_1.txt*, *eig_2.txt*, etc.

The system matrices are acquired by damping the ANSYS assembled global matrix file *.FULL and are written in the, so called, Harwell-Boeing file format [39]. In view of minimizing storage requirements only the diagonal entries and either the upper or the lower triangular part of the system matrices are saved. Thus, the conversion of the Harwell-Boeing format into the Matrix Market format requires an extra formulation of the form:

$$\mathbf{A} = \mathbf{A}_{LT} + \mathbf{A}_{LT}^T - \mathbf{A}_d, \quad (\text{A.1})$$

where \mathbf{A}_{LT} and \mathbf{A}_d annotate the lower-triangular part of the symmetric matrix \mathbf{A} and the diagonal matrix \mathbf{A} , respectively.

Table A.1: ANSYS FE data required for import into MORPACK

FE data	ANSYS GUI
1. Mass matrix	Utility Menu>Files>List>Binary Files>Matrix
2. Stiffness matrix	Utility Menu>Files>List>Binary Files>Matrix
3. Damping matrix (if required)	Utility Menu>Files>List>Binary Files>Matrix
4. Number of total nodes	Utility Menu>List>Status>Global Status
5. Eigenvector	Main Menu>General Postproc>List Results >Nodal Solution
6. Eigenfrequency vector	Main Menu>General Postproc>Results Summary
7. DoF list	Utility Menu>List>Nodes
8. Master DoF list	Main Menu>Solution>Master DOFs >User Selected>List All
9. DoF ordering	Utility Menu>Files>List>Binary Files>Other
10. Fixed DoF list (if required)	Utility Menu>List>Loads>DOF Constraints >On All Nodes

The *DoF ordering* file (9. in Table A.1 - located at the fourth record of the ANSYS results file *.RST) contains the information regarding the DoF allocation in the damped system matrices, i.e. which DoF represents the first entry of the matrix, etc. The ANSYS eigenvector listing commands result in listing the eigenvector DoF in increasing order starting from node name 1 until node name n , with n being the maximum defined node in the structure. Therefore, the *DoF ordering* information is also utilized for sorting the eigenvectors according to the sorting of the associated system matrices. In case of directly importing the ANSYS system matrices and eigenvectors (procedure I), the orthogonality properties of the mass matrix is a sufficient criterion to verify the correct data conversion.

The data gathered in Table A.1 constitute the general set of importable FE information in view of operating MORPACK. Depending on the designated procedure (I or II) only a certain subset thereof is required.

A.3 Procedures I & II

The selection of the algorithmic procedure is conducted by starting the MORPACK GUI, as depicted in Fig. A.1. A short description for each procedure is given within the *Procedure GUI* environment (Fig. A.1) and the available input data options are stated. According the FE information of Table A.1 and depending on the procedure selection, the user should provide the files listed in Table A.2.

It is noted that in case of a fixed FE structure the fixed input data should be used for initiating the first procedure, whereas the input data of the associated free structure should be provided for the second procedure along with the vector of fixed DoF (Table

Table A.2: MORPACK: Procedure I & II - Input data from Table A.1

ANSYS Structure	Procedure I	Procedure II
Free	1. – 4., 7. – 9.	1. – 9.
Fixed	1. – 4., 7. – 9. of the associated free structure plus 10.	1. – 10. of the actual fixed structure

A.2). The system is grounded later on during the application of the MOR interface.

In general, the second procedure, being less ANSYS-dependent results, in a faster computation of the imported data and it is considered as the default procedure in the MORPACK toolbox.

Nevertheless, the utilization of the first procedure is highly advised in case of very large FE models ($n_{dim} > 5 \cdot 10^5$), the eigenvalue analysis of which might fail within the Matlab code. Herewith, the required modal analysis data is acquired in the ANSYS code (with the help of the integrated sparse iterative solvers and/or the lumped mass approximation method) and provided in the MORPACK environment for further usage. Additionally, the first procedure is suitable for importing FE data - written in the Matrix Market file format - obtained from other FEM software packages, e.g. Msc Nastran (Appendix A.5).

A.4 MORPACK GUI

The initiation of MORPACK begins with the first GUI as depicted in Fig. A.1, the description of which is ascertained in the following panel manner, i.e.

- MORPACK: Model Order Reduction PACKAGE GUI
 - ANSYS-MORPACK Procedures: either Procedure I or II.
 - Data Source: the user is enabled to browse within the MORPACK root-folder to locate the created FE data folder.

Thereafter, the *Apply* button is automatically activated and the second, namely, the ANSYS-MATLAB Conversion GUI begins (Fig. A.2):

- ANSYS-MATLAB Conversion GUI
 - System matrices: the user is enabled to automatically browse in the user-created FE folder in order to input the designated system matrices.
 - Structure Nodes: input a number representing the total nodes of the structure.
 - Fixed DoF: No or Yes. If Yes, then the user is enabled to automatically browse in the user-created FE folder in order to input the designated fixed DoF file.
 - Eigenvectors: the user is enabled to automatically browse in the user-created FE folder in order to input the designated eigenvalue analysis data of the full

model. In case of numerous eigenvector files, only one should be selected and the rest is conducted by the MORPACK code.

- *Nr. to convert*: input a number of either the saved eigenvector files (procedure I) or the desired eigenvectors to be computed (procedure II).
- *Node Notation*: the user is enabled to automatically browse in the user-created FE folder in order to input the designated total and (or) master DoF.
- *DoF Ordering*: the user is enabled to automatically browse in the user-created FE folder in order to input the designated DoF ordering file.

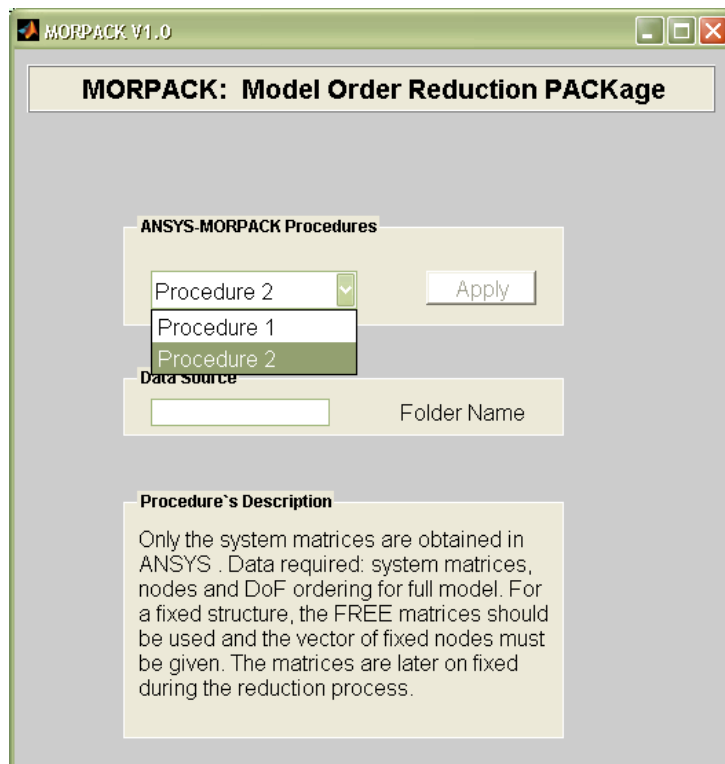


Fig. A.1: MORPACK - Procedure GUI

The completion of the above (depending on the procedure selection) allows the data conversion (*Convert Files* button) and a validation thereof (*Check Converted Files* button), which leads to the second *FE-MATLAB Check* GUI (Fig. A.3):

- *FE-MATLAB Check* GUI
 - *Matrix Non Zero Structure*: the sparse structure of the selected system matrix is visualized.
 - *Orthogonality Check/Eigenfrequency*: the selected modal matrices and the eigenfrequencies are visualized.

Thereafter (*Reduction/MCC* button), the *Second Order Model Order Reduction* GUI follows (Fig. A.4) is activated, the functionality of which is shortly outlined in the following:

- *Second Order Model Order Reduction GUI*
 - *Model Reduction Method*: selection of the MOR scheme.
 - *Enter Solver Approach*: either direct or iterative solution. In case of the latter, the user can choose either to define or not the preconditioner's fill in, and to apply or not the diagonal perturbation methodology by indicating the value of the k -parameter (Section 4.1). A MORPACK predefined k -spectrum is available.

The diagonal perturbation methodology might be applied in case of choosing to directly solve the MOR problem during the explicit application of a BT technique or the two-step approaches involving a BT technique.

- *DoF Ordering*: No or Yes. If Yes, the user is enabled to browse in the MORPACK folder, where the converted data is saved. On the upper-left corner of the browser's window the name of the file to be utilized is annotated by the MORPACK code. Data required are the: DoF list, DoF ordering, and the master DoF list.
- *MOR Data*: input the number of the start eigenfrequency for the Dynamic MOR method (Subsection 2.4.2) or the number of the required IRS iteration steps in case of the IRS MOR (Subsection 2.4.23). This holds also for the associated two-step version of the aforementioned MOR methods.
- *Enter Dimension*: the dimension of the ROM has to be appointed. The first box copes with the first ROM's dimension during the two-step MOR scheme and the second box for denoting the dimension of either the final ROM during the two-step MOR scheme or the dimension of the ROM during a one-step MOR approach.
- *Eigenvect. to compute*: indicate the number of the ROM's eigenvectors to compute. It should not be greater than the number of eigenvectors of the associated full model.
- *Craig-Bampton Modes*: indicate the number of modes of the CB set in case of the explicit CMS or a CMS related one-step or two-step MOR method (Section 2.5)
- *FE System Matrices*: the user is enabled to automatically browse into the MORPACK folder, where the converted data is saved, to select the system matrices. Depending on the procedure (I or II) different *.mat files are required, the names of which are automatically denoted on the upper-left corner of the browser's window.

The MOR scheme starts (*Reduce* button) and after the ROM is computed, the *Model Correlation Criteria GUI* can be activated (*Model Correlation* button) (Fig. A.5):

- *Model Correlation Criteria GUI*
 - *Free or Fixed*: the free or fixed nature of the ROM is indicated.
 - *Criterion*: both the selected MCC and the sparse structure of the system matrices can be visualized (*Apply* and *Check* buttons, respectively). The visualization of the results differs according to the chosen procedure (I or II).

If the ROM's dynamic properties do not comply with the user's requirements, the MCC GUI window can be closed and the MOR is restarted by indicating either a different MOR or appointing a different master DoF file. The latter is feasible only in case of the second procedure and under the assumption of a different master DoF FE file to have been provided by the user. Otherwise, the *Standard Input Data Properties* GUI (Fig. A.6) is started (*SID Definition* button):

- *Standard Input Data Properties* GUI
 - *MOR Used*: the applied MOR scheme is once more indicated.
 - *Fixed Model*: the free or fixed nature of the ROM is denoted. Herewith, the appropriate SID algorithms are appointed for the correct computation of the elastic body's properties (Eq. (5.31) - (5.39)).
 - *ROM Correlation*: in case a MOR scheme belonging to the *Non physical subspace reduction-expansion methods* category was used (Section 2.3), the *Back-projection control* application level (Subsection 6.1.2) is activated (*Apply* button). A visualized NRFD criterion follows, which validates the dynamic properties of the back-projected ROM. Two message types are available, namely, *OK* and *WRONG*, both indicating if the ROM is SIMPACK importable or not, respectively.
 - *SID File Name*: the name of the SID file should be indicated
 - *SID Initial Data*: certain initial parameter data required for the SID generation should be given, e.g. the damping coefficient (default is the natural damping coefficient), the utilized FE units, and the lists of the total and master DoF, respectively (automatic MORPACK browser)

The generated SID file is saved in the *SID Files* folder under the name construction *Date_Name_MOR.SID_FEM*, e.g. *15.08.1979_piston_ICMS.SID_FEM*.

Herewith, the GUI description of the MORPACK toolbox is completed. It should be mentioned that depending on the chosen procedure as well as the applied MOR scheme only certain of the previously outlined fields should be considered. In this regard, MORPACK automatically deactivates the non-required fields or buttons (colored gray and no action is allowed) and thus, the user need only to follow the designated (white colored) active fields.

A.5 Compatibility with commercial FEM software packages

The current MORPACK version also supports sorted FE system matrices (Eq. (2.43)) - written in the Market Matrix file format - generated from other FEM software packages, e.g. Msc Nastran. In this case, the first procedure should be activated and the first two GUIs should be skipped. Only the free or fixed nature of the FE structure should be indicated in the first *ANSYS-MATLAB Conversion* GUI. The MOR GUI is accessed as previously described and thereafter, the generated ROM can be validated (MCC).

Nevertheless, further adjustments are required for the adaptation of the SID GUI when coping with non-ANSYS FE data.

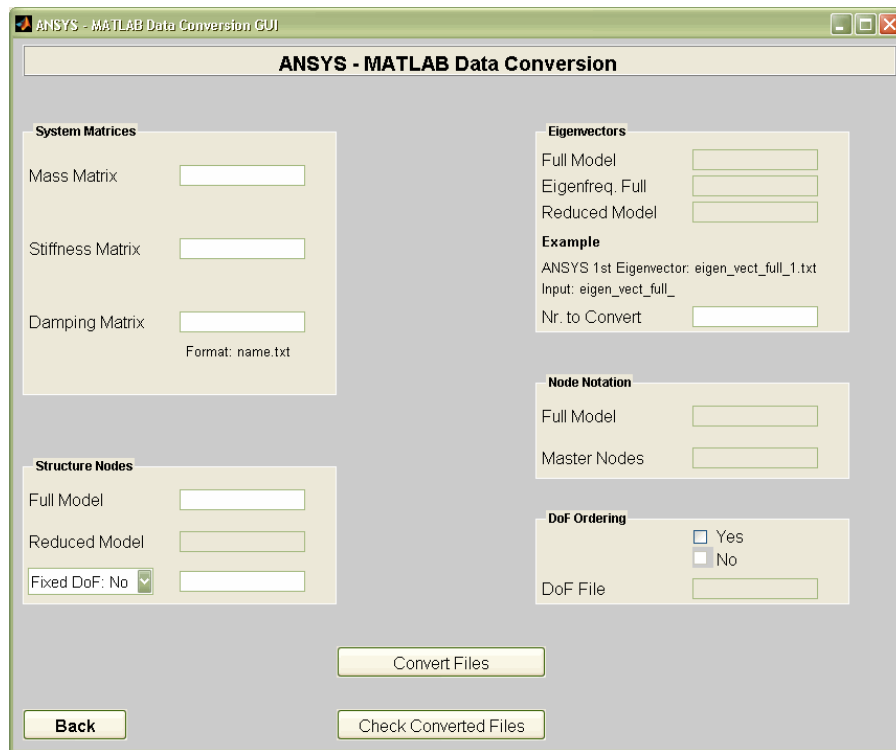
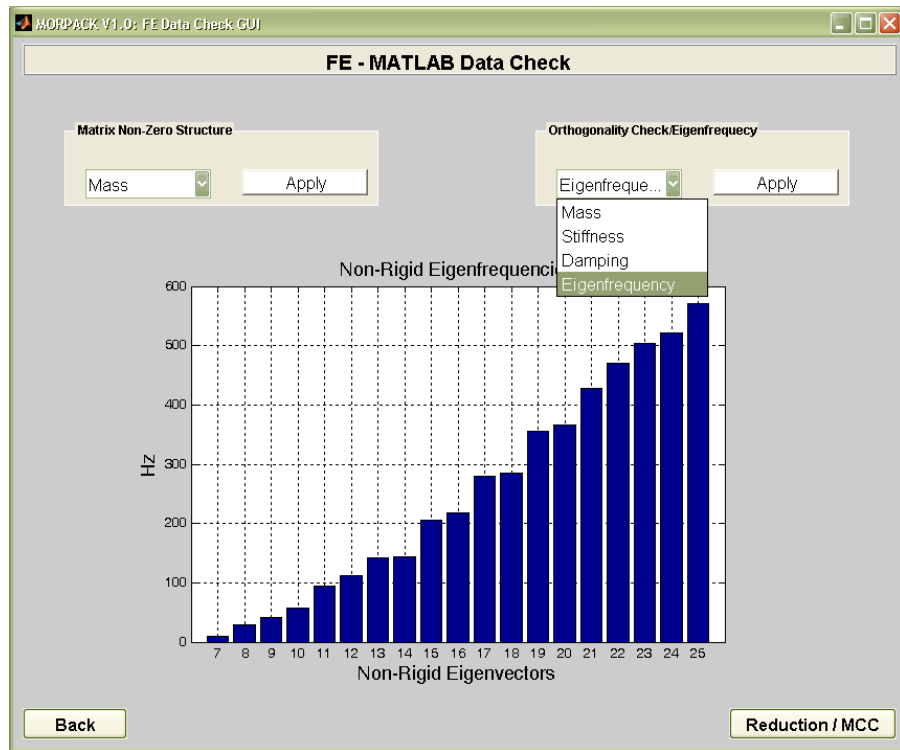
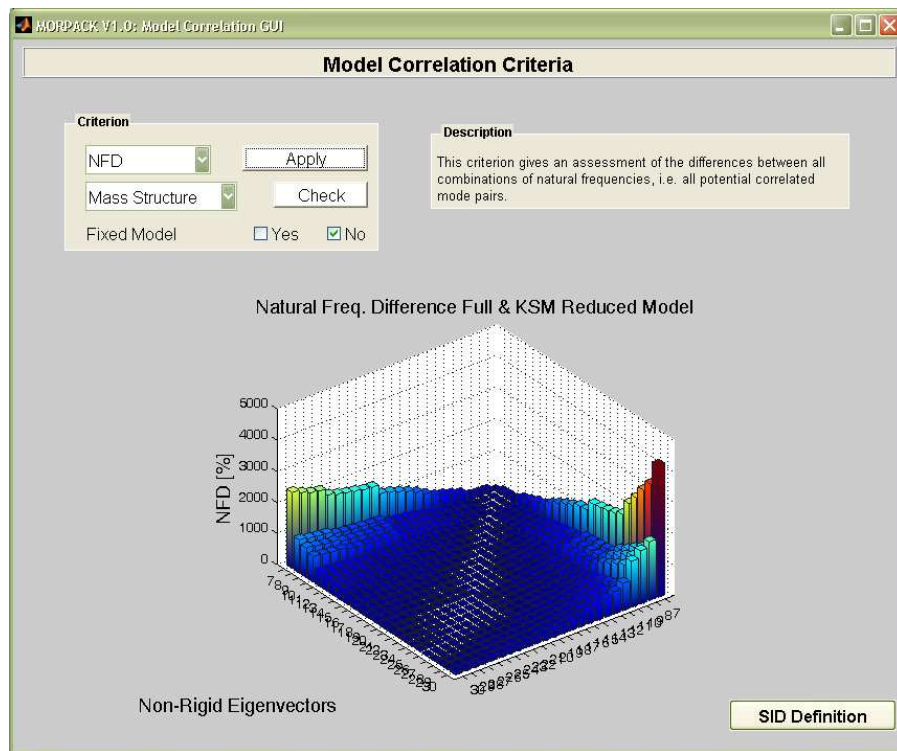
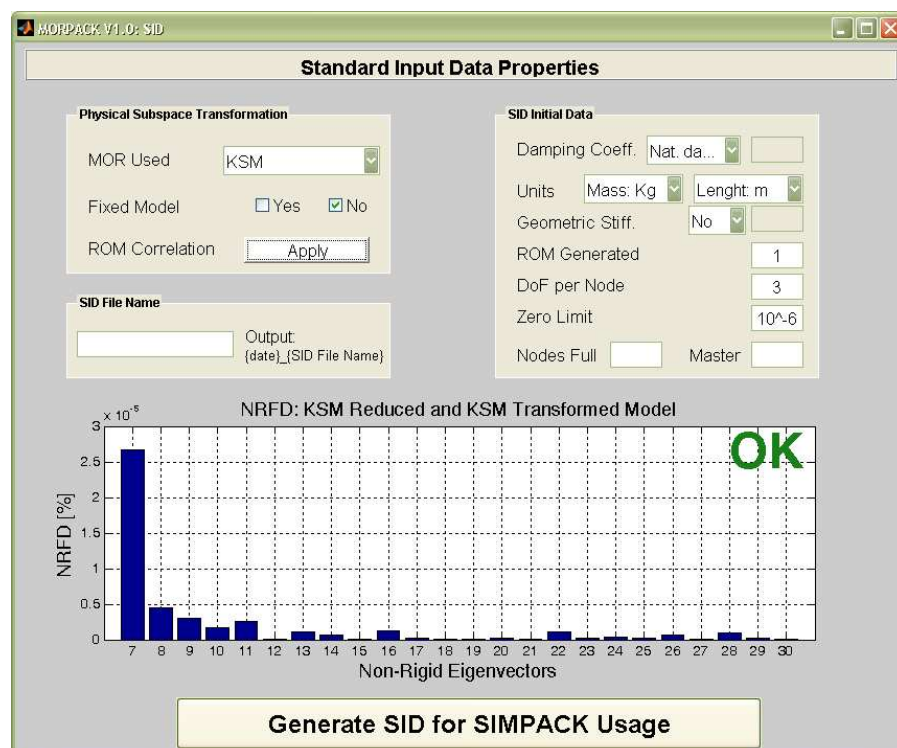


Fig. A.2: MORPACK: ANSYS-MATLAB Data Conversion GUI

Fig. A.3: MORPACK: *FE-MATLAB Check* GUIFig. A.4: MORPACK: *Second Order Model Order Reduction* GUI

Fig. A.5: MORPACK: *Model Correlation Criteria* GUIFig. A.6: MORPACK: *Standard Input Data Properties* GUI

